

**DOCTORAL THESIS**

# Screen-printed pH Sensors based on Ruthenium(IV) Oxide for Measurement in Food Samples

Maryna Lazouskaya

TALLINN UNIVERSITY OF TECHNOLOGY  
DOCTORAL THESIS  
14/2023

**Screen-printed pH Sensors based on  
Ruthenium(IV) Oxide for Measurement  
in Food Samples**

MARYNA LAZOUSKAYA



TALLINN UNIVERSITY OF TECHNOLOGY

School of Science

Department of Chemistry and Biotechnology

This dissertation was accepted for the defence of the degree 11 April 2023

**Supervisor:** Associate professor Ott Scheler  
Department of Chemistry and Biotechnology  
School of Science, Tallinn University of Technology  
Tallinn, Estonia

**Opponents:** Associate professor Toonika Rinke  
Institute of Chemistry  
Faculty of Science and Technology, University of Tartu  
Tartu, Estonia

Senior Research Fellow Alan O’Riordan  
Emerging Materials and Devices  
Micro & Nano Systems Centre  
Tyndall National Institute  
Cork, Ireland

**Defence of the thesis:** 26 May 2023, Tallinn

**Declaration:**

Hereby I declare that this doctoral thesis, my original investigation, and achievement, submitted for the doctoral degree at Tallinn University of Technology has not been submitted for a doctoral or equivalent academic degree. The work reported in this thesis was carried out in the Center of Food and Fermentation Technologies (a.k.a. TFTAK) and supported by European Commission through Horizon-2020 MSCA-ITN project AQUASENSE (grant agreement H2020-MSCA-ITN-2018-813680) and partially supported by Graduate School in Biomedicine and Biotechnology receiving funding from the European Regional Development Fund under program ASTRA 2014-2020.4.01.16-0032 in Estonia.

Maryna Lazouskaya

-----  
signature



Copyright: Maryna Lazouskaya, 2023

ISSN 2585-6898 (publication)

ISBN 978-9949-83-968-1 (publication)

ISSN 2585-6901 (PDF)

ISBN 978-9949-83-969-8 (PDF)

Printed by Auratrükk

TALLINNA TEHNIKAÜLIKOOL  
DOKTORITÖÖ  
14/2023

**Ruteenium(IV) oksiidil põhinevad  
siiditrükiga pH-andurid toiduproovide  
mõõtmiseks**

MARYNA LAZOUSKAYA





# Contents

List of Publications .....	7
Author's Contribution to the Publications .....	8
Introduction .....	9
1 Theory and Literature Overview .....	11
1.1 pH measurement in food samples .....	11
1.1.1 Potentiometric sensors.....	11
1.1.2 Potentiometric sensors based on polymers .....	12
1.1.3 Potentiometric biosensors .....	13
1.1.4 Systems consisting of novel working and reference electrodes.....	14
1.1.5 Conclusion .....	15
1.2 Principles of potentiometric pH measurement .....	15
1.3 Metal oxides for pH sensing.....	17
1.4 Ruthenium(IV) oxide .....	18
1.5 Nafion membrane as a protective layer in pH-sensitive electrodes .....	19
2 Aims of the Thesis .....	22
3 Materials and Methods.....	23
3.1 Fabrication of the RuO <sub>2</sub> electrodes (Publications I-III).....	23
3.2 Modification of the fabricated electrodes with Nafion membrane (Publication II) and investigation of the properties (Publications II, IV-VII) .....	23
3.3 Electrochemical characterization of the fabricated electrodes .....	24
3.3.1 Setup.....	24
3.3.2 Electrochemical characteristics .....	24
3.4 Measurement in real-life samples .....	27
4 Results and Discussion .....	28
4.1 Fabrication parameters for the screen printing of the RuO <sub>2</sub> pH electrodes (Publications I and II).....	28
4.2 Fabrication parameters for the deposition of the Nafion membrane and properties of the RuO <sub>2</sub> -Nf electrodes (Publications II-VI) .....	30
4.2.1 Concentration of Nafion casting solution (Publication IV) .....	30
4.2.2 Number of Nafion layers (Publication II) .....	31
4.2.3 Time needed for deposition of one layer (Publication II) .....	33
4.2.4 Drying temperature (Publication II).....	33
4.2.5 Stability of the readings of the RuO <sub>2</sub> -Nf electrodes (Publication II) .....	35
4.2.6 Cross-sensitivity of the RuO <sub>2</sub> -Nf electrodes (Publication III) .....	35
4.2.7 Reusability of the fabricated RuO <sub>2</sub> -Nf electrodes (Publication VI) .....	36
4.3 Performance of the fabricated RuO <sub>2</sub> -Nf electrodes in food samples (Publications III and VII) .....	36
4.3.1 Measurement in dairy samples (Publication III) .....	37
4.3.2 Continuous measurement in milk during coagulation .....	38
4.3.3 Cleaning after measurement in dairy samples (Publication VII) .....	39
Conclusion.....	40
References .....	41
Acknowledgements.....	48

Abstract.....	49
Lühikokkuvõte.....	50
Appendix 1 .....	51
Appendix 2 .....	69
Appendix 3 .....	83
Appendix 4 .....	95
Appendix 5 .....	101
Appendix 6 .....	107
Appendix 7 .....	113
Curriculum vitae.....	119
Elulookirjeldus.....	120

## List of Publications

The list of author's publications, based on which the thesis has been prepared:

### Journal Articles (code 1.1)

- I K. Uppuluri, M. Lazouskaya, D. Szwagierczak, K. Zaraska, and M. Tamm, "Fabrication, potentiometric characterization, and application of screen-printed RuO<sub>2</sub> pH electrodes for water quality testing," [Sensors](#), vol. 21, no. 5399, 2021.
- II M. Lazouskaya, O. Scheler, V. Mikli, K. Uppuluri, K. Zaraska, and M. Tamm, "Nafion protective membrane enables using ruthenium oxide electrodes for pH measurement in milk," [Journal of the Electrochemical Society](#), vol. 168, no. 107511, 2021.
- III Maryna Lazouskaya, Iuliia Vetik, Martti Tamm, Kiranmai Uppuluri, and Ott Scheler "Binary RuO<sub>2</sub>-CuO electrodes outperform RuO<sub>2</sub> electrodes when measuring pH in food samples," [ACS Omega](#), vol. 8, pp. 13275-13284, 2023.

### Conference articles (code 3.1)

- IV M. Lazouskaya, M. Tamm, O. Scheler, K. Uppuluri, and K. Zaraska, "Nafion as a protective membrane for screen-printed pH-sensitive ruthenium oxide electrodes," [Proceedings of IEEE Biennial Baltic Electronics Conference \(BEC\)](#), vol. 2020-October, pp. 18–21, 2020, Tallinn, Estonia.
- V K. Uppuluri, M. Lazouskaya, D. Szwagierczak, and K. Zaraska, "Influence of temperature on the performance of Nafion coated RuO<sub>2</sub> based pH electrodes," in [IEEE International Conference on Flexible and Printable Sensors and Systems \(FLEPS\)](#), 2021, Manchester, United Kingdom.
- VI M. Lazouskaya, O. Scheler, K. Uppuluri, K. Zaraska, and M. Tamm, "Reusability of RuO<sub>2</sub>-Nafion electrodes, suitable for potentiometric pH measurement," in [IEEE International Conference on Flexible and Printable Sensors and Systems \(FLEPS\)](#), 2022, Vienna, Austria.
- VII M. Lazouskaya, I. Vetik, O. Scheler, K. Uppuluri, N. Razmi, K. Zaraska, and M. Tamm, "Cleaning procedure for the screen printed RuO<sub>2</sub>-based pH electrodes," in [IEEE Sensors Conference](#), 2022, Dallas, Texas, USA.



## **Author's Contribution to the Publications**

Contribution to the papers in this thesis are (according to CREDiT taxonomy):

- I Methodology, formal analysis, writing – original draft preparation, writing – review and editing, visualization.
- II Conceptualization, methodology, validation, formal analysis, investigation, resources, data curation, writing – original draft preparation, visualization.
- III Conceptualization, methodology, validation, formal analysis, investigation, resources, data curation, writing – original draft preparation, writing – review and editing, visualization.
- IV Conceptualization, methodology, validation, formal analysis, investigation, resources, data curation, writing – original draft preparation, visualization.
- V Conceptualization, methodology, data curation, writing – original draft preparation, visualization.
- VI Conceptualization, methodology, validation, formal analysis, investigation, resources, data curation, writing – original draft preparation, visualization.
- VII Conceptualization, methodology, validation, formal analysis, investigation, resources, data curation, writing – original draft preparation, visualization.

## Introduction

The assessment of the quality of food products has always been and always will be one of the biggest responsibilities of food researchers. The quality of any food product is evaluated based on various parameters, including adulteration, physical properties, chemical composition, sensory attributes, etc. (Azad & Ahmed, 2016; Biswas & Mandal, 2020; Cheng et al., 2015; Toldrá, 2017). One of the key parameters in food manufacture and food quality analysis is pH. pH is known to be related to food quality and freshness (Abbas et al., 2008; Hopkins et al., 2014; Loudon et al., 2019; Matarneh et al., 2017), can be used to monitor microbial growth in dairy products (Poghossian et al., 2019) and is suitable to reveal mastitis and inflammatory infection in cattle (Kandeel et al., 2019).

At present, to determine the pH of food products, a standard potentiometric method is used (e.g. [ISO 11289:1993](#), [ISO 7238:2004](#)). Potentiometric determination of pH is based on the measurement of the electrochemical potential change between a pH-sensitive electrode and a reference electrode immersed into the test solution. The glass electrode used in conventional pH meters is a combination of pH-sensitive and reference electrodes incorporated in one glass body. However, due to its high cost, fragility of the glass body of the electrode, and possible contamination of samples and the reference junction, novel materials and methods are thoroughly investigated.

Several metal oxides were investigated over the years for application in pH measurement (Manjakkal et al., 2020). Researchers focus their attention on the hydrogen-sensitive metal oxides (e.g., ZnO, SnO<sub>2</sub>, IrO<sub>2</sub>, TiO<sub>2</sub>, Ta<sub>2</sub>O<sub>5</sub>) (Kurzweil, 2009; Manjakkal et al., 2020). The majority of the oxides have a wide pH range; however, they suffer from noticeable hysteresis that affects the precision of consequent measurements (Kurzweil, 2009). Among the investigated metal oxides, RuO<sub>2</sub> shows good accuracy, low hysteresis, and excellent performance even in the presence of bacteria on the electrode surface (Zhuiykov, 2009).

However, not much attention has been paid so far to the application of the RuO<sub>2</sub> electrodes in real-life samples. Moreover, there is a gap in knowledge regarding the application of novel pH samples to real-life measurements. Most of the research articles concentrate on the fabrication of the electrodes and the characterization of their sensitivity and accuracy in aqueous media. This thesis presents the investigation into the application of potentiometric RuO<sub>2</sub> sensors for pH measurement in food samples. Food samples, especially dairy products, are among the most challenging samples to work with due to their complex compositions. Fats in food samples are known to interfere with pH measurement by blocking the surface of the electrodes and hindering the charge transfer (Upreti et al., 2004). The first part of this thesis is dedicated to the optimization of the electrochemical characteristics of RuO<sub>2</sub> electrodes. Here discussion focuses on the influence of parameters of fabrication of the electrodes (such as sintering temperature and ink composition) on the sensitivity, linearity, hysteresis and drift. Following, the second chapter directs its attention to the key component of making RuO<sub>2</sub> electrodes work in food samples – the Nafion™ (Nafion) membrane. The discussion incorporates the investigation of the properties of the membrane, as well as the electrochemical performance of the Nafion-covered

electrodes. Finally, the third chapter describes the application of the RuO<sub>2</sub> electrodes for pH measurement in real-life samples. Here the results of pH measurement in dairy products are presented and a cleaning approach for the maintenance of the electrodes is proposed.

# 1 Theory and Literature Overview

## 1.1 pH measurement in food samples

The standard procedure of pH measurement is regulated by the International Organization for Standardization (ISO) by standards such as [ISO 11289:1993](#) and [ISO 7238:2004](#). The ISO recommends the standard potentiometric method for pH measurement. The theory of potentiometric pH measurement will be discussed in detail in section 1.2.

At present, different methods are scrutinized to find the one allowing fabricating the pH-electrode that would not suffer from asymmetry potential, fragility, or inability to measure pH in some matrices (Bühlmann et al., 2001; Upreti et al., 2004). The most promising results in pH measurement applications are observed for optical sensors, electrochemical sensors, and sensors based on field-effect transistors. Nevertheless, the methods themselves present less interest than miniature and portable sensors that could be used not only in laboratory analysis but also for the modernization of active manufacturing lines for on-line monitoring. Potentiometric sensors attract the most attention as they do not require expensive equipment and are easy to operate.

### 1.1.1 Potentiometric sensors

The potentiometric method (or Potentiometry) is a cheap and simple method that allows determining the pH in a matter of seconds. Potentiometric detection relies on the selective identification of ions, present in the investigated solution (Karastogianni et al., 2016).

Even though a big diversity of pH-sensitive electrodes is known and widely used for various purposes<sup>1</sup>, the conventional glass electrode (CGE) is the only type of electrode that is used for pH measurement in food research. The CGE is used in a common pH meter as a combination of a working electrode (WE) and a reference electrode (RE) in one glass body that is called a probe. For the safety and convenience of the measurement, the probe can be covered with stainless steel or inert polymeric material (e.g., polyvinylidene fluoride or polyethyleneimine). One such solution is commercialized by Frontmatec (Denmark). The manufacturer offers a [pH probe \(Figure 1\)](#), covered with a protective steel case with a telescopic sleeve. However, since the CGE has such drawbacks as high cost, brittleness, and therefore the possibility to contaminate food samples with dangerous shattered glass, novel materials that could replace the CGE in standard potentiometric pH measurement are investigated.

In 1986, Korkeala et al. (Korkeala et al., 1986) compared several types of glass electrodes when determining the pH of meat samples. The investigated electrodes showed a significant statistical difference in the calculated pH value.

In 2003, Eftekhari (Eftekhari, 2003) fabricated a pH-sensitive electrode by dip-coating an aluminium rod with lead oxide (PbO<sub>2</sub>). The electrode showed a sensitivity of 57.8 mV/pH against the saturated calomel electrode. The author mentions that the electrode was studied in soft drinks and fruit juices with satisfactory results, however, no data is presented in the study. Furthermore, the author indicated that the fabricated electrode is not suitable for pH measurement in complex samples.

---

<sup>1</sup> such as Normal Hydrogen Electrode, quinhydrone electrode, dropping mercury electrode, antimony electrode, etc.



Figure 1. pH\*K21 pH-probe manufactured by Frontmtec, Denmark (the image was taken from [Frontmtec website](#)).

In 2008, Liao and Chou (Liao & Chou, 2008) reported a sputtered ruthenium(IV) oxide ( $\text{RuO}_2$ ) film on a silicon wafer as a solid-state pH-electrode. The electrode showed a sensitivity of 55.6 mV/pH and a difference of 0.14 and 0.50 pH units from the CGE in coke and milk respectively.

In 2015, Manjakkal et al. (Manjakkal et al., 2015) fabricated a binary oxide electrode, based on the screen-printed mixture of  $\text{RuO}_2$  and tin(IV) oxide ( $\text{SnO}_2$ ) on top of alumina ( $\text{Al}_2\text{O}_3$ ) substrate. Authors demonstrated that their  $\text{RuO}_2$ - $\text{SnO}_2$  pH-sensitive electrodes have a sensitivity of 56.5 mV/pH and a pH difference of 0.21 pH units from CGE in lemon juice.

In 2018, Lonsdale et al. (Lonsdale, Shylendra, et al., 2018) presented a solid-state pH sensor that incorporated magnetron-sputtered  $\text{RuO}_2$  as the pH-sensitive material. The sensor showed a linear pH response with a sensitivity of 56.6 mV/pH. The electrode was tested in coke, beer, wine, and juice samples and demonstrated a deviation of less than 0.05 pH units from the CGE.

### 1.1.2 Potentiometric sensors based on polymers

While metals and metal oxides are the most intensively investigated materials for the fabrication of pH-sensors, metal-based sensors based still have the disadvantage of being toxic and not flexible, therefore, limiting the application of such sensors. At present, polymer-based pH sensors are investigated for point-of-care applications (Yoon et al., 2020). Two types of polymer-based pH sensors can be distinguished: (i) metal oxide pH-electrode covered with a protective polymeric membrane, e.g., Nafion<sup>TM</sup> (Lonsdale, Shylendra, et al., 2018; Lonsdale, Wajrak, et al., 2018; K. Xu et al., 2018) and (ii) metal or graphite electrodes covered with a pH-sensitive polymer. Polymer-based sensors are biocompatible, cheap, and flexible, and can be realized on different substrates, including carbon fibre (Yoon et al., 2020), paper (Kawahara et al., 2018), and textiles (Jose et al., 2021; Parilla et al., 2016). Polyaniline (Jose et al., 2021; Lakard et al., 2005, 2007; Yoon et al., 2020) and polypyrrole (Lakard et al., 2005; Mo et al., 2003; Shiu et al., 1999) are the most studied pH-sensitive polymers.

However, only a few papers address the application of the polymer-based pH sensor for measurement in real-life samples. Such an article was written by Upreti et al. (Upreti et al., 2004). Four combinations of polymers were used in that study: tridodecylamine ( $\text{R}_3\text{N}$ ) or octadecyl isonicotinate was mixed with plasticisers bis(2-ethylhexyl) sebacate (DOS) or o-nitrophenyl octyl ether (oNPOE). Among the studied polymer mixtures, only those based on  $\text{R}_3\text{N}$  were suitable for measurement in real-life samples. The fabricated electrodes were tested in milk, 20% cheese emulsion, and 70% cheese emulsion.

The difference in pH measured with R<sub>3</sub>N/DOS electrode from the CGE was equal to 0.05, 0.25, and 0.01 pH units for milk, 20%, and 70% cheese emulsions respectively. For the R<sub>3</sub>N/oNPOE electrode, the pH difference was equal to 0.01, 0.01, and 0.15 pH units for milk, 20% and 70% cheese emulsions respectively.

Another article was published in 2011 by Li et al. (Q. Li et al., 2011). The authors presented an indium tin oxide (ITO)-based electrode modified with electropolymerized bisphenol A. The electrode exhibited a sensitivity of 58.6 mV/pH and was tested in diluted milk and grape juice solutions. The deviation of the pH measured with the fabricated electrode from the CGE did not exceed 0.12 and 0.23 pH units for diluted milk and grape juice respectively.

In 2019, Park et al. (Park et al., 2019) reported a flexible potentiometric pH sensor that incorporated polyaniline as pH-sensitive material. Polyaniline was deposited on a carbon electrode screen-printed on a polyethylene terephthalate (PET) substrate via dilute chemical polymerization. Prior to polyaniline deposition, the carbon and silver inks were screen printed on the PET substrate to create WE and conductive channels respectively. The fabricated electrodes exhibited a sensitivity of 60.4 mV/pH and were tested in milk and on an apple to monitor the spoilage of the sample. The pH values measured with a fabricated electrode during 48 hours of monitoring of milk spoilage were similar to those of the CGE. For the monitoring of apple spoilage, no reference to CGE was performed.

In 2020, Yoon et al. (Yoon et al., 2020) used a polyaniline-coated electrode as a WE. The substrate was fabricated by coating carbon fibre with a self-healing polymer. The same materials were also used for the fabrication of the RE, with the only difference being that the RE was covered with Ag|AgCl instead of polyaniline. The electrode exhibited a pH sensitivity of 58.1 mV/pH and was tested on real-life human fluids and fruits. Unfortunately, the authors did not present the numerical values of measured pH.

### 1.1.3 Potentiometric biosensors

Electrochemical biosensors can be described as devices, in which a biolayer is used to identify the specific ions in the sample solution. The biolayer can be represented by various materials, including amino acids, enzymes, bacteria, yeast, DNA, antigens, etc. (Vargas-Bernal et al., 2012) (Figure 2). The biolayer responds directly to the presence of a detectable component and generates a signal, depending on the concentration of that component. The main drawbacks of the utilization of biosensors are related to their short stability and shelf-life (Panjan et al., 2017; Shaver & Arroyo-Currás, 2022).

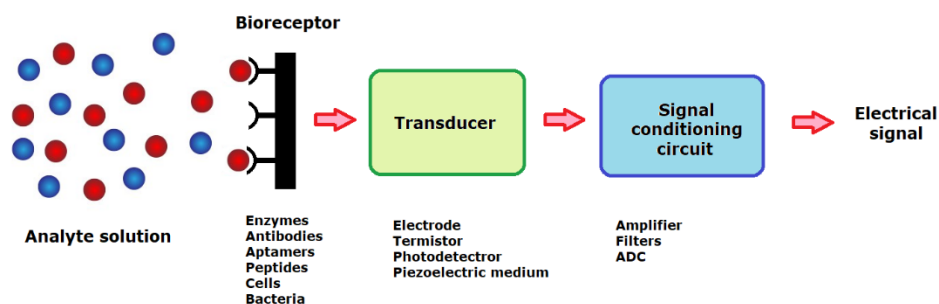


Figure 2. Schematic representation of a biosensor. Interaction of the biolayer with the analyte solution initiate a signal that is later converted to an electrical signal.

In 2018 Zuaznabar-Gardona and Frago (Zuaznabar-Gardona & Frago, 2018) presented a potentiometric pH sensor based on a polydopamine pH-sensitive layer. Dopamine film was electro- and self-polymerized on a glassy carbon electrode that contained a carbon nano-onion layer. The fabricated electrodes exhibited sensitivities of 58.3 and 60.1 mV/pH for electro- and self-polymerized dopamine respectively. In real-life samples, the deviation of the pH measured with the fabricated electrodes and the CGE was 0.08, 0.22, and 0.16 pH units for vinegar, pineapple juice, and milk respectively.

In 2020, Hu et al. (Hu et al., 2020) reported a potentiometric pH sensor based on a graphite electrode modified with tryptophan residues by cyclic voltammetry. Tryptophan was used as pH-sensitive material due to dependency on pH of the tryptophan oxidation. Tryptophan is one of the most commonly oxidized residues of aromatic amino acids in proteins. The sensor exhibited a sensitivity of 52 mV/pH and low deviation from CGE when used in milk and coke (below 0.15 pH units).

#### **1.1.4 Systems consisting of novel working and reference electrodes**

The inability of the conventional glass electrode to work in complex media (Eftekhari, 2003; Upreti et al., 2004) cannot be overcome by simply replacing the pH-sensitive working electrode; attention also should be paid to the reference electrode. The reference electrode is known to suffer from the potential drift and inconsistency of reading when used in viscous samples (Amemiya et al., 2007; Mugica et al., 2022). Therefore, alternatives to the conventional glass working electrode are investigated together with the alternatives to the glass Ag|AgCl reference electrode.

In 2017, Li et al. (Q. Li et al., 2017) described their RE electrode based on Ti/Au/Ag/AgCl ion-selective field-effect transistor (ISFET). The electrode was modified with a porous poly(vinyl butyral) membrane and was used together with a poly(ethylene terephthalate)-covered indium tin oxide as a WE. The potentiometric system showed a pH difference exceeding 0.50 pH units in coke, orange juice, beer, milk, and other studied samples.

In 2018, Xu et al. (K. Xu et al., 2018) incorporated an antimony film on top of a copper substrate as a WE together with a Ag|AgCl RE onto a printed circuit board. The WE was additionally modified with a Nafion membrane and the RE was modified with a graphene-chitosan membrane. This potentiometric system showed a pH sensitivity of 54.5 mV/pH and a pH difference from CGE of 0.19 and 0.11 pH units for coke and vinegar respectively.

Also in 2018, Lonsdale et al. (Lonsdale, Wajrak, et al., 2018) incorporated a modification of their previously reported RuO<sub>2</sub>-based pH-sensitive electrode and a pH-sensor. The working electrode was fabricated by covering the magnetron sputtered RuO<sub>2</sub> pH-sensitive electrode with protective layers of magnetron-sputtered Ta<sub>2</sub>O<sub>5</sub> and drop-casted Nafion. The RE was fabricated by modifying the WE with an acrylic well filled with PVB-SiO<sub>2</sub> junction material. The fabricated WE exhibited a sensitivity of 55.3 mV/pH and the pH-sensor was tested in real-life beverages: coke, sports drink, vinegar, several beer samples, and 2% fat milk. The sensor showed excellent performance with the measured pH value deviation of less than 0.08 pH units from the CGE.

In 2022, Mu et al. (Mu et al., 2022) reported a hydrogel-based flexible pH system. The sensor consisted of ITO as WE directly laser-scribed on a PET substrate, and an Ag|AgCl RE screen-printed on an ITO/PET substrate. The WE and RE electrodes were

covered with a hydrogel consisting of sodium carboxymethylcellulose and calcium alginate. The reported sensor showed a sensitivity of 49 mV/pH and was used to detect total volatile nitrogen (TVB-N) that is highly correlated to fish spoilage (Kyra et al., 1997; Kyra & Lougovois, 2002). Since the components of volatile organics ionize the hydrogel,  $\text{OH}^-$  is released and a change in pH is observed. The sensors were successfully used to identify the end of the shelf life of tilapia fish.

### 1.1.5 Conclusion

At present, potentiometric sensors for pH measurement remain the most investigated alternative to the CGE not only from the point of general application but from the point of application in food samples that are complex matrices, in which new alternative sensors cease to work. The development of new potentiometric sensors has a big advantage over other sensors: their work is based on the same principles as the CGE and they allow to use the same electronic devices with the new electrodes as used with the CGE, therefore making the transition to the use of the newly developed pH electrodes less expensive and more probable.

Over the years, potentiometric pH sensors were shown to have excellent pH sensitivity, fast response and accurate pH measurement in aqueous samples. However, most of the research in the field of pH sensors focuses on the materials, fabrication and application of the sensors in aqueous samples and does not address applicability to real-life samples. Much more research is needed to be conducted to make sure that the proposed alternative pH electrodes will prove themselves useful in real-life applications, including food products that are one of the most difficult to work with.

## 1.2 Principles of potentiometric pH measurement

The potentiometric pH measurement requires the construction of an electrochemical cell that primarily consists of (i) a measuring device – a potentiostat, a voltmeter, a galvanometer, etc., (ii) a working electrode (WE) – an electrode where the analytical reaction is taking place and (iii) a reference electrode (RE) that provides a stable and well-known potential (Figure 3).

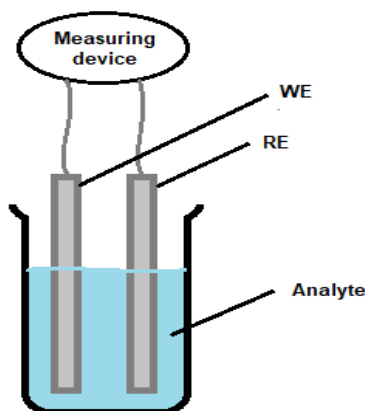


Figure 3. Schematic representation of an electrochemical cell.



The electrical characteristic of an electrochemical cell is electrochemical potential<sup>2</sup> (potential). The potential of an electrochemical cell (E) is determined as the difference in potentials of the two half-reactions happening on the WE and RE:

$$E = E_{WE} - E_{RE} \quad (1)$$

where  $E_{WE}$  is the electrochemical potential of the reaction, taking place on the WE, V;  $E_{RE}$  is the electrochemical potential of the reaction, taking place on the RE, V.

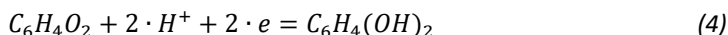
If  $E > 0$ , the reaction proceeds spontaneously, and if  $E < 0$ , the reaction proceeds only with the supply of energy from an external current source. Furthermore, if the RE is grounded, its potential is equal to zero, and the potential of the electrochemical cell is equal to the potential of the WE. This allows determining the activities of the ions participating in the electrochemical reaction on the working electrode according to the Nernst equation (Amemiya et al., 2007):

$$x \cdot Ox + n \cdot e \rightleftharpoons y \cdot Red \quad (2)$$

$$E_{Ox/Red} = E_{Ox/Red}^0 + \frac{R \cdot T}{n \cdot F} \ln \frac{[Red]^y}{[Ox]^x} \quad (3)$$

where **Ox** is the oxidized form of the electrode's material, **Red** is the reduced form of the electrode's material; **n** is the number of electrons transferred in the balanced Red/Ox equation; x and y are reaction coefficients;  $E_{Ox/Red}$  is the electrochemical potential of the reaction (2), V;  $E_{Ox/Red}^0$  is the standard electrochemical potential<sup>3</sup>, V; **R** is the universal gas constant, 8.314 J/mol·K; **T** is the temperature, K; **F** is the Faraday constant, 96485 J; **[Ox]** and **[Red]** are the activities of oxidized and reduced forms respectively.

For example, the reaction taking place on the quinhydrone WE is described by the following equations:



$$E_{C_6H_4O_2/C_6H_4(OH)_2} = E_{C_6H_4O_2/C_6H_4(OH)_2}^0 + \frac{R \cdot T}{2 \cdot F} \ln \frac{[C_6H_4O_2] \cdot [H^+]^2}{[C_6H_4(OH)_2]} \quad (5)$$

where  $C_6H_4O_2$  and  $C_6H_4(OH)_2$  are quinone and quinhydrone respectively.

When substituting the constraints and switching from natural logarithm to decimal logarithm, equation (5) takes the form of (6):

$$E_{C_6H_4O_2/C_6H_4(OH)_2} = E_{C_6H_4O_2/C_6H_4(OH)_2}^0 + 0.059 \cdot \ln [H^+] \quad (6)$$

When substituting  $-\ln[H^+]$  with pH, equation (6) takes the form of (7)

$$E_{C_6H_4O_2/C_6H_4(OH)_2} = E_{C_6H_4O_2/C_6H_4(OH)_2}^0 - 0.059 \cdot \text{pH} \quad (7)$$

Or in general, for any pH-sensitive electrode

$$E_{Ox/Red} = E_{Ox/Red}^0 - 0.059 \cdot \text{pH} \quad (8)$$

Equation (8) allows determining the pH value of the sample by determining the electrochemical potential of the electrode in the sample solution. The value by which pH is multiplied (0.059 V for equation (8)) is called the sensitivity of the electrode. The value of 0.059 V (or, more commonly, 59 mV) is called Nernstian sensitivity and is considered the theoretical sensitivity of an electrode.

<sup>2</sup> Electrochemical potential of an electrochemical cell is also sometimes referred to as electromotive force (Emf).

<sup>3</sup> Standard potential is a measure of the individual potential of a reversible electrode (in equilibrium) in a standard state (concentration 1 mol l<sup>-1</sup>, pressure 1 atm and temperature 25 °C).

### 1.3 Metal oxides for pH sensing

The idea of utilizing metal oxides for pH sensing was first suggested in 1947 by Perley and Godshalk (Perley & Godshalk, 1947) and has been investigated since 1982 (Katsube et al., 1982).

According to Fog and Buck, there are several possible mechanisms of the pH sensitivity of metal oxides (Fog, A.; Buck, 1984):

- 1 Ion exchange in the surface layer;
- 2 Equilibrium between the two oxidizing forms of the metal;
- 3 Hydrogen intercalation;
- 4 Oxygen intercalation;
- 5 Steady-speed corrosion of the material.

The authors also indicate that the most probable mechanism for pH sensing is oxygen intercalation: due to non-stoichiometric oxygen content in the oxides, the activity of oxygen in the solid phase should also be considered when calculating the electrode potential.

However, in 1998 Mihell and Atkinson (Mihell & Atkinson, 1998) studied the pH-response of planar RuO<sub>2</sub> electrodes and came to a conclusion that pH response of the electrode is due to the ionic exchange in the surface groups. When metal oxide contacts with an aqueous solution, the dissociative adsorption of water on the surface of the metal oxide leads to the formation of hydroxide groups. Authors attributed the pH-response of the RuO<sub>2</sub> electrode to the interaction between protons and hydroxide groups on the surface of metal oxide (Mihell & Atkinson, 1998).

According to Gláb et al. (Gláb et al., 1989), a metal oxide should satisfy the following criteria:

- ✓ Should be stable;
- ✓ Should not react with interfering ions in all the solutions over a wide pH range;
- ✓ Metal oxide should be reproducible;
- ✓ Should be able to participate in electrode reaction.

Other requirements to the pH electrodes come from the application of the electrodes: in some applications, such as environmental monitoring in food processing, the toxicity of the materials plays key role. For biomedical application, the flexibility and bendability of the sensors can be important. In general, it is desired to have (i) excellent pH-sensitivity and selectivity, (ii) a cost-effective fabrication road and (iii) a straightforward way of integration of sensors into existing applications (Manjakkal et al., 2020).

Among the metal oxides, RuO<sub>2</sub> demonstrates the most favourable characteristics: Nernstian sensitivity, fast response and low drift rate (Figure 4). Comparison of the pH electrodes based on RuO<sub>2</sub> to pH electrodes based on other metal oxides reveals that RuO<sub>2</sub> electrodes have excellent performance, however, the biggest disadvantage is their cost (Manjakkal et al., 2020).

### 1.4 Ruthenium(IV) oxide

Ruthenium oxide (IV) is the most stable oxygen-containing compound of ruthenium (Drozdzov et al., 2007). Ruthenium oxide (IV) is a blue-black powder with a rutile structure ( $a=4.51$ ;  $c=3.11$  Å) (Figure 5) and a melting point of around 1200 °C (Remy, 1956).

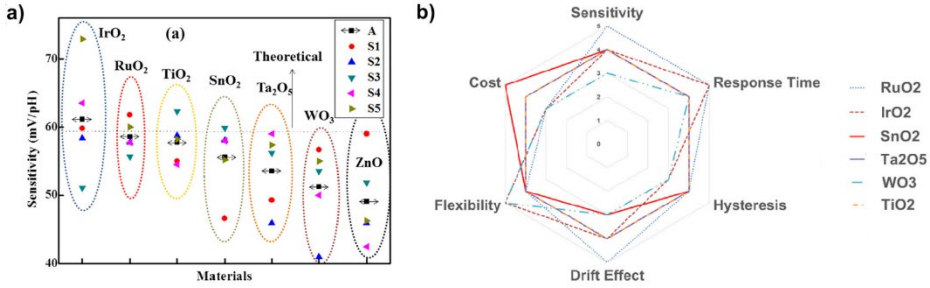


Figure 4. The sensitivity of the pH sensor depends on the material it is made from and the method utilized to fabricate the sensors. Among the investigated metal oxides (a), RuO<sub>2</sub> showed the sensitivity closest to the theoretical Nernstian response (horizontal grey dotted line). Sensors from different batches are indicated as S1, S2, S3, S4, and S5, while A is the average sensitivity. The overall performance of RuO<sub>2</sub> (b) is also exceeding other investigated oxides. Reproduced from Manjakkal et al., 2020.

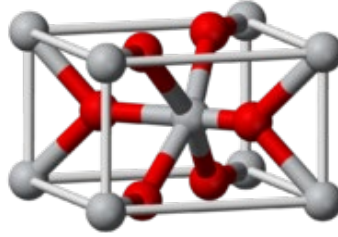
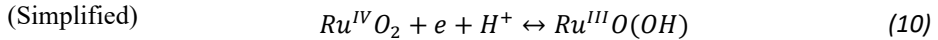
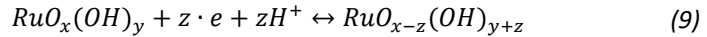


Figure 5. Structure of ruthenium(IV) oxide. Reproduced from Wikipedia.

The electrochemical response of the RuO<sub>2</sub> to the pH change can be described by the equations (9) and (10) (Lonsdale, 2018):



The Nernst equation for this process takes the form of (11)

$$E = E^0 + \frac{R \cdot T}{z \cdot F} \cdot \ln \frac{a_{Ru^{III}}}{a_{Ru^{IV}} \cdot a_{H^+}} \quad (11)$$

Considering that the values of metals activities approximate 1 in solid state and substituting the constants, (11) takes the form of (8).

The fabrication method is known to influence the properties of the RuO<sub>2</sub> electrodes (Table 1). Among the various fabrication methods proposed for electrodes based on metal oxides, the most convenient is screen printing (Manjakkal et al., 2020). From Figure 6a, it can be seen that screen printing allowed to get more reproducible sensitivity of the fabricated electrodes with the mean sensitivity being closer to the theoretical value of 59 mV/pH. The screen-printing technique allows producing electrodes of different sizes and shapes, fast and at a low cost (Zhang et al., 2021). Furthermore, utilizing screen printing approach it is possible to fabricate electrodes with small hysteresis and drift without sacrificing sensitivity and life time of the electrodes (Figure 6b). The printing is commonly described as follows: a roller moving across the screen stencil forces ink or other printable materials past the threads of the woven mesh that supports an ink-blocking stencil to achieve a specifically patterned layer of ink on a suitable substrate. Different woven meshes are prepared to print different parts of the electrode.

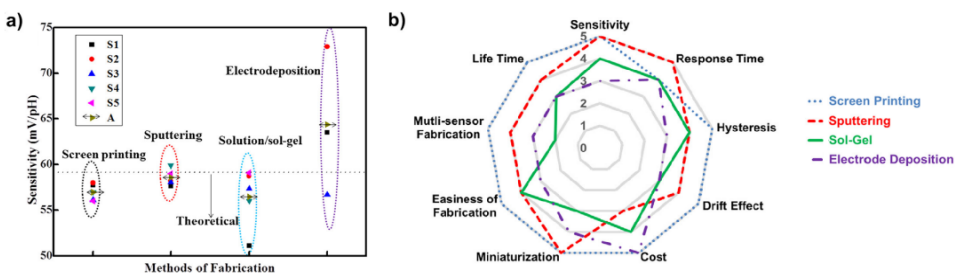


Figure 6. A comparison of the fabrication approaches has demonstrated that sputtering allows reproducibly fabricate electrodes with the sensitivity closest to the theoretical Nernstian response (a). However, even though screen printing is the second best, it has several advantages over the sputtering approach: lower cost and compatibility with mass-production, longer lifetime and compatibility with the fabrication of multi-sensors (b). Sensors from different batches (a) are indicated as S1, S2, S3, S4, and S5, while A is average sensitivity. Reproduced from Manjakkal et al., 2020.

The printing proceeds as a layer-by-layer deposition, where each layer undergoes solidification by thermal treatment. After printing of all the required layers, the surface is covered with an insulative coating (M. Li et al., 2012; Metters et al., 2011).

## 1.5 Nafion membrane as a protective layer in pH-sensitive electrodes

Nafion is a perfluorinated sulfonic acid (PFSA) ionomer that consists of a fluorocarbon backbone (hydrophobic) and a randomly tethered side chain with a terminal sulphur oxoacid group (Figure 7). Nafion was developed by Walter Grot for Dupont de Nemours (Wilmington, Delaware, USA) in the late 1960s and was the first commercial PFSA ionomer (Grot, 1982). Nowadays, Nafion is the most widely used PFSA ionomer. Nafion is used in the manufacture of fuel cells as a proton exchange membrane (Peighambardoust et al., 2010; Selim et al., 2022) and fabrication of electrochemical sensors as a protective membrane (Lonsdale, Wajrak, et al., 2017; Senthil Kumar et al., 2022) or for detection of ketones (Lucero et al., 2022).

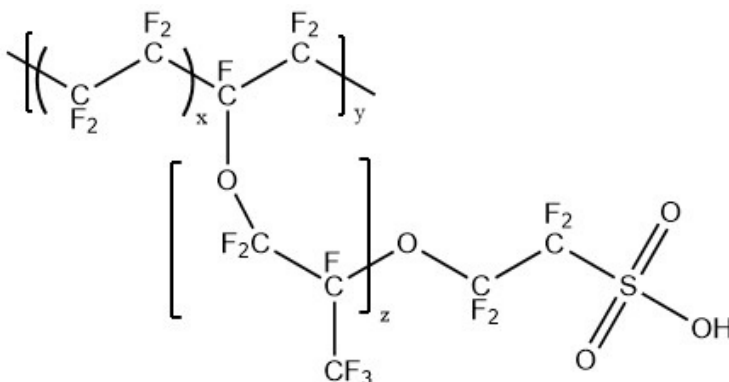


Figure 7. Chemical structure of Nafion.

Similarly to other PFSA ionomers, Nafion has a unique property of enhanced ion and solvent permittivity: the difference in hydrophilic nature of the fluorocarbon backbone and terminal sulphur oxoacid group allows phase separation that increases with the amount of solvent volume.

The permittivity towards  $H^+$  ions is explained by the Grotguss mechanism (Agmon, 1995): diffusion of protons inside the water network via the exchange of bonded  $H^+$  between neighbouring water molecules. During the hydration process, the water molecules ionize the sulfonic acid groups to form  $SO_3^- \cdot (H_3O)^+$  ions (Kusoglu & Weber, 2017). However, a further increase in the number of water molecules within the polymer network ( $\lambda^4 \approx 1-2$ ) leads to the dissociation of  $H^+$  from the  $SO_3^-$  groups and the formation of complex ions with water (e.g.,  $H_9O_4^+$ ,  $H_5O_2^+$ ). Hydrophilic domains enhance phase separation formed in the polymer network. When  $\lambda > 2$ , domains form an interconnected network, allowing the transport of ions and water molecules through the polymer network. Absorption of water continues till  $\lambda \approx 5-6$  when a solvation shell of water molecules is formed around each  $SO_3^- H^+$  (Kusoglu & Weber, 2017). This solvation shells of water together with the interconnected water network allow for excellent proton conductivity of Nafion.

Proton conductivity of the Nafion membrane is of key importance in electrochemical electrodes sensitive to cations: since the Nafion membrane consists of negatively charged groups, only small positive cations can travel through the polymer network (Kusoglu & Weber, 2017). This property of the Nafion membrane is of great importance for pH measurement in real-life food samples. The majority of food samples contain proteins and fats that interfere with pH measurement due to the contamination of the sensor. Nevertheless, if an electrode is covered with a Nafion membrane, the proteins in food samples that carry negative charges of  $\approx -15 \dots -30$  mV (Tan et al., 2014) cannot pass through the Nafion membrane due to the electrostatic repulsion (Figure 8).

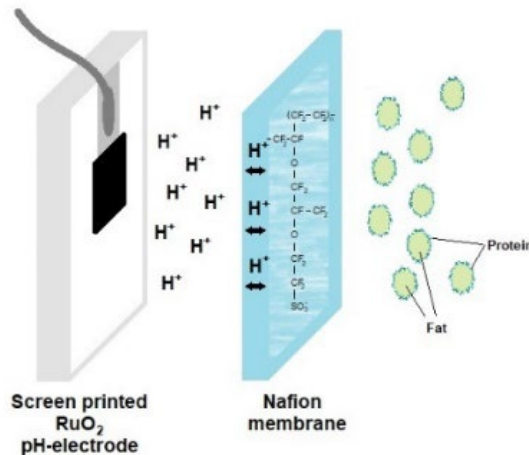


Figure 8. Schematic representation of the application of the Nafion membrane. Reproduced from **Publication II**.

<sup>4</sup>  $\lambda$  is the water content that is defined as the number of water molecules per mole of sulfonic-acid groups.

Table 1. Fabrication method and material and properties of previously reported RuO<sub>2</sub> pH-electrodes. Reproduced from **Publication I**.

Deposition method	Electrode sensitive material	Substrate	Sensitivity, mV/pH	E <sup>0</sup> , mV	R <sup>2</sup>	pH range	Response time, s	T, °C	Hysteresis, mV	Drift, mV/h	Reference
Electro-chemical deposition	RuO <sub>2</sub>	Au wire	59.3	521	N/A	2.0 - 12.0	N/A	N/A	N/A	N/A	(Pásztor et al., 1993)
		Au disk	60.5	N/A	0.999	2.0 – 11.0	7	N/A	N/A	N/A	(Shim et al., 2012)
		Pt	56.2	596	0.999	4.0 - 10.0	N/A	37.5	N/A	N/A	(Mingels et al., 2019)
		Pt-Ti	59.3	609	0.999	4.0 - 10.0	N/A	37.5	N/A	N/A	(Mingels et al., 2019)
Screen-printing	RuO <sub>2</sub>	Polyester foil	51.2	606	N/A	2.0 – 10.0	N/A	N/A	N/A	N/A	(Koncki & Mascini, 1997)
		Al <sub>2</sub> O <sub>3</sub>	56	N/A	N/A	2.0 – 12.0	120	N/A	N/A	N/A	(Manjakkal, Zaraska, et al., 2016)
	RuO <sub>2</sub> -Ta <sub>2</sub> O <sub>5</sub>	Al <sub>2</sub> O <sub>3</sub>	68.2	N/A	0.987	2.0 – 12.0	15	N/A	10	N/A	(Manjakkal, Zaraska, et al., 2016)
	RuO <sub>2</sub> -Ta <sub>2</sub> O <sub>5</sub>	Al <sub>2</sub> O <sub>3</sub>	56	N/A	N/A	2.0 – 12.0	15	N/A	N/A	N/A	(Manjakkal, Cvejic, et al., 2016)
	RuO <sub>2</sub> -SnO <sub>2</sub>	Al <sub>2</sub> O <sub>3</sub>	56.5	631	0.998	2.0 – 12.0	9	N/A	7	N/A	(Manjakkal et al., 2015)
	RuO <sub>2</sub> -Cu <sub>2</sub> O	Al <sub>2</sub> O <sub>3</sub>	47.4	N/A	N/A	2.0 – 13.0	N/A	21	N/A	N/A	(Zhuiykov, Kats, et al., 2011)
	RuO <sub>2</sub> -La <sub>2</sub> O <sub>3</sub>	Al <sub>2</sub> O <sub>3</sub>	49.3	N/A	N/A	2.0 – 12.0	N/A	19	N/A	N/A	(Zhuiykov, Marney, et al., 2011)
	RuO <sub>2</sub> -TiO <sub>2</sub>	Al <sub>2</sub> O <sub>3</sub>	56.6	630	0.999	2.0 – 11.0	15	N/A	5	N/A	(Manjakkal et al., 2014)
RuO <sub>2</sub> -Pt	Al <sub>2</sub> O <sub>3</sub> -Pt	58	640	N/A	2.0 – 13.0	2-Jan	23	~ 0	1.5	(Zhuiykov, 2009)	
Sol-gel Pechini	RuO <sub>2</sub> -CNT	Au, Co, steel	63.1	647	1	2.0 – 12.0	50	N/A	N/A	N/A	(Kahram et al., 2014)
	RuO <sub>2</sub> -TiO <sub>2</sub>	Ti	56	N/A	0.998	2.0 – 12.0	N/A	25	N/A	N/A	(Pocrička et al., 2006)
Radio-Frequency Magnetron Sputtering	RuO <sub>2</sub>	Pt wire	60	913	N/A	2.0 – 12.0	90	25	30	3	(McMurray et al., 1995)
		Ordered m/p carbon	57.8	598	0.999	2.0 – 12.0	180	22	3.14	19	(Lonsdale, Wajrak, et al., 2017)
			58.4	670	0.999	4.0 – 10.0	30	22	1.13	5	(Lonsdale, Maurya, et al., 2017)
		Carbon	59.2	800	1	4.0 – 10.0	25	22	5.44	20.5	(Lonsdale, Maurya, et al., 2017)
		Pt	58.6	925	0.999	4.0 – 10.0	20	22	6.45	23.4	(Lonsdale, Maurya, et al., 2017)
		Si	55.6	N/A	N/A	1.0 – 13.0	<1	N/A	4.36	0.38	(Liao & Chou, 2008)
		Si	51.7	N/A	0.978	2.0 – 10.0	N/A	N/A	N/A	N/A	(Yao et al., 2020)
		Si	55.8	N/A	0.998	2.0 – 10.0	N/A	N/A	N/A	N/A	(Yao et al., 2020)
	Si	56	N/A	N/A	1.0 - 12.0	N/A	N/A	N/A	N/A	(Chou et al., 2005)	
	RuO <sub>2</sub>	Al <sub>2</sub> O <sub>3</sub>	73.8	N/A	0.998	4.0 - 10.0	3	22	~ 5	N/A	(Sardarinejad et al., 2015)
		Al <sub>2</sub> O <sub>3</sub>	58.8	N/A	0.999	2.0 – 12.0	30	22	1.3	2.9	(Lonsdale, Wajrak, et al., 2018)
RuO <sub>2</sub> -Ta <sub>2</sub> O <sub>5</sub> -Nafion	Al <sub>2</sub> O <sub>3</sub>	55.3	288	1	2.0 – 12.0	136	22	0.7	7.2	(Lonsdale, Wajrak, et al., 2018)	
RuO <sub>2</sub> -CNT	Ta	55.5	643	1	2.0 – 12.0	40	25	10.2	~ 3	(B. Xu & Zhang, 2010)	

## **2 Aims of the Thesis**

The main objective of the thesis was to fabricate a potentiometric pH electrode based on ruthenium(IV) oxide for pH measurement in food samples.

To reach the aim of the thesis, the workflow was separated into the following steps:

- Aim 1 Find the fabrication parameters for the screen printing of ruthenium(IV) oxide pH electrodes.
- Aim 2 Find fabrication parameters for the deposition of the protective Nafion membrane. Investigate the properties of the ruthenium(IV) oxide pH electrodes covered with the Nafion membrane.
- Aim 3 Investigate the performance of the fabricated electrodes in food samples and during food processing.

### 3 Materials and Methods

Detailed description of the materials in methods can be found in the corresponding publications. This section is dedicated to briefly introducing utilized experimental procedures.

#### 3.1 Fabrication of the RuO<sub>2</sub> electrodes (Publications I-III)

Ruthenium(IV) oxide electrodes were fabricated by screen printing technique that consisted of 4 main steps (Figure 9a): (i) screen printing of conductive layer (Ag layer), (ii) screen printing of pH-sensitive layer (RuO<sub>2</sub> layer), (iii) attachment of copper wire to later connect an electrode to a measuring device, and (iv) insulating the electrical contact with silicone-based resin. The dimensions of the fabricated RuO<sub>2</sub> electrodes are presented in Figure 9b,c. Furthermore, in *Publication I* the influence of the sintering temperature on the performance of the RuO<sub>2</sub> electrodes was investigated. The properties of the fabricated RuO<sub>2</sub> electrodes are discussed in *Publications I, II, IV* and *V*.

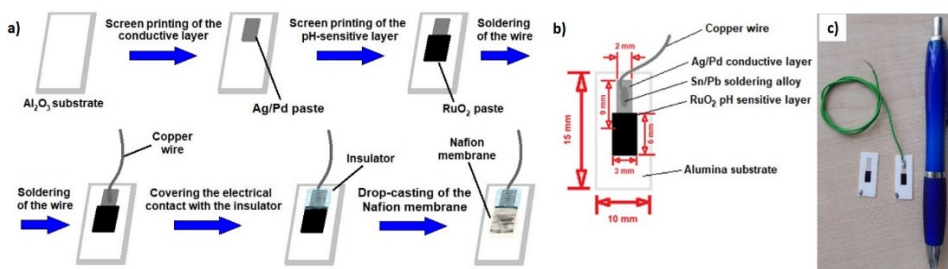


Figure 9. The RuO<sub>2</sub> electrodes were fabricated by screen printing of a conductive layer of Ag/Pd on an Al<sub>2</sub>O<sub>3</sub> substrate and consequently printing of the pH-sensitive layer of RuO<sub>2</sub>. (a) After the thermal treatment of both printed layers, a copper wire was attached to the Ag/Pd layer via soldering with a Pb/Sn alloy. For the fabrication of the RuO<sub>2</sub>-Nf electrode, the RuO<sub>2</sub> part of the RuO<sub>2</sub> electrode was covered with Nafion membrane by drop-casting technique. The fabricated electrodes had small dimensions (b). A photograph of the fabricated electrodes is presented in figure (c) for the visualization of the fabricated electrodes. Adopted from *Publication III*.

#### 3.2 Modification of the fabricated electrodes with Nafion membrane (Publication II) and investigation of the properties (Publications II, IV-VII)

In *Publication II* the conditions and parameters of the deposition of the Nafion membrane were investigated. The following conditions of the deposition were evaluated: (i) concentration of Nafion solution, (ii) number of Nafion layers, (iii) the time between layers deposition and (iv) drying temperature. The performance of the modified electrodes was evaluated on the basis of (i) membrane morphology, (ii) performance in milk, (iii) electrochemical characteristics (sensitivity, hysteresis and drift) and (iv) stability over long period of time. In *Publication VI*, the reusability of the RuO<sub>2</sub> electrodes after Nafion membrane deterioration was investigated and in *Publication VII* the cleaning procedure for the fabricated electrodes is discussed.leaning approach is one of the most important steps in accurate pH measurement. Usage of the electrode that was not properly cleaned can lead not only to false readings, but also the cross-contamination of



the next sample and possible destruction of the electrode in use. Furthermore, in *Publication V* the reversibility of thermal treatment of the Nafion membrane was investigated.

### 3.3 Electrochemical characterization of the fabricated electrodes

#### 3.3.1 Setup

The setup for the work with the fabricated RuO<sub>2</sub>-based electrodes consisted of the units presented in [Table 2](#) and [Figure 10](#). To evaluate the performance of the fabricated electrode, several parameters were evaluated: sensitivity (or the basis of the Nernst equation) and linearity (R<sup>2</sup>), hysteresis and drift rate.

*Table 2. Electrochemical setup used in this work.*

Unit	Electrode and equipment used	Function
Working electrode	RuO <sub>2</sub> , RuO <sub>2</sub> -Nf, RuO <sub>2</sub> -CuO, RuO <sub>2</sub> -CuO-Nf electrodes	pH-sensitive electrode
	Standard glass ion-selective Ag AgCl KCl electrode (HI1053P, Hanna Instruments, USA)	Accurate pH measurement
Reference electrode	Standard glass ion-selective Ag AgCl KCl electrode (HI1053P, Hanna Instruments, USA)	Stable potential readings
Measuring device	Data Acquisition (DAQ) device, USB-6259, National Instruments, USA	Recording of the data
Power supply	High-performance digital power supply (E3631A, Agilent, USA) with an interference-free input voltage of 12 V	Powering up the measuring device
Software	LabVIEW program (National Instruments, USA)	Registering the data

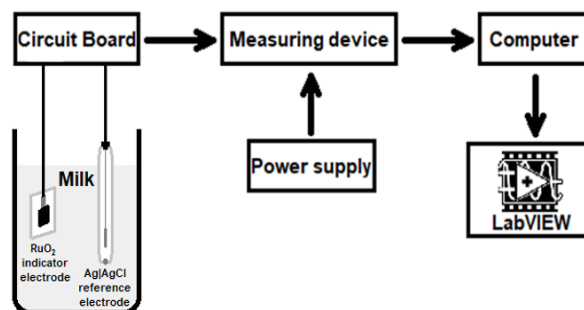


*Figure 10. Schematic representation of the setup used in this work. Reproduced from **Publication III**.*

#### 3.3.2 Electrochemical characteristics

##### Sensitivity

As mentioned in section 1.2, sensitivity rises from the Nernst equation and is used to evaluate the performance of an electrode and to calculate the pH of the sample from the measured potential value. Sensitivity is determined by checking the response of an electrode to pH change. For that, several buffer solutions of different pH are prepared

and the potential of an electrode in these solutions is recorded. In this work, citric, phosphate and carbonate buffers were prepared in pH ranges 3-6, 7-8 and 9.2-11.8 respectively. The buffers were prepared according to (Dawson, P.; Elliott, D.; Elliott, A.; Johns, 1991). The pH of the buffers was determined with a conventional pH meter (Seven2Go Advanced Single-Channel Portable pH Meter, Mettler Toledo, Switzerland).

The theoretical (expected) response of the pH sensor depends on the temperature and at a temperature of 21 °C should be equal to 58.4 mV/pH (Table 3). However, the sensitivity of printed electrodes most of the time is different from the theoretical response and depends not only on the materials used for the fabrication of the electrode but also on the fabrication methods and conditions (Kurzweil, 2009; Manjakkal et al., 2020; Zhuiykov, 2012).

Table 3. Theoretical sensitivity at common room temperatures.

T, °C	Theoretical sensitivity, mV/pH	T, °C	Theoretical sensitivity, mV/pH	T, °C	Theoretical sensitivity, mV/pH
16	57.4	21	58.4	26	59.4
17	57.6	22	58.6	27	59.6
18	57.8	23	58.8	28	59.8
19	58.0	24	59.0	29	60.0
20	58.2	25	59.2	30	60.2

The sensitivity [mV/pH],  $E^0$  [mV] and linearity of the response ( $R^2$ ) of the fabricated electrodes were determined by measuring the electrochemical potential in pH buffers and plotting the measured electrochemical potential as a function of the pH (Figure 11). The value of the potential was taken 90 seconds after immersing the electrode into a solution to let the electrode reach stable potential readings). The values of sensitivity and  $E^0$  were determined from the linear equation calculated from the least squares regression.

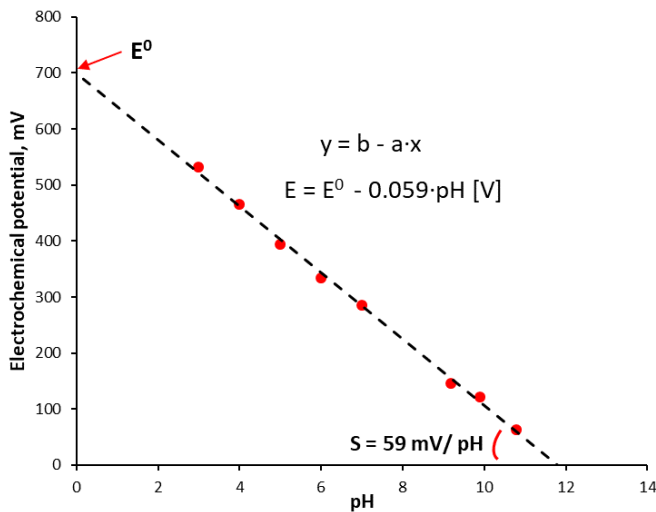


Figure 11. An example of a pH-electrode calibration curve.

## Hysteresis

Hysteresis [mV] is the so-called 'memory effect' of an electrode and is used to describe the impact of previous measurements on the current one (Figure 12). Hysteresis is related to the composition of the double layer on the surface of an electrode and the changes happening in the double layer when an electrode is exposed to solutions of different pH. The pH measurement loop is known to impact the hysteresis of pH electrodes fabricated from metal oxides (Manjakkal et al., 2020). Hysteresis of the fabricated electrodes was determined by measuring the pH of the buffers cyclically: the electrodes were exposed to pH buffer solutions from pH 3 to 7 and back to 3 (3–5–7–5–3) and from pH 11 to 7 and back to 11 (11–9–7–9–11) to evaluate acidic and basic hysteresis respectively. After submerging a fabricated electrode into a buffer solution, the electrochemical potential was recorded for 5 minutes and the value of hysteresis was determined by comparing the potential at pH 3. The electrode was rinsed with distilled water in between the measurement in the buffer solutions.

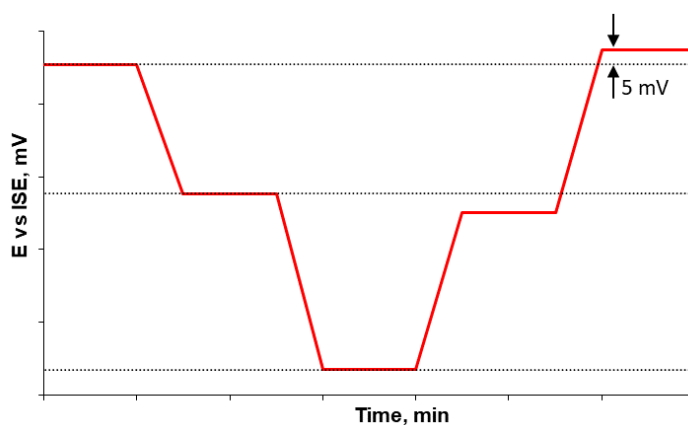


Figure 12. An example of a hysteresis graph.

## Drift

Drift [mV/h] of an electrode is a change of the potential of an electrode with time. Drift can be used to determine the reliability of an electrode and its applicability for continuous measurement. The drift was determined by the method of the slope of the line of line-of-best-fit after monitoring the potential of an electrode continuously for 2 hours by calculating the change of the potential in 1 hour period.

## Cross-sensitivity

Solid-state electrodes designed to measure pH can sometimes be cross-sensitive to other ions in the sample (Figure 13) (Manjakkal et al., 2015; Manjakkal, Zaraska, et al., 2016). Therefore, the sensitivity of the fabricated RuO<sub>2</sub>-Nf electrodes was evaluated in the presence of interfering ions. Change of the sensitivity of the fabricated electrodes was evaluated in the presence of chlorides of common cations – LiCl, KCl, NaCl, and NH<sub>4</sub>Cl. For that, the sensitivity of the fabricated electrodes was first measured in buffer solutions as described in section 3.3.2 and then in the same buffer with the addition of the above-mentioned compound (the concentration of the compound was 0.1 M).

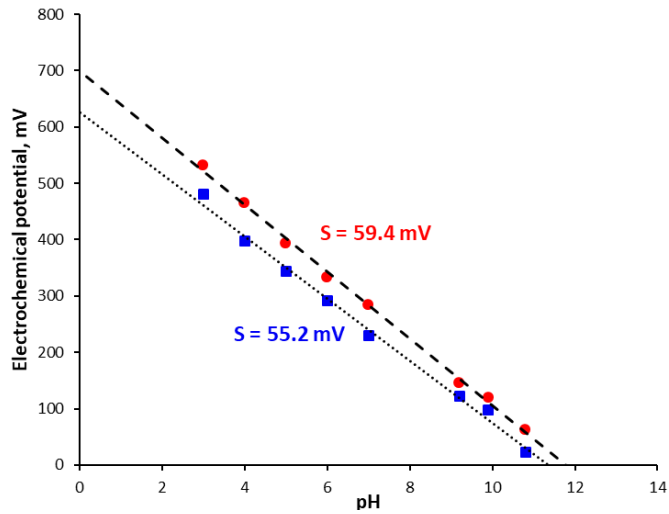


Figure 13. An example of the sensitivity of the  $\text{RuO}_2$  electrode in the absence (red) and in the presence of interfering ions (blue).

### 3.4 Measurement in real-life samples

In *Publication III*, the performance of the  $\text{RuO}_2\text{-Nf}$  electrodes in food samples was investigated. Among others, pH measurement in dairy products was conducted. The electrodes were pre-calibrated by two-point calibrating procedure and then used to measure pH of a dairy sample. The performance of the fabricated electrode was evaluated based on formula (12). All the measurements were made in triplicate for 2 electrodes.

$$pH_{\text{difference}} = pH_{\text{fabricated}} - pH_{\text{CGE}} \quad (12)$$

Furthermore, continuous measurement of pH change during milk coagulation was performed. For that, first, continuous measurement in milk sample was performed over a period of 1 hour and then the electrode was cleaned and used for pH measurement during milk coagulation. Coagulation of milk was shown to happen during first 5 minutes of the experiment. The pH change was monitored for 35 minutes. The measurement was conducted for 2 electrodes in parallel.

## 4 Results and Discussion

### 4.1 Fabrication parameters for the screen printing of the RuO<sub>2</sub> pH electrodes (Publications I and II)

Sintering temperature is known to impact the properties of the solid-state electrodes fabricated from metal oxides: higher sintering temperatures lead to improved crystallinity, increased density and lower porosity of the fabricated layer, therefore, forming compact microstructures (Javanbakht et al., 2016; Oketola et al., 2022; Syaizwadi et al., 2018). Furthermore, an increase in sintering temperature leads to lower electrical resistance and therefore improved electrical characteristics (Syaizwadi et al., 2018). For the fabricated screen-printed RuO<sub>2</sub> electrodes, the morphology and microstructure of the RuO<sub>2</sub> layers did not change much with the sintering temperature (Figure 14). All three electrode types, RuO<sub>2</sub>-800, RuO<sub>2</sub>-850 and RuO<sub>2</sub>-900, had low porosity and grain size of ~0.5-2.0 μm. However, better adhesion of the RuO<sub>2</sub> ink to the Al<sub>2</sub>O<sub>3</sub> substrate was observed for the electrodes sintered at 800 °C.

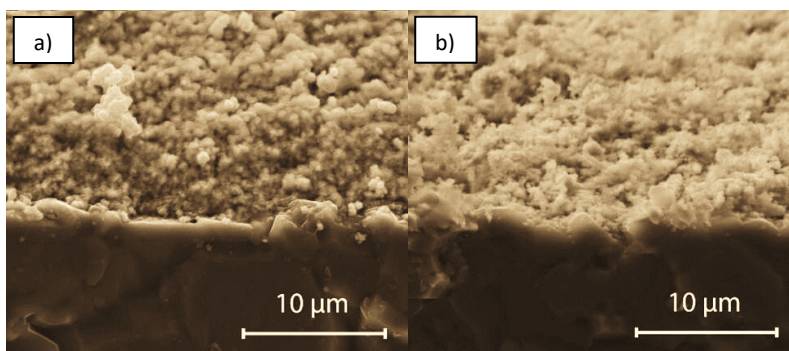


Figure 14. Scanning Electron Microscopy images (cross-section) of the RuO<sub>2</sub> electrodes sintered at (a) 800 °C and (b) 900 °C. Reproduced from **Publication I**.

Next, the electrochemical characteristics of the fabricated RuO<sub>2</sub> electrodes were investigated (Table 4). The fabricated electrodes exhibited sensitivity close to the theoretical Nernstian response and excellent linearity of the response to the pH change ( $R^2 > 0.094$ ) with sensitivity values slightly improving with the increase of the sintering temperature (Table 4). The drift was small for all three electrode types and was below 1 mV/h. The hysteresis was smaller for the acidic loop; furthermore, the hysteresis was the smallest for the RuO<sub>2</sub> electrodes sintered at 850 °C (4.6 mV and 26.3 mV for acidic and basic hysteresis respectively). All the 3 electrode types showed characteristics similar to those previously published by different authors (Table S1 in **Publication I**). Considering all the electrochemical characteristics, RuO<sub>2</sub>-850 electrodes were selected for further studies. Therefore, in the upcoming paragraphs phrase ‘RuO<sub>2</sub> electrodes’ will imply ‘RuO<sub>2</sub> electrodes sintered at 850 °C’.

Next, the stability of the readings of the fabricated electrodes was investigated. The results are presented in Figure 15. The sensitivity of the electrodes was changing for the first 4 weeks of conditioning. This change of sensitivity is explained by the slow speed of the formation of the double layer on the surface of the RuO<sub>2</sub> electrodes. It was shown before (Kurzweil, 2009; Pásztor et al., 1993) that solid-state electrodes need some time to reach stable composition of the double layer.

Table 4. Electrochemical characteristics of the RuO<sub>2</sub> electrodes sintered at different temperatures. Adopted from **Publication I**.

	Electrode type		
	RuO <sub>2</sub> -800	RuO <sub>2</sub> -850	RuO <sub>2</sub> -900
S, mV/pH	61.8 ± 1.0	60.5 ± 1.4	56.1 ± 2.1
E <sup>0</sup> , mV	681.9 ± 5.0	664.2 ± 11.3	624.0 ± 27.8
R <sup>2</sup>	0.996	0.997	0.996
Hysteresis A, mV	25.1	4.6	1.2
Hysteresis B, mV	35.4	26.3	40.4
Drift, mV/h	0-5	0-5	0-5

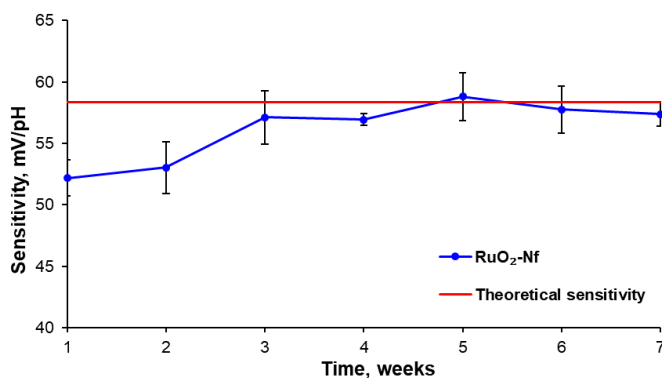


Figure 15. Change of the RuO<sub>2</sub> electrode sensitivity (Y-axis) with time. The sensitivity was changing for the first 4 weeks of storage in water and reached stable sensitivity values on 5<sup>th</sup> week.

RuO<sub>2</sub> solid-state electrodes were previously shown to work in aqueous samples and even in some more complex samples, such as coke and juices (Liao & Chou, 2008; Manjakkal et al., 2015). However, screen-printed RuO<sub>2</sub> electrodes do not work well in milk (Figure 16). Therefore, it was decided to cover the pH-sensitive part of the RuO<sub>2</sub> screen-printed electrode with a Nafion membrane. From Figure 16, it can be seen that Nafion-covered RuO<sub>2</sub> electrodes exhibit excellent pH dependency, identical to the CGE.

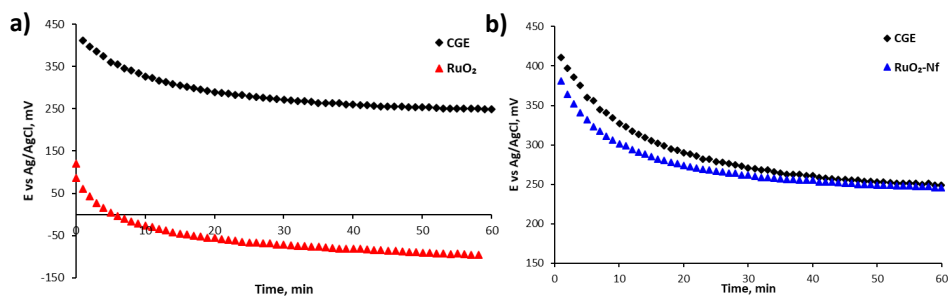


Figure 16. After placing the RuO<sub>2</sub> electrode in milk (**a**, red), its electrochemical potential abruptly dropped to negative values, indicating that electrodes cannot be used to measure the pH of the milk sample. On the other hand, the potential of the RuO<sub>2</sub>-Nf electrode (**b**, blue) was similar to the CGE. Modified from **Publication II**.

## 4.2 Fabrication parameters for the deposition of the Nafion membrane and properties of the RuO<sub>2</sub>-Nf electrodes (Publications II-VI)

After discovering the improved performance of the RuO<sub>2</sub> electrodes after covering them with the Nafion membrane, it was necessary to devote more attention to the deposition of the Nafion membrane. The parameters of the deposition of the Nafion membrane, such as method of membrane casting and its conditions (e.g., annealing temperature, pre-treatment, humidity), as well as polymer characteristics of Nafion (equivalent weight, length of side chain) are known to impact the proton conductivity of the membrane (Kusoglu & Weber, 2017). Among the deposition techniques reported by different authors (Table 1 in **Publication II**), drop-casting of Nafion solution is the most common one. However, there is a big difference in how Nafion membranes were drop-casted. The previously published papers vary in the thickness of the Nafion membrane and drying temperature.

### 4.2.1 Concentration of Nafion casting solution (Publication IV)

The influence of the Nafion concentration on the performance of the RuO<sub>2</sub>-Nf electrodes was evaluated by utilizing 5 % Nafion solutions diluted with 1:1 mixture of distilled water and ethanol to the following concentrations (v/v %): 1, 2.5 and 5. The sensitivity of the fabricated electrodes was monitored for 3 weeks and the results are presented in [Figure 17](#). It can be seen that, when the 5 % Nafion solution to cover the RuO<sub>2</sub> electrodes, the RuO<sub>2</sub>-Nf electrodes had the sensitivity, closest to the theoretical Nernstian response. Therefore, 5 % Nafion solution was selected for further studies.

To be certain that Nafion solution evenly covers the surface of the RuO<sub>2</sub> electrodes, the optical microscopy images of the electrodes with and without Nafion coatings were taken. [Figure 18](#) demonstrates that is evenly distributed over the RuO<sub>2</sub> microparticles, creating a uniform protective layer.

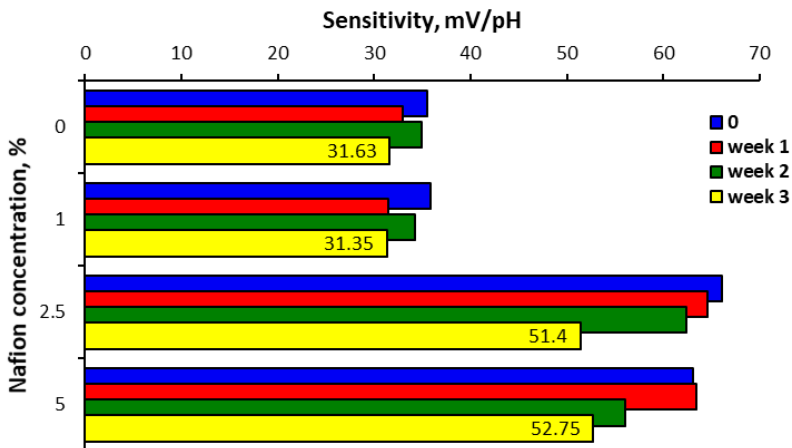


*Figure 17. Change of the sensitivity for the RuO<sub>2</sub>-Nf electrodes fabricated from the solutions with Nafion concentration of 1, 2.5 and 5 %. The sensitivity was measured before covering the RuO<sub>2</sub> electrodes with Nafion membrane (blue), 1 (red), 2 (green) and 3 (yellow) weeks after the covering. Adopted from **Publication IV**. © 2020 IEEE.*

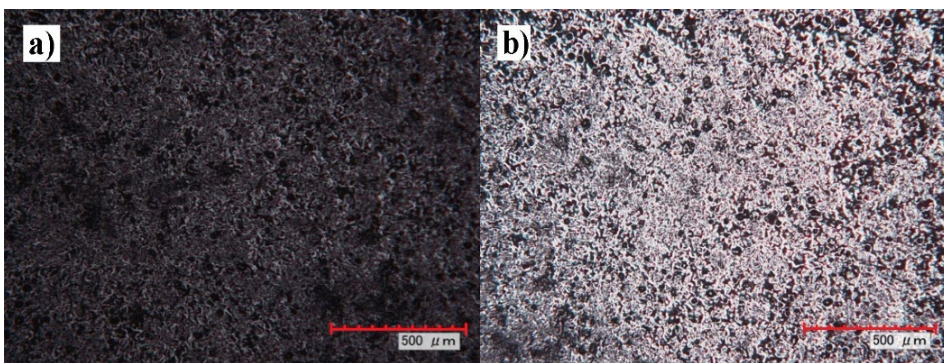


Figure 18. Digital optical microscopy images of  $\text{RuO}_2$  (a) and  $\text{RuO}_2\text{-Nf}$  (b) electrodes. The images were taken at the same light exposure. Reproduced from **Publication V**. © 2022 IEEE.

#### 4.2.2 Number of Nafion layers (Publication II)

The thickness of Nafion is important from the point of real-life applicability: the pH electrodes that were used in a food sample should be thoroughly cleaned before the next use to avoid cross-contamination and false pH readings. Therefore, the Nafion membrane should withstand cleaning. That can be achieved by increasing the thickness of the Nafion membrane. The types of electrodes were fabricated to investigate the proper thickness of Nafion membrane:  $\text{RuO}_2\text{-Nf}_1$ ,  $\text{RuO}_2\text{-Nf}_3$  and  $\text{RuO}_2\text{-Nf}_5$ .

First, the physical appearance of the deposited membrane was evaluated using SEM (Figure 19). All the 3 electrode types had some defects in the Nafion membrane (cracks and pores), and the size and number of defects increased with the thickness of the Nafion membrane (Table 5). The size of the defects can be important from the point of application of the electrodes, since the defect can be bigger than the size of some sample components<sup>5</sup> and, therefore, lead to contamination of the  $\text{RuO}_2$  pH-sensitive layer that was observed in milk test for the  $\text{RuO}_2\text{-Nf}_5$  electrodes.

Furthermore, the electrochemical characteristics of the fabricated electrodes were investigated. All the fabricated electrodes showed linear response with sensitivity values close to the theoretical Nernstian response of 58.4 mV/pH (at a temperature of 21 °C) with the sensitivity slightly decreasing with the increase of the thickness of the Nafion membrane Table 5. For the  $\text{RuO}_2\text{-Nf}_5$  electrodes, the linearity was 0.942 and the hysteresis exceeded 20 mV. This can be due to the longer time needed for the ions to travel through a thicker Nafion membrane and agrees well with the findings of Lonsdale (Lonsdale, 2018).

The preliminary test in milk samples (Figure 20) showed excellent performance of  $\text{RuO}_2\text{-Nf}_3$  electrodes even during the third application for measurement in milk. Therefore, the  $\text{RuO}_2\text{-Nf}_3$  electrodes with the 7.47  $\mu\text{m}$  thickness of the Nafion membrane were selected for further investigation.

<sup>5</sup> For example, the size of fat globules is around 2-6  $\mu\text{m}$  (Phadungath, 2005; Xu et al., 2016) that is smaller than defects in Nafion membrane for  $\text{RuO}_2\text{-Nf}_5$  electrodes.



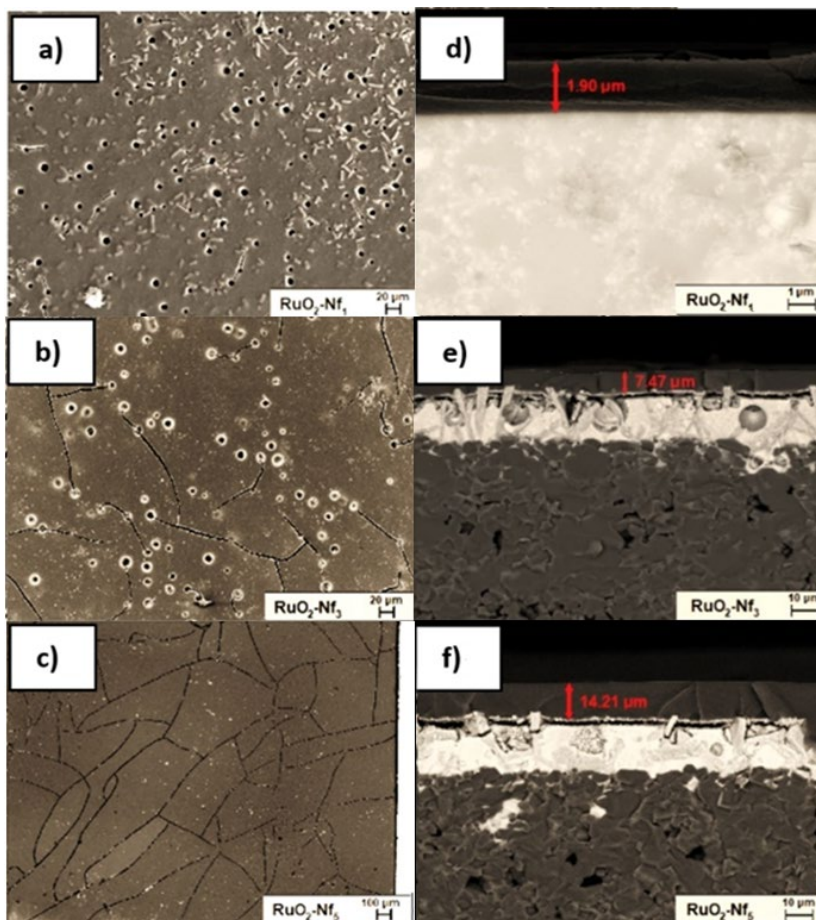


Figure 19. Scanning Electron Microscopy images (a-c) and cross-sections (d-f) of the fabricated  $\text{RuO}_2\text{-Nf}$  electrodes: (a, d)  $\text{RuO}_2\text{-Nf}_1$ , (b, e)  $\text{RuO}_2\text{-Nf}_3$  and (c, f)  $\text{RuO}_2\text{-Nf}_5$ . Reproduced from **Publication II**.

Table 5. Characteristics of  $\text{RuO}_2\text{-Nf}_1$ ,  $\text{RuO}_2\text{-Nf}_3$  and  $\text{RuO}_2\text{-Nf}_5$  electrodes. Reproduced from **Publication II**.

Characteristic	Electrode type		
	$\text{RuO}_2\text{-Nf}_1$	$\text{RuO}_2\text{-Nf}_3$	$\text{RuO}_2\text{-Nf}_5$
Nafion membrane thickness, $\mu\text{m}$	1.9	7.5	14.2
Defects in the Nafion layer	Pores	Pores and cracks of $\sim 2\text{-}4 \mu\text{m}$ width	Cracks of $\sim 10 \mu\text{m}$ width
Time needed for the deposition of all Nafion layers, hours	2	6	10
S, mV/pH	$57.0 \pm 0.7$	$56.5 \pm 0.3$	$55.1 \pm 0.4$
$E^0$ , mV	$684.1 \pm 2.3$	$693.2 \pm 3.8$	$603.9 \pm 32.5$
$R^2$	0.997	0.995	0.942
Hysteresis A, mV	$11 \pm 1$	$10 \pm 2$	$20 \pm 3$
Hysteresis B, mV	$17 \pm 9$	$24 \pm 6$	$32 \pm 5$
Drift, mV/h	14-15	25-35	25-35
Performance in milk	+	+	+
Reusability in milk	+	++	+

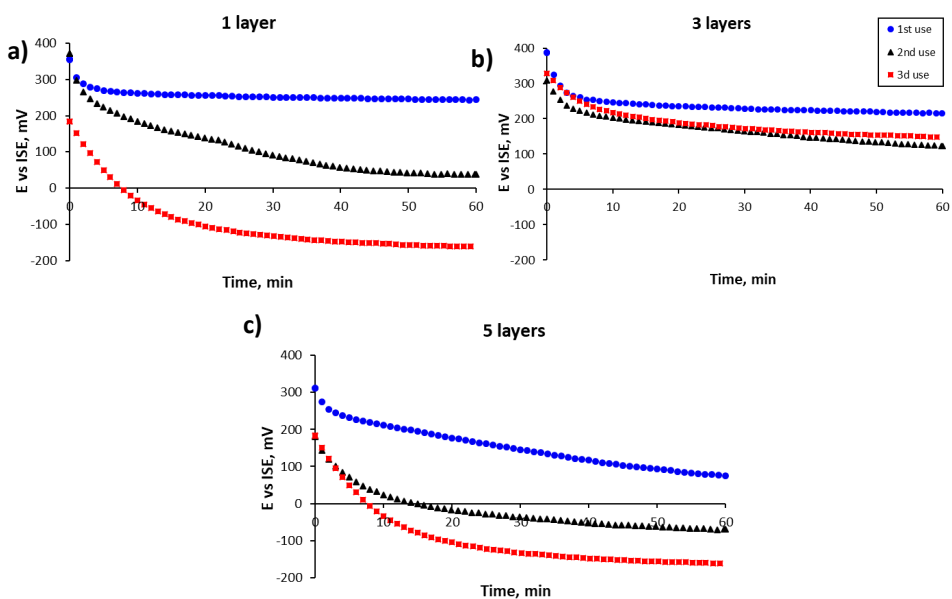


Figure 20. Performance of the RuO<sub>2</sub>-Nf electrodes ((a) – RuO<sub>2</sub>-Nf<sub>1</sub>, (b) – RuO<sub>2</sub>-Nf<sub>3</sub>, (c) – RuO<sub>2</sub>-Nf<sub>5</sub>) was evaluated by placing them in a milk sample and continuously measuring the electrochemical potential for 1 hour. Furthermore, the electrodes were used 3 times (blue – first use, black – second use, red – third use) to evaluate whether the electrodes can be used repeatedly. RuO<sub>2</sub>-Nf<sub>3</sub> showed the best performance. Reproduced from **Publication II**.

#### 4.2.3 Time needed for deposition of one layer (Publication II)

Next, the time necessary for the drying of one layer of the Nafion membrane was investigated. As can be seen from the data presented in Table 6, the best characteristics of the RuO<sub>2</sub>-Nf<sub>3</sub> electrodes were achieved when the Nafion layers were allowed to dry for 2 hours in between the layer deposition. In this case, more uniform values of the sensitivity were achieved with better linearity of the pH response.

Table 6. Characteristics of the RuO<sub>2</sub>-Nf<sub>3</sub> electrodes with different drying time. Reproduced from **Publication II**.

Characteristic	Drying time of one layer of Nafion		
	0.5 h	1 h	2 h
S, mV/pH	53.1 ± 0.5	56.2 ± 10.9	<b>60.5 ± 2.1</b>
E <sup>0</sup> , mV	601.5 ± 131.7	549.0 ± 90.3	<b>680.9 ± 10.3</b>
R <sup>2</sup>	0.981	0.978	<b>0.984</b>
Hysteresis A, mV	10 ± 2	11 ± 4	<b>4 ± 2</b>
Hysteresis B, mV	24 ± 6	21 ± 17	25 ± 4
Drift, mV/h	25-35	30-35	20-25

#### 4.2.4 Drying temperature (Publication II)

It was previously reported (Kusoglu & Weber, 2017), that pre-heating and annealing of the Nafion membrane allow improving the proton conductivity of the membrane. Furthermore, thermal treatment of the membrane allows increasing mechanical stability of the membrane (Kusoglu & Weber, 2017), which is important for real-life application of the RuO<sub>2</sub>-Nf electrode from the point of their susceptibility to cleaning. Xu and co-authors previously reported (K. Xu et al., 2016) enhanced mechanical and thermal

properties of the Nafion membrane dried at 80 °C. However, no explanation was given regarding why the temperature of 80 °C was selected. Hence, in this study, the range of temperatures from room temperature to 80 °C and its influence on the properties of the Nafion membrane was investigated.

The electrochemical characteristics of the RuO<sub>2</sub>-Nf<sub>3</sub> electrodes dried at different temperatures are presented in Table 7. The RuO<sub>2</sub>-Nf<sub>3</sub> electrodes dried at 60 and 80 °C showed good performance and provided better protection to the RuO<sub>2</sub> screen-printed layer (Figure 21). Apparently, the thermal treatment improved the mechanical stability of the Nafion membrane allowing for better protection of the screen-printed RuO<sub>2</sub> layer underneath due to the increased entanglement of polymer chains and coalescence of Nafion particles (Kim et al., 2015; Mauritz & Moore, 2004).

In real-life situations, it can be necessary to measure pH in samples of not room temperature, but elevated temperatures. For instance, acid-induced milk coagulation is carried out at a temperature of 40 °C (Phadungath, 2005). However, it is worth mentioning that the proton conductivity of the Nafion membrane is known to decrease with the temperature (Alberti et al., 2013). Therefore, the performance of the RuO<sub>2</sub>-Nf<sub>3</sub> electrodes was performed at temperatures 25, 30, 35 and 40 °C (Table 8). The best performance was achieved for the RuO<sub>2</sub>-Nf<sub>3</sub> electrodes dried at 80 °C (smaller hysteresis and drift, and a more linear increase of the sensitivity with temperature).

Table 7. Characteristics of the RuO<sub>2</sub>-Nf<sub>3</sub> electrodes dried at different temperatures. Reproduced from Publication II.

Characteristic	Drying temperature, °C			
	21	40	60	80
S, mV/pH	60.5 ± 2.1	48.9 ± 1.0	52.0 ± 2.0	52.2 ± 2.1
E <sup>0</sup> , mV	680.9 ± 10.3	554.0 ± 23.9	667.3 ± 19.9	485.7 ± 21.2
R <sup>2</sup>	0.984	0.995	0.994	0.983
Hysteresis A, mV	4 ± 2	22 ± 2	10 ± 3	8 ± 5
Hysteresis B, mV	24 ± 1	21 ± 3	19 ± 10	14 ± 4
Drift, mV/h	20-25	10-20	10-20	20-30

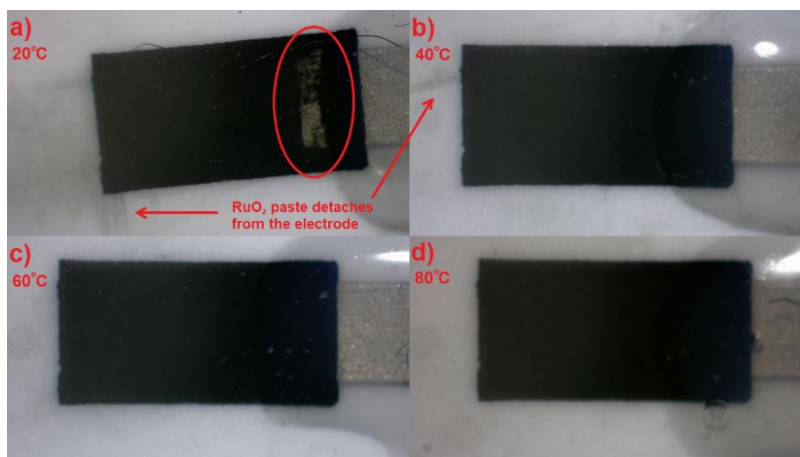


Figure 21. Images of the state of the RuO<sub>2</sub>-Nf<sub>3</sub> electrodes after use as pH -electrodes (Nafion membrane is removed) for the Nafion membrane dried at (a) 20, (b) 40, (c) 60 and (d) 80 °C. The electrodes dried at higher temperatures exhibited better protection of the RuO<sub>2</sub> screen-printed layer from the decay. Reproduced from Publication II.

Table 8. Electrochemical characteristics of the RuO<sub>2</sub>-Nf electrodes tested in heated samples. Adopted from **Publication II**.

Characteristic	Temperature of the sample, °C			
	25	30	35	40
<b>RuO<sub>2</sub>-Nf<sub>3</sub> electrodes dried at 60 °C</b>				
S, mV/pH	52.3 ± 2.0	54.5 ± 2.1	54.7 ± 6.8	56.4 ± 10.7
E <sup>0</sup> , mV	641.6 ± 8.8	556.3 ± 29.9	596.8 ± 17.4	645.6 ± 11.5
R <sup>2</sup>	0.997	0.972	0.952	0.956
Hysteresis A, mV	12 ± 7	11 ± 6	17 ± 8	28 ± 10
Hysteresis B, mV	12 ± 5	23 ± 9	26 ± 2	32 ± 10
Drift, mV/h	15-25	10-15	5-15	5-15
<b>RuO<sub>2</sub>-Nf<sub>3</sub> electrodes dried at 80 °C</b>				
S, mV/pH	53.5 ± 2.3	54.0 ± 0.8	54.5 ± 2.2	54.7 ± 2.2
E <sup>0</sup> , mV	640.7 ± 75.7	548.1 ± 16.3	506.2 ± 41.9	583.6 ± 58.2
R <sup>2</sup>	0.985	0.979	0.985	0.995
Hysteresis A, mV	8 ± 1	15 ± 6	12 ± 2	15 ± 7
Hysteresis B, mV	20 ± 6	17 ± 1	15 ± 9	20 ± 10
Drift, mV/h	5-20	5-15	10-20	10-15

#### 4.2.5 Stability of the readings of the RuO<sub>2</sub>-Nf electrodes (Publication II)

Solid-state electrodes require initial conditioning in water or buffer solutions that is needed to reach stable Ru(IV)/Ru(III) ratio in the fabricated electrodes (Manjakkal et al., 2014; Zhuiykov, 2009). The fabricated RuO<sub>2</sub>-Nf electrodes reached stable sensitivity values on the third week of conditioning (Figure 22), while RuO<sub>2</sub> electrodes required over one month of conditioning in water (Figure 22).

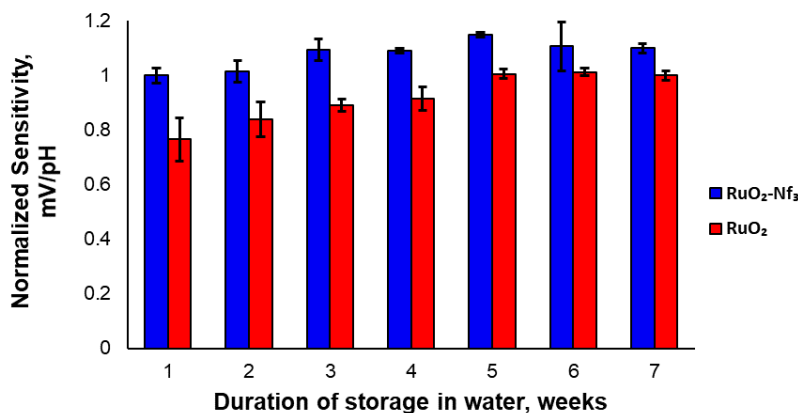


Figure 22. Change of sensitivity of the RuO<sub>2</sub> (red) and RuO<sub>2</sub>-Nf<sub>3</sub> (blue) electrodes with time. The sensitivity was normalized against the value of the sensitivity on week 7. The RuO<sub>2</sub>-Nf<sub>3</sub> reached stable sensitivity values in a shorter time compared to the RuO<sub>2</sub> electrodes. Adopted from **Publication II**.

#### 4.2.6 Cross-sensitivity of the RuO<sub>2</sub>-Nf electrodes (Publication III)

It was previously demonstrated, that only small positively charged ions can impact the performance of screen-printed RuO<sub>2</sub> electrodes (Manjakkal et al., 2020). Furthermore, Nafion membranes are known to have high ion mobility towards smaller cations and the negative charge of sulfonate groups in the Nafion backbone causes lower mobility towards anions (Kusoglu & Weber, 2017). Therefore, the cross-sensitivity of the fabricated RuO<sub>2</sub>-Nf

electrodes was tested in presence of  $\text{Na}^+$ ,  $\text{K}^+$ ,  $\text{Li}^+$  and  $\text{NH}_4^+$  utilizing chloride salts of these cations since  $\text{Cl}^-$  ions were shown to not alter the sensitivity of the  $\text{RuO}_2$  electrodes (Manjakkal et al., 2020). The results are presented in Figure 23. The presence of interfering cations in concentrations of 0.1 M did not significantly change the sensitivity of the  $\text{RuO}_2$ -Nf electrodes except for  $\text{NH}_4^+$ . The increase of sensitivity in presence of  $\text{NH}_4\text{Cl}$  was 2.83 mV/pH can be due to the presence of ammonia in the aqueous solution that can the composition of a double-layer on the surface of the  $\text{RuO}_2$  electrodes (Kurzweil, 2009). Nonetheless, the linearity of the response of the  $\text{RuO}_2$ -Nf electrodes toward the pH change was above 0.99 for all the investigated cases.

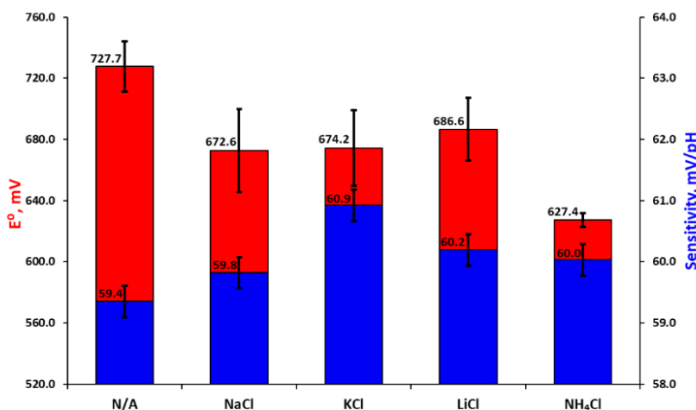


Figure 23.  $\text{RuO}_2$ -Nf electrodes are not sensitive to the presence of cations in buffer solutions at concentrations up to 0.1 M. The  $E^0$  of the fabricated electrodes (red, primary Y-axis) did not change much in the presence of interfering cations. The sensitivity of the fabricated electrodes (blue, secondary Y-axis) remained close to the theoretical Nernstian response indicating only negligible sensitivity towards most common interfering ions. Adopted from Publication III.

#### 4.2.7 Reusability of the fabricated $\text{RuO}_2$ -Nf electrodes (Publication VI)

Next, the reusability of the  $\text{RuO}_2$ -Nf electrodes after deterioration of Nafion membrane was investigated. Nafion membrane is a soft membrane, that is partially soluble in water and, therefore, might wear off with time. Here, the possibility of recover the  $\text{RuO}_2$  electrodes and repeatedly cover them with new Nafion membrane was investigated. The results are presented in Table 9. It can be seen that all the electrochemical characteristics were worsening with the next usage: the sensitivity,  $R_2$  and  $E^0$  were decreasing, whereas hysteresis a and B were increasing. Nonetheless, at room temperature the  $\text{RuO}_2$ -Nf electrodes exhibited acceptable characteristics and, therefore, can be used repeatedly but only at temperatures around 25 °C.

### 4.3 Performance of the fabricated $\text{RuO}_2$ -Nf electrodes in food samples (Publications III and VII)

Notwithstanding the number of papers dealing with the development and fabrication of new pH sensors published every year, only a few of them report application on other samples than buffer solutions. This is due to the fact that solid-state electrode face difficulties when measuring in real-life samples (Figure 16). The same applies to the CGE: not only electrode requires extensive cleaning, but also should be properly used for accurate pH measurement (Galster, 1991).

Table 9. Electrochemical characteristics of the RuO<sub>2</sub>-Nf electrodes, covered with Nafion 3 times and tested in samples of varying temperature. Reproduced from **Publication VI**. © 2020 IEEE.

Characteristic	Temperature of the sample, °C			
	25	30	35	40
<b>First coating</b>				
S, mV/pH	53.5 ± 2.3	54.0 ± 0.8	54.5 ± 2.2	54.7 ± 2.2
E <sup>0</sup> , mV	640.7 ± 75.7	548.1 ± 16.3	506.2 ± 41.9	583.6 ± 58.2
R <sup>2</sup>	0.985	0.979	0.985	0.995
Hysteresis A, mV	8 ± 1	15 ± 6	12 ± 2	15 ± 7
Hysteresis B, mV	20 ± 6	17 ± 1	15 ± 9	20 ± 10
Drift, mV/h	5-20	5-15	10-20	10-15
<b>Second coating</b>				
S, mV/pH	49.5 ± 5.8	40.4 ± 6.8	47.8 ± 5.0	33.3 ± 4.8
E <sup>0</sup> , mV	537.9 ± 23.4	350.7 ± 18.1	425.9 ± 18.1	259.6 ± 80.4
R <sup>2</sup>	0.994	0.952	0.977	0.876
Hysteresis A, mV	24 ± 7	9 ± 4	20 ± 7	28 ± 1
Hysteresis B, mV	9 ± 2	11 ± 3	20 ± 4	8 ± 7
Drift, mV/h	0-15	0-20	0-20	0-15
<b>Third coating</b>				
S, mV/pH	53.7 ± 1.5	27.7 ± 7.4	28.1 ± 5.8	13.7 ± 4.2
E <sup>0</sup> , mV	522.8 ± 22.3	342.6 ± 117.6	260.5 ± 51.0	67.7 ± 64.8
R <sup>2</sup>	0.975	0.966	0.941	0.831
Hysteresis A, mV	20 ± 4	19 ± 1	24 ± 4	22 ± 5
Hysteresis B, mV	4 ± 1	7 ± 4	20 ± 4	10 ± 2
Drift, mV/h	10-20	5-15	10-20	10-20

#### 4.3.1 Measurement in dairy samples (Publication III)

The RuO<sub>2</sub>-Nf electrodes, together with RuO<sub>2</sub>-CuO-Nf electrodes were tested for accurate pH measurement in different samples, including juices, carbonated and caffeinated beverages in the [MSc thesis of Iuliia Vetik](#) and will not be discussed here. In this study, the main attention was paid to the application of the fabricated electrodes to one of the most challenging samples – dairy samples that have denser textures and contain fats and proteins that interfere with pH measurement. The results of the pH measurement in dairy samples are presented in [Figure 24](#). It is worth mentioning that response time also increased from 5 minutes for milk and yoghurt to 10 minutes for sour cream, cottage and melted cheese.

It can be seen that for milk, yoghurt, sour cream and cottage cheese the difference in pH readings from the CGE was below 0.5 pH units and only for the melted cheese sample that had the densest texture the pH difference was around 3 pH units. For the second CGE that was used as a reference, the pH difference was reaching 0.1 pH units for denser samples. However, the difference of 0.5 pH units is still considered good as it is similar to those observed by other researchers for different sensing materials used in different samples (section 1.1). This finding correlated well with the recent investigation by Chawang et al. (Chawang et al., 2022), where the authors have demonstrated the influence of the viscosity of the sample on the performance of the iridium oxide electrode.

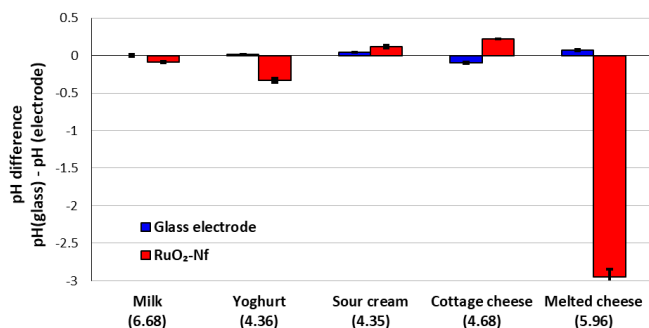


Figure 24. Results of pH measurement in dairy samples. The fabricated RuO<sub>2</sub>-Nf electrodes had error below 0.5 pH units in all samples except for melted cheese where the error was 2.95 pH units. Adopted from **Publication III**.

### 4.3.2 Continuous measurement in milk during coagulation

Monitoring the pH during the milk coagulation allows producing cheese with better quality (e.g., texture, taste) (Fox et al., 1990; Lucey et al., 2003). However, at present, there is no method that would allow continuous measurement of pH. Currently, pH is measured using the point method, when the pH of a sample is measured, e.g., every hour with cleaning in between the measurements (Rosca et al., 2019). Developing an electrode that would allow measurement of pH during the milk coagulation could allow more precise determination of cheese cutting time. Therefore, the fabricated electrodes were tested for applicability for pH measurement during milk coagulation. As demonstrated in Figure 16, RuO<sub>2</sub>-Nf electrodes exhibit behavior similar to the CGE when measuring in milk for one hour. In this study, an enzyme was used to induce milk coagulation. Since during enzymatic coagulation pH value should remain the same, it was expected to observe the constant response from the fabricated electrodes during milk coagulation. However, the pH measured with the fabricated RuO<sub>2</sub>-Nf electrode was gradually increasing by 2.76 and 3.15 pH units during the 35 min of measurement for electrodes 1 and 2 respectively (Figure 25). At the same time, the change of the measured pH with the CGE was only 0.06 pH units. Thus, even though RuO<sub>2</sub>-Nf electrodes show good performance in milk, they are not yet suitable for measurement during milk coagulation and once again indicated the inapplicability of the RuO<sub>2</sub>-Nf electrodes for denser samples.

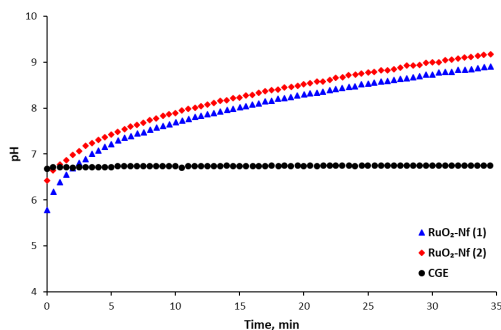


Figure 25. Change of pH value measured with the CGE (black) and 2 RuO<sub>2</sub>-Nf (blue and red) electrodes in parallel during milk coagulation. While the CGE showed stable pH readings, the fabricated RuO<sub>2</sub>-Nf electrodes failed to accurately measure the pH.

### 4.3.3 Cleaning after measurement in dairy samples (Publication VII)

The reusability of the RuO<sub>2</sub>-Nf electrodes was discussed in section 4.2.7, however, actual reusability of any electrode implies a correct cleaning procedure that allow to maintain the active surface of an electrode in-between the measurement. Therefore, here the cleaning of RuO<sub>2</sub>-Nf electrode after the usage in milk is discussed below. Four approach that are commonly advised for the cleaning of pH electrodes were investigated: (i) [removal of fats and oils] mechanical cleaning with surfactants: (ii) [removal of protein residues] cleaning with acidic pepsin solution; (iii) [removal of mineral deposits] acidic cleaning. The results are presented in Figure 26. The sensitivity of RuO<sub>2</sub>-Nf electrodes improved after any of the cleaning approaches, however, the sensitivity of the RuO<sub>2</sub>-Nf electrodes in all the cases was changing during first 24 hours after cleaning, indicating that conditioning of the RuO<sub>2</sub>-Nf electrodes is necessary prior to the next usage (similarly to the CGE). This conditioning is necessary to allow the double layer, consisting of H<sup>+</sup> and OH<sup>-</sup> ions to form on the surface of the electrodes (Manjakkal et al., 2020). The smallest change in sensitivity was observed for the RuO<sub>2</sub>-Nf electrodes cleaned with the acidic pepsin solution, hence, making this cleaning approach the most favourable once amongst investigated options.

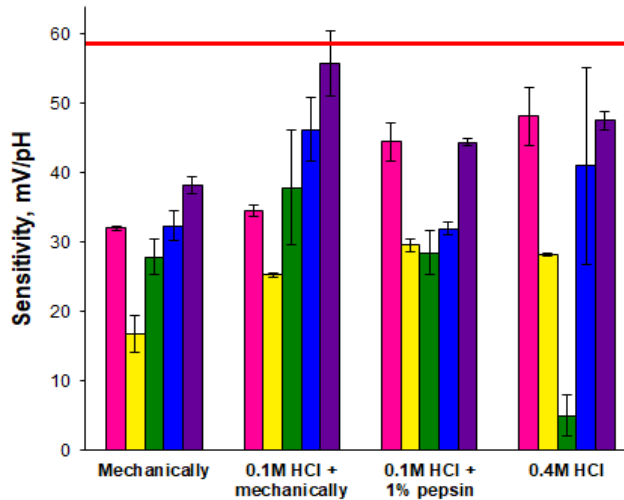


Figure 26. Change of the sensitivity of the RuO<sub>2</sub>-Nf electrodes with cleaning: initial sensitivity (pink), sensitivity after using in milk (yellow), sensitivity straight after cleaning (green), sensitivity 12 hours after cleaning (blue) and sensitivity 24 hours after cleaning (purple). Red line indicates theoretical Nernstian sensitivity. Reproduced from **Publication VII**. © 2022 IEEE.



## Conclusion

In this dissertation, solid-state RuO<sub>2</sub> are brought forward in order to replace fragile and expensive conventional glass electrode in the pH measurement of food samples.

The aims declared in the beginning of the thesis were reached with the following outcome:

Aim 1 Find the fabrication parameters for the screen printing of ruthenium(IV) oxide pH electrodes.

To reach the first aim of the thesis, the RuO<sub>2</sub> electrodes were fabricated by screen printing and the influence of the sintering temperature on the performance of the fabricated electrodes was discussed. Sintering temperature of 850 was selected as optimal for the fabrication of the RuO<sub>2</sub> electrodes with the best characteristics.

Aim 2 Find fabrication parameters for the deposition of the protective Nafion membrane. Investigate the properties of the ruthenium(IV) oxide pH electrodes covered with the Nafion membrane.

To reach the second aim, a protective membrane of Nafion™ was deposited and demonstrated to allow pH measurement in milk. Therefore, the properties of the Nafion™ membrane were investigated next. The conditions for the deposition of the Nafion™ membrane (thickness, drying time and temperature) were selected from the point of their effect on the electrochemical characteristics of the RuO<sub>2</sub> electrodes. Furthermore, it was demonstrated that the Nafion™ membrane improves the durability of the RuO<sub>2</sub> electrodes.

Aim 3 Investigate the performance of the fabricated electrodes in food samples and during food processing.

To reach the third aim, the fabricated electrodes were used for the pH measurement of dairy samples. The fabricated electrodes covered with Nafion™ protective membrane showed good performance in dairy samples and only failed to accurately measure pH in melted cheese. Apparently, not only the composition but also the texture of the samples can affect the performance of the screen-printed RuO<sub>2</sub> electrodes. Next, an attempt was made to use the fabricated electrodes for continuous measurement during milk coagulation. The experiment demonstrated, that even though the fabricated electrodes can be used for continuous monitoring of milk over 15 hours, they yet fail to measure pH during milk coagulation. Nevertheless, the reported electrodes can be successfully employed for pH measurement of different real-life samples and are suitable for continuous pH measurement that make them of potential interest for food researchers and food industry for on-line and in-line pH monitoring.

## References

- Abbas, K. A., Mohamed, A., Jamilah, B., & Ebrahimian, M. (2008). A review on correlations between fish freshness and pH during cold storage. *American Journal of Biochemistry and Biotechnology*, 4(4), 416–421. <https://doi.org/10.3844/ajbbsp.2008.416.421>
- Agmon, N. (1995). The Grotthuss mechanism. *Chemical Physics Letters*, 244(5–6), 456–462. [https://doi.org/10.1016/0009-2614\(95\)00905-J](https://doi.org/10.1016/0009-2614(95)00905-J)
- Alberti, G., Narducci, R., di Vona, M. L., & Giancola, S. (2013). More on Nafion conductivity decay at temperatures higher than 80 °C: Preparation and first characterization of in-plane oriented layered morphologies. *Industrial and Engineering Chemistry Research*, 52(31), 10418–10424. <https://doi.org/10.1021/ie303628c>
- Amemiya, S., Arning, M. D., Baur, J. E., Bergren, A. J., Chen, S., Ciabonu, M., Cliffel, D. E., Creager, S., Demaille, C., Denuault, G., Dryfe, R. A. W., Edwards, G. A., Ewing, A. G., Fan, F. F., Fernandez, J., Forster, R. J., Haram, S. K., Holt, K. B., Keyes, T. E., ... Zoski, C. G. (2007). *Handbook of Electrochemistry* (C. Zoski, Ed.; First edit). Elsevier.
- Azad, T., & Ahmed, S. (2016). Common milk adulteration and their detection techniques. *International Journal of Food Contamination*, 3(22), 1–9. <https://doi.org/10.1186/s40550-016-0045-3>
- Biswas, A. K., & Mandal, P. K. (2020). *Meat quality analysis* (A. K. Biswas & P. K. Mandal, Eds.). Academic press. <https://doi.org/10.1016/B978-0-12-819233-7.00001-X>
- Bühlmann, P., Hayakawa, M., Ohshiro, T., Amemiya, S., & Umezawa, Y. (2001). Influence of natural, electrically neutral lipids on the potentiometric responses of cation-selective polymeric membrane electrodes. *Analytical Chemistry*, 73(14), 3199–3205. <https://doi.org/10.1021/ac0015016>
- Chawang, K., Bing, S., & Chiao, J. C. (2022). Effects of Viscosity and Salt Interference for Planar Iridium Oxide and Silver Chloride pH Sensing Electrodes on Flexible Substrate. *Chemosensors*, 10(9). <https://doi.org/10.3390/chemosensors10090371>
- Cheng, J. H., Sun, D. W., Zeng, X. A., & Liu, D. (2015). Recent advances in methods and techniques for freshness quality determination and evaluation of fish and fish fillets: a review. *Critical Reviews in Food Science and Nutrition*, 55(7), 1012–1225. <https://doi.org/10.1080/10408398.2013.769934>
- Chou, J. C., Liu, S. I., & Chen, S. H. (2005). Sensing characteristics of ruthenium films fabricated by radio frequency sputtering. *Japanese Journal of Applied Physics, Part 1: Regular Papers and Short Notes and Review Papers*, 44(3), 1403–1408. <https://doi.org/10.1143/JJAP.44.1403>
- Dawson, P.; Elliott, D.; Elliott, A.; Johns, K. (1991). *Directory Biochemist*. Mir.
- Drozdov, V. P., Zlomanov, G. N., & Mazo, F. M. (2007). *Neorganicheskaya khimiya [Inorganic chemistry]* (J. D. Tretyakov, Ed.). Akademiya.
- Eftekhari, A. (2003). pH sensor based on deposited film of lead oxide on aluminum substrate electrode. *Sensors and Actuators, B: Chemical*, 88(3), 234–238. [https://doi.org/10.1016/S0925-4005\(02\)00321-0](https://doi.org/10.1016/S0925-4005(02)00321-0)
- Fog, A.; Buck, R. (1984). Electronic semiconducting oxides as pH sensors. *Sensors and Actuators*, 5, 137–146. [https://doi.org/10.1016/0250-6874\(84\)80004-9](https://doi.org/10.1016/0250-6874(84)80004-9)
- Fox, P. F., Lucey, J. A., & Cogan, T. M. (1990). Glycolysis and related reactions during cheese manufacture and ripening. *Critical Reviews in Food Science and Nutrition*, 29(4), 237–253. <https://doi.org/10.1080/10408399009527526>

- Galster, H. (1991). *pH measurement: Fundamentals, methods, applications, instrumentation*. VCH Verlagsgesellschaft.
- Głáb, S., Hulanicki, A., Edwall, G., Folke, F., Ingman, I., & Koch, W. F. (1989). Metal-metal oxide and metal oxide electrodes as pH sensors. *Critical Reviews in Analytical Chemistry*, 21(1), 29–47. <https://doi.org/10.1080/10408348908048815>
- Grot, W. G. (1982). Nafion Membrane and its Applications. In U. Landau, E. Yeager, & D. Kortan (Eds.), *Electrochemistry in Industry* (pp. 73–87). Springer, Boston, MA. <https://doi.org/10.1007/978-1-4684-4238-0>
- Hopkins, D. L., Ponnampalam, E. N., van de Ven, R. J., & Warner, R. D. (2014). The effect of pH decline rate on the meat and eating quality of beef carcasses. *Animal Production Science*, 54, 407–413. <https://doi.org/10.1071/AN12314>
- Hu, G., Li, N., Zhang, Y., & Li, H. (2020). A novel pH sensor with application to milk based on electrochemical oxidative quinone-functionalization of tryptophan residues. *Journal of Electroanalytical Chemistry*, 859. <https://doi.org/10.1016/j.jelechem.2020.113871>
- Javanbakht, M., Salahinejad, E., & Hadianfard, M. J. (2016). The effect of sintering temperature on the structure and mechanical properties of medical-grade powder metallurgy stainless steels. *Powder Technology*, 289, 37–43. <https://doi.org/10.1016/j.powtec.2015.11.054>
- Jose, M., Mylavarapu, S. K., Bikkarolla, S. K., Machiels, J., Sankaran, K. J., McLaughlin, J., Hardy, A., Thoelen, R., & Deferme, W. (2021). Printed pH sensors for textile-based wearables: a conceptual and experimental study on materials, deposition technology, and sensing principles. *Advanced Engineering Materials*, 2101087. <https://doi.org/10.1002/adem.202101087>
- Kahram, M., Asnavandi, M., & Dolati, A. (2014). Synthesis and electrochemical characterization of sol-gel-derived RuO<sub>2</sub>/carbon nanotube composites. *Journal of Solid State Electrochemistry*, 18, 993–1003. <https://doi.org/10.1007/s10008-013-2346-2>
- Kandeel, S. A., Megahed, A. A., Ebeid, M. H., & Constable, P. D. (2019). Ability of milk pH to predict subclinical mastitis and intramammary infection in quarters from lactating dairy cattle. *Journal of Dairy Science*, 102(2), 1417–1427. <https://doi.org/10.3168/jds.2018-14993>
- Karastogianni, S., Girousi, S., & Sotiropoulos, S. (2016). pH: Principles and measurement. In *Encyclopedia of Food and Health* (1st ed., Issue 4). Elsevier Ltd. <https://doi.org/10.1016/B978-0-12-384947-2.00538-9>
- Katsube, T., Lauks, I., & Zemel, J. N. (1982). pH-sensitive sputtered iridium oxide films. *Sensors and Actuators*, 2, 399–410. [https://doi.org/10.1016/0250-6874\(81\)80060-1](https://doi.org/10.1016/0250-6874(81)80060-1)
- Kawahara, R., Sahatiya, P., Badhulika, S., & Uno, S. (2018). Paper-based potentiometric pH sensor using carbon electrode drawn by pencil. *Japanese Journal of Applied Physics*, 57(4). <https://doi.org/10.7567/JJAP.57.04FM08>
- Kim, Y. S., Welch, C. F., Hjelm, R. P., Mack, N. H., Labouriau, A., & Orler, E. B. (2015). Origin of toughness in dispersion-cast Nafion membranes. *Macromolecules*, 48, 2161–2172. <https://doi.org/10.1021/ma502538k>
- Koncki, R., & Mascini, M. (1997). Screen-printed ruthenium dioxide electrodes for pH measurements. *Analytica Chimica Acta*, 351, 143–149. [https://doi.org/10.1016/S0003-2670\(97\)00367-X](https://doi.org/10.1016/S0003-2670(97)00367-X)
- Korkeala, H., Mäki-Petäys, O., Alanko, T., & Sorvettula, O. (1986). Determination of pH in meat. *Meat Science*, 18, 121–132. [https://doi.org/10.1016/0309-1740\(86\)90088-4](https://doi.org/10.1016/0309-1740(86)90088-4)

- Kurzweil, P. (2009). Metal oxides and ion-exchanging surfaces as pH sensors in liquids: State-of-the-art and outlook. *Sensors*, 9(6), 4955–4985. <https://doi.org/10.3390/s90604955>
- Kusoglu, A., & Weber, A. (2017). New insights into perfluorinated sulfonic-acid ionomers. *Chemical Reviews*, 117, 987–1104. <https://doi.org/10.1021/acs.chemrev.6b00159>
- Kyrana, V. R., & Lougovois, V. P. (2002). Sensory, chemical and microbiological assessment of farm-raised European sea bass (*Dicentrarchus labrax*) stored in melting ice. *International Journal of Food Science and Technology*, 37(3), 319–328. <https://doi.org/10.1046/j.1365-2621.2002.00572.x>
- Kyrana, V. R., Lougovois, V. P., & Valsamis, D. S. (1997). Assessment of shelf-life of maricultured gilthead sea bream (*Sparus aurata*) stored in ice. *International Journal of Food Science and Technology*, 32(4), 339–347. <https://doi.org/10.1046/j.1365-2621.1997.00408.x>
- Lakard, B., Herlem, G., Lakard, S., Guyetant, R., & Fahys, B. (2005). Potentiometric pH sensors based on electrodeposited polymers. *Polymer*, 46(26), 12233–12239. <https://doi.org/10.1016/j.polymer.2005.10.095>
- Lakard, B., Segut, O., Lakard, S., Herlem, G., & Gharbi, T. (2007). Potentiometric miniaturized pH sensors based on polypyrrole films. *Sensors and Actuators, B: Chemical*, 122(1), 101–108. <https://doi.org/10.1016/j.snb.2006.04.112>
- Liao, Y. H., & Chou, J. C. (2008). Preparation and characteristics of ruthenium dioxide for pH array sensors with real-time measurement system. *Sensors and Actuators, B: Chemical*, 128(2), 603–612. <https://doi.org/10.1016/j.snb.2007.07.023>
- Li, M., Li, Y. T., Li, D. W., & Long, Y. T. (2012). Recent developments and applications of screen-printed electrodes in environmental assays-A review. *Analytica Chimica Acta*, 734, 31–44. <https://doi.org/10.1016/j.aca.2012.05.018>
- Li, Q., Li, H., Zhang, J., & Xu, Z. (2011). A novel pH potentiometric sensor based on electrochemically synthesized polybisphenol A films at an ITO electrode. *Sensors and Actuators, B: Chemical*, 155(2), 730–736. <https://doi.org/10.1016/j.snb.2011.01.038>
- Li, Q., Tang, W., Su, Y., Huang, Y., Peng, S., Zhuo, B., Qiu, S., Ding, L., Li, Y., & Guo, X. (2017). Stable thin-film reference electrode on plastic substrate for all-solid-state ion-sensitive field-effect transistor sensing system. *IEEE Electron Device Letters*, 38(10), 1469–1472. <https://doi.org/10.1109/LED.2017.2732352>
- Lonsdale, W. (2018). *Development, manufacture and application of a solid-state pH sensor using ruthenium oxide* [Doctorate Theses, Edith Cowan University]. <https://ro.ecu.edu.au/theses/2095>
- Lonsdale, W., Maurya, D. K., Wajrak, M., & Alameh, K. (2017). Effect of ordered mesoporous carbon contact layer on the sensing performance of sputtered RuO<sub>2</sub> thin film pH sensor. *Talanta*, 164(November 2016), 52–56. <https://doi.org/10.1016/j.talanta.2016.11.020>
- Lonsdale, W., Shylendra, S. P., Brouwer, S., Wajrak, M., & Alameh, K. (2018). Application of ruthenium oxide pH sensitive electrode to samples with high redox interference. *Sensors and Actuators, B: Chemical*, 273(July), 1222–1225. <https://doi.org/10.1016/j.snb.2018.07.022>
- Lonsdale, W., Wajrak, M., & Alameh, K. (2017). Effect of conditioning protocol, redox species and material thickness on the pH sensitivity and hysteresis of sputtered RuO<sub>2</sub> electrodes. *Sensors and Actuators B: Chemical*, 252, 251–256. <https://doi.org/10.1016/j.snb.2017.05.171>

- Lonsdale, W., Wajrak, M., & Alameh, K. (2018). Manufacture and application of RuO<sub>2</sub> solid-state metal-oxide pH sensor to common beverages. *Talanta*, *180*(December 2017), 277–281. <https://doi.org/10.1016/j.talanta.2017.12.070>
- Loudon, K. M. W., Tarr, G., Lean, I. J., Polkinghorne, R., Mcgilchrist, P., Dunshea, F. R., Gardner, G. E., & Pethick, D. W. (2019). The impact of pre-slaughter stress on beef eating quality. *Animals*, *9*(612). <https://doi.org/10.3390/ani9090612>
- Lucero, A. M., Orozco, M., Navarro, N., & Collins, V. (2022). Sensitivity of Nafion Films to Organic Substances, Especially Ketones. *Advances in Polymer Technology*, *2022*. <https://doi.org/10.1155/2022/1025653>
- Lucey, J. A., Johnson, M. E., & Horne, D. S. (2003). Invited review: Perspectives on the basis of the rheology and texture properties of cheese. In *Journal of Dairy Science* (Vol. 86, Issue 9, pp. 2725–2743). American Dairy Science Association. [https://doi.org/10.3168/jds.S0022-0302\(03\)73869-7](https://doi.org/10.3168/jds.S0022-0302(03)73869-7)
- Manjakkal, L., Cvejic, K., Kulawik, J., Zaraska, K., Socha, R. P., & Szwagierczak, D. (2016). X-ray photoelectron spectroscopic and electrochemical impedance spectroscopic analysis of RuO<sub>2</sub>-Ta<sub>2</sub>O<sub>5</sub> thick film pH sensors. *Analytica Chimica Acta* *931*, 47–56. <https://doi.org/10.1016/j.aca.2016.05.012>
- Manjakkal, L., Cvejic, K., Kulawik, J., Zaraska, K., Szwagierczak, D., & Socha, R. P. (2014). Fabrication of thick film sensitive RuO<sub>2</sub>-TiO<sub>2</sub> and Ag/AgCl/KCl reference electrodes and their application for pH measurements. *Sensors and Actuators, B: Chemical*, *204*, 57–67. <https://doi.org/10.1016/j.snb.2014.07.067>
- Manjakkal, L., Cvejic, K., Kulawik, J., Zaraska, K., Szwagierczak, D., & Stojanovic, G. (2015). Sensing mechanism of RuO<sub>2</sub>-SnO<sub>2</sub> thick film pH sensors studied by potentiometric method and electrochemical impedance spectroscopy. *Journal of Electroanalytical Chemistry*, *759*, 82–90. <https://doi.org/10.1016/j.jelechem.2015.10.036>
- Manjakkal, L., Szwagierczak, D., & Dahiya, R. (2020). Metal oxides based electrochemical pH sensors: Current progress and future perspectives. *Progress in Materials Science*, *109*, 1–31. <https://doi.org/10.1016/j.pmatsci.2019.100635>
- Manjakkal, L., Zaraska, K., Cvejic, K., Kulawik, J., & Szwagierczak, D. (2016). Potentiometric RuO<sub>2</sub>-Ta<sub>2</sub>O<sub>5</sub> pH sensors fabricated using thick film and LTCC technologies. *Talanta*, *147*, 233–240. <https://doi.org/10.1016/j.talanta.2015.09.069>
- Matarneh, S. K., England, E. M., Scheffler, T. L., & Gerrard, D. E. (2017). The conversion of muscle to meat. In F. Toldra (Ed.), *Lawrie's Meat Science: Eighth Edition* (8th ed., pp. 159–185). Woodhead Publishing. <https://doi.org/10.1016/B978-0-08-100694-8.00005-4>
- Mauritz, K. A., & Moore, R. B. (2004). State of understanding of Nafion. *Chemical Reviews*, *104*(10), 4535–4585. <https://doi.org/10.1021/cr0207123>
- McMurray, H. N., Douglas, P., & Abbot, D. (1995). Novel thick-film pH sensors based on ruthenium dioxide-glass composites. *Sensors and Actuators: B. Chemical*, *28*(1), 9–15. [https://doi.org/10.1016/0925-4005\(94\)01536-Q](https://doi.org/10.1016/0925-4005(94)01536-Q)
- Metters, J. P., Kadara, R. O., & Banks, C. E. (2011). New directions in screen printed electroanalytical sensors: An overview of recent developments. *Analyst*, *136*(6), 1067–1076. <https://doi.org/10.1039/c0an00894j>
- Mihell, J. A., & Atkinson, J. K. (1998). Planar thick-film pH electrodes based on ruthenium dioxide hydrate. *Sensors and Actuators B*, *48*, 505–511.
- Mingels, R. H. G., Kalsi, S., Cheong, Y., & Morgan, H. (2019). Iridium and Ruthenium oxide miniature pH sensors: Long-term performance. *Sensors and Actuators, B: Chemical*, *297*(126779). <https://doi.org/10.1016/j.snb.2019.126779>

- Mo, X., Wang, J., Wang, Z., & Wang, S. (2003). Potentiometric pH responses of fibrillar polypyrrole modified electrodes. *Sensors and Actuators, B: Chemical*, *96*(3), 533–536. [https://doi.org/10.1016/S0925-4005\(03\)00634-8](https://doi.org/10.1016/S0925-4005(03)00634-8)
- Mu, B., Dong, Y., Qian, J., Wang, M., Yang, Y., Nikitina, M. A., Zhang, L., & Xiao, X. (2022). Hydrogel coating flexible pH sensor system for fish spoilage monitoring. *Materials Today Chemistry*, *26*, 101183. <https://doi.org/10.1016/j.mtchem.2022.101183>
- Mugica, M. M., McGuinness, K. L., & Lawrence, N. S. (2022). Electropolymerised pH Insensitive Salicylic Acid Reference Systems: Utilization in a Novel pH Sensor for Food and Environmental Monitoring. *Sensors*, *22*(2). <https://doi.org/10.3390/s22020555>
- Oketola, A., Jamiru, T., Adegbola, A. T., Ogunbiyi, O., Sadiku, R., & Salifu, S. (2022). Influence of sintering temperature on the microstructure, mechanical and tribological properties of ZrO<sub>2</sub> reinforced spark plasma sintered Ni–Cr. *International Journal of Lightweight Materials and Manufacture*, *5*(2), 188–196. <https://doi.org/10.1016/j.ijlmm.2022.01.002>
- Panjan, P., Virtanen, V., & Sesay, A. M. (2017). Determination of stability characteristics for electrochemical biosensors via thermally accelerated ageing. *Talanta*, *170*(April), 331–336. <https://doi.org/10.1016/j.talanta.2017.04.011>
- Parilla, M., Canovas, R., Jeerapan, I., Andrade, F. J., & Wang, J. (2016). A textile-based stretchable multi-ion potentiometric sensor. *Advanced Healthcare Materials*, *5*, 996–1001. <https://doi.org/10.1002/adhm.201600092>
- Park, H. J., Yoon, J. H., Lee, K. G., & Choi, B. G. (2019). Potentiometric performance of flexible pH sensor based on polyaniline nanofiber arrays. *Nano Convergence*, *6*(1). <https://doi.org/10.1186/s40580-019-0179-0>
- Pásztor, K., Sekiguchi, A., Shimo, N., Kitamura, N., & Masuhara, H. (1993). Electrochemically-deposited RuO<sub>2</sub> films as pH sensors. *Sensors and Actuators: B: Chemical*, *13*(14), 561–562. [https://doi.org/10.1016/0925-4005\(93\)85091-N](https://doi.org/10.1016/0925-4005(93)85091-N)
- Peighambardoust, S. J., Rowshanzamir, S., & Amjadi, M. (2010). Review of the proton exchange membranes for fuel cell applications. *International Journal of Hydrogen Energy*, *35*, 9349–9384. <https://doi.org/10.1016/j.ijhydene.2010.05.017>
- Perley, G. A., & Godshalk, J. B. (1947). *Cell for pH measurements* (Patent No. 2416949). U.S. Patent and trademark office.
- Phadungath, C. (2005). The mechanism and properties of acid-coagulated milk gels. *Songklanakarin J. Sci. Technol.*, *27*(2), 433–448.
- Pocrička, L. A., Gonçalves, C., Grossi, P., Colpa, P. C., & Pereira, E. C. (2006). Development of RuO<sub>2</sub>-TiO<sub>2</sub> (70-30) mol% for pH measurements. *Sensors and Actuators, B: Chemical*, *113*(2), 1012–1016. <https://doi.org/10.1016/j.snb.2005.03.087>
- Poghossian, A., Geissler, H., & Schöning, M. J. (2019). Rapid methods and sensors for milk quality monitoring and spoilage detection. *Biosensors and Bioelectronics*, *140*(April), 111272. <https://doi.org/10.1016/j.bios.2019.04.040>
- Remy, H. (1956). *Treatise on Inorganic Chemistry. Second volume*. Elsevier.
- Rosca, C. M., Popescu, M., Patrascioiu, C., & Stancu, A. (2019). Comparative Analysis of pH Level Between Pasteurized and UTH Milk Using Dedicated Developed Application. *Revista de Chimie*, *70*(11), 3917–3920. <http://www.revistadechimie.ro>
- Sardarnejad, A., Maurya, D. K., & Alameh, K. (2015). The pH sensing properties of RF sputtered RuO<sub>2</sub> thin-film prepared using different Ar/O<sub>2</sub> flow ratio. *Materials*, *8*(6), 3352–3363. <https://doi.org/10.3390/ma8063352>

- Selim, A., Szijjártó, G. P., & Tompos, A. (2022). Insights into the Influence of Different Pre-Treatments on Physicochemical Properties of Nafion XL Membrane and Fuel Cell Performance. *Polymers*, *14*. <https://doi.org/10.3390/polym14163385>
- Senthil Kumar, P., Sreeja, B. S., Krishna Kumar, K., & Padmalaya, G. (2022). Investigation of Nafion coated GO-ZnO nanocomposite behaviour for sulfamethoxazole detection using cyclic voltammetry. *Food and Chemical Toxicology*, *167*. <https://doi.org/10.1016/j.fct.2022.113311>
- Shaver, A., & Arroyo-Currás, N. (2022). The challenge of long-term stability for nucleic acid-based electrochemical sensors. *Current Opinion in Electrochemistry*, *32*, 100902. <https://doi.org/10.1016/j.coelec.2021.100902>
- Shim, J. H., Kang, M., Lee, Y., & Lee, C. (2012). A nanoporous ruthenium oxide framework for amperometric sensing of glucose and potentiometric sensing of pH. *Microchimica Acta*, *177*, 211–219. <https://doi.org/10.1007/s00604-012-0774-9>
- Shiu, K. K., Song, F. Y., & Lau, K. W. (1999). Effects of polymer thickness on the potentiometric pH responses of polypyrrole modified glassy carbon electrodes. *Journal of Electroanalytical Chemistry*, *476*(2), 109–117. [https://doi.org/10.1016/S0022-0728\(99\)00372-1](https://doi.org/10.1016/S0022-0728(99)00372-1)
- Syaizwadi, S. M., Noradilah, S. S., Sabri, M. G. M., Rafizah, W. A. W., Syara, K., & Lee, O. J. (2018). Effect of Sintering Temperature on Zinc Oxide Varistor Ceramics. *IOP Conference Series: Materials Science and Engineering*, *440*(1). <https://doi.org/10.1088/1757-899X/440/1/012037>
- Tan, T. J., Wang, D., & Moraru, C. I. (2014). A physicochemical investigation of membrane fouling in cold microfiltration of skim milk. *Journal of Dairy Science*, *97*, 4759–4771. <https://doi.org/10.3168/jds.2014-7957>
- Toldrá, F. (2017). The Storage and Preservation of Meat: III-Meat Processing. In F. Toldrá (Ed.), *Lawrie's Meat Science: Eighth Edition* (8th ed., pp. 265–296). Elsevier Ltd. <https://doi.org/10.1016/B978-0-08-100694-8.00009-1>
- Upreti, P., Metzger, L. E., & Bühlmann, P. (2004). Glass and polymeric membrane electrodes for the measurement of pH in milk and cheese. *Talanta*, *63*, 139–148. <https://doi.org/10.1016/j.talanta.2003.12.020>
- Vargas-Bernal, R., Rodríguez-Miranda, E., & Herrera-Prez, G. (2012). Evolution and expectations of enzymatic biosensors for pesticides. In *Pesticides - Advances in Chemical and Botanical Pesticides* (Issue Chapter 14, pp. 329–356). InTech. <https://doi.org/10.5772/46227>
- Xu, B., & Zhang, W. (2010). Modification of vertically aligned carbon nanotubes with RuO<sub>2</sub> for a solid-state pH sensor. *Electrochimica Acta*, *55*, 2859–2864. <https://doi.org/10.1016/j.electacta.2009.12.099>
- Xu, K., Zhang, X., Chen, C., & Geng, M. (2018). Development and performance of an all-solid-stated pH sensor based on modified membranes. *International Journal of Electrochemical Science*, *13*(3), 3080–3090. <https://doi.org/10.20964/2018.03.04>
- Xu, K., Zhang, X., Hou, K., Geng, M., & Zhao, L. (2016). The effects of antimony thin film thickness on antimony pH electrode coated with nafion membrane. *Journal of the Electrochemical Society*, *163*(8), B417–B421. <https://doi.org/10.1149/2.0191608jes>
- Yao, X., Vepsäläinen, M., Isa, F., Martin, P., Munroe, P., & Bendavid, A. (2020). Advanced RuO<sub>2</sub> Thin Films for pH Sensing Application. *Sensors*, *20*(6432). <https://doi.org/10.3390/s20226432>

- Yoon, J. H., Kim, S. M., Park, H. J., Kim, Y. K., Oh, D. X., Cho, H. W., Lee, K. G., Hwang, S. Y., Park, J., & Choi, B. G. (2020). Highly self-healable and flexible cable-type pH sensors for real-time monitoring of human fluids. *Biosensors and Bioelectronics*, *150*(November 2019), 111946. <https://doi.org/10.1016/j.bios.2019.111946>
- Zhang, Y., Zhu, Y., Zheng, S., Zhang, L., Shi, X., He, J., Chou, X., & Wu, Z.-S. (2021). Ink formulation, scalable applications and challenging perspectives of screen printing for emerging printed microelectronics. *Journal of Energy Chemistry*. <https://doi.org/10.1016/j.jechem.2021.08.011>
- Zhuyikov, S. (2009). Morphology of Pt-doped nanofabricated RuO<sub>2</sub> sensing electrodes and their properties in water quality monitoring sensors. *Sensors and Actuators, B: Chemical*, *136*(1), 248–256. <https://doi.org/10.1016/j.snb.2008.10.030>
- Zhuyikov, S. (2012). Solid-state sensors monitoring parameters of water quality for the next generation of wireless sensor networks. *Sensors and Actuators, B: Chemical*, *161*(1), 1–20. <https://doi.org/10.1016/j.snb.2011.10.078>
- Zhuyikov, S., Kats, E., Marney, D., & Kalantar-Zadeh, K. (2011). Improved antifouling resistance of electrochemical water quality sensors based on Cu<sub>2</sub>O-doped RuO<sub>2</sub> sensing electrode. *Progress in Organic Coatings*, *70*(1), 67–73. <https://doi.org/10.1016/j.porgcoat.2010.10.003>
- Zhuyikov, S., Marney, D., & Kats, E. (2011). Investigation of electrochemical properties of La<sub>2</sub>O<sub>3</sub>-RuO<sub>2</sub> thin-film sensing electrodes used in sensors for the analysis of complex solutions. *International Journal of Applied Ceramic Technology*, *8*(5), 1192–1200. <https://doi.org/10.1111/j.1744-7402.2010.02562.x>
- Zuaznabar-Gardona, J. C., & Fragoso, A. (2018). A wide-range solid state potentiometric pH sensor based on poly-dopamine coated carbon nano-onion electrodes. *Sensors and Actuators, B: Chemical*, *273*(January), 664–671. <https://doi.org/10.1016/j.snb.2018.06.103>



## Acknowledgements

I would like to thank the European Commission for supporting the research presented in this work through the Marie Skłodowska-Curie Actions (MSCA) Innovative Training Network (ITN) in wAter and Food Quality monitoring using Autonomous SENSors and IntelligENt Data Gathering and Analysis ([Aguasense](#)) project [H2020-MSCA-ITN-2018-813680]. I would like to personally thank Kiranmai Uppuluri and Nasrin Razmi for inspiring me to work harder on my project.

I would also like to thank the Center of Food and Fermentation Technologies (a.k.a. [TFTAK](#)) for being my host organization for 3 years and allowing me to use their premises to conduct my research.

I would like to thank my supervisor Ott Scheler for being a supervisor, who takes great care of his PhD students; for teaching me a lot about how to make my research more readable and interesting to the scientific community and society; for being understanding and supportive.

I would like to thank my family for supporting my decision to move to Estonia and get my PhD far away from home. I would like to thank my 'Estonian family' – Aleksandra Zahharova, Terje Tilk, and Iuliia Vetik – who were supporting me through the darkest time and who believed in me the most. Pursuing PhD is a journey and journeys are always easier and faster with friends. And I believe mine would have been impossible without these people.

## Abstract

### Screen-printed pH sensors based on ruthenium(IV) oxide for measurement in food samples

The quality of water and food on its basis (dairy, meat and fish products) is a matter of great concern. One of the most essential food quality parameters is pH. It can be used to monitor the quality of fermentation processes, evaluate freshness and reveal impurities in food samples. At present, pH of food products is determined by a standard potentiometric method based on the measurement of the electrochemical potential change between a pH-sensitive and a reference electrode immersed into the test solution. The glass electrodes in conventional pH meters are a combination of pH-sensitive and reference electrodes incorporated in one glass body. However, due to its high cost, fragility of the glass body of the electrode, possible contamination of samples and the reference junction, as well as inability of continuous measurement, glass electrode cannot be implemented for monitoring of on-line industrial processes. Therefore, novel materials and methods are thoroughly investigated.

One of the most investigated alternatives to conventional glass electrode is electrochemical sensors based on metal oxides. These sensors are easy to fabricate, exhibit good sensitivity and linear response, with some of them being compatible with conventional pH meters. Among the metal oxides, suitable for pH measurement, ruthenium(IV) oxide ( $\text{RuO}_2$ ) has proven itself to be the most beneficial one, due to its optimum performance characteristics, such as excellent pH sensitivity, low drift and hysteresis, consistent performance even in bacteria-rich environment. However, even though the  $\text{RuO}_2$ -based pH sensors exhibit excellent performance in aqueous media, the actual challenge is to make these sensors applicable to real-life samples due to the complexity of their composition.

This work presents research dedicated to improve the performance of  $\text{RuO}_2$  electrodes. The reliable pH measurement with the screen-printed  $\text{RuO}_2$  electrodes was achieved by covering them with a protective Nafion™ membrane. This manuscript is tackling on the (i) fabrication and properties of the  $\text{RuO}_2$  electrodes, (ii) fabrication and properties of the Nafion™ membrane, as well as (iii) application of the developed electrodes for measurement in food samples.

## Lühikokkuvõte

### Ruteenium(IV)oksiidil põhinevad siiditrükiga pH-andurid toiduproovide mõõtmiseks

Vee ja sellel põhineva toidu (piima-, liha- ja kalatooted) kvaliteedi kontroll on toidutööstuses väga oluline. Üks oluline toidukvaliteedi parameeter on pH. Seda saab kasutada käärimisprotsesside kvaliteedi jälgimiseks, toidu värskuse hindamiseks ja lisandite tuvastamiseks toiduproovides. Tavaliselt määratakse tänapäeval toiduainete pH standardse potentsiomeetrilise meetodiga, mis põhineb elektrokeemilise potentsiaali muutuse mõõtmisel pH-tundliku ja katselahusesse sukeldatud võrdluselektroodi vahel. Klaaselektroodid tavalistes pH-meetrites koosnevad pH-tundlikest ja võrdluselektroodidest, mis on ühendatud ühte klaasist korpusesse. Klaaselektroodi ei saa kasutada *on-line* tööstusprotsesside jälgimiseks kuna neil on kõrge hind, elektroodi klaaskeha on habras, and saastuvad kiiresti ja ei ned saa kasutada pideva mõõtmise režiimis. Seetõttu uuritakse põhjalikult uudeid alternatiivseid materjale ja meetodeid pH mõõtmiseks toidutööstuses.

Üks enim uuritud alternatiive tavapärasele klaaselektroodile on metalloksiididel põhinevad elektrokeemilised andurid. Neid andureid on lihtne valmistada, neil on hea tundlikkus ja lineaarne vastus ja mõned neist ühilduvad ka tavapäraste pH-meetritega. Ruteenium(IV) oksiid ( $\text{RuO}_2$ ) on osutunud kõige kasulikumaks metallioksiidiks pH mõõtmise jaoks tänu oma headele mõõtmis omadustele, nagu suurepärase pH tundlikkus, madal triiv ja hüsterees ja ühtlane töö isegi bakteririkas keskkonnas. Kuigi  $\text{RuO}_2$ -põhistel pH-anduritel on vesikeskkonnas suurepäraseid omadused on neid seni olnud väga keeruline rakendada kuna päriselu proovide jaoks tööstuses.

Selles doktoritöös pühenduti  $\text{RuO}_2$  elektroodide töökindluse parandamisele toidutööstuse jaoks. Usaldusväärne pH mõõtmine siiditrüki meetodil valmistatud  $\text{RuO}_2$  elektroodidega saavutati kui and olid kaetud kaitsva Nafion<sup>TM</sup> membraaniga. See käsikiri käsitleb (i)  $\text{RuO}_2$  elektroodide valmistamist ja omadusi, (ii) Nafion<sup>TM</sup> membraani valmistamist ja omadusi, samuti (iii) väljatöötatud elektroodide kasutamist toiduproovide analüüsil.

# Appendix 1

## Publication I

K. Uppuluri, M. Lazouskaya, D. Szwagierczak, K. Zaraska, and M. Tamm, "Fabrication, Potentiometric Characterization, and Application of Screen-Printed RuO<sub>2</sub> pH Electrodes for Water Quality Testing," *Sensors*, 21(16), 2021.



## Article

# Fabrication, Potentiometric Characterization, and Application of Screen-Printed RuO<sub>2</sub> pH Electrodes for Water Quality Testing

Kiranmai Uppuluri <sup>1</sup> , Maryna Lazouskaya <sup>2,3</sup> , Dorota Szwagierczak <sup>1,\*</sup> , Krzysztof Zaraska <sup>1</sup>  and Martti Tamm <sup>2</sup>

<sup>1</sup> Lukaszewicz Research Network—Institute of Microelectronics and Photonics, Kraków Division, ul. Zabłocie 39, 30-701 Kraków, Poland; kiranmai.uppuluri@imif.lukasiewicz.gov.pl (K.U.); krzysztof.zaraska@imif.lukasiewicz.gov.pl (K.Z.)

<sup>2</sup> Center of Food and Fermentation Technologies, Akadeemia tee 15A, 12618 Tallinn, Estonia; maryna.lazouskaya@tftak.eu (M.L.); martti@tftak.eu (M.T.)

<sup>3</sup> Department of Chemistry and Biotechnology, School of Science, Tallinn University of Technology, Ehitajate tee 5, 19086 Tallinn, Estonia

\* Correspondence: dorota.szwagierczak@imif.lukasiewicz.gov.pl

**Abstract:** Screen-printed sensing electrodes attract much attention for water pollution monitoring due to their small size, physical and chemical durability, and low cost. This paper presents the fabrication and broad potentiometric characterization of RuO<sub>2</sub> pH sensing electrodes deposited by screen printing on alumina substrates and sintered in the 800–900 °C temperature range. All the fabricated electrodes showed close to Nernstian sensitivity, good linearity, fast response, small drift, low hysteresis, and low cross-sensitivity toward various interfering cations and anions. Furthermore, decreasing the sintering temperature led to better adhesion of the RuO<sub>2</sub> layer and a negligible response to interfering ions. The measurements in real-life samples from different water sources showed that the fabricated electrodes are on par with conventional glass electrodes with a maximum deviation of 0.11 pH units, thus indicating their potential for application in water quality monitoring.

**Keywords:** ruthenium oxide; screen printing; pH electrode; potentiometric sensor; sintering temperature; water pollution monitoring



**Citation:** Uppuluri, K.; Lazouskaya, M.; Szwagierczak, D.; Zaraska, K.; Tamm, M. Fabrication, Potentiometric Characterization, and Application of Screen-Printed RuO<sub>2</sub> pH Electrodes for Water Quality Testing. *Sensors* **2021**, *21*, 5399. <https://doi.org/10.3390/s21165399>

Academic Editor: Peter Kruse

Received: 16 July 2021

Accepted: 7 August 2021

Published: 10 August 2021

**Publisher's Note:** MDPI stays neutral with regard to jurisdictional claims in published maps and institutional affiliations.



**Copyright:** © 2021 by the authors. Licensee MDPI, Basel, Switzerland. This article is an open access article distributed under the terms and conditions of the Creative Commons Attribution (CC BY) license (<https://creativecommons.org/licenses/by/4.0/>).

## 1. Introduction

The pollution of rivers and lakes creates a great danger for the environment and human health. Pollution can originate from industrial wastewaters, municipal sewage, and substances used in agriculture (fertilizers, pesticides, and manure). At present, the quality of water is determined against numerous parameters: electrical conductivity, turbidity, dissolved oxygen, toxic inorganic and organic substances, etc. [1]. However, the determination of all the parameters is time-consuming, and sometimes an express test is needed.

A change in pH can be a simple and fast signal of a pollution appearance in water [2,3]. Thus, the availability of cheap, accurate, and stable pH sensors is of high importance. pH sensors, developed in the last decades, vary in detection principles, sensing materials, and fabrication methods [3–9]. One of the most effective and inexpensive techniques of pH detection is the potentiometric method where the pH of the sample is determined by measuring the potential difference between a pH-sensitive electrode and a reference electrode. The value of the pH is calculated from the Nernst equation [10].

Among the sensing materials investigated for pH detection, metal oxide-based electrodes are well-known for their potential to overcome such drawbacks of glass electrode as fragility (and related risk of contamination with dangerous shattered glass) and poor stability in harsh conditions (strong alkaline or acidic solutions, high pressure, and high temperature) [11,12].

The pH sensing mechanism of metal oxide electrodes is governed by several electrochemical phenomena at the electrode–electrolyte interphase, including adsorption, dissociation, diffusion of ions, hydration, redox processes, electrical double layer formation, and charge transfer [13–16].

In their fundamental work [13], Fog and Buck analyzed the applicability and pH sensing mechanism of a few metal oxides: PtO<sub>2</sub>, IrO<sub>2</sub>, RuO<sub>2</sub>, OsO<sub>2</sub>, Ta<sub>2</sub>O<sub>5</sub>, and TiO<sub>2</sub>. Among the investigated metal oxides, ruthenium (IV) oxide (RuO<sub>2</sub>) was indicated as the most appropriate material for the pH-sensitive electrodes owing to its mixed electronic-ionic conductivity, relatively low sintering temperature, high sensitivity close to the Nernstian behavior, fast response, low hysteresis, broad pH diapason, resistance to corrosive conditions, chemical and thermal stability, and biocompatibility [6]. Furthermore, among the expensive oxides of the platinum metals group, RuO<sub>2</sub> is the cheapest one.

Several techniques were used for the deposition of ruthenium oxide-based pH-sensitive electrodes on a substrate. A lot of attention was paid to thin-film methods, including nanostructured film deposition from suspension [17,18], magnetron sputtering [19–23], sol-gel [24,25], the Pechini method [26,27], and electrodeposition [28]. Besides the investigation of pure RuO<sub>2</sub> layers, numerous studies were devoted to RuO<sub>2</sub> mixed or doped with other metal oxides (TiO<sub>2</sub> [26,29], Ta<sub>2</sub>O<sub>5</sub> [30], SnO<sub>2</sub> [31], Cu<sub>2</sub>O [18], and La<sub>2</sub>O<sub>3</sub> [32]), glasses [33–35], or carbon nanotubes [20,25].

Among thick-film methods, the most attractive is screen printing [30,35–38]. This technique is simple, cheap, and flexible in design and manufacturing, and typically provides relatively dense and mechanically strong layers with a thickness ranging from a few to a few tens of micrometers, well-adhering to different substrates. The screen-printing method consists of the deposition of layers of functional materials (metals, glass, and ceramics) on a suitable substrate. The pattern of each layer is fabricated by using a printable thick-film paste and a screen with a stainless steel or polyester mesh that has a predetermined design. A squeegee moves the paste across the screen and forces the material to pass through. After one layer of material has been printed, it undergoes thermal treatment.

The printable material usually consists of conductive, semiconducting, or dielectric particles mixed with binders (e.g., cellulose acetate), solvents (e.g., terpineol), and modifying agents [35,37]. For less demanding applications, cheap polymer-based thick-film pastes cured at low temperatures can be used. However, the best properties of screen printed layers, close to those of bulk functional materials, are attained after complete burnout of organic constituents and subsequent sintering at a proper high temperature (typically 850–900 °C for RuO<sub>2</sub>). To avoid oxidation of metallic components at high temperatures, increase conductivity and/or improve pH sensing performance, noble metal (Pt, Pd, Au) additives are often used in thick-film technology [36]. However, little attention has been paid so far to the influence of the sintering temperature on the properties of the fabricated pH-sensitive electrodes. Moreover, most of the previous research on RuO<sub>2</sub>-based pH electrodes used commercial pastes or mixed oxides and was conducted at a laboratory scale with applications limited to few types of water samples and beverages.

Here, we present the fabrication process and potentiometric investigation of RuO<sub>2</sub> pH electrodes sintered at three different temperatures: 800, 850, and 900 °C. The areas of investigation include performance characteristics such as sensitivity, response time, drift, hysteresis, and cross-sensitivity with other ions in the solution.

The aim of this work was to verify the applicability of fabricated electrodes for environmental, municipal, and industrial water quality monitoring and investigate their precision. To realize this goal, the pH of real-life samples from different water sources were measured using the RuO<sub>2</sub> electrodes and compared with the pH values obtained using a glass electrode. Additionally, cross-sensitivity of the fabricated RuO<sub>2</sub> electrodes to the ionic contaminants that can be found in environmental water due to overfertilization of agricultural lands was evaluated. Another important objective was to show that lowering the sintering temperature, which enables reduction of the environmental and economic impact

from the point of view of the firing process, does not negatively impact the performance of the pH electrode.

## 2. Materials and Methods

### 2.1. Preparation of RuO<sub>2</sub> Paste

Ruthenium oxide paste for screen printing was prepared by mixing anhydrous RuO<sub>2</sub> powder (density: 6.95 g/cm<sup>3</sup>, Sigma Aldrich, St. Louis, MO, USA) with ethyl cellulose (analytical grade purity) and terpineol (anhydrous, Fluka Analytical, Switzerland) in an agate mortar. Mixing was carried out for 20 min to achieve optimal consistency of the paste.

### 2.2. Fabrication of RuO<sub>2</sub> Electrodes for Potentiometric Sensors

Standard alumina (Al<sub>2</sub>O<sub>3</sub>, 96%) plates were chosen as the substrates for the pH electrodes due to their compatibility with thick films and high tolerance toward various environmental conditions. First, Ag/Pd thick-film paste (9695, Electro-Science Laboratories, King of Prussia, PA, USA) was screen-printed on the substrates, dried at 120 °C for 15 min, and fired at 860 °C for 30 min. Freshly prepared RuO<sub>2</sub> paste was then screen printed on the substrates in such a way that the RuO<sub>2</sub> layer slightly overlapped the Ag/Pd conducting layer. After drying at 120 °C for 15 min, electrodes were sintered at 800 °C (RuO<sub>2</sub>-800), 850 °C (RuO<sub>2</sub>-850), or 900 °C (RuO<sub>2</sub>-900) for one hour. Three RuO<sub>2</sub> electrodes were prepared for each sintering temperature. Next, electrical contact was attached to an open end of the conducting layer by soldering a copper wire. To avoid any contact between the conducting layer and the electrolyte, the electrical contact and the conducting layer were covered with noncorrosive polydimethylsiloxane coating (DOWSIL™ 3140 RTV Coating, Dow Chemical Company, Midland, MI, USA), and the sensitive area was left uncovered. Finally, the silicone resin cover was hardened at room temperature for 48 h. The schematic representation of the various stages of fabrication of RuO<sub>2</sub> electrodes is presented in Figure 1.

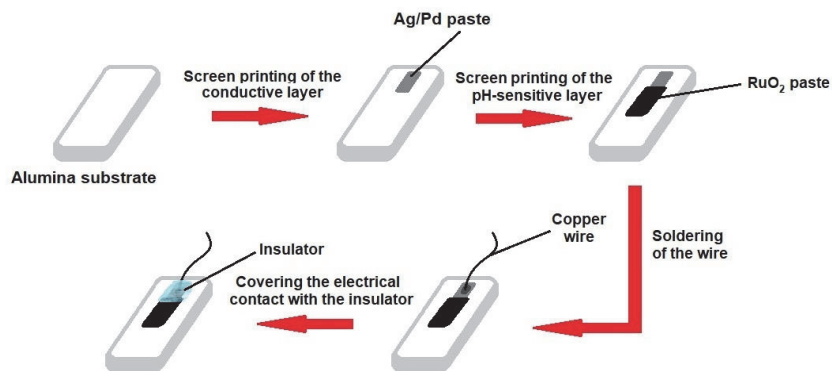


**Figure 1.** Schematic representation of the fabrication process of RuO<sub>2</sub> electrodes.

### 2.3. Microstructural Studies

Scanning electron microscopy (SEM) and energy dispersive spectroscopy (EDS) (Nova Nano SEM 200 with EDAX Genesis EDS system, FEI, Hillsboro, OR, USA) were used to examine the microstructure and elemental composition of the fabricated electrodes.

### 2.4. Electrochemical Studies

Electrode potential was measured by standard potentiometric technique. The fabricated RuO<sub>2</sub> electrodes were used as pH-sensitive electrodes; meanwhile, an ion-selective glass electrode (ISE, Ag|AgCl|KCl, Hydromet, Poland) was used as a reference electrode. To minimize signal loss, electrodes were attached to a unity gain buffer amplifier (LMC6044, Texas Instruments, Dallas, TX, USA) which was further connected to a voltage



input module (9205, National Instruments, Austin, TX, USA). LABVIEW software (National Instruments, Austin, TX, USA) was utilized to record all measured data.

#### 2.4.1. pH Measurements

Potentiometric determination of pH relies on selective identification of  $H^+$  ions present in the investigated solution [39]. The standard potentiometric setup consists of an electrochemical cell and a measuring device (potentiometer, voltmeter, multimeter, etc.). The electrochemical cell consists of a sensing electrode, sensitive to pH change, and a reference electrode (usually silver chloride electrode).

The electrical characteristic of an electrochemical cell is electromotive force (*Emf*). The *Emf* of the cell is determined as the difference in electrode potentials ( $E$ ) of the two half-reactions proceeding at the sensing and reference electrodes. Usually, the reference electrode is grounded, its potential is considered equal to zero, and the *Emf* of the cell is equal to the potential of the sensing electrode.

The half-reaction taking place on the sensing electrode is quantitatively explained by the Nernst equation:

$$E = E^0 - \frac{R \cdot T}{n \cdot F} \cdot \ln \frac{[Red]}{[Ox]}, \quad (1)$$

where  $E^0$  is standard potential,  $V$ ;  $R$  is the universal gas constant, 8.314 J/K·mol;  $T$  is temperature,  $K$ ;  $n$  is the number of the electrodes participating in the redox reaction;  $F$  is the Faraday constant, 96,485 C/mol; and  $[Red]$  and  $[Ox]$  are the activities of reduced and oxidized forms of the electrode material, respectively, mol/L. The standard potential is a measure of the individual potential of the reversible electrode (in equilibrium) in the standard state (concentration 1 mol/L, pressure 1 atmosphere and temperature 25 °C).

For the  $RuO_2$  electrode, the mechanism of pH-sensing can be explained by a simplified equation [11]:



The Nernst equation for this process takes the following form:

$$E = E^0_{Ru^{IV}/Ru^{III}} - \frac{R \cdot T}{n \cdot F} \cdot \ln \frac{[Ru^{III}]}{[Ru^{IV}] \cdot [H^+]}, \quad (3)$$

where  $[Ru^{III}]$ ,  $[Ru^{IV}]$ , and  $[H^+]$  are activities or  $Ru^{IV}O_2$ ,  $Ru^{III}O(OH)$ , and  $H^+$ , respectively, mol/L.

Considering that the values of metal activities approximate 1 in solid-state and substituting the constants, at room temperature ( $T = 22$  °C), Equation (3) takes the following form:

$$E = E^0_{Ru^{IV}/Ru^{III}} - 0.0583 \cdot \lg [H^+] \quad (4)$$

The value of 58.3 mV is called electrode sensitivity or theoretical Nernst response at  $T = 22$  °C. At the given temperature, the sensitivity value should be the same for all the pH-sensitive electrodes when  $n = 1$ . However, in practice deviation from the theoretical response is observed (see Table S1) [33,34,40].

As a conditioning protocol, all electrodes were immersed in distilled water for 24 h prior to their first measurement in order to hydrate pH-sensitive surfaces.

The sensitivity of the fabricated electrodes was determined by measuring the *Emf* of the electrochemical cell (the potential difference between the reference electrode and the fabricated pH-sensitive electrode) as a function of pH. For that, electrodes were submerged into buffer solutions of pH range from 1 to 14. Buffers were purchased from Chempur (Piekary Śląskie, Poland) and used as received. The pH of the solution was monitored with a combined glass electrode (ELMETRON, Zabrze, Poland).

The *Emf* was recorded for 5 min with data points being collected every 10 s. The *Emf* at the specific pH was determined as the average value of the last 10 data points. Electrode sensitivity,  $E^0$ , and linearity of the response were determined by plotting the electrode potential as a function of pH and calculating the equation describing this dependency

using the least-squares approach. Electrode sensitivity was calculated as the slope of the linear equation,  $E^0$  was calculated as the potential at pH = 0 by extrapolating the data, and the linearity of the response of the electrode to pH change was calculated as correlation coefficient ( $R^2$ ).

#### 2.4.2. Response Time, Drift Rate, and Hysteresis

The response time was determined as the time needed for the electrode potential to reach 90% of the stable value.

To measure the drift of electrode response in time, electrodes were left overnight in distilled water, and the drift rate (in mV/h) was calculated using the slope of the line-of-best-fit approach.

To study the hysteresis, the memory effect of an electrode, the fabricated electrodes were exposed to a series of pH buffers. First, the electrodes were exposed to a pH change from acidic to basic (pH change 1.1 → 4.1 → 7.0 → 10.0 → 13.4), and then, the same pH changes were carried out in the opposite direction. Electrode response was recorded for 3 min after submerging the electrode into a new buffer solution. Electrodes were washed with distilled water and dried with a pressure gun after each measurement.

#### 2.4.3. Cross-Sensitivity

The interference of ions with the performance of the fabricated  $\text{RuO}_2$  electrodes was evaluated by measuring the *Emf* of the cell and determining the sensitivity of the electrodes in the presence of KCl,  $\text{KNO}_3$ ,  $\text{NH}_4\text{NO}_3$ , and  $(\text{NH}_4)_3\text{PO}_4$ . For that, the abovementioned salts were added to buffer solutions to reach the concentration of 0.01 M. Electrodes were immersed into the samples for 5 min, and their *Emf* response was recorded.

#### 2.5. Measurements of Real-Life Samples

The fabricated electrodes were used to measure the pH values of different types of water samples: distilled and tap water, mineral water and water from a river and two lakes. Samples were stored at 4 °C prior to any measurement.

Commercially available “Wysoviańska” still water was used as mineral water. River water samples were collected from the Vistula River (Kraków, Poland).

Lake water samples were collected from Zakrzówek Lake (Lake Z, Kraków, Poland, Figure 2a) from the surface and the depth of 6 m and the surface of a mountain lake—Lake M (Lake Morskie Oko in Tatra Mountains, Poland, Figure 2b).

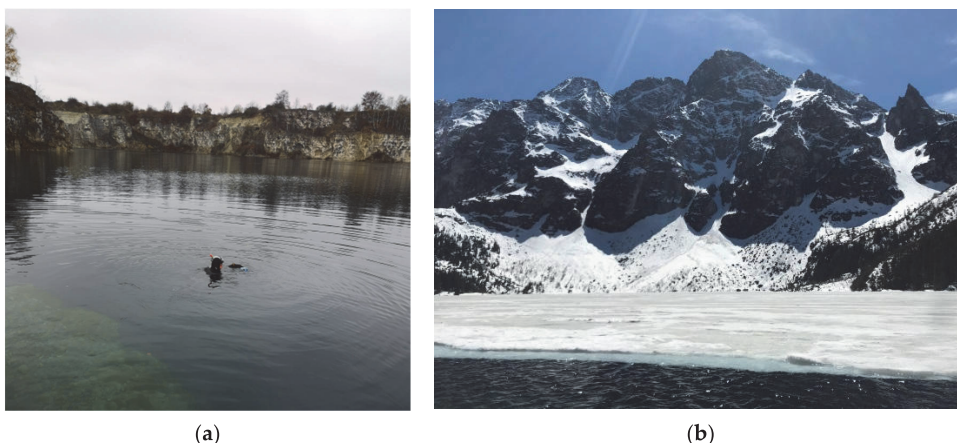


**Figure 2.** (a) Diver collecting samples from Zakrzówek Lake in Kraków, Poland, and (b) Lake Morskie Oko in Tatra Mountains, Poland.

### 3. Results and Discussion

#### 3.1. Microstructure of RuO<sub>2</sub> Electrodes

Thermal treatment temperature was previously shown to affect the properties of metal oxide solid-state electrodes due to change in relative density and/or crystallinity with temperature. The sensing layer morphology significantly impacts its sensing performance [17,21,41,42]. For the fabricated RuO<sub>2</sub> electrodes, there was only a slight change in surface morphology and microstructure of the layers sintered at different temperatures in the range of 800–900 °C. The EDS analysis confirmed the presence of both ruthenium and oxygen in the fabricated pH-sensitive layers. SEM images of fractured cross-sections of the electrodes screen printed on Al<sub>2</sub>O<sub>3</sub> substrates (Figure 3) indicated that both the RuO<sub>2</sub>-800 and the RuO<sub>2</sub>-900 electrodes were characterized by small porosity and uniform, fine-grained microstructure with grain sizes of 0.5–2 μm. However, for RuO<sub>2</sub>-800 electrodes (Figure 3a), improved adhesion to the substrate was observed, probably due to their lower porosity related to densification proceeding with a higher contribution of the amorphous phase at grain boundaries. Higher content of pores in the sensing layer can entail scattering of the charge carriers, leading to reduced carrier mobility and decreased sensitivity [41].

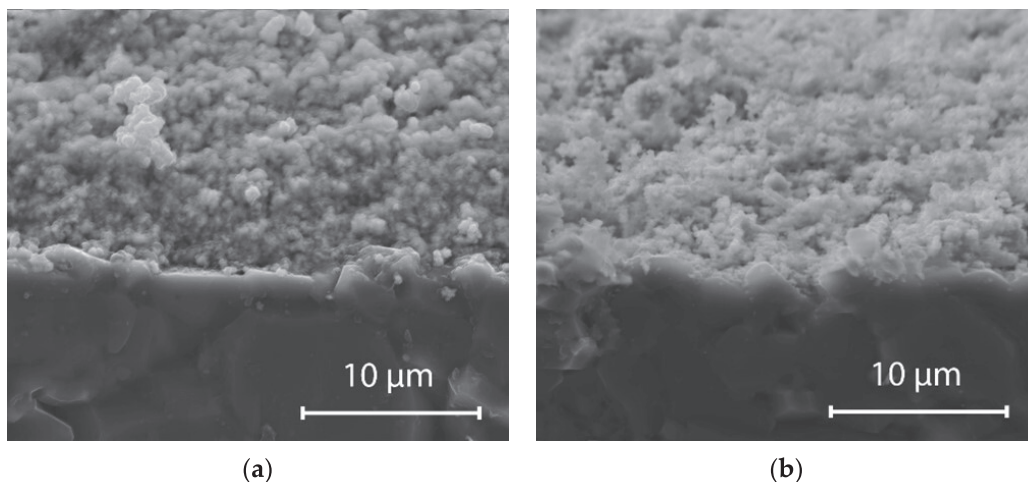


**Figure 3.** SEM images of the cross-sections of fired electrodes screen printed on alumina substrate: (a) RuO<sub>2</sub>-800 and (b) RuO<sub>2</sub>-900.

#### 3.2. Sensitivity of the Fabricated Electrodes

Sensitivity is the key characteristic of an electrode that allows determining if the electrode is working properly. The pH sensitivity of the fabricated RuO<sub>2</sub> electrode was determined by exposing the electrodes to buffer solutions of different pH and calculating the slope of the Nernst equation for the electrodes based on measured *Emf*. The results are presented in Figure 4 and Table 1. It can be seen that the sensitivity is close to the theoretical response with good linearity ( $R^2 = 0.994 - 0.996$ ) for all the electrodes. Furthermore, the sensitivity values are slightly decreasing with an increase in sintering temperature. Therefore, decreasing the sintering temperature of the RuO<sub>2</sub> pH electrodes does not negatively impact their sensitivity and can be implemented to reduce the power consumption that is needed to achieve higher firing temperatures in the furnace.

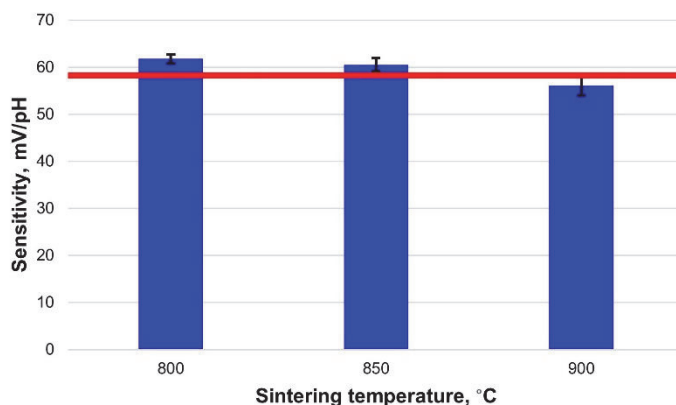


**Figure 4.** Comparison of the sensitivity of the fabricated electrodes sintered at different temperatures with the theoretical Nernstian response (red line).

**Table 1.** Potentiometric characteristics of the fabricated electrodes.

Electrode Type	Sensitivity, mV/pH		$E^0$ , mV	$R^2$	Response Time, s		Drift Rate, mV/h
	Theoretical	Observed			pH ≤ 7	pH > 7	
RuO <sub>2</sub> -800	58.9	61.8 ± 1.0	681.9 ± 5.0	0.996	2 ± 0	36 ± 1	0.1–0.2
RuO <sub>2</sub> -850		60.5 ± 1.4	664.2 ± 11.3	0.994	2 ± 0	34 ± 0	0.1–0.9
RuO <sub>2</sub> -900		56.1 ± 2.1	624.0 ± 27.9	0.996	2 ± 0	26 ± 2	0.1–0.4

The sensitivity of the pH electrodes under investigation became stable almost immediately. Moreover, the response is faster than that of the RuO<sub>2</sub> electrodes fabricated from the commercial paste containing a glass addition [43].

### 3.3. Long-Term Stability and Repeatability

It was previously shown that solid-state electrodes might require some time to reach stable sensitivity values [17,29]. However, no significant change in sensitivity for all the fabricated electrodes was noticed over two weeks of usage (Figure 5, Table S2). The daily variation in temperature was taken into account, and the observed sensitivity values were normalized according to expected theoretical sensitivity at a given temperature. The sensitivity values of RuO<sub>2</sub>-800, RuO<sub>2</sub>-850, and RuO<sub>2</sub>-900 electrodes remained close to the theoretical value and did not significantly change over time. Furthermore, the decrease in sensitivity with sintering temperature, observed during the first usage of the electrodes, did not occur during further measurements.

The porosity and surface oxidation states of the RuO<sub>2</sub> layer can be impacted due to the ageing of an electrode [17]. Nevertheless, in our study, ageing did not impact the pH sensing properties of the electrodes even though they were only conditioned once before the first measurement. The pH sensitivity of RuO<sub>2</sub>-850 and RuO<sub>2</sub>-900 electrodes fabricated six months earlier and stored in the air was only reduced by 2.7 and 6.5 mV/pH, respectively. For general water quality monitoring, the pH is not expected to change very rapidly and frequently. However, the fabricated electrodes were repeatedly subjected to fast changes in pH range 1–13.4. The stability in sensitivity over days thereby exhibits the endurance of RuO<sub>2</sub> to multiple measurements in electrolytes with varying pH across a wide range. Therefore, fabricated electrodes exhibit not only long-term stability in operation but also have a long shelf life. Moreover, the loss in sensitivity over 6 months was lower at a lower sintering temperature.

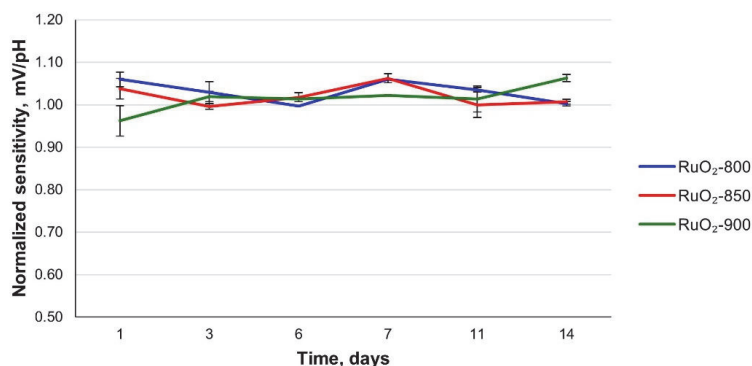


**Figure 5.** Sensitivity of the RuO<sub>2</sub>-800, RuO<sub>2</sub>-850, and RuO<sub>2</sub>-900 electrodes as a function of time.

### 3.4. Drift and Response Time

For continuous measurements that can last for hours, an important characteristic of an electrode is the drift rate. Drift rate is used to evaluate if the readings of an electrode maintain the same over a long period of observation. The values of the drift rate for the electrodes are presented in Table 1. These values remained small and did not exceed 1 mV/h.

Both the potential drift of an electrode and the response time are closely related to the mechanisms that govern them. Based on the material composition, drift of the  $E_{mf}$  during pH measurement in RuO<sub>2</sub> electrodes can be caused due to slow hydration of the pH-sensitive layer or slow H<sup>+</sup> ions diffusion [17]. Other critical aspects of the RuO<sub>2</sub> electrode that determine the drift of potential are homogeneity, porosity and thickness of the pH-sensitive layer, and composition and structure of the pH-sensitive material [17]. For a given temperature and electrode composition, the drift rate is expected to be small as it does not significantly depend on the interface between the pH-sensitive surface and the electrolyte, while pores at grain boundaries trapping H<sub>2</sub> govern the H<sup>+</sup> ions transport through this layer [17]. Therefore, the low drift rate related to fast surface hydration and H<sup>+</sup> diffusion experienced by the fabricated RuO<sub>2</sub> electrodes could be attributed to their single-phase composition without additives and the uniform microstructure.

Response time is the characteristic that tells how long one needs to wait before the electrode reaches stable potential readings. Response time plays an important role when a fast change in pH must be detected. All the fabricated electrodes showed a response time of 2–36 s (Table 1).

The disadvantage of pure RuO<sub>2</sub> could be lesser adhesion to the substrate [17]. To overcome it, glass can be added to the screen-printing paste [33,35]. However, the addition of glass has been reported to increase the response time due to reduced porosity of the printed layer and diffusion rate of protons [6]. The choice of the best RuO<sub>2</sub>-based composition is therefore strongly dependent on the requirements of the user and the area of the sensor application. In our research, we have similarly experienced that the layer made of commercial RuO<sub>2</sub> paste containing glass particles adheres better to the alumina substrate than a layer of pure RuO<sub>2</sub>. However, the slightly weaker mechanical strength and integrity of the latter do not impact its sensitivity to pH as shown in Section 3.2.

The response at the pH < 7.0 is almost instantaneous (2 s). However, as the pH increases, the response time also increases, and at pH 13, the maximum response time of 52 s is observed. The negative effect of pH increase on the response time can be attributed to the low concentration of H<sup>+</sup> ions at higher pH values [6]. Furthermore, compared to the OH<sup>−</sup> ions that are bigger and diffuse more slowly, H<sup>+</sup> ions are small, which makes their diffusion in the RuO<sub>2</sub> layer faster and therefore facilitates relevant ion exchange [6].

### 3.5. Hysteresis

Another important characteristic of an electrode is hysteresis. Differences in the *Emf* values at the same pH occur when the measurement is repeated multiple times. The analysis of this phenomenon, also known as the memory effect, allows for estimating if the previous measurement affects the consequent. To evaluate the hysteresis, the fabricated electrodes were exposed to a series of pH buffer changes. The RuO<sub>2</sub> electrodes exhibited a small hysteresis effect (Figure 6). All the fabricated electrodes showed hysteresis values not exceeding 21 mV when the pH changing started from the acidic region (1.1 → 13.4 → 1.1). For the opposite direction of pH change (13.4 → 1.1 → 13.4), the hysteresis values did not exceed 25 mV. These results show that all electrodes have a proper response to pH changes. The lowest hysteresis was observed for the RuO<sub>2</sub>-850 electrodes.

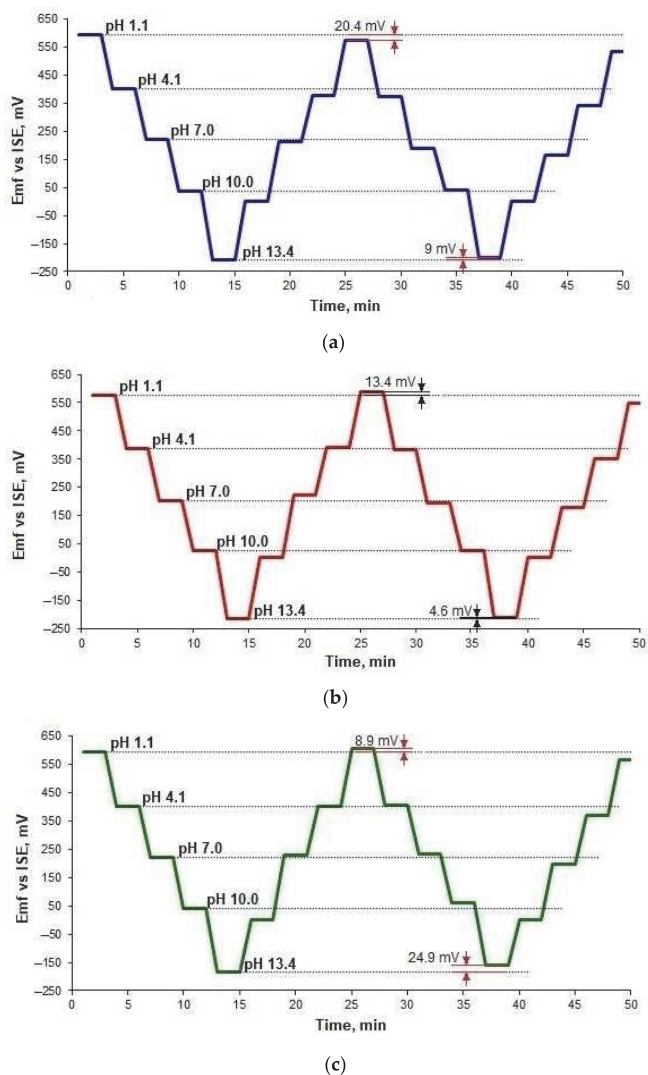


**Figure 6.** Hysteresis of the RuO<sub>2</sub>-800 (a), RuO<sub>2</sub>-850 (b), and RuO<sub>2</sub>-900 (c) electrodes for the pH 1.1→4.1→7→10→13.4→10→7→4.1→1.1→4.1→7→10→13.4→10→7→4.1→1.1 loop.

The pH measurement loop and crystalline properties of the pH-sensitive material are two factors that mainly influence the hysteresis effect in metal oxide-based pH electrodes [6]. The hysteresis effect in this study was higher for all electrodes when pH change started from the basic to acidic region ( $13.4 \rightarrow 1.1 \rightarrow 13.4$ ) because  $\text{OH}^-$  ions diffuse slower than  $\text{H}^+$  ions in the  $\text{RuO}_2$  layer. This finding is in agreement with previous studies [6,20,23]. However, it can be seen that similar to the response time, the hysteresis effect was also lower for higher sintering temperature, which may be attributed to higher porosity.

### 3.6. Cross-Sensitivity

One of the main limitations of the usage of metal oxide pH electrodes is the sensitivity of the electrode to interfering ions. The interferences caused by various ions were investigated by measuring the sensitivity in the presence of  $\text{K}^+$  and  $\text{NH}_4^+$  cations and  $\text{Cl}^-$ ,  $\text{NO}_3^-$ , and  $\text{PO}_4^{3-}$  anions. The observed pH sensitivities in the presence of the interfering ions for all three types of electrodes are listed in Table 2. Furthermore, Table S1 presents the comparison of electrode properties and sensitivity characteristics of  $\text{RuO}_2$ -based pH sensors reported previously by other authors with those obtained in this work.

**Table 2.** Sensitivity characteristics of the electrodes in presence of interfering salts.

	Sensitivity, mV/pH	$E^0$ , mV	$R^2$
$\text{RuO}_2$ -800			
No added salt	$59.1 \pm 0.2$	$647.0 \pm 0.1$	0.982
KCl	$58.9 \pm 1.1$	$630.3 \pm 18.9$	0.992
$\text{KNO}_3$	$59.7 \pm 0.2$	$684.3 \pm 3.8$	0.999
$\text{NH}_4\text{NO}_3$	$58.5 \pm 0.6$	$633.9 \pm 6.5$	1.000
$(\text{NH}_4)_3\text{PO}_4$	$58.0 \pm 2.3$	$686.15 \pm 0.0$	0.998
$\text{RuO}_2$ -850			
No added salt	$59.0 \pm 0.4$	$642.4 \pm 0.7$	0.998
KCl	$55.8 \pm 0.2$	$585.3 \pm 41.7$	0.996
$\text{KNO}_3$	$54.4 \pm 2.2$	$550.8 \pm 100.1$	0.997
$\text{NH}_4\text{NO}_3$	$59.0 \pm 0.8$	$642.0 \pm 0.2$	1.000
$(\text{NH}_4)_3\text{PO}_4$	$57.0 \pm 1.4$	$654.3 \pm 16.1$	0.995
$\text{RuO}_2$ -900			
No added salt	$61.5 \pm 1.1$	$645.6 \pm 17.0$	0.998
KCl	$56.4 \pm 0.6$	$642.3 \pm 14.5$	0.999
$\text{KNO}_3$	$58.0 \pm 0.7$	$674.9 \pm 14.2$	0.999
$\text{NH}_4\text{NO}_3$	$57.9 \pm 0.3$	$629.4 \pm 1.3$	0.999
$(\text{NH}_4)_3\text{PO}_4$	$59.9 \pm 1.0$	$695.2 \pm 13.1$	0.996

The  $E_{mf}$  versus pH plots for the  $\text{RuO}_2$ -800 electrode in the presence of interfering ions are presented in Figure 7. For  $\text{RuO}_2$ -850 and  $\text{RuO}_2$ -900 electrodes, similar behavior was observed. All the fabricated electrodes exhibited close to the Nernstian response and did not show any significant deviation from the theoretical sensitivity in distilled water when no salt was added (Table 2).

In general, the effect of the interfering salts was small, especially for  $\text{RuO}_2$ -800 sensing electrodes fired at the optimal temperature of  $800^\circ\text{C}$ . However, in the case of  $\text{RuO}_2$ -850 and  $\text{RuO}_2$ -900 electrodes, a decrease in sensitivity was observed. The maximum impact observed was a reduction of  $5.1\text{ mV/pH}$  for  $\text{RuO}_2$ -850 in the presence of  $0.01\text{ mol/L}$  of KCl.  $\text{K}^+$  ion is smaller in size as compared to  $\text{NH}_4^+$ , and therefore, it has higher mobility. Due to its faster diffusion into the double layer at the sensing surface of the  $\text{RuO}_2$  electrode, it influences the sensitivity of the electrode more than the bigger and slower  $\text{NH}_4^+$  cation. The most distinct deviation in the  $E^0$  potential observed for  $(\text{NH}_4)_3\text{PO}_4$  (for  $\text{RuO}_2$ -800 and  $\text{RuO}_2$ -900 electrodes) implies that the phosphate changes the contribution of  $\text{Ru}^{4+}$  and  $\text{Ru}^{3+}$  ions governing the redox reaction in the sensing layer. Such shifts in the  $E^0$  values

were attributed by Lonsdale et al. [21] to the changes in the  $\text{Ru}^{4+}/\text{Ru}^{3+}$  ratio caused by oxidizing/reducing agents.

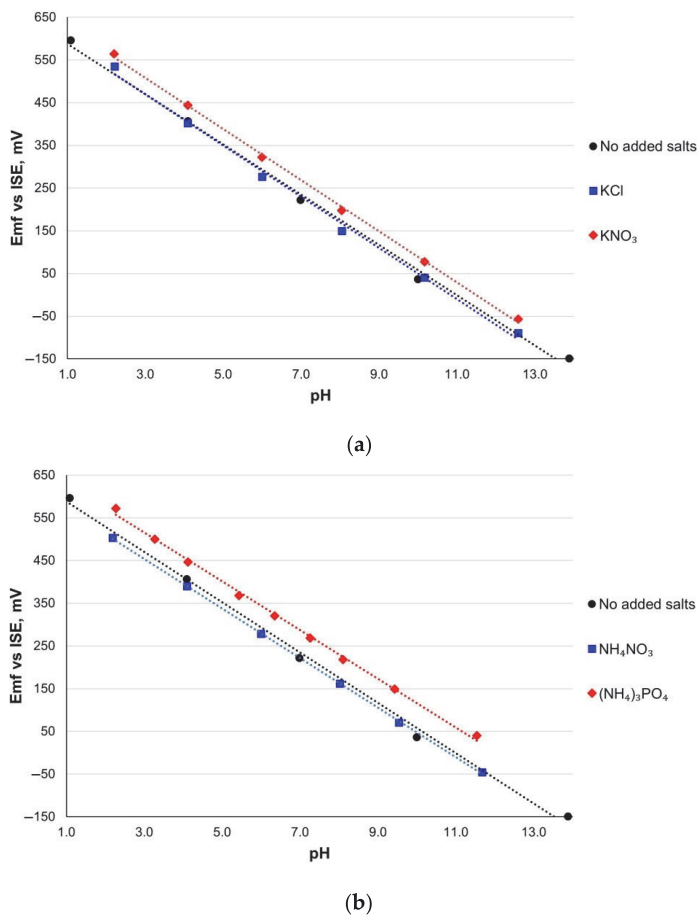


**Figure 7.** The electrochemical response of the RuO<sub>2</sub>-800 electrodes to the pH change in the presence of (a) potassium salts: (a) KCl and KNO<sub>3</sub> and (b) ammonia salts: NH<sub>4</sub>NO<sub>3</sub> and (NH<sub>4</sub>)<sub>3</sub>PO<sub>4</sub> in comparison with the response without added salts.

The lack of interference from various ions in the solution may be due to the undoped composition of the sensing layer based on pure RuO<sub>2</sub> used to fabricate the sensors. In the study by Labrador et al. [38], where commercial RuO<sub>2</sub> paste was used, interference from halides, carbonates, and sulfates were attributed to the presence of lead (II) oxide (PbO), which causes the formation of insoluble products with the anions. Commercial RuO<sub>2</sub> paste contains lead borosilicates because it aids in modifying material properties such as temperature coefficient of expansion of the glass phase [44]. Pocrifka et al. [26] reported a pH electrode developed by mixing RuO<sub>2</sub> with 30 mol.% TiO<sub>2</sub> that was insensitive toward cations (Li<sup>+</sup>, Na<sup>+</sup>, and Ca<sup>2+</sup>) without a significant improvement in the pH sensitivity when compared to the undoped RuO<sub>2</sub> electrode.

In this study, it was stated that a pure RuO<sub>2</sub> sensing electrode is capable of being uninfluenced by various interfering ions without the addition of lead borosilicate-based glass phase or TiO<sub>2</sub>. This indicates that the addition of PbO to RuO<sub>2</sub> only assists in improving the thick-film properties of the pH electrode, such as sheet resistivity, adhesion, low temperature coefficient of resistance, and low noise indices [44]. Similarly, the advantage



of adding TiO<sub>2</sub> is less related to improvement in sensitivity and selectivity, and it has more to do with lowering the cost [26] and avoiding corrosion by oxidation of RuO<sub>2</sub> to RuO<sub>4</sub> or RuO<sub>4</sub><sup>2-</sup> [45]. Therefore, the additives to pure RuO<sub>2</sub> may have an adverse, favorable, or neutral impact on the cross-sensitivity of the pH electrode depending on the properties of the additive, and the decision of their use rests upon the requirements and priorities of the researchers and manufacturers.

All the compounds used in the cross-sensitivity experiment performed in this study are also agricultural fertilizers used for plant growth, and the combined presence of nitrogen, phosphorus, and potassium in the composition gives such fertilizers the common name N-P-K fertilizers. Albeit their great contribution to tackling the ever-growing global demand for food, N-P-K fertilizers are also notorious for nutrient pollution through groundwater contamination and surface run-off from farms to in-land waters. In order to be absorbed by the plant's root hair cells, fertilizers must be soluble in water, and the water solubility of KNO<sub>3</sub>, KCl, and NH<sub>4</sub>NO<sub>3</sub> is 100%, whereas for (NH<sub>4</sub>)<sub>3</sub>PO<sub>4</sub>, it is 35% [46]. Therefore, the low cross-sensitivity of fabricated RuO<sub>2</sub> pH electrodes makes them suitable for measurement in water that has been contaminated by fertilizers and is rich in nutrients. Applicability of such pH sensing without interference from ions such as K<sup>+</sup>, NO<sub>3</sub><sup>-</sup>, NH<sub>4</sub><sup>+</sup>, and PO<sub>4</sub><sup>3-</sup> ranges from water quality monitoring in agriculture to municipal and industrial wastewater treatment.

### 3.7. Performance of pH Electrodes in Real-Life Water Samples

The fabricated electrodes were tested in several water samples to evaluate their applicability to real-life measurements. The results obtained for distilled, mineral, tap, river, and lake water are presented in Table 3. The pH values measured with the fabricated electrodes were similar to those measured with a conventional glass electrode with the maximum discrepancy of 0.11 pH units observed for Lake M water samples. Furthermore, all the fabricated electrodes showed good uniformity of the measured pH value, with the standard deviation not exceeding 0.13 pH units.

**Table 3.** pH values of water samples measured with a glass electrode and the fabricated RuO<sub>2</sub> electrodes.

Water Sample	pH Values Measured with			
	Glass Electrode	RuO <sub>2</sub> -800	RuO <sub>2</sub> -850	RuO <sub>2</sub> -900
Distilled water	7.30	7.29 ± 0.04	7.29 ± 0.01	7.27 ± 0.00
Mineral water	5.74	5.75 ± 0.01	5.74 ± 0.01	5.75 ± 0.00
Tap water	8.32	8.35 ± 0.05	8.39 ± 0.01	8.33 ± 0.07
River water	8.05	8.12 ± 0.01	8.11 ± 0.00	8.12 ± 0.00
Lake Z water (surface)	8.04	7.97 ± 0.11	8.04 ± 0.01	7.93 ± 0.02
Lake Z water (deep)	8.12	8.06 ± 0.07	8.13 ± 0.01	8.08 ± 0.11
Lake M water (surface)	6.75	6.84 ± 0.08	6.83 ± 0.11	6.86 ± 0.13

The highest difference between the measurement by glass electrode and the fabricated RuO<sub>2</sub> electrodes was only 0.11 units for surface water of Lake Z and Lake M measured by RuO<sub>2</sub>-900 electrode. The RuO<sub>2</sub>-850 electrode exhibited the closest to the glass electrode pH value and a very small variation (±0.01 pH units) in parallel readings for all water samples except Lake M water.

The industrially manufactured and commercially available mineral water tested in this study contains cations such as Na<sup>+</sup>, Ca<sup>+</sup>, Mg<sup>+</sup>, and K<sup>+</sup>, and anions such as HCO<sub>3</sub><sup>-</sup>, SO<sub>4</sub><sup>2-</sup>, Cl<sup>-</sup>, and F<sup>-</sup>. In 2017, an analysis of municipal tap water in Krakow, Poland, revealed the presence of calcium, magnesium, and nitrates in it [47]. The quality of water in the Vistula River is quite impacted by urbanization, and a high content of contaminants such as NH<sub>4</sub><sup>+</sup>, K<sup>+</sup>, Ca<sup>2+</sup>, Mg<sup>2+</sup>, Zn<sup>2+</sup>, Mn<sup>2+</sup>, Fe<sup>2+</sup>, Fe<sup>3+</sup>, etc., can be found in it [48]. Until 1991, Lake Z was an upper Jurassic limestone quarry, and a 2003 study by Galas [49] reported high conductivity and chloride content of water due to infiltration from the nearby Vistula

River. Lake M was reported to have a cadmium concentration of about  $0.13 \text{ mg/dm}^3$  due to anthropogenic activities [50].

The obtained results of the measurements of the water samples highlight the effectiveness of the fabricated  $\text{RuO}_2$  pH electrodes in the presence of various chemical species and elements. Therefore, reported electrodes are capable of functioning accurately in environmental, industrial, and municipal water quality monitoring.

#### 4. Conclusions

Thick-film pH-sensitive electrodes based on pure  $\text{RuO}_2$  without the addition of glass or other metal oxides were successfully prepared by screen printing and subsequent sintering at different temperatures. Excellent sensing characteristics were attained owing to the single-phase composition of the electrodes, their high conductivity, and good electrochemical and catalytic properties of  $\text{RuO}_2$ . The advantageous properties comprised the Nernstian behavior in a broad pH range of 1–13 with the sensitivity of 56.1–61.8 mV/pH, fast response of 2 s for  $\text{pH} \leq 7$ , low hysteresis, good long-term stability, and high resistance to cross-sensitivity from various interfering cations and anions. The analysis of the influence of sintering temperature of  $\text{RuO}_2$  electrodes on the performance of potentiometric pH electrodes showed small differences for the samples sintered at 800, 850, and 900 °C. However, a sintering temperature of 800 °C should be preferred not only from the economic and ecological point of view but also for the better adhesion of the  $\text{RuO}_2$  layer to the alumina substrate and its lowest cross-sensitivity. Furthermore, the excellent applicability of the fabricated electrodes for the pH measurements of real-life water samples (tap, mineral, river, and lake water) was proved in this work. The water samples used in the study exposed the  $\text{RuO}_2$  pH-sensitive layers to a variety of chemical elements, and the precise pH measurement in such conditions showed their ability to function correctly in different environments. In most water samples, the electrodes sintered at 850 °C showed the best precision and repeatability. The developed screen-printed potentiometric electrodes seem to be promising candidates for online monitoring systems of water quality due to their excellent pH sensing performance and potential for miniaturization and wireless measurement data transfer.

**Supplementary Materials:** The following are available online at <https://www.mdpi.com/article/10.3390/s21165399/s1>: Table S1. Summary of  $\text{RuO}_2$ -based pH electrode characteristics reported previously and in this work, Table S2. Change of the sensitivity of the fabricated electrodes with time.

**Author Contributions:** Conceptualization, K.U. and D.S.; methodology, K.U., M.L., and D.S.; software, K.Z.; validation, K.U.; formal analysis, K.U. and M.L.; investigation, K.U.; resources, K.U., K.Z.; data curation, K.U.; writing—original draft preparation, K.U., M.L., and D.S.; writing—review and editing, M.L. and D.S.; visualization, K.U. and M.L.; supervision, D.S.; project administration, K.Z., M.T.; funding acquisition, K.Z. and M.T. All authors have read and agreed to the published version of the manuscript.

**Funding:** This research was funded by the European Commission through the AQUASENSE (H2020-MSCA-ITN-2018-813680) project.

**Institutional Review Board Statement:** Not applicable.

**Informed Consent Statement:** Not applicable.

**Data Availability Statement:** Data are contained within the article or the Supplementary Materials. The LabView block diagram is available upon request from the authors.

**Acknowledgments:** The authors would like to thank Andrzej Kapusta for assistance in screen printing and sample collection from Vistula River. The authors are also grateful to Bogdan Puz for the acquisition of the samples from Zakrzówek Lake and Jerzy Krypel for the acquisition of the samples from Morskie Oko Lake.

**Conflicts of Interest:** The authors declare no conflict of interest.

## References

1. Hassan Omer, N. Water quality parameters. In *Water Quality-Science, Assessments and Policy*; IntechOpen Ltd.: London, UK, 2019; pp. 1–18.
2. Boyd, C.E.; Tucker, C.S.; Viriyatum, R. Interpretation of pH, Acidity, and Alkalinity in Aquaculture and Fisheries. *N. Am. J. Aquac.* **2011**, *73*, 403–408. [[CrossRef](#)]
3. Poghosian, A.; Baade, A.; Emons, H.; Schöning, M. Application of ISFETs for pH measurement in rain droplets. *Sens. Actuators B: Chem.* **2001**, *76*, 634–638. [[CrossRef](#)]
4. Chan, L.C.Z.; Moghaddam, G.K.; Wang, Z.; Lowe, C.R. Miniaturized pH Holographic Sensors for the Monitoring of *Lactobacillus casei* Shiota Growth in a Microfluidic Chip. *ACS Sens.* **2019**, *4*, 456–463. [[CrossRef](#)] [[PubMed](#)]
5. John, G.T.; Goelling, D.; Klimant, I.; Schneider, H.; Heinzle, E. PH-sensing 96-well microtitre plates for the characterization of acid production by dairy starter cultures. *J. Dairy Res.* **2003**, *70*, 327–333. [[CrossRef](#)]
6. Manjakkal, L.; Szwagierczak, D.; Dahiya, R. Metal oxides based electrochemical pH sensors: Current progress and future perspectives. *Prog. Mater. Sci.* **2020**, *109*, 100635. [[CrossRef](#)]
7. Oh, H.; Lee, K.J.; Baek, J.; Yang, S.S.; Lee, K. Development of a high sensitive pH sensor based on shear horizontal surface acoustic wave with ZnO nanoparticles. *Microelectron. Eng.* **2013**, *111*, 154–159. [[CrossRef](#)]
8. Khan, M.I.; Mukherjee, K.; Shoukat, R.; Dong, H. A review on pH sensitive materials for sensors and detection methods. *Microsyst. Technol.* **2017**, *23*, 4391–4404. [[CrossRef](#)]
9. Yuqing, M.; Jianrong, C.; Keming, F. New technology for the detection of pH. *J. Biochem. Biophys. Methods* **2005**, *63*, 1–9. [[CrossRef](#)]
10. Karastogianni, S.; Girosi, S.; Sotiropoulos, S. *pH: Principles and Measurement*, 1st ed.; Elsevier Ltd.: Amsterdam, The Netherlands, 2016; ISBN 9780123849533.
11. Kurzweil, P. Metal Oxides and Ion-Exchanging Surfaces as pH Sensors in Liquids: State-of-the-Art and Outlook. *Sensors* **2009**, *9*, 4955–4985. [[CrossRef](#)]
12. Hall, D.G. Ion-Selective Membrane Electrodes: A General Limiting Treatment of Interference Effects. *J. Phys. Chem.* **1996**, *100*, 7230–7236. [[CrossRef](#)]
13. Fog, A.; Buck, R.P. Electronic semiconducting oxides as pH sensors. *Sens. Actuators* **1984**, *5*, 137–146. [[CrossRef](#)]
14. Yates, D.E.; Levine, S.; Healy, T.W. Site-binding model of the electrical double layer at the oxide/water interface. *J. Chem. Soc. Faraday Trans. 1 Phys. Chem. Condens. Phases* **1974**, *70*, 1807–1818. [[CrossRef](#)]
15. Kurzweil, P. Precious metal oxides for electrochemical energy converters: Pseudocapitance and pH dependence of redox processes. *J. Power Sources* **2009**, *190*, 189–200. [[CrossRef](#)]
16. Jadon, A.; Rossi, C.; Djafari-Rouhani, M.; Estève, A.; Pech, D. Interaction of hydrogen with the bulk, surface and subsurface of crystalline RuO<sub>2</sub> from first principles. *Phys. Open* **2021**, *7*, 100059. [[CrossRef](#)]
17. Zhuyikov, S. Morphology of Pt-doped nanofabricated RuO<sub>2</sub> sensing electrodes and their properties in water quality monitoring sensors. *Sens. Actuators B Chem.* **2009**, *136*, 248–256. [[CrossRef](#)]
18. Zhuyikov, S.; Kats, E.; Marney, D.; Kalantar-Zadeh, K. Improved antifouling resistance of electrochemical water quality sensors based on Cu<sub>2</sub>O-doped RuO<sub>2</sub> sensing electrode. *Prog. Org. Coat.* **2011**, *70*, 67–73. [[CrossRef](#)]
19. Sardarnejad, A.; Maurya, D.; Khaled, M.; Alameh, K. Temperature effects on the performance of RuO<sub>2</sub> thin-film pH sensor. *Sens. Actuators A Phys.* **2015**, *233*, 414–421. [[CrossRef](#)]
20. Xu, B.; Zhang, W.-D. Modification of vertically aligned carbon nanotubes with RuO<sub>2</sub> for a solid-state pH sensor. *Electrochim. Acta* **2010**, *55*, 2859–2864. [[CrossRef](#)]
21. Lonsdale, W.; Wajrak, M.; Alameh, K. Effect of conditioning protocol, redox species and material thickness on the pH sensitivity and hysteresis of sputtered RuO<sub>2</sub> electrodes. *Sens. Actuators B Chem.* **2017**, *252*, 251–256. [[CrossRef](#)]
22. Lonsdale, W.; Shylendra, S.P.; Wajrak, M.; Alameh, K. Application of all solid-state 3D printed pH sensor to beverage samples using matrix matched standard. *Talanta* **2019**, *196*, 18–21. [[CrossRef](#)]
23. Liao, Y.-H.; Chou, J.-C. Preparation and characteristics of ruthenium dioxide for pH array sensors with real-time measurement system. *Sens. Actuators B Chem.* **2008**, *128*, 603–612. [[CrossRef](#)]
24. Armelao, L.; Barreca, D.; Moraru, B. A molecular approach to RuO<sub>2</sub>-based thin films: Sol–gel synthesis and characterisation. *J. Non-Cryst. Solids* **2003**, *316*, 364–371. [[CrossRef](#)]
25. Kahram, M.; Asnavandi, M.; Dolati, A. Synthesis and electrochemical characterization of sol–gel-derived RuO<sub>2</sub>/carbon nanotube composites. *J. Solid State Electrochem.* **2013**, *18*, 993–1003. [[CrossRef](#)]
26. Pocrifka, L.; Gonçalves, C.; Grossi, P.; Colpa, P.; Pereira, E. Development of RuO<sub>2</sub>-TiO<sub>2</sub> (70–30)mol% for pH measurements. *Sens. Actuators B Chem.* **2006**, *113*, 1012–1016. [[CrossRef](#)]
27. Sadig, H.R.; Li, C. Applying a Novel Polymeric Precursor Derived by Capillary-Gravitational Coating in Fabrication of Nanostructured Tri- Metal Oxide-Based pH Sensing Electrode. *IEEE Sens. J.* **2020**, *20*, 12512–12521. [[CrossRef](#)]
28. Shim, J.H.; Kang, M.; Lee, Y.; Lee, C. A nanoporous ruthenium oxide framework for amperometric sensing of glucose and potentiometric sensing of pH. *Microchim. Acta* **2012**, *177*, 211–219. [[CrossRef](#)]
29. Manjakkal, L.; Cvejic, K.; Kulawik, J.; Zaraska, K.; Szwagierczak, D.; Socha, R.P. Fabrication of thick film sensitive RuO<sub>2</sub>-TiO<sub>2</sub> and Ag/AgCl/KCl reference electrodes and their application for pH measurements. *Sens. Actuators B Chem.* **2014**, *204*, 57–67. [[CrossRef](#)]

30. Manjakkal, L.; Cvejic, K.; Kulawik, J.; Zaraska, K.; Socha, R.P.; Szwagierczak, D. X-ray photoelectron spectroscopic and electrochemical impedance spectroscopic analysis of RuO<sub>2</sub>-Ta<sub>2</sub>O<sub>5</sub> thick film pH sensors. *Anal. Chim. Acta* **2016**, *931*, 47–56. [[CrossRef](#)]
31. Manjakkal, L.; Cvejic, K.; Kulawik, J.; Zaraska, K.; Szwagierczak, D.; Stojanovic, G. Sensing mechanism of RuO<sub>2</sub>-SnO<sub>2</sub> thick film pH sensors studied by potentiometric method and electrochemical impedance spectroscopy. *J. Electroanal. Chem.* **2015**, *759*, 82–90. [[CrossRef](#)]
32. Zhuyikov, S.; Marney, D.; Kats, E. Investigation of Electrochemical Properties of La<sub>2</sub>O<sub>3</sub>-RuO<sub>2</sub> Thin-Film Sensing Electrodes Used in Sensors for the Analysis of Complex Solutions. *Int. J. Appl. Ceram. Technol.* **2011**, *8*, 1192–1200. [[CrossRef](#)]
33. McMurray, H.; Douglas, P.; Abbot, D. Novel thick-film pH sensors based on ruthenium dioxide-glass composites. *Sens. Actuators B Chem.* **1995**, *28*, 9–15. [[CrossRef](#)]
34. Lazouskaya, M.; Tamm, M.; Scheler, O.; Uppuluri, K.; Zaraska, K. Nafion as a protective membrane for screen-printed pH-sensitive ruthenium oxide electrodes. In Proceedings of the 2020 17th Biennial Baltic Electronics Conference (BEC), Tallinn, Estonia, 6–8 October 2020; pp. 1–4.
35. Manjakkal, L.; Synkiewicz, B.; Zaraska, K.; Cvejic, K.; Kulawik, J.; Szwagierczak, D. Development and characterization of miniaturized LTCC pH sensors with RuO<sub>2</sub> based sensing electrodes. *Sens. Actuators B Chem.* **2016**, *223*, 641–649. [[CrossRef](#)]
36. Li, M.; Li, Y.-T.; Li, D.-W.; Long, Y.-T. Recent developments and applications of screen-printed electrodes in environmental assays—A review. *Anal. Chim. Acta* **2012**, *734*, 31–44. [[CrossRef](#)] [[PubMed](#)]
37. Antuña-Jiménez, D.; González-García, M.B.; Hernández-Santos, D.; Fanjul-Bolado, P. Screen-Printed Electrodes Modified with Metal Nanoparticles for Small Molecule Sensing. *Biosensors* **2020**, *10*, 9. [[CrossRef](#)]
38. Labrador, R.H.; Soto, J.; Martínez-Mañez, R.; Coll, C.; Benito, A.; Ibáñez, J.; García-Breijo, E.; Gil, L. An electrochemical characterization of thick-film electrodes based on RuO<sub>2</sub>-containing resistive pastes. *J. Electroanal. Chem.* **2007**, *611*, 175–180. [[CrossRef](#)]
39. Council of Europe. Potentiometric determination of pH. In *European Pharmacopoeia 5.0*; Council of Europe: Strasbourg, France, 2005; pp. 26–27. ISBN 978-9287152817.
40. Lonsdale, W.; Wajrak, M.; Alameh, K. RuO<sub>2</sub> pH Sensor with Super-Glue-Inspired Reference Electrode. *Sensors* **2017**, *17*, 2036. [[CrossRef](#)]
41. Yao, X.; Vepsäläinen, M.; Isa, F.; Martin, P.; Munroe, P.; Bendavid, A. Advanced RuO<sub>2</sub> Thin Films for pH Sensing Application. *Sensors* **2020**, *20*, 6432. [[CrossRef](#)]
42. Mingels, R.; Kalsi, S.; Cheong, Y.; Morgan, H. Iridium and Ruthenium oxide miniature pH sensors: Long-term performance. *Sens. Actuators B Chem.* **2019**, *297*, 126779. [[CrossRef](#)]
43. Uppuluri, K.; Lazouskaya, M.; Szwagierczak, D.; Zaraska, K. Influence of temperature on the performance of Nafion coated RuO<sub>2</sub> based pH electrodes. In Proceedings of the 2021 IEEE International Conference on Flexible and Printable Sensors and Systems (FLEPS), Manchester, UK, 20–23 June 2021; pp. 1–4.
44. Hrovat, M.; Bencan, A.; Belavič, D.; Holc, J.; Dražič, G. The influence of firing temperature on the electrical and microstructural characteristics of thick-film resistors for strain gauge applications. *Sens. Actuators A Phys.* **2003**, *103*, 341–352. [[CrossRef](#)]
45. Osman, J.R.; Crayston, J.A.; Pratt, A.; Richens, D.T. RuO<sub>2</sub>-TiO<sub>2</sub> mixed oxides prepared from the hydrolysis of the metal alkoxides. *Mater. Chem. Phys.* **2008**, *110*, 256–262. [[CrossRef](#)]
46. Vitosh, M.L.; Fertilizers, N.-P.-K. *Types, Uses and Characteristics*; Extension Bulletin E—Cooperative Extension Service; Michigan State University: East Lansing, MI, USA, 1983.
47. Jachimowski, A. Factors Affecting Water Quality in a Water Supply Network. *J. Ecol. Eng.* **2017**, *18*, 110–117. [[CrossRef](#)]
48. Aleksander-Kwaterczak, U.; Plenzler, D. Contamination of small urban watercourses on the example of a stream in Krakow (Poland). *Environ. Earth Sci.* **2019**, *78*, 1–13. [[CrossRef](#)]
49. Galas, J. Limnological study on a lake formed in a limestone quarry (Kraków, Poland). *I. Water chemistry. Pol. J. Environ. Stud.* **2003**, *12*, 297–300.
50. Sobczyk, W.; Mateusz, W.; Małgorzata, P. Physical and Chemical Indicators of Surface Waters of the Tatra National Park. *J. Ecol. Eng.* **2020**, *21*, 174–179. [[CrossRef](#)]



## Appendix 2

### Publication II

M. Lazouskaya, O. Scheler, V. Mikli, K. Uppuluri, K. Zaraska, and M. Tamm, "Nafion Protective Membrane Enables Using Ruthenium Oxide Electrodes for pH Measurement in Milk," *Journal of the Electrochemical Society*, V. 168, N. 10, 2021.





## Nafion Protective Membrane Enables Using Ruthenium Oxide Electrodes for pH Measurement in Milk

Maryna Lazouskaya,<sup>1,2,z</sup>  Ott Scheler,<sup>1</sup>  Valdek Mikli,<sup>3</sup> Kiranmai Uppuluri,<sup>4</sup>   
 Krzysztof Zaraska,<sup>4</sup>  and Martti Tamm<sup>2</sup>

<sup>1</sup>Department of Chemistry and Biotechnology, School of Science, Tallinn University of Technology, 19086 Tallinn, Estonia

<sup>2</sup>Center of Food and Fermentation Technologies, 12618 Tallinn, Estonia

<sup>3</sup>Department of Material and Environmental Technology, School of Engineering, Tallinn University of Technology, 19086 Tallinn, Estonia

<sup>4</sup>Lukasiewicz Research Network—Krakowski Instytut Technologiczny, 30-418, Krakow, Poland

The application of conventional glass electrodes for pH measurement in food samples has a serious drawback: glass is fragile and should be handled with care in order to prevent breaking and thus contaminating the food with dangerous shattered fragments. The implementation of all-solid-state sensors allows for pH measurements without this contamination risk but their application in food samples is scarce due to their inability to be used in complex food matrices that contain fats, proteins, yeasts, etc. We can solve this problem by coating solid-state RuO<sub>2</sub> electrodes with a semi-permeable protective Nafion<sup>TM</sup> membrane layer. We show that covering screen printed potentiometric RuO<sub>2</sub> electrodes with Nafion membrane using a drop-casting technique does not alter the performance of the electrodes in milk samples and provides similar results to the conventional glass electrode. Furthermore, we discovered that thermal treatment of Nafion-layers at 80 °C for 2 h after each layer deposition optimises the performance of the electrodes, makes them usable even in heated aqueous solutions, and increases their lifetime.

© 2021 The Author(s). Published on behalf of The Electrochemical Society by IOP Publishing Limited. This is an open access article distributed under the terms of the Creative Commons Attribution 4.0 License (CC BY, <http://creativecommons.org/licenses/by/4.0/>), which permits unrestricted reuse of the work in any medium, provided the original work is properly cited. [DOI: 10.1149/1945-7111/ac2d3c]



Manuscript submitted July 9, 2021; revised manuscript received September 28, 2021. Published October 29, 2021.

pH is one of the essential quality parameters in water and food quality control that can be used as an express indicator of:

- I. Meat quality (high pH values can be an indicator of poor meat texture);<sup>1–5</sup>
- II. Fish freshness (an increase of pH with storage duration);<sup>6–9</sup>
- III. Microbial growth in dairy products;<sup>10</sup>
- IV. Inflammatory infection in cattle.<sup>11</sup>

At present, pH is measured by the means of potentiometry utilising a conventional glass electrode. However, glass electrodes are known to be fragile and have the potential to contaminate water or food with dangerous shattered glass fragments.

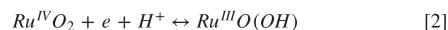
Several alternatives to glass electrodes have been proposed in the last couple of decades by various researchers, including ion-selective field-effect transistors (ISFET),<sup>12</sup> electrodes based on pH-sensitive polymers,<sup>13</sup> and metal oxides.<sup>14,15</sup> Amongst these, metal oxides have attracted the most attention, with some already having been successfully tested for water pollution monitoring<sup>4</sup> and pH measurement in common beverages.<sup>16</sup> According to a study by Manjakkal et al.,<sup>15</sup> Ruthenium oxide IV (RuO<sub>2</sub>) is the most suitable for pH electrode fabrication due to its comparatively low cost, high sensitivity, fast response time, low hysteresis and drift effect.

The working principle of metal oxide pH electrodes is fundamentally the same as conventional glass electrodes. It relies on the selective identification of the H<sup>+</sup> ions present in sample.<sup>14</sup> Electrodes sensitive to H<sup>+</sup> ions are therefore called indicator electrodes. The measuring setup for H<sup>+</sup> determination is called an electrochemical cell and consists of an (i) indicator electrode, (ii) reference electrode, and (iii) measuring device (potentiometer, voltmeter, multimeter, etc.).<sup>17,18</sup> The electrical characteristic of an electrochemical cell is electrochemical potential (hereafter referred to as potential). The potential of cell (E) is determined as the difference in electrode potentials of the half-reactions taking place at the electrodes:

$$E = E_{\text{ind}} - E_{\text{ref}} \quad [1]$$

where E<sub>ind</sub> is the potential of the reaction taking place at the indicator electrode, V; and E<sub>ref</sub> is the potential of the reaction taking place at the reference electrode, V. Usually, the reference electrode is grounded, its potential is considered equal to zero, and the potential of the electrochemical cell is, therefore, equal to the potential of the indicator electrode.

The half-reaction taking place on the ruthenium oxide (IV) electrode was previously studied and described as follows:<sup>14</sup>



This reaction is quantitatively described by the Nernst equation:

$$E = E^0_{\text{Ru}^{\text{IV}}/\text{Ru}^{\text{III}}} - \frac{R \cdot T}{n \cdot F} \cdot \ln \frac{a_{\text{Ru}^{\text{III}}}}{a_{\text{Ru}^{\text{IV}}} \cdot a_{\text{H}^+}} \quad [3]$$

where E<sup>0</sup> is standard potential<sup>9</sup>, V; R is the universal gas constant, 8.314 J/K·mol; T is the temperature, K; n is the number of electrodes participating in the redox reaction; F is the Faraday constant, 96485 C mol<sup>-1</sup>; a<sub>Ru<sup>IV</sup></sub> and a<sub>Ru<sup>III</sup></sub> are the activities of Ru<sup>IV</sup>O<sub>2</sub> and Ru<sup>III</sup>O(OH) respectively, mol l<sup>-1</sup>, a<sub>H<sup>+</sup></sub> is the activity of H<sup>+</sup> ions, mol l<sup>-1</sup>.

Considering that the value of the activities of metals is approximately 1 in a solid-state and substituting the constants at room temperature (T = 21 °C), Eq. 3 takes the following form:

$$E = E^0_{\text{Ru}^{\text{IV}}/\text{Ru}^{\text{III}}} - 0.0584 \cdot \lg[\text{H}^+] \quad [4]$$

Equation 4 allows determining pH from the measured potential value. The value of 0.0584 V pH<sup>-1</sup> (or 58.4 mV pH<sup>-1</sup>) is called electrode sensitivity or the theoretical Nernst response at the temperature of 21 °C and is determined by the calibration of the electrode in buffer solutions of known pH.

Despite being similar to the glass electrode's performance in aqueous media,<sup>13,15,18</sup> the application of metal oxide pH-electrodes in food samples is limited due to the interference of fat and proteins (fat and proteins can adsorb on the electrode surface and block the measurement). This limitation can be overcome by covering the

<sup>9</sup>Standard potential is a measure of the individual potential of a reversible electrode (in equilibrium) in a standard state (concentration 1 mol l<sup>-1</sup>, pressure 1 atmosphere and temperature 25 °C).



electrode's pH-sensitive area with a semi-permeable membrane that allows only  $H^+$  ions (protons) to pass through, thus protecting the electrode from contamination. One of the substances widely used for electrochemical and bio-sensor protection is Nafion<sup>TM</sup> (hereafter referred to as Nafion).<sup>12,19–22</sup>

Nafion is a random copolymer that consists of hydrophobic fluorocarbon chain and terminal hydrophilic sulfone groups (Fig. 1). Nafion belongs to the group of perfluorinated sulfonic acid (PFSA) ionomers known for their ionic conductivity, chemical and mechanical stability and application as proton-exchange membranes (PEM).<sup>23,24</sup> Nafion was the first commercial PFSA ionomer developed by Walter Grot for DuPont (DuPont de Nemours, Inc., Wilmington, Delaware, USA) in the late 1960s.<sup>25</sup> Nonetheless, even at present, Nafion is the most widely used PFSA ionomer due to its excellent proton conductivity.<sup>26</sup>

The proton conductivity of fully hydrated Nafion is explained by structural diffusion (Grotguss mechanism); protons travel through the hydrogen bond in the water network inside the polymer membrane via the rotation and reorientation of water molecules.<sup>27</sup> According to Gierke's model [26], water molecules are retained in polymer clusters by hydrophilic sulfone groups that are connected into channels and therefore provide a continuous flow of protons across the polymer membrane. The transfer of protons starts with the dissociation of protons as the result of the breakage of the  $SO_3-H$  bond. Dissociated protons then form complex ions with water (hydronium— $H_3O^+$ , Eigen cation— $H_9O_4^+$  and Zundel cation— $H_5O_2^+$ ) and travel through the water network.

Proton conductivity of Nafion depends on membrane deposition and treatment-related parameters (deposition technique, annealing/boiling temperature) among other parameters (equivalent weight of polymer and length of its side chain, humidity, and temperature of the sample, etc.).<sup>26</sup> In previously reported papers (Table I), the Nafion membrane was predominantly deposited by drop-casting of a commercially available solution<sup>b</sup> on the electrode surface. However, approaches developed by different authors varied in (i) number of Nafion layers and (ii) drying method (Table I).

The aim of this study was to investigate if coverage of the  $RuO_2$  electrodes with Nafion improves electrodes' performance in real-life samples and how the Nafion deposition condition affects the main characteristics of the pH electrode—sensitivity, hysteresis, drift rate. The  $RuO_2$  electrodes used in this study were fabricated by the screen printing method and are suitable for potentiometric pH measurement.

## Experimental

**Fabrication of screen printed ruthenium oxide electrodes.**—Electrodes were fabricated similarly to previously reported protocols.<sup>42,43</sup> The schematic representation of the fabrication steps is presented in Fig. 2a. First, a conductive layer of Ag/Pd thick film paste with the resistivity of  $3\text{--}6\text{ m}\Omega\text{ sq}^{-1}$  (9695, Electro-Science Laboratories<sup>c</sup>, USA) was screen printed on an alumina substrate, dried at  $120\text{ }^\circ\text{C}$  for 15 min, and consequently sintered at  $850\text{ }^\circ\text{C}$  for 1 h. After cooling down, a pH-sensitive layer of  $RuO_2$ -glass paste with the resistivity of  $10\text{ k}\Omega\text{ sq}^{-1}$  (3914, Electro-Science Laboratories, USA) was printed on top of the substrate in such a way that layers of  $RuO_2$  and Ag/Pd partly overlap. After screen printing of the  $RuO_2$  layer, the substrates were once again dried at  $120\text{ }^\circ\text{C}$  for 15 min and consequently sintered at  $850\text{ }^\circ\text{C}$  for 1 h. After printing and sintering of both layers, copper wire was connected to the conductive layer of Ag/Pd via soldering with a resin core solder (grade  $Sn_{60}Pb_{40}$ , HQ, Nedis, Netherlands). The next and final step was shielding the electrical connections with a polydimethylsiloxane coating (DOWSIL<sup>TM</sup> 3140 RTV Coating, Dow Chemical Company, USA).

**Deposition of nafion.**—The fabricated  $RuO_2$  electrodes were modified with a Nafion protective layer using the drop-casting

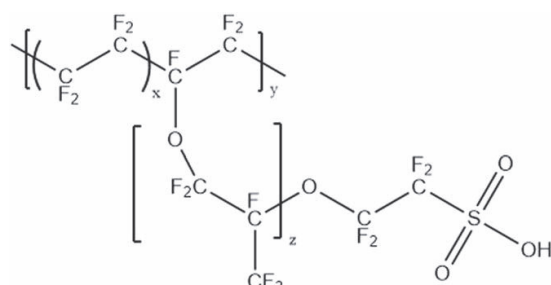


Figure 1. Chemical structure of Nafion.

technique. For that, a 5% solution of Nafion in a mixture of lower aliphatic alcohols and water (Nafion 117, Sigma Aldrich, USA) was used.

To investigate the influence of Nafion coating on electrode characteristics, we fabricated Nafion-modified Ruthenium oxide ( $RuO_2$ -Nf) electrodes varying in (i) number of Nafion layers, (ii) time between layers deposition, and (iii) drying temperature.

**Multilayered films.**—To investigate the influence of the thickness of the Nafion membrane on the performance of the  $RuO_2$  electrodes,  $RuO_2$  electrodes were modified with 1, 3 and 5 layers of Nafion. The samples were named  $RuO_2$ -Nf<sub>1</sub>,  $RuO_2$ -Nf<sub>3</sub> and  $RuO_2$ -Nf<sub>5</sub> respectively.

**$RuO_2$ -Nf<sub>1</sub> electrodes.**— $10\text{ }\mu\text{l}$  of 5% Nafion solution was drop-casted on the  $RuO_2$  layer and air-dried at room temperature. Nafion was applied in such a way that only the  $RuO_2$  layer got covered. The electrodes were left to air-dry at room temperature overnight.

**$RuO_2$ -Nf<sub>3</sub> electrodes.**—Modification of  $RuO_2$  electrodes with 3 layers of Nafion was carried as layer-by-layer deposition. First,  $10\text{ }\mu\text{l}$  of 5% Nafion solution were drop-casted on the  $RuO_2$  layer and air-dried at room temperature for 2 h. Then the procedure was repeated 2 more times, therefore, forming 3 layers of Nafion. After the last layer was deposited, the electrodes were left to air-dry at room temperature overnight.

**$RuO_2$ -Nf<sub>5</sub> electrodes.**—Modification of  $RuO_2$  electrodes with 5 layers of Nafion was similar to that of  $RuO_2$ -Nf<sub>3</sub> electrodes. First,  $10\text{ }\mu\text{l}$  of 5% Nafion solution was drop-casted on the  $RuO_2$  layer and air-dried at room temperature for 2 h. The procedure was then repeated 4 more times, therefore, forming 5 layers of Nafion. After the last layer was deposited, the electrodes were left to air-dry at room temperature overnight.

**Time between layer deposition.**—To evaluate the appropriate time needed for one layer to dry, we applied  $10\text{ }\mu\text{l}$  of 5% Nafion solution on the electrodes and varied the layer drying time by 30 min, 1 h and 2 h. Here we deposited 3 layers of Nafion to achieve  $RuO_2$ -Nf<sub>3</sub>. After all the layers were applied, the electrodes were left to air-dry at room temperature overnight.

**Drying temperature.**—In order to enhance the mechanical and thermal strength of the Nafion membrane, we also fabricated the  $RuO_2$ -Nf<sub>3</sub> electrodes that were dried in a laboratory incubator (BD 53, Binder, Germany) at  $40\text{ }^\circ\text{C}$ ,  $60\text{ }^\circ\text{C}$ , and  $80\text{ }^\circ\text{C}$  for 2 h in between layer deposition. After all the layers were deposited and dried in the incubator, the electrodes were left to air-dry at room temperature overnight.

**Electrochemical characterization.**—It was shown previously<sup>44</sup> that screen printed  $RuO_2$  electrodes require preliminary conditioning (storage) in water for the double layer formation at the pH-sensitive

<sup>b</sup>Nafion 117, 5% Nafion solution in a mixture of low aliphatic alcohols, Sigma Aldrich, USA.

<sup>c</sup>Now part of Ferro Corporation, Mayfield Heights, Ohio, USA.

Table I. Comparison of previously reported electrochemical sensors covered with Nafion.

Detecting species	Nafion deposition technique	Nafion solution	Volume of the solution	Number of layers	Drying method	References
<b>Amperometric sensors and biosensors</b>						
H <sub>2</sub> O <sub>2</sub>	Drop-casting	0.25%–1.25% solution in 90% alcohol	3 $\mu$ l	1	Air-dried at room temperature	12
H <sub>2</sub> O <sub>2</sub>	Drop-casting	N/A	20 $\mu$ l	1	Air-dried for 2 h and for another 20 min at 85 °C	13
Glucose	Dip-coating	1% solution diluted with propanol-2	N/A	3	N/A	28
Glucose	Drop-casting	1% solution in 95% alcohol	2 $\mu$ l	1	Air-dried at room temperature	29
Glucose	Drop-casting	5% solution (Sigma) <sup>a)</sup>	N/A	1	Air-dried at room temperature	30
Oxygen	Spin-coating	5% solution (Sigma)	N/A	1	Air-dried at room temperature, thermally annealed	31
<b>Voltammetric sensors</b>						
Dopamine	Dip-coating	N/A	N/A	2–3	Air-dried at room temperature	32
Norepinephrine						
Serotonin						
Uric acid	Drop-casting	0.5%–5.0% solution	10 $\mu$ l	1	Air-dried at room temperature	33
1-aminopyrene	Drop-casting	1% solution	4 $\mu$ l	1	N/A	34
Ondansetron	Drop-casting	0.5% Nafion solution in ethanol	5 $\mu$ l of the suspension <sup>b)</sup>	1	Air-dried at room temperature	35
Morphine						
<b>Potentiometric sensors</b>						
pH	Dip-coating Spin-coating	5% or 10% solution	N/A	1	Dried at 60 °C for 1 h and for 30 min at 210 °C	36
pH	Dip-coating	5% solution (Sigma)	N/A	3	Cured at 230 °C for 15 min under vacuum	37
pH	Drop-casting	5% solution (Sigma)	50 $\mu$ l	1	Cured at 230 °C for 15 min under vacuum	37, 38
pH	Drop-casting	5% solution (Sigma)	N/A	3	Dried at 60 °C under vacuum for 2 h and for another 2 h at 80 °C	39
pH	Drop-casting	5% solution (Sigma)	5 $\mu$ l	1	Air-dried at room temperature for 12 h	40
Uric acid	Drop-casting	1% solution in methanol	5 $\mu$ l	1	Air-dried at room temperature	41
<b>Impedimetric sensors</b>						
pH	Drop-casting	5% solution (Sigma)	1 ml	5	Air-dried for 2 h after all the layers were casted	22
Zink ions	N/A	N/A	N/A	N/A	N/A	21

a) 5% solution of Nafion in a mixture of lower aliphatic alcohols and water produced by Sigma-Aldrich. b) Suspension of 5  $\mu$ l of the Multiwalled carbon nanotubes-Nafion.

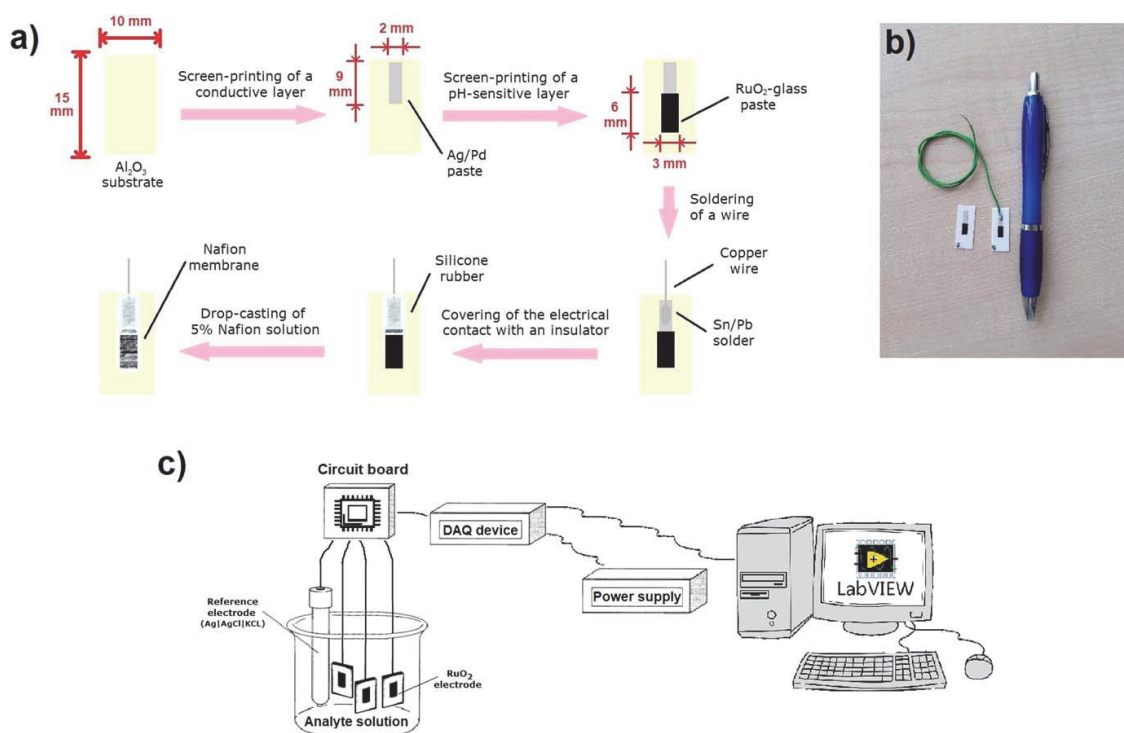


**Figure 2.** Electrodes were fabricated by a screen printing technique (a), schematic representation of the fabrication steps). The electrodes were made of a rectangular shape with sizes 15 mm (length), 10 mm (width), and 2 mm (thickness) (b) with attached copper wire that connects the electrodes to the microcontroller (c).

surface.<sup>15</sup> This initial conditioning is required for electrodes to reach a stable working state. Therefore, prior to any measurement, electrodes were left in distilled water for one week.

All the measurements were conducted in parallel with 3 electrodes for each modification at room temperature (21 °C) if not specified otherwise.

**Setup.**—All the essential characteristics of the fabricated electrodes ( $E^0$ , sensitivity, hysteresis, drift rate) were measured by the standard potentiometric measurement. For that, a galvanic cell consisting of fabricated  $\text{RuO}_2$ -Nafion indicator electrodes and a standard glass ion-selective  $\text{Ag}|\text{AgCl}|\text{KCl}$  (HI1053P, Hanna Instruments, USA) was used as a reference electrode and as an indicator electrode for comparison purposes (Fig. 1c). For the convenience of measurement, several indicator electrodes and one reference electrode were connected to the measuring device (Data Acquisition (DAQ) device, USB-6259, National Instruments, USA) through a circuit board with galvanic connections. A high-performance digital power supply (E3631A, Agilent, USA) was used to get an interference-free input voltage of 12 V to power up the measuring device. The potential difference between the indicator electrodes and the reference electrode was monitored using the LabVIEW program (National Instruments, USA).

The performance of the  $\text{RuO}_2$ -Nf electrodes was evaluated from the point of the following parameters: sensitivity, hysteresis, and drift rate.

**Sensitivity.**—Sensitivity is determined as the response of the electrode to the change of pH. Ideally, the sensitivity of an electrode should be close to  $58.4 \text{ mV pH}^{-1}$  (at a temperature of 21 °C), which is called the theoretical Nernst response. At the given temperature, the sensitivity value of  $58.4 \text{ mV pH}^{-1}$  should be observed for all the

pH-sensitive electrodes when  $n = 1$  (see Eqs 3 and 4). However, in practice, deviation from the theoretical response is observed.<sup>42,43,45–47</sup> Therefore, all the electrodes (including conventional glass electrodes) require calibrating of the electrode in buffer solutions of several different pH.

The sensitivity and  $E^0$  were evaluated by determining the electrochemical potential in pH buffers in the range of 3.0–11.0 pH units and plotting the measured electrochemical potential as a function of the pH. Sensitivity was determined as the slope of the function, while  $E^0$  was determined by extrapolation of the function until the intersection with the Oy axis. The electrochemical potential was recorded 5 min after immersing the electrodes in the solution in order to reach stable values. Citric ( $\text{HOC}(\text{CO}_2\text{H})(\text{CH}_2\text{CO}_2\text{H})_2$ — $\text{Na}_2\text{HPO}_4$ ), phosphate ( $\text{NaH}_2\text{PO}_4$ — $\text{Na}_2\text{HPO}_4$ ) and bicarbonate buffer ( $\text{Na}_2\text{CO}_3$ — $\text{NaHCO}_3$ ) solutions were prepared before each measurement in accordance with<sup>48</sup> All the salts were purchased anhydrous from Sigma Aldrich. The pH of the buffers was determined with a conventional pH-meter (Seven2Go Advanced Single-Channel Portable pH Meter, Mettler Toledo, Switzerland).

Cross-sensitivity of the  $\text{RuO}_2$ -Nf electrodes to other cations (e.g.  $\text{Li}^+$ ,  $\text{Na}^+$ ,  $\text{K}^+$ ,  $\text{NH}_4^+$ ,  $\text{Ca}^{2+}$ ,  $\text{Mg}^{2+}$ , etc.) was not tested in this study. We would like to kindly ask the reader to refer to the following articles: cross-selectivity and cross-sensitivity of Nafion membrane<sup>26,49</sup> and cross-sensitivity of  $\text{RuO}_2$  pH-sensitive screen printed layer.<sup>15,50</sup>

**Hysteresis.**—Another important characteristic of an electrode is hysteresis. Hysteresis is determined as the difference in potential readings of an electrode when the electrode is used to measure the acidity of several solutions of differing pH. Hysteresis is associated with changes in the double layer on the surface of an electrode when the electrode is exposed to a solution of a different pH. Hysteresis

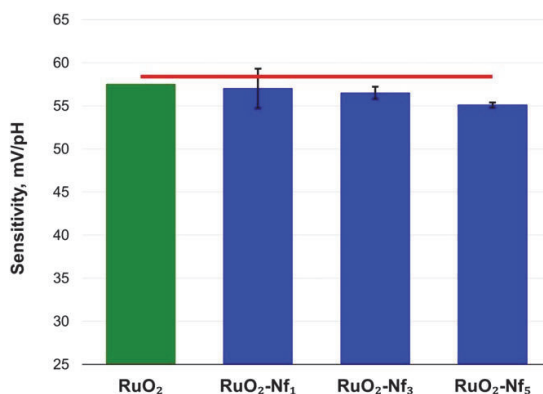


**Figure 3.** The sensitivity of Nafion-covered electrodes (was similar to that of uncovered RuO<sub>2</sub> electrodes (green) and close to the theoretical value (red)). There is a slight decrease of sensitivity with an increasing number of Nafion layers but sensitivity remains close to the control nevertheless. This decrease can be explained by the increase in Nafion thickness.

can be measured for the entire pH diapason (pH 1–14) or only for the acidic or basic region. Hysteresis is usually measured mV.

The hysteresis (memory effect) was determined by exposing the fabricated electrodes to buffer solutions of different pH. The hysteresis was determined for 2 pH cycles: acidic (3–5–7–5–3) and basic (11–9–7–9–11). The electrochemical potential was recorded for 5 min in each buffer. Between measurements, the electrodes were blotted with a paper towel and rinsed with distilled water.

**Drift rate.**—Another parameter that we evaluated was the drift rate—the change in the electrode reading with time. This characteristic is important for continuous measurements and is measured in mV h<sup>-1</sup>.

The drift rate was determined using the slope of the line-of-best-fit method. For that, the potential change was continuously measured for 2 h and the drift rate was calculated as the average difference between initial and final potential values per one hour.

**Measurement at elevated temperatures.**—To evaluate the performance of the fabricated electrodes in heated samples, sensitivity, hysteresis, and drift rate were determined at buffer solutions heated to 25 °C, 30 °C, 35 °C and 40 °C. Buffer solutions were heated to the selected temperature with a magnetic stirrer with an integrated temperature control plane (RT 15, IKA, Germany). The temperature of the solutions was monitored with a digital laboratory thermometer and the deviation from the desired temperature was kept at ±0.5 °C.

**Measurement in milk.**—Commercially available milk (2.5% ultra pasteurised Latte Piim, Tere, Estonia) was used for the pH measurement in real-life samples. Milk samples were heated to room temperature (21 °C) and the potential of the electrodes was recorded for one hour. A conventional glass pH-electrode (HI1053P, Hanna Instruments, USA) was used to compare the performance of RuO<sub>2</sub> and RuO<sub>2</sub>-Nf electrodes.

**Scanning electron microscopy (SEM).**—SEM images of the fabricated electrodes were recorded with the use of a high-resolution field emission scanning electron microscope ZEISS ULTRA-55 (EHT = 20 kV, resolution 1 nm, Carl Zeiss AG, Germany). Prior to measurement, the fabricated electrodes were coated with a thin layer of Pt by a precision ion etching coating system PECS 682 (Gatan—Ametek, USA).

**Optical microscopy.**—To evaluate the state of the RuO<sub>2</sub> layer of RuO<sub>2</sub>-Nf electrodes after the characterisation procedures, a stereo microscope SMZ-171-TLED (Motic, China) was used. The

specifications of the microscope are as follows: optical system—Greenough type, observation tube—trinocular head, inclination—45 degrees.

## Results and Discussion

**Nafion membrane does not alter the sensitivity of RuO<sub>2</sub> electrodes.**—Properties of the RuO<sub>2</sub>-Nf electrodes can be divided into two groups: (i) properties determined by RuO<sub>2</sub> pH-sensitive layer and (ii) properties determined by Nafion protective membrane. The properties and performance of RuO<sub>2</sub> electrodes themselves were previously studied by S. Zhuiykov<sup>51</sup> and L. Manjakkal and coworkers.<sup>52</sup> Properties of Nafion membrane depend on numerous parameters such as deposition method, concentration and volume of the applied solution, polymer properties of Nafion (e.g., length of side chain), solvent, deposition temperature, number of applied layers (for multilayered films), the time between layers deposition, etc. In our study, we selected the drop-casting deposition technique due to its simplicity and cost-effectiveness. Furthermore, we used a constant concentration and volume of the Nafion solution (10 μl of 5% Nafion solution per one layer). This way, we could dwell upon depositing multilayered films. Multilayered films were of the greatest importance as a thicker Nafion membrane would be more susceptible to the mechanical cleaning that is required after measurement in real-life samples.

After the electrodes reached stable sensitivity values, we compared the properties of electrodes with a different number of Nafion layers: RuO<sub>2</sub>-Nf<sub>1</sub>, RuO<sub>2</sub>-Nf<sub>3</sub> and RuO<sub>2</sub>-Nf<sub>5</sub>. RuO<sub>2</sub>-Nf electrodes were compared after one month of conditioning in water (Fig. 3, Table A.1). All the fabricated electrodes showed sensitivity values close to Nernstian response (58.4 mV pH<sup>-1</sup> at 21 °C) and similar to that of a conventional glass electrode (58.8 mV pH<sup>-1</sup>).

Furthermore, RuO<sub>2</sub>-Nf<sub>1</sub> and RuO<sub>2</sub>-Nf<sub>3</sub> electrodes showed only a slight difference in their performance in addition to being similar to that of a commercially available glass electrode (Table A.1). In the case of RuO<sub>2</sub>-Nf<sub>5</sub> electrodes, there is a decrease in sensitivity and linearity of response as well as an increase of hysteresis. This can be due to the fact that a thicker Nafion membrane in the case of RuO<sub>2</sub>-Nf<sub>5</sub> electrodes (Table II) requires more time for ion diffusion from the solution to the RuO<sub>2</sub> layer. This finding is in agreement with the studies by Lonsdale.<sup>37</sup> Nevertheless, all the electrodes showed acceptable drift rate and hysteresis compared to those previously reported for RuO<sub>2</sub> electrodes fabricated by different methods for different precursors and substrates.<sup>38,51,53–55</sup>

**Nafion-coated electrodes reach working conditions faster than bare RuO<sub>2</sub> electrodes.**—It was previously demonstrated that

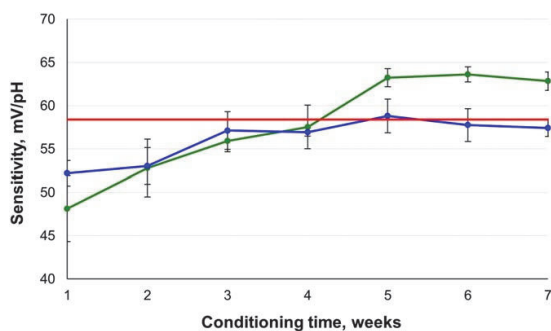


**Figure 4.** RuO<sub>2</sub>-Nafion electrodes (blue) need 3 weeks of conditioning in distilled water compared to 5 weeks for uncovered RuO<sub>2</sub> electrodes (green) to reach stable sensitivity values close to theoretical response (red).

solid-state RuO<sub>2</sub> electrodes require initial conditioning in water or phosphate buffer before the first usage to reach equilibria with the protons in the solution.<sup>42,44,46</sup> For the fabricated RuO<sub>2</sub>-Nf electrodes, stable sensitivity values were observed after 3 weeks of conditioning in distilled water (Fig. 7). For RuO<sub>2</sub> electrodes, the sensitivity kept changing after one month of conditioning in water.

**An increase in Nafion thickness leads to an increase of the defects in the Nafion membrane.**—Furthermore, RuO<sub>2</sub>-Nf electrodes were compared by the physical properties of the Nafion membrane. The SEM images of the electrodes are presented in the Appendix (Fig. A-1). We observed some unevenness and cracking of the coating in the Nafion membrane for all the fabricated electrodes; the amount and size of those defects increased with the increase in the thickness of the Nafion membrane (Table II). The size of defects is crucial for the application of the electrodes in real-life samples, for example, milk proteins have sizes of 0.1–0.25 μm<sup>56,57</sup> and the milk fat globules have sizes of 0.1–15 μm (with an average size of the milk fat globule being 2–6 μm).<sup>58,59</sup> Since for RuO<sub>2</sub>-Nf<sub>3</sub> and RuO<sub>2</sub>-Nf<sub>5</sub> electrodes the size of defects in Nafion-membrane is comparable and even exceed the sizes of main components of food samples, 3 and 5 layers of Nafion might not protect electrodes from contamination.

**Two hours is the optimal time for layer deposition.**—After determining that 3 layers of Nafion are optimal, we investigated the influence of time between the Nafion layers deposition on the electrode performance. The data presented in Fig. 5 and Table A-I suggest that if another layer of Nafion is applied too early before the previous layer has dried properly, the reproducibility of electrodes decreases and there is a huge deviation in electrodes' characteristics. A lesser deviation in electrodes' characteristics (with values comparable to the characteristics observed for the conventional glass electrode) was achieved when drying time was equal to 2 h.

**Thermal treatment of the Nafion membrane during the layers deposition improves the performance of the electrodes.**—Proton conductivity of the Nafion membrane is known to be lower for pre-heated and annealed membranes.<sup>26</sup> On the other hand, thermal treatment of the Nafion membrane improves the mechanical

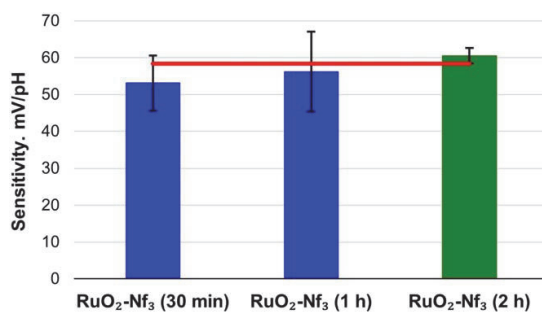


**Figure 5.** RuO<sub>2</sub>-Nf<sub>3</sub> electrodes that were allowed to dry for 2 h between Nafion layer deposition (green) showed better uniformity of sensitivity and were closer to theoretical response (red).

properties of the membrane.<sup>26</sup> According to,<sup>39</sup> drying the Nafion membrane at 80 °C allows for enhancing the mechanical and thermal properties of the membrane. However, the authors did not explain why the temperature of 80 °C was selected. Therefore, we determined characteristics of the Nafion-covered electrodes air-dried for different drying temperatures.

The proton conductivity of the Nafion membrane is also known to depend on temperature.<sup>26</sup> Additionally, in some real-life applications, measurement in heated samples is needed (e.g. measurement of pH during acid-induced coagulation of milk<sup>60</sup>). To evaluate the performance of Nafion covered electrodes in samples of elevated temperature, we determined the characteristics of the thermally treated RuO<sub>2</sub>-Nf<sub>3</sub> electrodes in the buffer solutions heated to 25 °C, 30 °C, 35 °C and 40 °C. We did not investigate higher operating temperatures as (i) proton conductivity decreases with the temperature of the solution,<sup>61</sup> and (ii) in food applications, especially industrial processes, pH is usually measured at a temperature below 40 °C. Temperatures below room 20 °C were not studies as even though milk is stored at lower temperatures (around 4 °C), all the milk samples must be warmed before any further usage.

The results of the measurements are presented in the supplementary material (Table A-II). In Table III we present a comparison matrix with scores (on a scale of 0 to 6) of the overall performance of thermally treated RuO<sub>2</sub>-Nf<sub>3</sub> electrodes in samples of different temperatures. It can be seen that the best overall performance was observed for RuO<sub>2</sub>-Nf<sub>3</sub> electrodes dried at 80 °C. We did not investigate higher temperatures due to high power consumption and therefore, overall expensiveness that can lead to economical and ecological unprofitability.

**Thermal treatment of Nafion membrane during the layers deposition reduces decay of RuO<sub>2</sub> electrodes.**—After conducting measurements at elevated temperatures, we have noticed that on some electrodes, the RuO<sub>2</sub> layer started to wear off. We removed the Nafion membrane to see what the RuO<sub>2</sub> layer looks like. The Nafion was removed by soaking the electrodes in 50% (v/v) ethanol for 1 min and wiping it off with a paper towel.

The RuO<sub>2</sub> layer of RuO<sub>2</sub>-Nf<sub>3</sub> that was air-dried at room temperature has started to detach from the substrate, revealing the

**Table II.** Characteristics of RuO<sub>2</sub>-Nf electrodes with different thicknesses of Nafion membrane.

Characteristic	Electrode type		
	RuO <sub>2</sub> -Nf <sub>1</sub>	RuO <sub>2</sub> -Nf <sub>3</sub>	RuO <sub>2</sub> -Nf <sub>5</sub>
Nafion membrane thickness	1.9 μm	7.5 μm	14.2 μm
Defects in Nafion layer	Pores	Pores and cracks of ~2–4 μm width	Cracks of ~10 μm width
Time needed for the deposition of all Nafion layers	2 h	6 h	10 h

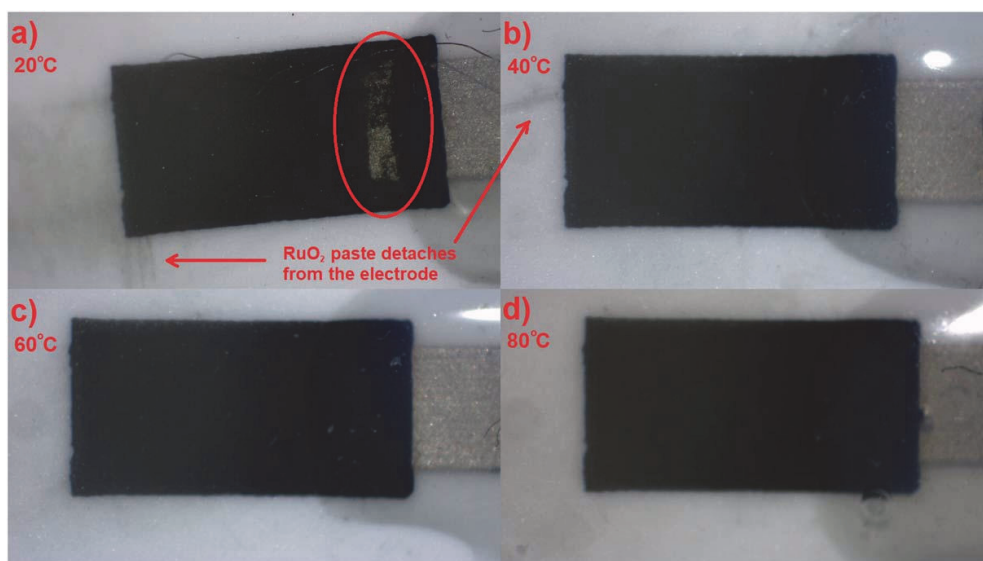


**Figure 6.** An increase of drying temperature during Nafion layers deposition allowed to make Nafion membranes that protected electrodes from the decay: for RuO<sub>2</sub>-Nf<sub>3</sub> electrodes that were dried at 21 °C (a), a more distinguished depletion of RuO<sub>2</sub> layer was observed compared to that of RuO<sub>2</sub>-Nf<sub>3</sub> electrodes dried at 40 °C (b), 60 °C (c) and 80 °C (d).

**Table III.** Comparison matrix for the performance<sup>a)</sup> of RuO<sub>2</sub>-Nf<sub>3</sub> electrodes dried at different temperatures.

Drying temperature \ Temperature of the sample	Temperature of the sample				
	21 °C	25 °C	30 °C	35 °C	40 °C
21 °C	3	3	4	2	2
40 °C	3	4	3	4	2
60 °C	5	4	5	3	3
80 °C	5	5	5	6	5

a) The performance of the electrodes was evaluated based on six parameters: sensitivity,  $E^0$ ,  $R^2$ , hysteresis in the acidic loop, hysteresis in the basic loop and drift rate. The performance was evaluated as good if 5–6 parameters were evaluated as positive, acceptable—3–4 parameters and bad—0–2 parameters. The parameters were evaluated as positive if: sensitivity—Deviation of Sensitivity from theoretical value did not exceed 10 mV pH<sup>-1</sup> and STD value was not exceeding 5 mV pH<sup>-1</sup>;  $E^0$ —STD value was not exceeding 50 mV;  $R^2$ —the value was not lower than 0.95; hysteresis—hysteresis value was < 15 mV and < 20 mV in acidic and basic loops respectively; drift rate—drift value was not exceeding 15 mV h<sup>-1</sup>.

Ag/Pd layer underneath (Fig. 6a). RuO<sub>2</sub>-Nf<sub>3</sub> electrodes that were dried at elevated temperatures, however, exhibited only slight deterioration of the RuO<sub>2</sub> layer. Apparently, the Nafion membrane was more mechanically durable, providing better protection for RuO<sub>2</sub> as well. Improved mechanical stability of thermally treated Nafion membranes is associated with increased entanglement of polymer chains and the coalescence of Nafion particles.<sup>62,63</sup>

**The RuO<sub>2</sub> electrode does not work in complex food samples (e.g., milk) without coating.**—At present, the application of RuO<sub>2</sub> electrodes for measurement in real-life samples is limited due to interference of fat, proteins, and other constituents that lead to an

abrupt drop of measured potential to negative values (Fig. 7a, red line). However, in our experiments, the RuO<sub>2</sub> electrodes that were covered with Nafion exhibited similar behaviour to the glass electrode in the milk sample (Fig. 7a, green line), indicating the applicability of RuO<sub>2</sub>-Nf electrodes for measurement in real-life samples. Improved performance of Nafion-covered electrodes can be explained by the structure of Nafion; the hydrophilic negatively charged sulfonate groups in Nafion block the anionic species from reaching the electrode surface and allow only cations (e.g. H<sup>+</sup>, Na<sup>+</sup>, K<sup>+</sup>) to pass through (Fig. 7b). As casein micelles and proteins in milk have a negative electric charge (zeta-potential around -15 ... -30 mV<sup>64</sup>), they cannot go through the Nafion membrane.

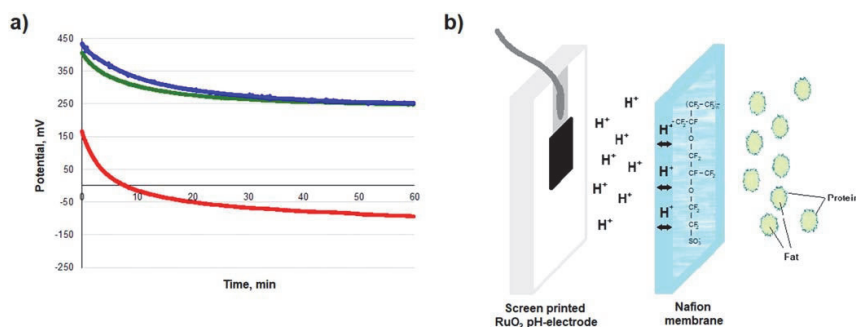


**Figure 7.** RuO<sub>2</sub>-Nf electrode (a, **green**) work just like conventional glass electrode (a, **blue**) from the point of the working diapason of potential and tendency of the potential change with time after exposure to the milk sample. Meanwhile, the RuO<sub>2</sub> electrode (a, **red**) is not suitable for measurement in complex samples like milk. Nafion acts as a semi-permeable membrane allowing only small positive ions to pass through (b).

**Table IV.** Characteristics of RuO<sub>2</sub>-Nf electrodes with different thicknesses of Nafion membrane.

Characteristic	Electrode type			
	RuO <sub>2</sub>	RuO <sub>2</sub> -Nf <sub>1</sub>	RuO <sub>2</sub> -Nf <sub>3</sub>	RuO <sub>2</sub> -Nf <sub>5</sub>
Sensitivity in water, mV pH <sup>-1</sup>	57.5 ± 2.3	57.0 ± 0.7	56.5 ± 0.3	55.1 ± 0.4
Performance in milk	-	+	+	-
Reusability in milk	-	+	++	-

Meanwhile, H<sup>+</sup> ions that are carriers of positive electric charge easily pass through the membrane.

**Coverage of RuO<sub>2</sub> electrodes with 3 layers of Nafion is optimal from the point of performance characteristics.**—To test the usability of RuO<sub>2</sub>-Nf<sub>3</sub> and RuO<sub>2</sub>-Nf<sub>5</sub> electrodes for measurement in real-life samples, we tested all the fabricated electrodes (RuO<sub>2</sub>, RuO<sub>2</sub>-Nf<sub>1</sub>, RuO<sub>2</sub>-Nf<sub>3</sub> and RuO<sub>2</sub>-Nf<sub>5</sub>) in milk. The results of the measurements are presented in Table IV and Fig. A.1. Despite the fact that the size of the defects in the Nafion layer for RuO<sub>2</sub>-Nf<sub>3</sub> electrodes was compatible with the average size of milk fat globules (2–4 and 2–6 μm respectively), RuO<sub>2</sub>-Nf<sub>3</sub> electrodes work fine in milk samples. Furthermore, RuO<sub>2</sub>-Nf<sub>3</sub> electrodes exhibited better reusability in milk samples in comparison to RuO<sub>2</sub>-Nf<sub>1</sub> and therefore, RuO<sub>2</sub> electrodes covered with 3 layers of Nafion were selected for further investigation. Reusability in milk was evaluated as an ability to preserve the behaviour of the electrode potential for several consequent measurements. In-between the measurements, electrodes were cleaned mechanically with a brush and chemically with surfactants, rinsed with distilled water, and left in water overnight.

### Conclusions

In this study, we have demonstrated that the introduction of a Nafion protecting membrane allows the usage of potentiometric RuO<sub>2</sub> electrodes for pH measurement in milk. We have evaluated the effect of the Nafion membrane on the performance of

potentiometric RuO<sub>2</sub> electrodes from the point of the most important electrode characteristics: sensitivity, hysteresis, and drift rate. Furthermore, we have demonstrated that by controlling Nafion deposition conditions, it is possible to enhance the physical stability of RuO<sub>2</sub> electrodes. The advantages of our electrodes are miniature size, firmness, and ability to measure pH in a complex matrix such as milk. The disadvantages of our electrodes are connected to their limited lifetime and the necessity of the reference electrode. Future plans include further investigation of RuO<sub>2</sub>-Nafion electrodes: re-coating of the electrodes when the Nafion membrane wears off, applicability for measurement pH in other food samples (e.g., meat products), development of a cleaning procedure (due to the softness of the Nafion membrane, a proper non-destructive way to clean the electrodes has to be developed), and the fabrication of a suitable all-solid-state reference electrode. The reported electrodes show potential to be used in the food industry and food research in general for on-line and in-line pH monitoring.

### Acknowledgments

This work was supported by the European Commission through the AQUASENSE project [H2020-MSCA-ITN-2018-813680]. Ott Scheler acknowledges support from the Tallinn University of Technology development program 2016–2022 [project code 2014-2020.4.01.16-0032].

### Appendix

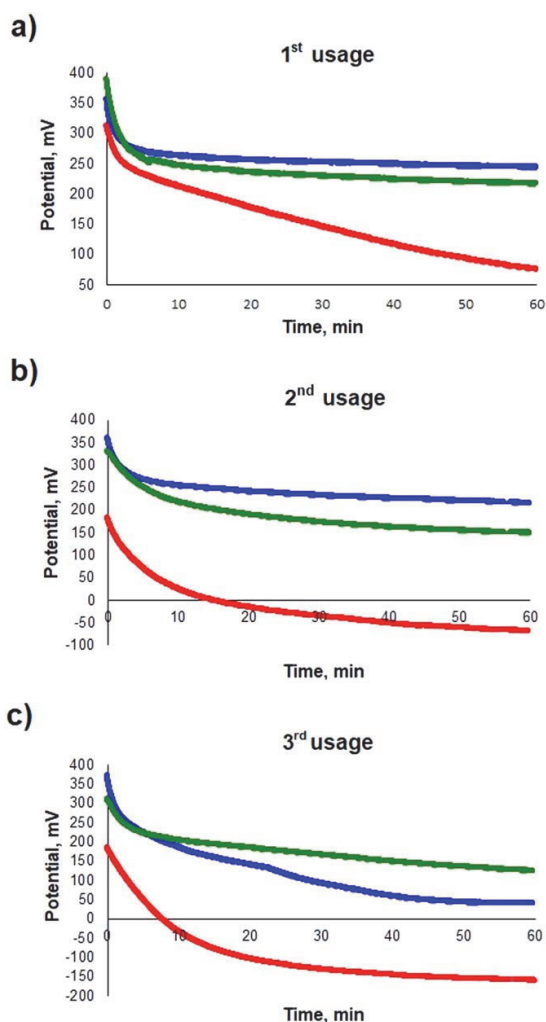


**Figure A-1.** RuO<sub>2</sub>-Nf<sub>1</sub> (blue) and RuO<sub>2</sub>-Nf<sub>3</sub> (green) electrodes showed similar performance in milk. RuO<sub>2</sub>-Nf<sub>5</sub> electrodes (red), however, exhibited a sharp decline of potential and cannot be used for pH measurement in milk samples. The change of electrodes' performance with more uses can be explained by damaging the Nafion membrane during cleaning of the electrodes in-between measurements. Further investigation is needed to develop the cleaning procedure.

**Table A-1.** Characteristics of RuO<sub>2</sub>-Nf electrodes for electrodes varying in number of Nafion layers and time between layers deposition.

Electrode type	Sensitivity, mV pH <sup>-1</sup>	E <sup>0</sup> , mV	R <sup>2</sup>	Hysteresis A, mV	Hysteresis B, mV	Drift, mV h <sup>-1</sup>
<b>RuO<sub>2</sub>-Nf, number of Nafion layers</b>						
RuO <sub>2</sub>	57.5 ± 2.3	566.3 ± 55.3	0.979	3 ± 2	5 ± 2	0–5
RuO <sub>2</sub> -Nf <sub>1</sub>	57.0 ± 0.7	684.1 ± 2.3	0.997	11 ± 1	17 ± 9	14–15
RuO <sub>2</sub> -Nf <sub>3</sub>	56.5 ± 0.3	693.2 ± 3.8	0.995	10 ± 2	24 ± 6	25–35
RuO <sub>2</sub> -Nf <sub>5</sub>	55.1 ± 0.4	603.9 ± 32.5	0.942	20 ± 3	32 ± 5	25–35
<b>RuO<sub>2</sub>-Nf<sub>3</sub>, time between Nafion layers deposition</b>						
30 min	53.1 ± 7.5	601.5 ± 131.7	0.981	10 ± 2	24 ± 6	25–35
1 h	56.2 ± 10.9	549.0 ± 90.3	0.978	11 ± 4	21 ± 17	30–35
2 h	60.5 ± 2.1	680.9 ± 10.3	0.984	4 ± 2	25 ± 4	20–25
<b>Glass electrode</b>						
	58.8 ± 3.4	705.7 ± 36.8	0.997	10 ± 2	12 ± 3	0–5



Table A-II. Characteristics of RuO<sub>2</sub>-Nf<sub>3</sub> electrodes dried at different temperatures, measured at varying sample temperature.

Temperature	Sensitivity, mV pH <sup>-1</sup>	Theoretical Sensitivity, mV pH <sup>-1</sup>	E <sup>0</sup> , mV	R <sup>2</sup>	Hysteresis A, mV	Hysteresis B, mV	Drift, mV h <sup>-1</sup>
<b>RuO<sub>2</sub>-Nf<sub>3</sub> dried at room temperature (21 °C)</b>							
21 °C	60.5 ± 2.1	58.4	680.9 ± 10.3	0.984	4 ± 2	24 ± 1	20–25
25 °C	56.6 ± 7.4	59.2	606.7 ± 44.5	0.980	27 ± 5	25 ± 4	10–20
30 °C	54.4 ± 4.2	60.2	571.4 ± 68.1	0.976	18 ± 9	10 ± 7	0–15
35 °C	45.9 ± 1.3	61.2	499.1 ± 59.1	0.934	21 ± 11	10 ± 6	5–10
40 °C	53.7 ± 5.0	62.2	592.4 ± 59.0	0.958	25 ± 7	32 ± 8	5–10
<b>RuO<sub>2</sub>-Nf<sub>3</sub> dried at 40 °C</b>							
21 °C	48.9 ± 1.0	58.4	554.0 ± 23.9	0.995	22 ± 2	21 ± 3	10–20
25 °C	47.9 ± 0.2	59.2	541.8 ± 25.8	0.978	13 ± 8	29 ± 13	10–15
30 °C	53.0 ± 2.3	60.2	516.2 ± 18.6	0.974	16 ± 2	25 ± 8	5–10
35 °C	49.9 ± 1.8	61.2	534.5 ± 12.0	0.977	12 ± 11	22 ± 15	5–10
40 °C	45.2 ± 9.3	62.2	504.8 ± 60.4	0.971	21 ± 8	20 ± 1	5–15
<b>RuO<sub>2</sub>-Nf<sub>3</sub> dried at 60 °C</b>							
21 °C	52.0 ± 2.0	58.4	667.3 ± 19.9	0.994	10 ± 3	19 ± 10	10–20
25 °C	52.3 ± 5.0	59.2	641.6 ± 8.8	0.997	12 ± 7	12 ± 5	15–25
30 °C	54.5 ± 2.1	60.2	556.3 ± 29.9	0.972	11 ± 6	23 ± 9	10–15
35 °C	54.7 ± 6.8	61.2	596.8 ± 17.4	0.952	17 ± 8	26 ± 2	5–15
40 °C	56.4 ± 10.7	62.2	645.6 ± 11.5	0.956	28 ± 10	32 ± 10	5–15
<b>RuO<sub>2</sub>-Nf<sub>3</sub> dried at 80 °C</b>							
21 °C	52.2 ± 2.1	58.4	485.7 ± 21.2	0.983	8 ± 5	14 ± 4	20–30
25 °C	53.5 ± 2.3	59.2	640.7 ± 75.7	0.985	8 ± 1	20 ± 6	5–20
30 °C	54.0 ± 0.8	60.2	548.1 ± 16.3	0.979	15 ± 6	17 ± 1	5–15
35 °C	54.5 ± 2.2	61.2	506.2 ± 41.9	0.985	12 ± 2	15 ± 9	10–20
40 °C	54.7 ± 2.2	62.2	583.6 ± 58.2	0.995	15 ± 7	20 ± 10	10–15

## ORCID

Maryna Lazouskaya  <https://orcid.org/0000-0003-2411-4267>  
 Ott Scheler  <https://orcid.org/0000-0002-8428-1350>  
 Kiranmai Uppuluri  <https://orcid.org/0000-0002-5725-252X>  
 Krzysztof Zaraska  <https://orcid.org/0000-0003-2298-7320>

## References

1. K. M. W. Loudon, K. M. W. Tarr, I. J. Lean, R. Polkinghorne, P. Megilchrist, F. R. Dunshea, G. E. Gardner, and D. W. Pethick, *Animals*, **9**, 612 (2019).
2. D. L. Hopkins, E. N. Ponnampalam, R. J. Van De Ven, and R. D. Warner, *Anim. Prod. Sci.*, **54**, 407 (2014).
3. P. Li, T. Wang, Y. Mao, Y. Zhang, L. Niu, R. Liang, L. Zhu, and X. Luo, *Sci. World J.*, **2014**, 174253 (2014).
4. P. G. Chambers and T. Grandin, *Guidelines for Humane Handling, Transport and Slaughter of Livestock*, ed. Gunter Heinz Thinnarat and Thinnarat Srisuvan (Food and Agriculture Organization of the United Nations (FAO), Rome, Italy) p. 3 (2001), <http://fao.org/3/a-x6909e.pdf>.
5. S. K. Matarneh, E. M. England, T. L. Scheffler, and D. E. Gerrard, *Lawrie's Meat Science*, ed. F. Toldra (Woodhead Publishing, Sawston, United Kingdom) 8th ed., 5, 159-185 (2017).
6. K. A. Abbas, A. Mohamed, B. Jamilah, and M. Ebrahimian, *Am. J. Biochem. Biotechnol.*, **4**, 416 (2008).
7. C. N. Ravishanker, T. M. R. Setty, and T. S. Shetty, *Indian J. Fish.*, **41**, 28 (1994).
8. V. R. Kyrana, V. P. Lougvois, and D. S. Valsamis, *Int. J. Food Sci. Tech.*, **32**, 339 (1997).
9. V. R. Kyrana and V. P. Lougvois, *Int. J. Food Sci. Technol.*, **37**, 319 (2002).
10. A. Poghosian, H. Geissler, and M. J. Schöning, *Biosens. Bioelectron.*, **140**, 111272 (2019).
11. S. A. Kandeel, A. A. Megahed, M. H. Ebeid, and P. D. Constable, *J. Dairy Sci.*, **102**, 1417 (2019).
12. J. Ping, X. Mao, K. Fan, D. Li, S. Ru, J. Wu, and Y. Ying, *Ionics (Kiel)*, **16**, 523 (2010).
13. N. Hamdi, J. Wang, and H. G. Monbouquette, *J. Electroanal. Chem.*, **581**, 258 (2005).
14. P. Kurzweil, *Sensors*, **9**, 4955 (2009).
15. L. Manjakkal, D. Szwagierczak, and R. Dahiya, *Prog. Mater. Sci.*, **109**, 1 (2020).
16. W. Lonsdale, S. P. Shylendra, S. Brouwer, M. Wajrak, and K. Alameh, *Sensors Actuators B Chem.*, **273**, 1222 (2018).
17. Council of Europe, *European Pharmacopoeia 5.0* (Council of Europe, Strasbourg, France) p. 26 (2005).
18. M. Khalil, S. Wang, J. Yu, R. L. Lee, and N. Liu, *J. Electrochem. Soc.*, **163**, B485 (2016).
19. K. Xu, X. Zhang, C. Chen, and M. Geng, *Int. J. Electrochem. Sci.*, **13**, 3080 (2018).
20. J. Chou, T. J. Ilgen, S. Gordon, A. D. Ranasinghe, E. W. McFarland, H. Metiu, and S. K. Buratto, *J. Electroanal. Chem.*, **632**, 97 (2009).
21. S. Zougar, O. Bechiri, S. Baali, R. Kherrat, M. Abbessi, N. Jaffrezic-Renault, and N. Fertikh, *Sens. Lett.*, **9**, 1 (2011).
22. P. Awasthi, R. Mukherjee, S. P. O. Kare, and S. Das, *RSC Adv.*, **6**, 102088 (2016).
23. S. J. Peighambaridou, S. Rowshanzamir, and M. Amjadi, *Int. J. Hydrogen Energy*, **35**, 9349 (2010).
24. K. Scott and A. K. Shukla, *Rev. Environ. Sci. Biotechnol.*, **3**, 273 (2004).
25. W. G. Grot, *Electrochemistry in Industry*, ed. U. Landau et al. (Springer, Boston, MA) p. 73 (1982).
26. A. Kusoglu and A. Weber, *Chem. Rev.*, **117**, 987 (2017).
27. N. Agmon, *Chem. Phys. Lett.*, **244**, 456 (1995).
28. X. Zhang, J. Wang, B. Ogorevc, and U. E. Spichiger, *Electroanalysis*, **11**, 945 (1999).
29. T. F. Tseng, Y. Yang, M. Chuang, S. Lou, M. Galik, G. Flechsig, and J. Wang, *Electrochem. Commun.*, **11**, 1819 (2009).
30. A. Olejnik, K. Siuzdak, J. Karczewski, and K. Grochowska, *Electroanalysis*, **31**, 1-11 (2019).
31. J. R. Marland, F. Moore, C. Dunare, A. Tsiamis, E. González-Fernández, E. O. Blair, S. Smith, J. G. Terry, A. F. Murray, and A. J. Walton, *IEEE Trans. Semicond. Manuf.*, **33**, 196 (2020).
32. G. Nagy, G. A. Gerhardt, A. F. Oke, M. E. Rice, R. N. Adams, R. B. Moore, M. N. Szentirmay, and C. R. Martin, *J. Electroanal. Chem.*, **188**, 85 (1985).
33. N. Stozhko, M. Bukharinova, L. Galperin, and K. Brainina, *Biosensors*, **8**, 5 (2018).
34. K. Zarei and H. Helli, *J. Electroanal. Chem.*, **749**, 10 (2015).
35. B. Nigović, M. Sadiković, and M. Sertić, *Talanta*, **122**, 187 (2014).
36. P. J. Kinlen, J. E. Heider, and D. E. Hubbard, *Sensors Actuators B Chem.*, **22**, 13 (1994).
37. W. Lonsdale, *Development, manufacture and application of a solid-state pH sensor using ruthenium oxide*, Edith Cowan University (2018). A thesis submitted in fulfilment of the requirement for the degree of Doctor of Philosophy <https://ro.ecu.edu.au/theses/2095/>.
38. W. Lonsdale, M. Wajrak, and K. Alameh, *Talanta*, **180**, 277 (2018).
39. K. Xu, X. Zhang, K. Hou, M. Geng, and L. Zhao, *J. Electrochem. Soc.*, **163**, B417 (2016).
40. S. Chinnathambi and G. Euverink, *J. Vis. Exp.*, **e58422**, 1 (2018), <https://www.jove.com/video/58422>.
41. S. M. U. Ali, Z. H. Ibulopo, M. Kashif, U. Hashim, and M. Willander, *Sensors*, **12**, 2787 (2012).
42. M. Lazouskaya, M. Tamm, O. Scheler, K. Uppuluri, and K. Zaraska, *Proc. Bienn. Balt. Electron. Conf.*, Tallinn, Estonia 6-8 October 2020(IEEE, Piscataway, New Jersey, USA) 18 (2020).
43. L. Manjakkal, K. Cvejin, J. Kulawik, K. Zaraska, and D. Szwagierczak, *Key Eng. Mater.*, **605**, 457 (2014).
44. L. Manjakkal, K. Cvejin, J. Kulawik, K. Zaraska, D. Szwagierczak, and R. P. Sochab, *Sensors Actuators B Chem.*, **204**, 57 (2014).
45. W. Lonsdale, D. K. Maurya, M. Wajrak, C. Y. Tay, B. J. Marshall, and K. Alameh, *Sensors Actuators B Chem.*, **242**, 1305 (2017).
46. K. Pásztor, A. Sekiguchi, N. Shimo, N. Kitamura, and H. Masuhara, *Sensors Actuators B Chem.*, **13**, 561 (1993).
47. H. N. McMurray, P. Douglas, and D. Abbot, *Sensors Actuators B Chem.*, **28**, 9 (1995).
48. P. Dawson, D. Elliott, A. Elliott, and K. Johns, *Directory Biochemist* (Mir, Moscow) p. 540 (1991).
49. S. Shi, A. Z. Weber, and A. Kusoglu, *Electrochim. Acta*, **220**, 517 (2016).
50. K. Uppuluri, M. Lazouskaya, D. Szwagierczak, K. Zaraska, and M. Tamm, *Sensors*, **21**, 5399 (2021).
51. S. Zhuiykov, *Sensors Actuators B Chem.*, **136**, 248 (2009).
52. L. Manjakkal, E. Djurdjic, K. Cvejin, J. Kulawik, K. Zaraska, and D. Szwagierczak, *Electrochim. Acta*, **168**, 246 (2015).
53. W. Lonsdale, M. Wajrak, and K. Alameh, *Sensors Actuators B Chem.*, **252**, 251 (2017).
54. W. Lonsdale, D. K. Maurya, M. Wajrak, and K. Alameh, *Talanta*, **164**, 52 (2017).
55. Y. H. Liao and J. C. Chou, *Sensors Actuators B Chem.*, **128**, 603 (2008).
56. E. Bijl, R. De Vries, H. Van Valenberg, and T. Huppertz, *Int. Dairy J.*, **34**, 135 (2014).
57. P. Hristov, I. Mitkov, D. Sirakova, I. Mehndgiiski, and G. Radoslavov, *Milk Proteins - From Structure to Biological Properties and Health Aspects*, ed. I. Gigli (IntechOpen, London) (2016).
58. A. Fleming, F. S. Schenkel, J. Chen, F. Malchiodi, R. A. Ali, B. Mallard, M. Sargolzaei, M. Corredig, and F. Miglior, *J. Dairy Sci.*, **100**, 1640 (2017).
59. V. Tatar, H. Mootse, A. Sats, T. Mahla, T. Kaart, and V. Poikalainen, *Agron. Res.*, **13**, 1112 (2015).
60. C. Phadungath, *Songklanakarini J. Sci. Technol.*, **27**, 433 (2005).
61. G. Alberti, R. Narducci, M. L. Di Vona, and S. Giancola, *Ind. Eng. Chem. Res.*, **52**, 10418 (2013).
62. K. A. Mauritz and R. B. Moore, *Chem. Rev.*, **104**, 4535 (2004).
63. Y. S. Kim, C. F. Welch, R. P. Hjelm, N. H. Mack, A. Labouriau, and E. B. Orler, *Macromolecules*, **48**, 2161 (2015).
64. T. J. Tan, D. Wang, and C. I. Moraru, *J. Dairy Sci.*, **97**, 4759 (2014).
65. S. Amemiya et al., *Handbook of Electrochemistry*, ed. C. Zoski (Elsevier, Amsterdam) 1st ed., p. 935 (2007).



## Appendix 3

### Publication III

M. Lazouskaya, Iuliia Vetik, Martti Tamm, Kiranmai Uppuluri, Ott Scheler, "Binary RuO<sub>2</sub>-CuO electrodes outperform RuO<sub>2</sub> electrodes in measuring the pH in food samples," *ACS Omega*, V. 8, P. 13275-13284, 2023.



# Binary RuO<sub>2</sub>–CuO Electrodes Outperform RuO<sub>2</sub> Electrodes in Measuring the pH in Food Samples

Maryna Lazouskaya,\* Iuliia Vetik, Martti Tamm, Kiranmai Uppuluri, and Ott Scheler

Cite This: *ACS Omega* 2023, 8, 13275–13284

Read Online

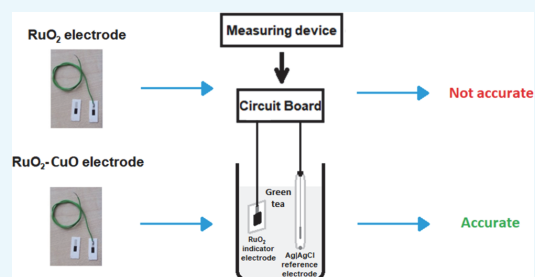
ACCESS |

Metrics & More

Article Recommendations

Supporting Information

**ABSTRACT:** Glass electrodes are the only type of pH-sensitive electrodes currently used in the food industry. While widely used, they have several disadvantages, especially in the areas of brittleness and price. Ruthenium(IV) oxide (RuO<sub>2</sub>) pH electrodes are a well-known alternative to conventional glass electrodes, providing improved durability and lower price. Nevertheless, partial substitution of RuO<sub>2</sub> with cupric oxide (CuO) would further lower the price and reduce the toxicity of the electrode. In this paper, we present the applicability of RuO<sub>2</sub>–CuO electrodes for pH measurement in food samples. The electrodes were fabricated by screen printing and covered with a protective Nafion membrane. In the experiments with food samples, the RuO<sub>2</sub>–CuO electrodes outperformed RuO<sub>2</sub> electrodes in measuring the pH with an almost twofold higher rate of accurate measurements. The utilization of CuO for the fabrication of pH electrodes allowed the accurate measurement of pH in a larger variety of food samples without compromising the response time.

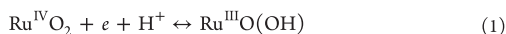


## INTRODUCTION

Screen-printed electrodes are a widely investigated alternative to bulky and fragile glass electrodes. Screen-printed electrodes are known to be cheap and sensitive and are capable of replacing conventional glass electrodes in pH measurements. Among the different screen-printed electrodes studied for pH measuring applications, ruthenium(IV) oxide (RuO<sub>2</sub>)-based electrodes have shown the best characteristics.<sup>1,2</sup> RuO<sub>2</sub>-based electrodes are highly sensitive to pH changes over a broad range and are chemically and thermally stable and biocompatible.<sup>1</sup>

Screen-printed electrodes based on RuO<sub>2</sub> have previously shown excellent pH sensitivity when used in water samples.<sup>3,4</sup> Screen printing is one of the simplest and cheapest methods for the fabrication of pH-sensitive solid-state electrodes.<sup>1</sup> It allows the deposition of layers with a thickness on the micrometer scale with excellent mechanical stability and good adherence to various substrates.<sup>3</sup> Screen-printed RuO<sub>2</sub> electrodes have close to Nernstian sensitivity and low hysteresis and drift rate in a wide pH range.<sup>1,3</sup>

The sensitivity of RuO<sub>2</sub> electrodes to the pH of the solution is based on the following reaction (simplified)<sup>2</sup>



The Nernst equation for the reaction 1 allows for a quantitative description

$$E = E_{\text{Ru}^{\text{IV}}/\text{Ru}^{\text{III}}}^0 - \frac{R \cdot T}{n \cdot F} \cdot \ln \frac{a_{\text{Ru}^{\text{III}}}}{a_{\text{Ru}^{\text{IV}}} \cdot a_{\text{H}^+}} \quad (2)$$

where  $E^0$  is the standard potential (individual potential of a reversible electrode (in equilibrium) in the standard state),  $V$ ;  $R$  is the universal gas constant, 8.314 J/K·mol;  $T$  is the temperature, K;  $n$  is the number of electrons participating in the redox reaction;  $F$  is the Faraday constant, 96485 C/mol;  $a_{\text{Ru}^{\text{IV}}}$  and  $a_{\text{Ru}^{\text{III}}}$  are the activities of Ru<sup>IV</sup>O<sub>2</sub> and Ru<sup>III</sup>O(OH), respectively, mol/L; and  $a_{\text{H}^+}$  is the activity of H<sup>+</sup> ions, mol/L.

Considering that the value of the activities of metals is approximately 1 in the solid state, substituting the constants at room temperature ( $T = 22$  °C) and replacing  $-\lg a_{\text{H}^+}$  with pH, eq 2 takes the following form

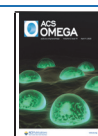
$$E = E_{\text{Ru}^{\text{IV}}/\text{Ru}^{\text{III}}}^0 + 58.6 \cdot \text{pH} \text{ (mV)} \quad (3)$$

eq 3 allows the determination of the pH of the solution by measuring the electrochemical potential of the RuO<sub>2</sub> electrode. Furthermore, in practice, the theoretical (Nernstian) sensitivity value of 58.6 mV/pH might not be observed.<sup>3</sup> The sensitivity is determined separately for each electrode by determining the

Received: January 26, 2023

Accepted: March 22, 2023

Published: March 30, 2023



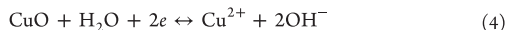
electrode potential in several buffer solutions and calibrating the electrode against buffers with known pH values.

The electrochemical potential of an electrode can be determined by connecting it to an electrochemical cell for potentiometric measurement. Such an electrochemical cell consists of (i) a measuring device—usually a galvanometer or voltmeter, (ii) an electrode of interest, which is called an indicator or working electrode (WE) (in our case—RuO<sub>2</sub> electrode), and (iii) a reference electrode (RE) with a stable potential that allows determining the potential of the indicator electrode (usually Ag/AgCl electrode) (Figure 1). The measuring device detects the difference in the electrochemical potentials between the indicator and the reference electrode.

At present, the application of screen-printed electrodes for pH measurement in food samples is limited due to the inability of electrodes to perform in complex media (e.g., containing fats or proteins).<sup>5</sup> Modification of screen-printed electrodes with a Nafion protective membrane was previously demonstrated to improve the performance of RuO<sub>2</sub> electrodes in milk.<sup>5</sup> Furthermore, the introduction of the Nafion membrane does not significantly alter the most important electrochemical characteristics of the pH-sensitive RuO<sub>2</sub> electrode.<sup>5</sup>

However, since ruthenium is a rare element,<sup>6</sup> it is not the best material to be used for the mass production of pH electrodes. Therefore, to improve the economic and ecological aspects of RuO<sub>2</sub> electrodes, it is possible to use binary oxides, where a part of RuO<sub>2</sub> is substituted with another oxide.<sup>4,7–10</sup> One of the oxides that can be used for this purpose is copper(II) oxide (CuO). Copper(II) oxide is easy to synthesize in various shapes (nanoribbons,<sup>11</sup> -flowers,<sup>11–13</sup> -wires,<sup>13</sup> -rods,<sup>14</sup> etc.) and sizes;<sup>12–14</sup> therefore, allowing the surface area to be improved. Due to its high specific surface area, chemical stability, electrocatalytic activity, and low price copper(II) oxide is widely used as an electrocatalyst,<sup>15</sup> supercapacitor,<sup>16</sup> photodetector,<sup>16</sup> and photocatalyst,<sup>16</sup> sensor for glucose,<sup>13,16</sup> humidity, and various gases,<sup>16</sup> such as ethanol,<sup>16,17</sup> hexanal,<sup>18</sup> acetone,<sup>19</sup> etc.<sup>19</sup> Furthermore, previous studies by Yang et al.<sup>20</sup> and Zaman et al.<sup>12</sup> have demonstrated

that CuO has a linear sub-Nernstian response to pH. The principle of pH sensitivity of metal oxides can be explained by binding theory: when metal oxide contacts with a solution, three types of surface charges are formed on the surface of metal oxide: negative (MO<sup>-</sup>), positive (MOH<sub>2</sub><sup>+</sup>), and neutral (MOH).<sup>21</sup> H<sup>+</sup> and OH<sup>-</sup> are attracted to negative and positive sites, respectively, leading to the formation of hydroxyl groups. For the RuO<sub>2</sub>, the reaction involving H<sup>+</sup> ions is described in eq 1, and for CuO, the reaction can be written as eq 4<sup>2</sup>



In this paper, the properties and performance of binary pH-sensitive electrodes based on a mixture of ruthenium and copper oxides (RuO<sub>2</sub>–CuO electrodes) are presented. The electrodes described in this study were fabricated by the screen printing and investigated by means of potentiometry.

## RESULTS AND DISCUSSION

**X-ray Diffraction Spectrum of the RuO<sub>2</sub>–CuO Electrodes.** In this study, the RuO<sub>2</sub>–CuO screen printing ink for the fabrication of the pH electrodes was made from commercially available RuO<sub>2</sub> and CuO nanoparticle powders. The X-ray diffraction (XRD) spectrum of the screen-printed and sintered RuO<sub>2</sub>–CuO ink is presented in Figure 2. The results correlate with the rutile structure for the RuO<sub>2</sub> (JCPDS 21-1172), the tenorite structure for CuO (JCPDS 98-009-2365), and the corundum structure for the Al<sub>2</sub>O<sub>3</sub>. Furthermore, evaluation of the peaks intensity revealed 46.8% of RuO<sub>2</sub>, 47.2% of CuO, and 6% Al<sub>2</sub>O<sub>3</sub> in the sample and therefore verifying the 1:1 mixing ratio of the metal oxides. The particle size calculated from the Scherrer equation was equal to 107 ± 13 nm. This finding correlates well with those observed by Manjakkal et al. for screen-printing inks fabricated by mixing RuO<sub>2</sub> with other oxides: Ta<sub>2</sub>O<sub>5</sub>, SnO<sub>2</sub>, and TiO<sub>2</sub>. For the RuO<sub>2</sub>–TiO<sub>2</sub>,<sup>7</sup> RuO<sub>2</sub>–SnO<sub>2</sub>,<sup>4</sup> and RuO<sub>2</sub>–Ta<sub>2</sub>O<sub>5</sub>,<sup>8,22</sup> the average grain size confirmed by scanning electron microscopy (SEM) was 100–260, 90–210, and 180–520 nm, respectively.

**Sensitivity of the RuO<sub>2</sub>–CuO Electrodes.** Screen printing is a cost-effective technique that is suitable for the mass production of all-solid-state electrodes.<sup>1,23</sup> Even though multiple parameters can be altered when depositing layers by the screen printing (e.g., changing the types of binders and

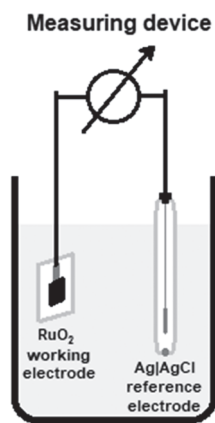


**Figure 1.** Schematic representation of an electrochemical cell. Primarily, an electrochemical cell for pH measurement consists of (i) a working electrode where the reaction involving H<sup>+</sup> ions takes place, (ii) a reference electrode that provides a stable and well-known potential, and (iii) a measuring device.

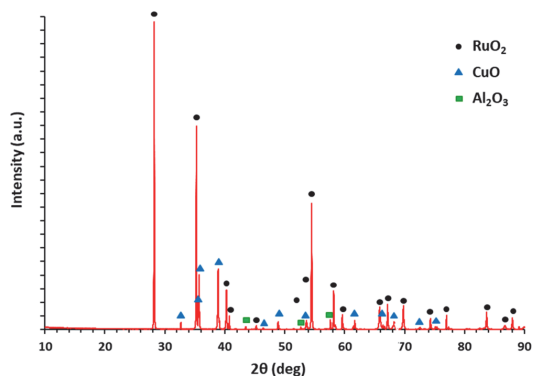


**Figure 2.** X-ray diffraction spectrum of the RuO<sub>2</sub>–CuO screen printed on the Al<sub>2</sub>O<sub>3</sub> substrate and sintered at 900 °C. RuO<sub>2</sub> and CuO were mixed at a 1:1 ratio.

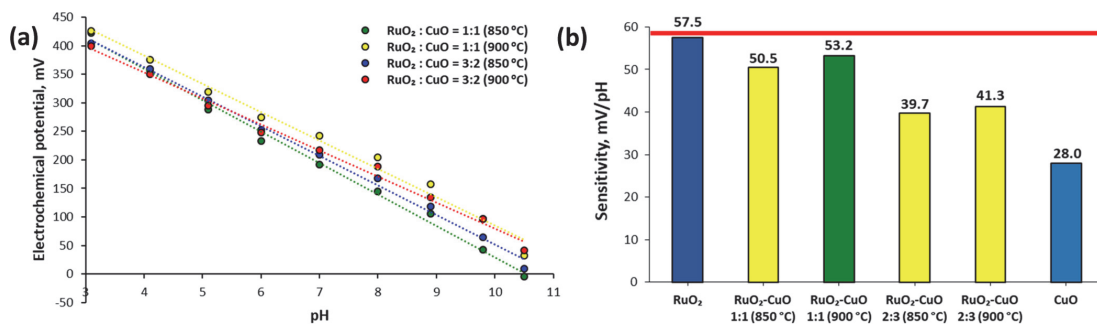


**Figure 3.** Among the fabricated electrodes, the RuO<sub>2</sub>-CuO electrodes with a RuO<sub>2</sub>:CuO ratio of 1:1 sintered at 900 °C (green) showed the best sensitivity. Graph (a) presents dependencies of the electrochemical potential of the fabricated RuO<sub>2</sub>-CuO electrodes (Y-axis) on pH (X-axis). Graph (b) presents the normalized sensitivity (Y-axis) of the fabricated RuO<sub>2</sub>-CuO electrodes compared to those of RuO<sub>2</sub> (purple) and CuO (blue) electrodes and theoretical sensitivity (red line). Red horizontal lines indicate the deviation of 5 mV/pH from the theoretical Nernstian response. The RuO<sub>2</sub>-CuO electrodes with a RuO<sub>2</sub>:CuO ratio of 1:1 sintered at 900 °C (green) were selected for further investigation. The data on the CuO electrodes were taken from ref.<sup>12</sup>

**Table 1.** Electrochemical Characteristics of the Glass Electrode and RuO<sub>2</sub>-Based pH Electrodes

electrode type	sensitivity, mV/pH	$E^0$ , mV	$R^2$	hysteresis A, mV	hysteresis B, mV	drift, mV/h
RuO <sub>2</sub>	57.5 ± 2.3	566.3 ± 55.3	0.979	3 ± 2	5 ± 2	0–5
RuO <sub>2</sub> -Nf	57.0 ± 0.7	684.1 ± 2.3	0.997	11 ± 1	17 ± 9	0–15
RuO <sub>2</sub> -CuO	54.3 ± 6.4	587.8 ± 15.6	0.989	5 ± 2	15 ± 2	0–5
RuO <sub>2</sub> -CuO-Nf	53.2 ± 1.6	575.3 ± 5.5	0.990	5 ± 2	20 ± 3	0–15
glass	58.8 ± 3.4	705.7 ± 36.8	0.997	10 ± 2	12 ± 3	0–5

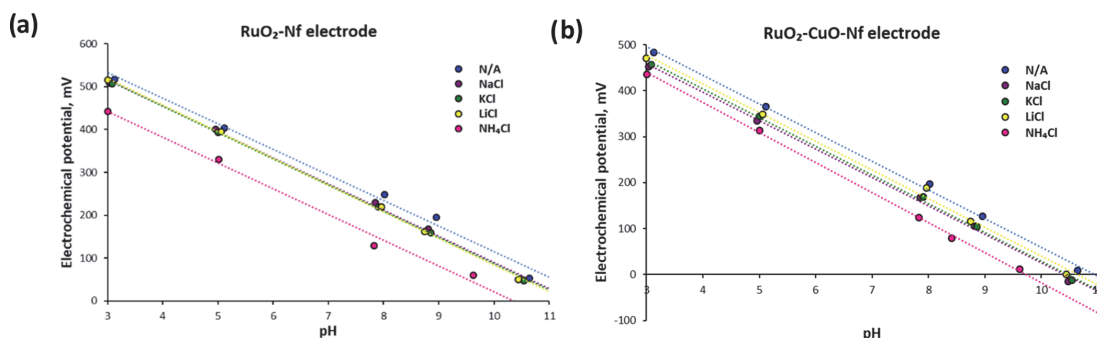


**Figure 4.** Electrochemical potential (Y-axis) of the fabricated RuO<sub>2</sub>-Nf (a) and RuO<sub>2</sub>-CuO-Nf (b) electrodes in the presence of Na<sup>+</sup> (purple), K<sup>+</sup> (green), Li<sup>+</sup> (yellow), and NH<sub>4</sub><sup>+</sup> (pink). The ammonium ion influenced the  $E^0$  value the most.

solvents and introducing additives), in our study, the following was investigated: (i) ratio of RuO<sub>2</sub> and CuO in the paste and (ii) sintering temperature. To determine the best RuO<sub>2</sub>-to-CuO ratio and sintering temperature, the fabricated electrodes were evaluated from the point of their sensitivity to pH changes. The results of the sensitivity measurement are presented in Figure 3 and Table S.1. The fabricated electrodes with a RuO<sub>2</sub> to CuO ratio of 1:1 sintered at 900 °C showed pH sensitivity similar to the sensitivity observed for RuO<sub>2</sub> electrodes and close to the theoretical sensitivity. Hence, these electrodes were selected for further study. For the RuO<sub>2</sub>-CuO electrodes with a greater amount of CuO, the sensitivity dropped by more than 10 mV/pH. This can be attributed to the lower sensitivity of CuO toward H<sup>+</sup> ions: Zaman et al.<sup>12</sup> previously reported sensor-based CuO nanoflowers that exhibited a near-Nernstian response of 28 mV/pH. In the

study by Yang et al.,<sup>20</sup> an extended gate effect transistor-based pH sensor that incorporated CuO nanowires showed pH sensitivity of 18.4 mV/pH. Furthermore, lower pH sensitivity for a lower concentration of RuO<sub>2</sub> correlates well with finding on electrodes fabricated from mixtures of RuO<sub>2</sub> with Ta<sub>2</sub>O<sub>5</sub>, TiO<sub>2</sub>, and SnO<sub>2</sub>.<sup>4,8,22</sup> Nevertheless, for RuO<sub>2</sub>-CuO electrodes with a RuO<sub>2</sub> to CuO ratio of 1:1, the pH sensitivity was closer to that of RuO<sub>2</sub> electrodes. This finding correlates well with the study by Manjakkal et al.<sup>8</sup> The author reported a pH sensor fabricated from a mixture of RuO<sub>2</sub> with tantalum(V) oxide (Ta<sub>2</sub>O<sub>5</sub>) mixed at RuO<sub>2</sub> to Ta<sub>2</sub>O<sub>5</sub> ratios of 7:3 and 3:7. The sensitivity of the RuO<sub>2</sub>-Ta<sub>2</sub>O<sub>5</sub> electrodes mixed at 7:3 ratio was equal to 56.17 mV/pH, whereas the sensitivity of the RuO<sub>2</sub>-Ta<sub>2</sub>O<sub>5</sub> electrodes mixed at 3:7 was equal to 35.3 mV/pH. Since the sensitivity of the RuO<sub>2</sub>-CuO electrodes with a RuO<sub>2</sub> to CuO ratio of 1:1 sintered at 900 °C was close to the



theoretical Nernstian sensitivity, other RuO<sub>2</sub> to CuO ratios were not investigated.

**Comparison of the RuO<sub>2</sub>–CuO Electrodes to the RuO<sub>2</sub> Electrodes.** For the selected RuO<sub>2</sub>–CuO electrodes with a RuO<sub>2</sub> to CuO ratio of 1:1 sintered at 900 °C, the remaining electrochemical characteristics were investigated and compared to those of a conventional glass electrode and RuO<sub>2</sub> electrodes. The characteristics of the electrodes are presented in Table 1. The fabricated RuO<sub>2</sub>–CuO electrodes showed good linearity ( $R^2 \sim 0.990$ ) and  $E^0$  values similar to those of RuO<sub>2</sub> electrodes. For Nafion-covered RuO<sub>2</sub> and RuO<sub>2</sub>–CuO electrodes, the electrochemical characteristics remained close to those of unmodified electrodes with slightly higher hysteresis and drift values since more time was required for ions to diffuse to the surface of the RuO<sub>2</sub> layer through the Nafion membrane.<sup>5,24</sup> Given that the Nafion membrane does not affect the performance of the RuO<sub>2</sub>–CuO electrodes, Nafion-covered electrodes were investigated for pH measurement in food samples.

**Cross-Sensitivity toward Interfering Ions.** Single-charged cations, such as Na<sup>+</sup>, K<sup>+</sup>, Li<sup>+</sup>, and NH<sub>4</sub><sup>+</sup>, can interfere with precise pH measurement. To study the influence of these cations on the performance of the fabricated electrodes, the sensitivity of the fabricated Nafion-modified electrodes was determined in their presence. The results are presented in Figure 4 and Table 2. The pH sensitivity of the fabricated electrodes was not affected by the presence of the studied cations: the largest deviation was observed for the RuO<sub>2</sub>–CuO–Nf electrode in the presence of NH<sub>4</sub><sup>+</sup> ions and was equal to 2.9 mV/pH. Nevertheless, the RuO<sub>2</sub>–Nf and RuO<sub>2</sub>–CuO–Nf electrodes showed good linearity with  $R^2$  values above 0.991. The drop in  $E^0$  values observed for both RuO<sub>2</sub>–Nf and RuO<sub>2</sub>–CuO–Nf electrodes in the presence of NH<sub>4</sub><sup>+</sup> ions can be due to the decreased conductivity of Nafion membrane caused by the reaction between the NH<sub>4</sub><sup>+</sup> and SO<sub>3</sub><sup>–</sup> groups in Nafion backbone.<sup>25</sup>

**pH of Water Samples.** The fabricated electrodes showed good performance in real-life water samples (Table 3). The average measurement accuracy was 0.23 and 0.05 pH units for the RuO<sub>2</sub>–Nf and RuO<sub>2</sub>–CuO–Nf electrodes, respectively. The fabricated electrodes exhibited a response similar to the conventional pH meter and a glass electrode with the maximum deviations of 0.36 and 0.12 pH units observed for RuO<sub>2</sub>–Nf and RuO<sub>2</sub>–CuO–Nf electrodes, respectively. Furthermore, all the fabricated electrodes showed good uniformity of the measured pH value (STD < 0.05 pH units).

**pH of Food Samples.** The performance of the solid-state pH electrodes in food samples can be different from their performance in diluted water samples or buffers due to a more complex composition or higher density. Even for measurement

**Table 2. Characteristics of the RuO<sub>2</sub>–Nf and RuO<sub>2</sub>–CuO–Nf Electrodes in the Presence of the Interfering Ions**

	RuO <sub>2</sub> –Nf			RuO <sub>2</sub> –CuO–Nf		
	sensitivity, mV/pH	$E^0$ , mV	$R^2$	sensitivity, mV/pH	$E^0$ , mV	$R^2$
no added salts	59.6	711.2	0.991	62.4	684.1	0.998
NaCl	60.9	699.9	0.998	61.9	644.2	0.998
KCl	61.2	698.9	0.999	62.4	654.4	0.999
LiCl	62.4	707.1	0.999	62.4	664.0	0.995
NH <sub>4</sub> Cl	60.1	622.9	0.991	65.3	634.8	0.999

**Table 3. pH Values Measured with a Conventional Glass Electrode, RuO<sub>2</sub>–Nf and RuO<sub>2</sub>–CuO–Nf Electrodes in Different Water Samples**

water sample	pH	glass electrode	RuO <sub>2</sub> –Nf	RuO <sub>2</sub> –CuO–Nf
tap water	7.7	7.69 ± 0.02	8.06 ± 0.01	7.68 ± 0.05
river water	7.34	7.35 ± 0.04	7.2 ± 0.05	7.35 ± 0.03
pond water	7.18	7.17 ± 0.02	6.99 ± 0.05	7.06 ± 0.04
seawater	7.54	7.55 ± 0.02	7.3 ± 0.01	7.5 ± 0.03

with a conventional glass electrode, adjustments should be made for proper pH measurement.<sup>26</sup> The literature on the application of solid-state pH electrodes is scarce; to our knowledge, there are only a few articles. In 2008, Liao and Chou<sup>27</sup> presented their working electrode, consisting of a RuO<sub>2</sub> film sputtered on top of a silicon wafer. Their electrodes exhibited pH differences of 0.14 and 0.50 pH units for coke and milk, respectively. In 2015, Manjakkal et al.<sup>4</sup> reported a screen-printed RuO<sub>2</sub>–SnO<sub>2</sub> WE that was tested in lemon juice and showed a pH difference from a conventional glass electrode of 0.21 pH units. In 2018, Xu et al.<sup>28</sup> reported their potentiometric system, consisting of a printed circuit board with two electrodes attached to it from the opposite sides: a sputtered antimony film on a copper substrate modified with a Nafion membrane as the WE and Ag/AgCl modified with a graphene-chitosan membrane as the RE. The reported electrodes showed pH differences of 0.19 and 0.11 pH units for coke and vinegar, respectively. Furthermore, Li et al.<sup>29</sup> reported their potentiometric system utilizing poly(ethylene terephthalate)-covered indium tin oxide as the WE and Ti/Au/Ag/AgCl covered with a porous poly(vinyl butyral) membrane ion-selective field-effect transistor as the RE. For their electrodes, the pH difference was above 0.50 pH units in all the studied samples (coke, orange juice, beer, milk, etc.). The authors suggested that the pH difference from a conventional glass electrode can be due to the interference of proteins, organics, and additives in the beverages. Lonsdale et al.<sup>30</sup> published their results on a WE that consisted of a RuO<sub>2</sub> film sputter-deposited on an alumina substrate and modified with a sputtered Ta<sub>2</sub>O<sub>5</sub> layer and drop-casted Nafion membrane. The electrodes showed excellent performance with pH differences not exceeding 0.08 pH units for the investigated samples, which included coke, beer, and milk. In 2020, Hu et al.<sup>31</sup> reported a potentiometric pH sensor based on a graphite electrode modified with tryptophan residues. The sensor exhibited a sensitivity of 52 mV/pH and a deviation from the CGE of 0.15 pH units when used in milk and coke. Another article published in 2020 by Vivaldi et al.<sup>32</sup> presented a screen-printed gold electrode modified with an indoaniline derivative as a pH-sensitive material. The sensor had a Nernstian response (56 mV/pH) and showed a deviation from the CGE of about 0.4 pH units when used in orange juice, milk, and tea.

The results of the pH measurements with the fabricated RuO<sub>2</sub>–Nf and RuO<sub>2</sub>–CuO–Nf electrodes are presented in Figure 5 and Table S.2. The ±0.5 pH units were used as a reference margin.

In caffeinated drinks, the fabricated electrodes showed a significant difference from the pH values measured with a conventional glass electrode. For the RuO<sub>2</sub>–Nf electrode, the pH difference exceeded 0.5 pH units, making these electrodes unsuitable for pH measurement in tea or coffee samples. The RuO<sub>2</sub>–CuO–Nf electrodes showed better performance: the

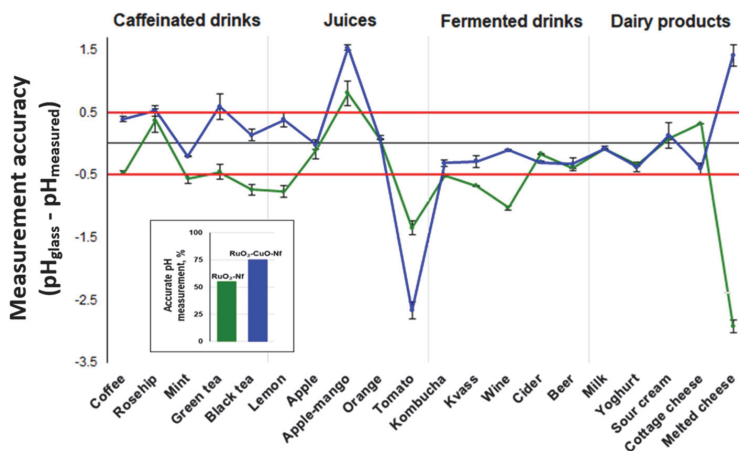


**Figure 5.** RuO<sub>2</sub>-CuO-Nf electrodes (blue) showed less scattered pH values measured for two electrodes in parallel compared to RuO<sub>2</sub>-Nf electrodes (green). Red horizontal lines (c) indicate the corridor or minimum (−0.5) and maximum (0.5) accepted errors. The accuracy of the electrodes was evaluated as a probability to measure the pH with the difference from the conventional glass electrode not exceeding 0.5 pH units. For the RuO<sub>2</sub>-Nf electrodes, the error exceeded 0.5 pH units in 45% of all measurements, and for RuO<sub>2</sub>-CuO-Nf electrodes, the error exceeded 0.5 pH units in only 25% of all measurements.

average pH difference was 0.36 pH units, with a pH difference exceeding 0.5 pH units only for the green tea sample (0.59 pH units).

The difference in the RuO<sub>2</sub>-Nf and RuO<sub>2</sub>-CuO-Nf electrode performance is more noticeable in the juice samples. Both electrode types showed errors exceeding 0.5 pH units in samples of higher density and thickness. Fruit juices contain ascorbic acid (reducing agent) that negatively affects the performance of metal oxide electrodes.<sup>30</sup> Furthermore, the viscosity of the samples can negatively affect the potential of a metal oxide electrode.<sup>33</sup> A more detailed study of this phenomenon is necessary and will be addressed in our future work.

The performance of the fabricated electrodes in fermented drinks was more accurate, with the RuO<sub>2</sub>-CuO-Nf electrodes showing an average pH difference of −0.27 pH units.

The investigation of the performance of the fabricated electrodes in dairy products revealed that both electrode types are suitable for pH measurement even in products with higher density. The fabricated electrodes only failed to measure the pH in melted cheese: the pH difference exceeded 1.4 pH units in both cases. For the melted cheese, the viscosity of the sample could have been the problem. In the dairy industry, measuring the pH of samples is a challenge. Usually, a homogenate is prepared by blending with water, and then, the pH of the homogenate is measured. In this study, we attempted to measure the pH of the product and not homogenate, thus, setting a challenging task. The challenges of measuring the pH in viscous samples correlate well with the findings of Chawang et al.,<sup>33</sup> where authors have demonstrated that the viscosity of starch significantly influenced the measured potential of the iridium oxide electrode.

Furthermore, it is worth mentioning that the response time (time needed for an electrode to reach stable potential) in caffeinated drinks did not exceed 90 s for either electrode type. In the case of fermented drinks, apple and lemon juices, milk, and yoghurt, the time to reach stable potential did not exceed 5 min. For the samples of thicker texture, such as apple-mango,

orange, and tomato juices, sour cream, cottage, and melted cheese, the measurement was conducted for almost 10 min.

Overall, the RuO<sub>2</sub>-Nf electrodes failed to accurately measure pH in 9 out of 20 investigated samples, while RuO<sub>2</sub>-CuO-Nf electrodes failed only in 5 out of 20 samples; thus, an almost twofold improvement in the performance of the pH electrodes was observed.

## CONCLUSIONS

In conclusion, electrodes based on binary oxide RuO<sub>2</sub> and CuO fabricated by a screen-printing technique were tested for pH measurement for the first time. The application of the electrodes in real-life food samples was possible due to the coverage of the electrodes with a Nafion protective membrane. The RuO<sub>2</sub>-CuO-Nf electrodes surpass RuO<sub>2</sub>-Nf electrodes in potentiometric pH measurement not only from the point of cost-effectiveness but also the overall performance in real-life samples. The proposed electrodes aim to replace fragile glass electrodes in the pH measurement of food samples. Since the reported electrodes are physically durable, they can be of interest to food researchers not only in research but also in industrial pH measurement. Binary electrodes are equal to both conventional glass electrodes and previously reported RuO<sub>2</sub> electrodes from the point of view of the electrochemical characteristics. Furthermore, RuO<sub>2</sub>-CuO pH electrodes covered with a protective Nafion membrane are compatible with pH measurements of common beverages and dairy products. Significant error, exceeding 0.5 pH units, was observed only when measuring specific juices and cheese. Apparently, the texture of the sample, as well as its composition, can affect the performance of the screen-printed RuO<sub>2</sub>-based electrode. In our future work, we plan to further investigate the influence of the abovementioned factors.

## MATERIALS AND METHODS

**Fabrication of RuO<sub>2</sub> Electrodes.** The electrodes were fabricated similarly to previously described methods.<sup>34</sup> Briefly, two layers were deposited on an alumina (Al<sub>2</sub>O<sub>3</sub>) substrate by

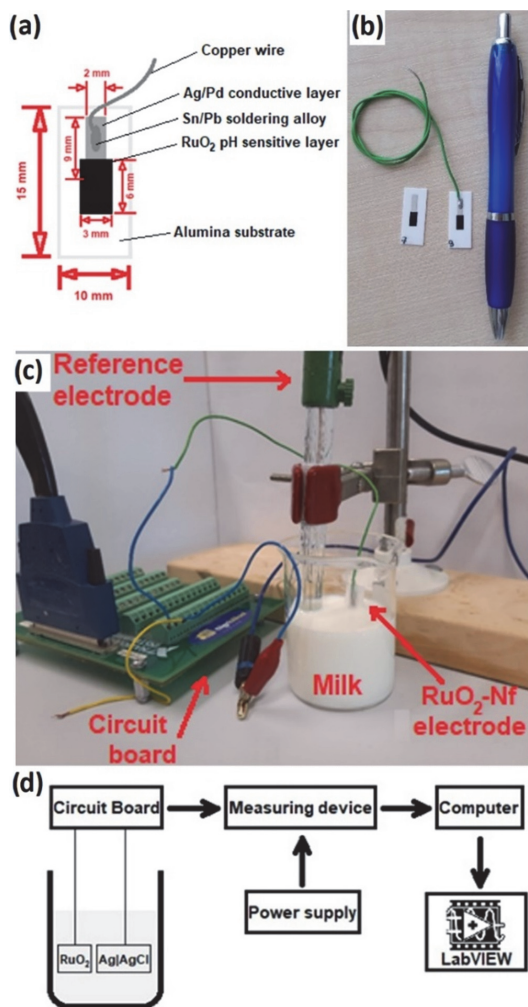


**Figure 6.** The RuO<sub>2</sub> electrodes were fabricated by screen printing a conductive Ag/Pd layer and pH-sensitive RuO<sub>2</sub> layer on an alumina substrate (a). A copper wire was connected to the conductive layer by soldering with a Pb/Sn alloy. In Figure (b), a pen is placed next to the fabricated sensors for comparison. For the electrochemical measurement, a fabricated electrode and a standard glass reference electrode were placed into a sample solution (c). In Figure (d), the scheme of the measuring setup is presented: the RuO<sub>2</sub> pH-sensitive electrode and Ag/AgCl reference electrode were connected to the measuring device via the circuit board. The measuring supply was powered with an input voltage of 12 V. The data were registered and monitored using the LabView program.

**Table 4. Water Samples Used for the Investigation of the Performance of the Fabricated Electrodes**

sample	pH	collection place
tap water	7.70	lab sink
river water	7.34	river near Toolese village, Estonia
pond water	7.18	pond near Toolese village
seawater	7.54	Kunda bay near Toolese village

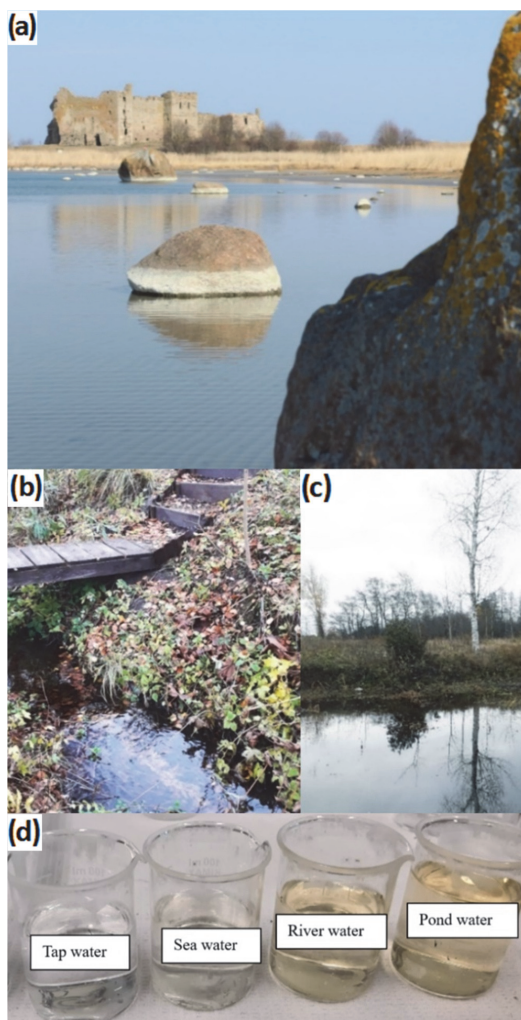


**Figure 7.** Photos of the places where water samples were collected: (a) Kunda bay of Baltic sea, (b) pond, and (c) river in Toolese village, (d) side-by-side comparison of collected water samples.

the screen printing: a conductive layer and a pH-sensitive layer. A conductive layer of Ag/Pd thick film paste (9695, Electro-Science Laboratories, King of Prussia, Pennsylvania) was printed first, and a pH-sensitive layer of commercially available RuO<sub>2</sub> paste (10 kΩ/sq, 3914, Electro-Science Laboratories, King of Prussia, Pennsylvania) was printed second. Furthermore, the RuO<sub>2</sub> layer was printed in such a way that it would partly overlap the conductive Ag/Pd layer. The substrates were dried at 120 °C for 15 min and consequently sintered at 850 °C for 1 h after the first printing step and at 900 °C for 1 h after the second printing step. After cooling the substrate, a copper wire was connected to the Ag/Pd layer by soldering with a Sn/Pb alloy. Finally, a protective layer of silicone rubber (DOWSIL 3140 RTV Coating, Dow Chemical Company, Midland, Michigan) was used to cover the conductive layer and the electric contact. The dimensions of the fabricated

Table 5. Food Samples Used for the Investigation of the Performance of the Fabricated Electrodes

sample	pH	manufacturer	sample	pH	manufacturer
<i>caffeinated drinks</i>			<i>fermented drinks</i>		
Rosehip tea	3.21	Herba, Germany	Kombucha	3.67	GUTsy, Portugal
coffee	5.08	Jacobs, Germany	Kvass	3.61	A. Le Coq, Estonia
mint tea	6.83	Herba, Germany	wine	3.42	Mirabeau, France
green tea	6.97	Tetley, U.K.	cider	3.22	A. Le Coq, Estonia
black tea	7.31	Tetley, U.K.	beer	4.38	Heineken, Netherlands
<i>juices</i>			<i>dairy products</i>		
lemon juice	2.55	ICA, Italy	milk	6.68	Valio, Estonia
apple juice	3.06	A. Le Coq, Estonia	yogurt	4.36	Valio, Estonia
apple-mango juice	3.80	A. Le Coq, Estonia	sour cream	4.35	Valio, Estonia
orange juice	3.93	A. Le Coq, Estonia	cottage cheese	4.68	Valio, Estonia
tomato juice	4.31	A. Le Coq, Estonia	melted cheese	5.96	Valio, Estonia

RuO<sub>2</sub> electrodes are presented in Figure 6a,b. The screen-printed RuO<sub>2</sub> electrodes were previously characterized by Manjakkal et al.<sup>35–37</sup>

**Fabrication of RuO<sub>2</sub>–CuO Electrodes.** The RuO<sub>2</sub>–CuO electrodes were fabricated similarly to the RuO<sub>2</sub>-based electrodes previously described by Manjakkal and co-workers.<sup>4,7,8</sup> The only difference was in the paste used for the deposition of the pH-sensitive layer. For the fabrication of the RuO<sub>2</sub>–CuO electrodes, the RuO<sub>2</sub>–CuO paste was prepared before screen printing. Anhydrous RuO<sub>2</sub> (99.9% pure, Sigma-Aldrich, USA) and CuO (average particle size 40–80 nm, 99.9% pure, Chempur, Germany) were mixed in an agate mortar. Ethylcellulose (analytical grade purity) and terpineol (anhydrous, Fluka Analytical) were added to the mortar as binders for the paste. The oxides were mixed for 20 min to achieve optimal consistency of the paste.

Two RuO<sub>2</sub>/CuO ratios were investigated to determine what part of RuO<sub>2</sub> can be successfully substituted with CuO without compromising the electrode performance: 1:1 and 2:3. All the other parameters of the fabrication remained the same.

Two different temperatures were used to investigate the influence of the sintering temperature on the properties of the RuO<sub>2</sub>–CuO electrodes: 850 and 900 °C. The sintering temperature was previously demonstrated to not affect RuO<sub>2</sub> electrodes.<sup>3</sup> All the other parameters of the fabrication remained the same.

The crystalline structure of the RuO<sub>2</sub>–CuO screen printing ink was conducted by the X-ray diffraction (XRD) analysis using a Empyrean diffractometer (Malvern Pananalytical, U.K.). The copper target (1.54 Å) was used to record the intensity of the diffraction in the range of 5–90° 2θ. Phase identification was performed according to the International Center for Diffraction Database (ICDD). Crystallite size was calculated from the Scherrer equation.<sup>38</sup> Scanning electron microscopy (SEM) and transmission electron microscopy (TEM) were not performed in this study.

**Deposition of the Nafion Membrane.** To make the fabricated electrodes suitable for measurement in dairy products, the fabricated electrodes were covered with a Nafion protective membrane by the drop-casting technique. The methodology for the Nafion membrane deposition was previously reported elsewhere.<sup>34</sup> Briefly, 10 μL of 5% solution of Nafion in a mixture of lower aliphatic alcohols and water (Nafion 117, Sigma-Aldrich, USA) was applied to cover the pH-sensitive area of the fabricated electrodes. Next, the electrodes were dried in a laboratory incubator (BD 53, Binder, Germany) at 80 °C for 2 h. The Nafion solution was

pipetted on the electrodes and dried in the laboratory incubator two more times, thus creating three layers of the Nafion membrane. After the last layer was dried in the laboratory incubator, the electrodes were left to air-dry at room temperature overnight. The RuO<sub>2</sub> and RuO<sub>2</sub>–CuO electrodes modified with Nafion were named RuO<sub>2</sub>–Nf and RuO<sub>2</sub>–CuO–Nf, respectively.

**Setup for Potentiometric Measurement.** All the measurements were performed in an electrochemical cell, as presented in Figure 6c,d. One of the fabricated electrodes (RuO<sub>2</sub>, RuO<sub>2</sub>–CuO, RuO<sub>2</sub>–Nf, or RuO<sub>2</sub>–CuO–Nf) and a standard glass ion-selective Ag|AgCl (RL-100, HYDROMET, Poland) reference electrode were connected to the measuring device (Data Acquisition (DAQ) device, USB-6259, National Instruments, USA) through a circuit board via galvanic connections. The measuring device was powered by a high-performance digital power supply (E3631A, Agilent, USA) with an input voltage of 12 V. The potential difference between a fabricated and the reference electrode was monitored and registered with the use of the LabVIEW program (National Instruments, USA).

**Determination of Electrochemical Characteristics.** The following characteristics were determined to evaluate the electrode performance: sensitivity and linearity, hysteresis and drift effects, and cross-sensitivity to interfering ions. The abovementioned characteristics were measured for a conventional glass electrode (HI1053P, Hanna Instruments, USA) as well. All the measurements were conducted in triplicate for 2 electrodes of the same kind if not specified otherwise.

All the electrochemical characteristics of the fabricated electrodes were evaluated after one month of conditioning in water. This preliminary condition is necessary for an electrode to reach stable working conditions.<sup>39</sup>

The sensitivity of the fabricated electrodes were determined by calibrating them against buffer solutions. Buffer solutions in the pH range of 3.0–11.0 were used. Buffers were freshly prepared from anhydrous salts (Sigma-Aldrich, Massachusetts) according to the procedure described by Dawson et al.<sup>40</sup> The pH of the buffers was determined with a conventional pH meter (Seven2Go Advanced Single-Channel Portable pH Meter, Mettler Toledo, Switzerland). To calibrate an electrode, the potential of the electrode was determined in several buffer solutions 90 s after immersing the electrode into a buffer solution. The values of the electrode potential (*Y*-axis) were plotted against the pH of the buffers (*X*-axis), and the sensitivity was determined as a slope of the function  $E = f(\text{pH})$

by the method of least squares.  $E^0$  was determined by extrapolating the function to the intersection with the Y-axis.

The sensitivity was determined for all the fabricated electrode types (RuO<sub>2</sub>, RuO<sub>2</sub>-CuO, RuO<sub>2</sub>-Nf, and RuO<sub>2</sub>-CuO-Nf) to evaluate whether the Nafion membrane is suitable for RuO<sub>2</sub>-CuO electrodes. Since the sensitivity of the RuO<sub>2</sub>-CuO electrodes with and without Nafion was similar (as for RuO<sub>2</sub> electrodes) and the electrodes without a Nafion protective layer ceased working in food samples, all of the following characteristics were evaluated for the RuO<sub>2</sub>-Nf and RuO<sub>2</sub>-CuO-Nf electrodes only.

The hysteresis (mV) is a characteristic of an electrode that is observed when the electrode has different potential values in the same media due to the previous electrode's exposure to a solution of different pH values. Hysteresis is associated with changes in the composition of the double layer on the surface of the electrode. Hysteresis of the fabricated electrodes was determined by exposing the electrodes to the buffer solutions in a loop manner. Two loops were investigated separately: an acidic loop (pH values of 3-5-7-5-3) and a basic loop (pH values of 11-9-7-9-11). A fabricated electrode and the reference electrode were placed into a buffer solution, and the potential was recorded 5 min after the submersion of the electrodes into the buffer. Then, the electrodes were rinsed with distilled water, gently tapped with a paper towel, and placed into the next buffer solution. Hysteresis was determined as the difference in the potential values of the electrode at pH 3.

The drift of the potential of an electrode (mV/h) is defined as a slow nonrandom change in the reading of an electrode with time. The drift of the electrode potential is associated with the diffusion of H<sup>+</sup> ions.<sup>41</sup> The drift rate of the fabricated electrodes was determined by recording the potential of an electrode for 2 h and calculating the average difference (per hour) in the potential values of an electrode at the beginning of the measurement and after 2 h of continuous potential measurement.

The presence of some of the compounds in the sample can affect the performance of a solid-state electrode.<sup>3,4,8</sup> The interference of ions with the performance of the fabricated electrodes was evaluated by determining the sensitivity of the electrodes in the presence of specific anions and cations. Buffer solutions additionally containing the chlorides of Li<sup>+</sup>, Na<sup>+</sup>, K<sup>+</sup>, and NH<sub>4</sub><sup>+</sup> at a concentration of 0.1 M were prepared (other cations were not investigated since the Nafion membrane allows only small ions to pass through<sup>25</sup>). The potential of the electrode was determined in the buffer solutions 90 s after immersing the electrode into each buffer.

The Electrical Impedance Spectroscopy (EIS) was not performed in this study; however, the capacitive characteristics of the RuO<sub>2</sub>-CuO electrodes are expected to be similar to those of RuO<sub>2</sub>-SnO<sub>2</sub> previously described by Manjakkal et al.<sup>4</sup> RuO<sub>2</sub>-CuO electrodes are expected to have more capacitive nature than RuO<sub>2</sub> electrodes. The Nyquist plot of RuO<sub>2</sub> consists of a bigger semi-circular arc in low frequency range that is due to adsorption of ions on the surface of the electrode.<sup>37</sup> For the CuO, the semi-circle which is observed in the higher frequency range and is due to the charge-transfer process of H<sup>+</sup>/OH<sup>-</sup> ions at the CuO/solution interface.<sup>14</sup>

The stability and the reusability of the RuO<sub>2</sub>-Nf electrodes was reported in our previous works.<sup>5,42</sup> Briefly, the stability of the RuO<sub>2</sub> electrodes was evaluated by monitoring the sensitivity over the course of 7 weeks. The sensitivity was changing during first 3 weeks and then remained at the same

value.<sup>5</sup> Furthermore, the RuO<sub>2</sub>-Nf electrodes were tested for 1 h-long measurement in milk and exhibited performance similar to the conventional glass electrode.<sup>5</sup> The RuO<sub>2</sub>-Nf electrodes were shown to be reusable by renewing the Nafion membrane.<sup>42</sup> The stability of the RuO<sub>2</sub>-CuO-Nf electrodes is similar to the RuO<sub>2</sub>-Nf electrodes.

**Measurement in Real-Life Samples.** The pH values of the samples were determined by two-point calibration, which is widely used in laboratory practice.<sup>26,43,44</sup> For this purpose, commercially available certified buffers (Certipur, Merk, New Jersey) with pH values of 4 and 7 were used. The RuO<sub>2</sub>-Nf or RuO<sub>2</sub>-CuO-Nf electrode was placed into a buffer solution of pH 7, and readings of the voltmeter were recorded for 5 min. Then, the electrode was rinsed with Milli-Q water and placed into a buffer solution of pH 4, and the potential was again measured for 5 min. The electrode was rinsed with Milli-Q water again and placed into a sample. The potential of the electrode was registered 5 min after placing the electrode into the sample. All the measurements were made in triplicate for two identical electrodes.

The performance of the fabricated electrodes was evaluated as the measurement accuracy determined as the difference in pH readings between a fabricated electrode (pH<sub>measured</sub>) and the pH meter (pH<sub>glass</sub>) on the basis of the following formula

$$\text{Measurement accuracy} = \text{pH}_{\text{measured}} - \text{pH}_{\text{glass}} \quad (5)$$

Water samples from different sources (Table 4 and Figure 7) were collected to evaluate the performance of the fabricated electrodes. The seawater was collected at the Kunda bay of the Baltic sea 3 meters from the shore. The pond water was collected from the surface of a small pond near Toole village, Haljala vald, Estonia. All of the samples were stored at 4 °C and allowed to warm up to room temperature prior to any measurement. The pH value of the collected samples was measured with a conventional pH meter.

All the food samples (Table 5) were purchased from a local grocery store. The samples were brought to room temperature (22 °C) prior to any measurements. A conventional pH meter was used to determine the pH values of the food samples.

## ■ ASSOCIATED CONTENT

### SI Supporting Information

The Supporting Information is available free of charge at <https://pubs.acs.org/doi/10.1021/acsomega.3c00538>.

Sensitivity values for the RuO<sub>2</sub>-CuO electrodes at different mixing ratios and sintering temperatures; pH values measured with a conventional glass electrode, RuO<sub>2</sub>-Nf and RuO<sub>2</sub>-CuO-Nf electrodes in different food samples (PDF)

## ■ AUTHOR INFORMATION

### Corresponding Author

Maryna Lazouskaya – School of Science, Department of Chemistry and Biotechnology, Tallinn University of Technology, 19086 Tallinn, Estonia; Center of Food and Fermentation Technologies (TFTAK), 12618 Tallinn, Estonia; [orcid.org/0000-0003-2411-4267](https://orcid.org/0000-0003-2411-4267); Phone: +372-5596-6379; Email: [maryna.lazouskaya@taltech.ee](mailto:maryna.lazouskaya@taltech.ee)

## Authors

Iuliia Vetik – School of Science, Department of Chemistry and Biotechnology, Tallinn University of Technology, 19086 Tallinn, Estonia

Martti Tamm – Center of Food and Fermentation Technologies (TFTAK), 12618 Tallinn, Estonia

Kiranmai Uppuluri – Łukasiewicz Research Network—Institute of Microelectronics and Photonics (Łukasiewicz—IMI), 30-701 Kraków, Poland

Ott Scheler – School of Science, Department of Chemistry and Biotechnology, Tallinn University of Technology, 19086 Tallinn, Estonia; [orcid.org/0000-0002-8428-1350](https://orcid.org/0000-0002-8428-1350)

Complete contact information is available at:

<https://pubs.acs.org/10.1021/acsomega.3c00538>

## Notes

The authors declare no competing financial interest.

## ACKNOWLEDGMENTS

This work was supported by the European Commission through the AQUASENSE project [project code H2020-MSCA-ITN-2018-813680]. Ott Scheler acknowledges support from the Tallinn University of Technology development program 2016–2022 [project code 2014-2020.4.01.16-0032]. The authors would like to thank Professor Magnus Willander for the review of the manuscript.

## REFERENCES

- (1) Manjakkal, L.; Szwagierczak, D.; Dahiya, R. Metal Oxides Based Electrochemical pH Sensors: Current Progress and Future Perspectives. *Prog. Mater. Sci.* **2020**, *109*, No. 100635.
- (2) Kurzweil, P. Metal Oxides and Ion-Exchanging Surfaces as pH Sensors in Liquids: State-of-the-Art and Outlook. *Sensors* **2009**, *9*, 4955–4985.
- (3) Uppuluri, K.; Lazouskaya, M.; Szwagierczak, D.; Zaraska, K.; Tamm, M. Fabrication, Potentiometric Characterization, and Application of Screen-Printed RuO<sub>2</sub> pH Electrodes for Water Quality Testing. *Sensors* **2021**, *21*, 5399.
- (4) Manjakkal, L.; Cvejnik, K.; Kulawik, J.; Zaraska, K.; Szwagierczak, D.; Stojanovic, G. Sensing Mechanism of RuO<sub>2</sub>-SnO<sub>2</sub> Thick Film pH Sensors Studied by Potentiometric Method and Electrochemical Impedance Spectroscopy. *J. Electroanal. Chem.* **2015**, *759*, 82–90.
- (5) Lazouskaya, M.; Scheler, O.; Mikli, V.; Uppuluri, K.; Zaraska, K.; Tamm, M. Nafion Protective Membrane Enables Using Ruthenium Oxide Electrodes for pH Measurement in Milk. *J. Electrochem. Soc.* **2021**, *168*, No. 107511.
- (6) Knunyants, I. L.; Zefirov, N. S.; Kulov, N. N. *Khimicheskaya Entsiklopediya [Chemical Encyclopedia]*; Knunyants, I. L.; Zefirov, N. S.; Kulov, N. N., Eds.; Sovietskaya enciklopediya: Moscow, 1965; Vol. 4.
- (7) Manjakkal, L.; Cvejnik, K.; Kulawik, J.; Zaraska, K.; Szwagierczak, D.; Socha, R. P. Fabrication of Thick Film Sensitive RuO<sub>2</sub>-TiO<sub>2</sub> and Ag/AgCl/KCl Reference Electrodes and Their Application for pH Measurements. *Sens. Actuators, B* **2014**, *204*, 57–67.
- (8) Manjakkal, L.; Zaraska, K.; Cvejnik, K.; Kulawik, J.; Szwagierczak, D. Potentiometric RuO<sub>2</sub>-Ta<sub>2</sub>O<sub>5</sub> pH Sensors Fabricated Using Thick Film and LTCC Technologies. *Talanta* **2016**, *147*, 233–240.
- (9) Zhuiykov, S.; Marney, D.; Kats, E. Investigation of Electrochemical Properties of La<sub>2</sub>O<sub>3</sub>-RuO<sub>2</sub> Thin-Film Sensing Electrodes Used in Sensors for the Analysis of Complex Solutions. *Int. J. Appl. Ceram. Technol.* **2011**, *8*, 1192–1200.
- (10) Zhuiykov, S.; Kats, E.; Marney, D. Potentiometric Sensor Using Sub-Micron Cu<sub>2</sub>O-Doped RuO<sub>2</sub> Sensing Electrode with Improved Antifouling Resistance. *Talanta* **2010**, *82*, 502–507.
- (11) Heng, B.; Qing, C.; Sun, D.; Wang, B.; Wang, H.; Tang, Y. Rapid Synthesis of CuO Nanoribbons and Nanoflowers from the Same Reaction System, and a Comparison of Their Supercapacitor Performance. *RSC Adv.* **2013**, *3*, 15719–15726.
- (12) Zaman, S.; Asif, M. H.; Zainelabdin, A.; Amin, G.; Nur, O.; Willander, M. CuO Nanoflowers as an Electrochemical pH Sensor and the Effect of pH on the Growth. *J. Electroanal. Chem.* **2011**, *662*, 421–425.
- (13) Li, C.; Yamahara, H.; Lee, Y.; Tabata, H.; Delaunay, J. J. CuO Nanowire/Microflower/Nanowire Modified Cu Electrode with Enhanced Electrochemical Performance for Non-Enzymatic Glucose Sensing. *Nanotechnology* **2015**, *26*, No. 305503.
- (14) Manjakkal, L.; Sakthivel, B.; Gopalakrishnan, N.; Dahiya, R. Printed Flexible Electrochemical pH Sensors Based on CuO Nanorods. *Sens. Actuators, B* **2018**, *263*, 50–58.
- (15) Koodlur Sannegowda, L.; Reddy, K. R. V.; Shivaprasad, K. H. Stable Nano-Sized Copper and Its Oxide Particles Using Cobalt Tetraamino Phthalocyanine as a Stabilizer; Application to Electrochemical Activity. *RSC Adv.* **2014**, *4*, 11367–11374.
- (16) Zhang, Q.; Zhang, K.; Xu, D.; Yang, G.; Huang, H.; Nie, F.; Liu, C.; Yang, S. CuO Nanostructures: Synthesis, Characterization, Growth Mechanisms, Fundamental Properties, and Applications. *Prog. Mater. Sci.* **2014**, *60*, 208–337.
- (17) Hsu, C. L.; Tsai, J. Y.; Hsueh, T. J. Ethanol Gas and Humidity Sensors of CuO/Cu<sub>2</sub>O Composite Nanowires Based on a Cu through-Silicon via Approach. *Sens. Actuators, B* **2016**, *224*, 95–102.
- (18) Kulkarni, S.; Kummara, S.; Gorthala, G.; Ghosh, R. CuO Nanoflake-Based Sensors for Detecting Linalool, Hexanal, and Methyl Salicylate. *ACS Agric. Sci. Technol.* **2022**, *2*, 1285–1291.
- (19) Steinhauer, S. Gas Sensors Based on Copper Oxide Nanomaterials: A Review. *Chemosensors* **2021**, *9*, 51.
- (20) Yang, T.-H.; Chang, S.-P.; Li, C.-W.; Chang, S.-J. *Sensing Performance of EGFET pH Sensors with CuO Nanowires Fabricated on Glass Substrate*; The Electrochemical Society: Honolulu, 2012.
- (21) Yates, D. E.; Levine, S.; Healy, T. W. Site-Binding Model of the Electrical Double Layer at the Oxide/Water Interface. *J. Chem. Soc., Faraday Trans. 1* **1974**, *70*, 1807–1818.
- (22) Manjakkal, L.; Cvejnik, K.; Kulawik, J.; Zaraska, K.; Socha, R. P.; Szwagierczak, D. X-Ray Photoelectron Spectroscopic and Electrochemical Impedance Spectroscopic Analysis of RuO<sub>2</sub>-Ta<sub>2</sub>O<sub>5</sub> Thick Film pH Sensors. *Anal. Chim. Acta* **2016**, *931*, 47–56.
- (23) Zhang, Y.; Zhu, Y.; Zheng, S.; Zhang, L.; Shi, X.; He, J.; Chou, X.; Wu, Z.-S. Ink Formulation, Scalable Applications and Challenging Perspectives of Screen Printing for Emerging Printed Microelectronics. *J. Energy Chem.* **2021**, *63*, 498–513.
- (24) Lonsdale, W. Development, Manufacture and Application of a Solid-State PH Sensor Using Ruthenium Oxide. Doctorate Theses, Edith Cowan University, 2018. <https://ro.ecu.edu.au/theses/2095>.
- (25) Kusoglu, A.; Weber, A. New Insights into Perfluorinated Sulfonic-Acid Ionomers. *Chem. Rev.* **2017**, *117*, 987–1104.
- (26) Galster, H. *pH Measurement: Fundamentals, Methods, Applications, Instrumentation*; VCH Verlagsgesellschaft: Weinheim, Germany, 1991.
- (27) Liao, Y. H.; Chou, J. C. Preparation and Characteristics of Ruthenium Dioxide for pH Array Sensors with Real-Time Measurement System. *Sens. Actuators, B* **2008**, *128*, 603–612.
- (28) Xu, K.; Zhang, X.; Chen, C.; Geng, M. Development and Performance of an All-Solid-State pH Sensor Based on Modified Membranes. *Int. J. Electrochem. Sci.* **2018**, *13*, 3080–3090.
- (29) Li, Q.; Tang, W.; Su, Y.; Huang, Y.; Peng, S.; Zhuo, B.; Qiu, S.; Ding, L.; Li, Y.; Guo, X. Stable Thin-Film Reference Electrode on Plastic Substrate for All-Solid-State Ion-Sensitive Field-Effect Transistor Sensing System. *IEEE Electron Device Lett.* **2017**, *38*, 1469–1472.
- (30) Lonsdale, W.; Wajrak, M.; Alameh, K. Manufacture and Application of RuO<sub>2</sub> Solid-State Metal-Oxide pH Sensor to Common Beverages. *Talanta* **2018**, *180*, 277–281.
- (31) Hu, G.; Li, N.; Zhang, Y.; Li, H. A Novel PH Sensor with Application to Milk Based on Electrochemical Oxidative Quinone-Functionalization of Tryptophan Residues. *J. Electroanal. Chem.* **2020**, *859*, No. 113871.

(32) Vivaldi, F.; Santalucia, D.; Poma, N.; Bonini, A.; Salvo, P.; del Noce, L.; Melai, B.; Kirchhain, A.; Kolivoška, V.; Sokolová, R.; Hromadová, M.; di Francesco, F. A Voltammetric pH Sensor for Food and Biological Matrices. *Sens. Actuators, B* **2020**, *322*, No. 128650.

(33) Chawang, K.; Bing, S.; Chiao, J. C. Effects of Viscosity and Salt Interference for Planar Iridium Oxide and Silver Chloride pH Sensing Electrodes on Flexible Substrate. *Chemosensors* **2022**, *10*, 371.

(34) Lazouskaya, M.; Tamm, M.; Scheler, O.; Uppuluri, K.; Zaraska, K. Nafion as a Protective Membrane for Screen-Printed pH-Sensitive Ruthenium Oxide Electrodes. In *Proceedings of the Biennial Baltic Electronics Conference, BEC*; IEEE, 2020; pp 18–21. DOI: 10.1109/BEC49624.2020.9276822.

(35) Manjakkal, L.; Cvejic, K.; Kulawik, J.; Zaraska, K.; Szwagierczak, D. A Low-Cost PH Sensor Based on RuO<sub>2</sub> Resistor Material. *Nano Hybrids* **2013**, *5*, 1–15.

(36) Manjakkal, L.; Synkiewicz, B.; Zaraska, K.; Cvejic, K.; Kulawik, J.; Szwagierczak, D. Development and Characterization of Miniaturized LTCC pH Sensors with RuO<sub>2</sub> Based Sensing Electrodes. *Sens. Actuators, B* **2016**, *223*, 641–649.

(37) Manjakkal, L.; Djurdjic, E.; Cvejic, K.; Kulawik, J.; Zaraska, K.; Szwagierczak, D. Electrochemical Impedance Spectroscopic Analysis of RuO<sub>2</sub> Based Thick Film pH Sensors. *Electrochim. Acta* **2015**, *168*, 246–255.

(38) Muniz, F. T. L.; Miranda, M. A. R.; Morilla Dos Santos, C.; Sasaki, J. M. The Scherrer Equation and the Dynamical Theory of X-Ray Diffraction. *Acta Crystallogr., Sect. A: Found. Adv.* **2016**, *72*, 385–390.

(39) Pásztor, K.; Sekiguchi, A.; Shimo, N.; Kitamura, N.; Masuhara, H. Electrochemically-Deposited RuO<sub>2</sub> Films as pH Sensors. *Sens. Actuators, B* **1993**, *14*, 561–562.

(40) Dawson, P.; Elliott, D.; Elliott, A.; Johns, K. *Directory Biochemist*; Mir: Moskow, 1991.

(41) Zhuiykov, S. Morphology of Pt-Doped Nanofabricated RuO<sub>2</sub> Sensing Electrodes and Their Properties in Water Quality Monitoring Sensors. *Sens. Actuators, B* **2009**, *136*, 248–256.

(42) Lazouskaya, M.; Scheler, O.; Uppuluri, K.; Zaraska, K.; Tamm, M. Reusability of RuO<sub>2</sub>-Nafion Electrodes, Suitable for Potentiometric PH Measurement. In *FLEPS 2022 - IEEE International Conference on Flexible and Printable Sensors and Systems, Proceedings*; IEEE, 2022. DOI: 10.1109/FLEPS53764.2022.9781521.

(43) Sheppard, N. F.; Guiseppe-Elie, A. PH Measurement. In *Measurement, Instrumentation, and Sensors Handbook*; Webster, J.; Eren, H., Eds.; CRC Press: Boca Raton, Florida, 2014 DOI: 10.1201/b15664.

(44) Metrohm. *Application Bulletin 188/3e. PH Measurement Technique*.

## Appendix 4

### Publication IV

M. Lazouskaya, M. Tamm, O. Scheler, K. Uppuluri, and K. Zaraska, "Nafion as a protective membrane for screen-printed pH-sensitive ruthenium oxide electrodes," *Proceedings of IEEE Biennial Baltic Electronics Conference (BEC)*, V. 2020-October, P. 18–21, 2020, Tallinn, Estonia.

© 2020 IEEE. Reprinted, with permission, from M. Lazouskaya, M. Tamm, O. Scheler, K. Uppuluri, and K. Zaraska, "Nafion as a protective membrane for screen-printed pH-sensitive ruthenium oxide electrodes," *Proceedings of IEEE Biennial Baltic Electronics Conference (BEC)*, October 2020





# Nafion as a protective membrane for screen-printed pH-sensitive ruthenium oxide electrodes

Maryna Lazouskaya  
Center of Food and Fermentation  
Technologies  
Department of Chemistry and  
Biotechnology  
Tallinn University of Technology  
Tallinn, Estonia  
maryna.lazouskaya@tftak.eu

Marti Tamm  
Center of Food and Fermentation  
Technologies  
Tallinn, Estonia  
martti@tftak.eu

Ott Scheler  
Department of Chemistry and  
Biotechnology  
Tallinn University of Technology  
Tallinn, Estonia  
ott.scheler@taltech.ee

Kiranmai Uppuluri  
Department of Microelectronics  
Institute of Electron Technology  
Krakow, Poland  
uskiranmai@ite.waw.pl

Krzysztof Zaraska  
Department of Microelectronics  
Institute of Electron Technology  
Krakow, Poland  
kzaraska@ite.waw.pl

**Abstract** — Solid-state electrodes have gained attention in past decades for application in pH sensing as a miniature and mechanically stable alternative to conventional fragile glass electrodes. As a material for solid-state electrodes ruthenium oxide has shown the best characteristics. In this study we investigated the sensitivity and stability of RuO<sub>2</sub> screen printed electrodes, produced from the commercially available conductive paste. To enhance the performance, electrodes were coated with Nafion protective layer. Influence of the concentration of Nafion coating solution, drop-casted on the sensitive area of the electrode, was investigated. RuO<sub>2</sub> pH electrodes covered with Nafion layer have shown super-Nernstian response and longer response time, which come into agreement with the result published by other authors previously.

**Keywords** — ruthenium oxide, solid-state pH electrodes, Nafion

## I. INTRODUCTION

Solid-state electrodes have advantages over conventional glass electrodes, such as high selectivity [1], shape and size alteration, costs and rates of production, as well as ease of integration with microelectronic components for real-time monitoring. Reports of fabrication and investigation of solid-state sensors based on oxides of Sn, Sb, Ti and metals of platinum group (Ir, Pd, Pt, Rh, Ru, Os) have already been published elsewhere [2], [3]. Among aforementioned metal oxides, RuO<sub>2</sub> is considered to be the most valuable due to its favourable properties, such as suitable sensitivity [1], [4] and selectivity [1], good response even in the presence of strong oxidizing and reducing agents [4], and unaltered performance of RuO<sub>2</sub> electrodes in presence of colonies of organic sediments [5]. Various fabrication methods of RuO<sub>2</sub> thick and thin films were published previously [6]–[10]; nevertheless, those methods do not allow to fabricate the layers of RuO<sub>2</sub> that would meet the requirements for electrodes, such as developed surface, phase composition, etc. Among methods, reported for solid-state electrodes fabrication [5], [11]–[15], screen printing is the one that allows achieving the best sensitivity and response time, is suitable for mass-production at a low-cost, fast and of various compositions and sizes [16].

However, such feature as an inability to conduct measurement in complex organic and biological media has yet to be overcome. Proteins and other macromolecules adsorb on the electrode surface and interfere with the performance of the electrode and therefore impede the measurement in food matrices (e.g. meat, fish, dairy products). One of the approaches to overcome this problem is to cover the electrode surface with a layer of inert material that will prevent adsorption of macromolecules and facilitate electron exchange between the electrode and the media [17]. The main coating material used for this purpose is Nafion: a perfluorinated ionomer that belongs to the proton-conducting polymers. The structure of incorporated perfluoro vinyl ether groups terminated with sulfonate groups onto a tetrafluoroethylene (PTFE) backbone determines the unique properties of Nafion, such as high proton exchange, chemical and temperature stability [18]–[20]. Nafion serves as a permselective membrane, allowing only protons to reach the electrode and blocking all other ionic species.

The aim of this work was to investigate the influence of Nafion coatings on the performance of RuO<sub>2</sub> electrodes fabricated by screen-printing technique.

## II. MATERIALS AND METHODS

### A. Fabrication of RuO<sub>2</sub> electrodes

The process of electrodes fabrication was the same as described in [21]. Shortly, an Ag/Pd thick film paste (ESL 9695) was used for a conductive layer fabrication and commercially available RuO<sub>2</sub> paste with the resistivity of 10 kΩ/sq (ESL, 3914) was used for sensitive layer fabrication on Alumina substrate respectively. The formation of one layer can be described as follows: a roller moving across the screen stencil forced corresponding paste past the threads of the woven mesh that supports an ink-blocking stencil to achieve a specifically patterned layer of ink on suitable substrate [22]. After each printing step, the substrates were dried at 120 °C for 15 min and consequently fired at 850 °C for 1 hour. After printing and firing of both layers, copper wires were connected to the conductive layer and a protective layer of silicone rubber (Dow Corning, 3140 RTV) was applied to secure the electrical connections. The sensitive area was remaining uncovered.

---

This work was supported by the European Commission through the AQUASENSE (H2020-MSCA-ITN-2018-813680) project. Ott Scheler acknowledges support from the Tallinn University of Technology development program 2016–2022 (project code 2014-2020.4.01.16-0032), 978-1-7281-9444-8/20/\$31.00 ©2020 European Union

### B. Electrochemical characterization

Prior to the utilization, solid-state electrodes were soaked in distilled water in order to reach a stable sensitivity value [15]. Such a step is required as the pH-sensitive surface requires some time to reach equilibria with the protons in the media [23]. Therefore, the electrodes were left in water for 1 week prior to any measurement or calibration. The subsequent change in potential was measured weekly.

The sensitivity of RuO<sub>2</sub> solid-state electrodes was investigated by the standard potentiometric measurement. The potential difference between the indicator and the reference electrode of the electrochemical cell was observed by a Multifunctional DAQ Device (National Instruments, USA) and analyzed using LabVIEW program. Standard glass ion-selective electrode Ag|AgCl|KCl (HYDROMET, Poland) (ISE) was used as a reference electrode. For the measurement of the hysteresis effect and cross-selectivity, the same equipment was utilized.

The electrodes response was evaluated by soaking the electrodes in the buffer solutions of the pH value in the range of 3.0 ... 11.0. The signal was recorded for 3-5 minutes for the value of the electromotive force to reach a stable value. The presence of Na<sup>+</sup>, K<sup>+</sup> and NH<sub>4</sub><sup>+</sup> is known to influence the performance of thick film electrodes [1]. Thus, to characterize the sensitivity of the fabricated electrodes, buffer solutions containing only a few ion types were used: phosphate, bicarbonate and citrate buffers. Buffer solutions were prepared before each measurement. Salts needed for buffers preparation were purchased anhydrous from Sigma Aldrich.

### C. Modification with Nafion

The developed RuO<sub>2</sub> electrodes were modified with a layer of Nafion (5% in a mixture of lower aliphatic alcohols and water, Nafion 117, Sigma Aldrich). For that 100 μL of Nafion solution (per 1 cm<sup>2</sup> of RuO<sub>2</sub> sensitive area) were drop-casted on electrode sensitive area in different concentrations: 1.0; 2.5 and 5.0 % and were left to air dry. To investigate the influence of Nafion coating on electrode sensitivity, modified electrodes were electrochemically characterized as described in section B. The measurements were conducted in parallel of two experiments for each concentration. To investigate the possibility of enhancement electrodes from the shelf by modifying them with Nafion membrane, the same procedures were applied.

### D. Determination of the hysteresis effect

The hysteresis effect (memory effect) of both modified and non-modified electrodes was measured for 2 different pH cycles: acidic (3-5-7-5-3) and basic (11-9-7-9-11). Electrode performance was evaluated by cycling the pH solution two times at 5 min intervals.

## III. RESULTS AND DISCUSSIONS

### A. Sensitivity and stability studies of the fabricated electrodes

The sensitivity of RuO<sub>2</sub> electrodes was estimated by the comparison of the theoretical Nernstian response with the slope of linear dependence of the electromotive force on pH. According to the Nernst equation, the difference in the potentials of the electrodes (E, mV) is proportional to the medium pH (1):

$$E = E_0 - 2.303(R \cdot T/n \cdot F) \cdot \text{pH} \quad (1)$$

where E<sub>0</sub> is the standard electrochemical potential, mV; R is the universal gas constant, 8.314 J/K/mol; F is the Faraday constant, 96500 C/mol; n is the number of electrons in the reaction between ruthenium oxide different oxidizing forms and T is temperature, °K. For a single electron process at 22 °C, Nernstian equation takes the form of (2):

$$E = E_0 - 58.56 \text{ pH} \quad (2)$$

where the value of 58.56 mV is called electrode sensitivity or Nernstian response.

Fig. 1a shows electrochemical potential shift with the change of pH for one of the fabricated electrodes. According to the Nernst equation, the dependence of the electrochemical potential on the pH of the potentiometric sensors of a RuO<sub>2</sub> thick film is described by the equation  $E = 787.84 - 63.78 \text{ pH}$  after 1-week storage (Fig. 1a, red line) and  $E = 683.85 - 58.65 \text{ pH}$  after 8 weeks storage (Fig. 1a, blue line) respectively. These results indicate that the one-week time interval is not sufficient for full surface hydration. Stable values of sensitivity and E<sub>0</sub> are reached only after 4 weeks of storage in water (Fig. 1b).

The storage of the electrodes in distilled water for 8 weeks has led to the sensitivity values from 30 to 59 mV/pH. Only for one out of four electrodes deviation from the Nernstian response was low, for the other three

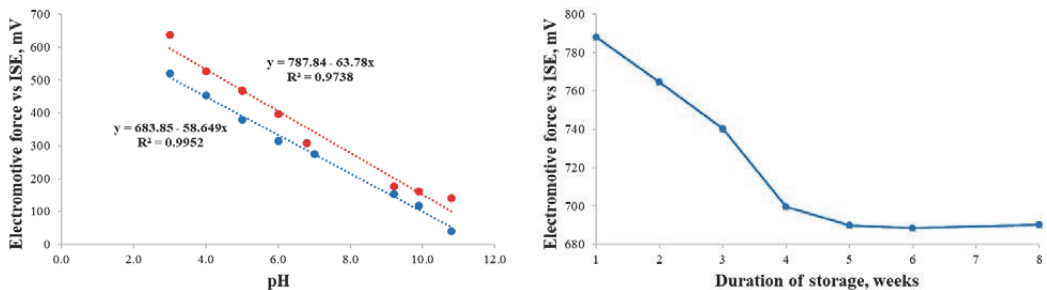


Fig. 1. Sensitivity and readings' stability of RuO<sub>2</sub> screen-printed electrodes: a) dependence of electromotive force on pH of the electrode after 1 week (red line) and 8 weeks (blue line) of storage in water; b) change of E<sub>0</sub> with storage time for one of the electrodes.

electrodes, however, the deviation exceeded 20%. Such high values of deviation indicate a need for modification of surface for better performance.

### B. Improved sensitivity of Nafion covered RuO<sub>2</sub> electrodes

The sensitivity of Nafion covered electrodes was measured continuously for 3 weeks. The values of the Nernstian response are presented in Fig. 2. Coverage of the electrode sensitive area with Nafion was found to improve the Nernstian response of the electrodes when using solutions with a higher concentration of Nafion. Uncovered electrodes showed stable sensitivity after 1 week of storage in water ( $\pm 3$  mV), however, electrodes covered with Nafion took 2 weeks to reach stable values due to slow proton transfer through Nafion chains [24]. Nevertheless, coverage of electrodes with Nafion led to increased reaction times (from 10-50 seconds to over 200 seconds). This is consistent with previous study by Lonsdale [25].

### C. Increased hysteresis loops of Nafion covered RuO<sub>2</sub> electrodes

The hysteresis effect (memory effect) of the fabricated thick film pH sensor for different cycles of pH changes is presented in Table I. Fig. 3 represent the hysteresis effect for the loops in the acidic region (pH 3-5-7-5-3). The difference in the reading at the same pH in the beginning and at the end of both loops was found to not exceed  $\pm 22$  mV and  $\pm 26$  mV for acidic and basic loops respectively. Electrodes, covered with Nafion have shown higher hysteresis effect, with hysteresis value increasing with the increase of the concentration of the Nafion solution used for electrodes modification (Table I). Increased hysteresis for Nafion covered electrodes can be explained by not sufficient time for full equilibrating of the Nafion layer with ions form the solution. Those results agree with the ones reported by Lonsdale, who also indicated that actual reaction time for solid-state electrodes is over 2 hours [25].

## IV. CONCLUSIONS

The coverage of pH-sensitive ruthenium oxide layer is necessary to improve electrode's performance in complex media, such as meat, fish, and dairy products, where proteins and fat adsorb on the electrode's surface and inhibit or block the sensing reaction. It was shown that covering the RuO<sub>2</sub> pH-sensitive electrodes with Nafion protective membrane leads to improved sensitivity, however,

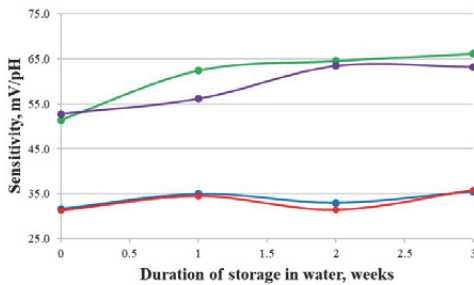


Fig. 2. Change in sensitivity of the RuO<sub>2</sub> screen-printed electrodes covered with Nafion after storage in water: red line – bare electrodes; blue line – electrodes covered with 1% Nafion solution; green line – electrodes covered with 2.5% Nafion solution; purple line – electrodes covered with 5% Nafion solution.

TABLE I. HYSTERESIS (IN mV) OF THE ELECTRODES COVERED WITH NAFION

pH loop	Concentration of the Nafion solution, %			
	0	1	2.5	5
3-5-7-5-3	10.3	10.2	15.5	22.0
11-9-7-9-11	11.5	14.3	18.8	26.0

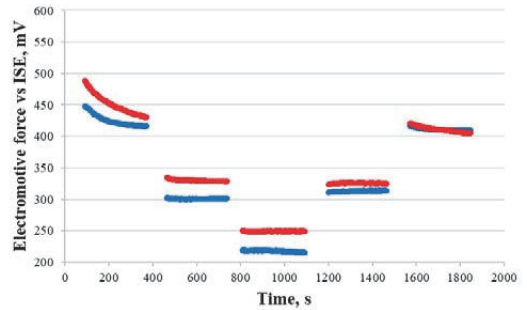


Fig. 3. Potential response change of RuO<sub>2</sub> screen-printed electrodes due to hysteresis effect for different solution pH values in the acidic loop (pH 3-5-7-5-3): red markers – bare electrode; blue markers – electrode covered with 5% Nafion solution.

increasing reaction times. In our future work, we will employ Nafion covered RuO<sub>2</sub> solid-state electrodes in above-mentioned media and will attempt to evaluate and eliminate the influence of real-life factors that take place in the industrial environment (e.g. temperature, pressure, electromagnetic and mechanical disturbance).

## REFERENCES

- [1] P. Kurzweil, "Metal oxides and ion-exchanging surfaces as pH sensors in liquids: State-of-the-art and outlook," *Sensors*, vol. 9, no. 6, pp. 4955–4985, 2009.
- [2] A. Power and A. Morrin, "Electroanalytical Sensor Technology," in *Electrochemistry*, InTech, 2013, p. 38.
- [3] E. Kress-Rogers, "Solid-state pH sensors for food applications," *Trends Food Sci. Technol.*, vol. 2, pp. 320–324, 1991.
- [4] R. Fog, A.; Buck, "Electronic semiconducting oxides as pH sensors," *Sensors and Actuators*, vol. 5, pp. 137–146, 1984.
- [5] S. Zhuiykov, "Morphology of Pt-doped nanofabricated RuO<sub>2</sub> sensing electrodes and their properties in water quality monitoring sensors," *Sensors Actuators, B Chem.*, vol. 136, no. 1, pp. 248–256, 2009.
- [6] S. Zhuiykov, "In situ FTIR study of oxygen adsorption on nanostructured RuO<sub>2</sub> thin-film electrode," *Ionics*, vol. 15, no. 4, pp. 507–512, 2009.
- [7] B. Y. Fugare and B. J. Lokhande, "Study on structural, morphological, electrochemical and corrosion properties of mesoporous RuO<sub>2</sub> thin films prepared by ultrasonic spray pyrolysis for supercapacitor electrode application," *Mater. Sci. Semicond. Process.*, vol. 71, no. April, pp. 121–127, 2017.
- [8] L. Armelao, D. Barreca, and B. Moraru, "A molecular approach to RuO<sub>2</sub>-based thin films: Sol-gel synthesis and characterisation," *J. Non. Cryst. Solids*, vol. 316, no. 2–3, pp. 364–371, 2003.
- [9] P. Gopal Ganesan and M. Eizenberg, "Chemical vapor deposited RuO<sub>2</sub> films: Interfacial adhesion study," *Mater. Sci. Eng. B Solid-State Mater. Adv. Technol.*, vol. 103, no. 3, pp. 213–218, 2003.

- [10] L. E. Papa, K. J. Schnoes, and D. Brasen, "Chemical Vapor Deposition of Ruthenium and Ruthenium Dioxide Films," *J. Electrochem. Soc.*, vol. 132, no. 11, pp. 2677–2685, 1985.
- [11] W. Lonsdale, D. K. Maurya, M. Wajrak, and K. Alameh, "Effect of ordered mesoporous carbon contact layer on the sensing performance of sputtered RuO<sub>2</sub> thin film pH sensor," *Talanta*, vol. 164, no. November 2016, pp. 52–56, 2017.
- [12] W. Lonsdale, M. Wajrak, and K. Alameh, "Effect of conditioning protocol, redox species and material thickness on the pH sensitivity and hysteresis of sputtered RuO<sub>2</sub> electrodes," *Sensors Actuators, B Chem.*, vol. 252, pp. 251–256, 2017.
- [13] L. A. Pocrifka, C. Gonçalves, P. Grossi, P. C. Colpa, and E. C. Pereira, "Development of RuO<sub>2</sub>-TiO<sub>2</sub> (70-30) mol% for pH measurements," *Sensors Actuators, B Chem.*, vol. 113, no. 2, pp. 1012–1016, 2006.
- [14] W. Lonsdale, M. Wajrak, and K. Alameh, "Manufacture and application of RuO<sub>2</sub> solid-state metal-oxide pH sensor to common beverages," *Talanta*, vol. 180, no. December 2017, pp. 277–281, 2018.
- [15] K. Pásztor, A. Sekiguchi, N. Shimo, N. Kitamura, and H. Masuhara, "Electrochemically-deposited RuO<sub>2</sub> films as pH sensors," *Sensors Actuators B Chem.*, vol. 13, no. 14, pp. 561–562, 1993.
- [16] M. Li, Y. T. Li, D. W. Li, and Y. T. Long, "Recent developments and applications of screen-printed electrodes in environmental assays-A review," *Anal. Chim. Acta*, vol. 734, pp. 31–44, 2012.
- [17] B. Lakard, O. Segut, S. Lakard, G. Herlem, and T. Gharbi, "Potentiometric miniaturized pH sensors based on polypyrrole films," *Sensors Actuators, B Chem.*, vol. 122, no. 1, pp. 101–108, 2007.
- [18] S. Motupally, A. J. Becker, and J. W. Weidner, "Diffusion of water in Nafion 115 membranes," *J. Electrochem. Soc.*, vol. 147, no. 9, pp. 3171–3177, 2000.
- [19] K. Scott and A. K. Shukla, "Polymer electrolyte membrane fuel cells: Principles and advances," *Rev. Environ. Sci. Biotechnol.*, vol. 3, pp. 273–280, 2004.
- [20] A. Siu, J. Schmeisser, and S. Holdcroft, "Effect of water on the low temperature conductivity of polymer electrolytes," *J. Phys. Chem. B*, vol. 110, pp. 6072–6080, 2006.
- [21] L. Manjakkal, K. Cvejic, J. Kulawik, K. Zaraska, and D. Szwagierczak, "The effect of sheet resistivity and storage conditions on sensitivity of RuO<sub>2</sub> based pH sensors," *Key Eng. Mater.*, vol. 605, pp. 457–460, 2014.
- [22] J. P. Metters, R. O. Kadara, and C. E. Banks, "New directions in screen printed electroanalytical sensors: An overview of recent developments," *Analyst*, vol. 136, no. 6, pp. 1067–1076, 2011.
- [23] L. Manjakkal, K. Cvejic, J. Kulawik, K. Zaraska, D. Szwagierczak, and R. P. Socha, "Fabrication of thick film sensitive RuO<sub>2</sub>-TiO<sub>2</sub> and Ag/AgCl/KCl reference electrodes and their application for pH measurements," *Sensors Actuators, B Chem.*, vol. 204, pp. 57–67, 2014.
- [24] K. A. Mauritz and R. B. Moore, "State of understanding of Nafion," *Chem. Rev.*, vol. 104, no. 10, pp. 4535–4585, 2004.
- [25] W. Lonsdale, "Development, manufacture and application of a solid-state pH sensor using ruthenium oxide (Doctoral dissertation)," Edith Cowan University, 2018.

## Appendix 5

### Publication V

K. Uppuluri, M. Lazouskaya, D. Szwagierczak, and K. Zaraska, "Influence of temperature on the performance of Nafion coated RuO<sub>2</sub> based pH electrodes," in *IEEE International Conference on Flexible and Printable Sensors and Systems (FLEPS)*, 2021, Manchester, United Kingdom.

© 2021 IEEE. Reprinted, with permission, from K. Uppuluri, M. Lazouskaya, D. Szwagierczak, and K. Zaraska, "Influence of temperature on the performance of Nafion coated RuO<sub>2</sub> based pH electrodes," in *IEEE International Conference on Flexible and Printable Sensors and Systems (FLEPS)*, June 2021



# Influence of temperature on the performance of Nafion coated RuO<sub>2</sub> based pH electrodes

Kiranmai Uppuluri<sup>1</sup>, Maryna Lazouskaya<sup>2,3</sup>, Dorota Szwagierczak<sup>1</sup>, Krzysztof Zaraska<sup>1</sup>

<sup>1</sup> Łukasiewicz Research Network–Institute of Microelectronics and Photonics, ul. Zablocie 39, Krakow, Poland

<sup>2</sup> Center of Food and Fermentation Technologies, Akadeemia tee 15A, Tallinn, Estonia

<sup>3</sup> Department of Chemistry and Biotechnology, Tallinn University of Technology, Ehitajate tee 5, Tallinn, Estonia  
[uskiranmai@ite.waw.pl](mailto:uskiranmai@ite.waw.pl)

**Abstract**— At present, ruthenium oxide (RuO<sub>2</sub>) based solid-state electrodes are investigated as an alternative to conventional glass electrode due to their low cost, chemical and physical durability, good sensitivity and fast response. Coverage of the solid-state electrodes with a protective membrane can improve the overall performance of the electrode and allow measurement in complex media, such as blood, food, biologically active environment. One of the well-known protective membranes for electrodes is Nafion. However, little is known about the performance of Nafion-covered electrodes used in heated samples. Here we present the investigation of the behaviour of ruthenium oxide (RuO<sub>2</sub>) based pH electrodes modified with Nafion protective membrane (RuO<sub>2</sub>-Nafion) at an elevated temperature of 80°C. RuO<sub>2</sub> electrodes were fabricated by screen printing technique. We compare the performance of the RuO<sub>2</sub>-Nafion electrodes was compared to that of unmodified RuO<sub>2</sub> electrodes. Both unmodified RuO<sub>2</sub> electrodes and RuO<sub>2</sub>-Nafion electrodes perform well at room temperature, showing sensitivity close to the theoretical value (58.4 and 62.4 mV/pH respectively), the fast response time (14 and 42 s respectively) and low drift rate (0.5 and 0.4 mV/h respectively). The sensitivity of the Nafion- covered electrodes was found to be higher at elevated temperature as well: 37.2 mV/pH compared to 33.4 mV/pH for unmodified electrodes. Furthermore, RuO<sub>2</sub>-Nafion electrodes showed a lower drift rate at elevated temperature (9.6 mV/h) compared to that of modified electrodes (34.8 mV/h).

**Keywords**—screen-printed pH electrode, RuO<sub>2</sub>, Nafion, temperature effect component

## I. INTRODUCTION

Presently, in laboratory practice, as well as on an industrial level, measurement of pH is carried out by the means of potentiometry with the use of a glass electrode. However, such disadvantages of glass electrode as fragility, limited lifetime and high price, make scientist search for a more feasible alternative. Such an alternative can be metal-oxide based electrode where metal oxide is used as a material sensitive to pH change [1], [2]. Among different oxides, studied for application in pH measurement [1], Ruthenium oxide (IV) (RuO<sub>2</sub>) shows the best characteristics (e.g. high sensitivity, low hysteresis and drift, relatively low price) [2]. Screen printing is one of the several techniques implemented for the fabrication of RuO<sub>2</sub> pH-sensitive electrodes [2]. Among reported methods, screen printing is the one that allows producing electrodes with the best characteristics at low cost and of various compositions

and sizes [3], [4]. Nevertheless, the inability to conduct measurement in complex organic and biological media has yet to be overcome. One of the approaches to overcome this difficulty is to modify the electrodes with Nafion protective membrane [5]–[7].

Nafion is a synthetic sulfonated tetrafluoroethylene based co-polymer discovered by Walter Grot in 1960 [8]. Nafion has received immense attention for its proton-conducting property and is known for its application in proton exchange membrane fuel cells (PEMFC) [9] and as a protective coating for electrochemical sensors [10]. Furthermore, Nafion was found to provide protection from certain ion interferences [11] and improve the sensitivity of electrodes in non-aqueous media [4], [5], [12].

Although it has been observed that Nafion coating can help to improve pH sensitivity at normal conditions, not much has been said about its performance at high temperatures. The behaviour of Nafion coatings at elevated temperature is of great importance since temperature directly influences pH whereas the hydration level influences the proton conductivity of Nafion [12].

This study aimed to investigate the influence of Nafion on the sensitivity of screen-printed RuO<sub>2</sub> based pH-sensitive electrodes. The influence of temperature on the ability of Nafion to improve response time and drift rate was also investigated.

## II. MATERIALS AND METHODS

### A. Fabrication of RuO<sub>2</sub> based pH-sensitive electrodes

The method adopted in this study for the fabrication of pH-sensitive electrodes was analogous to the process described in [13] and [14]. Aluminium oxide (Al<sub>2</sub>O<sub>3</sub>, 96%), a conventional inert material, was used as a substrate for the screen-printed sensitive electrodes. First, the conducting layer of silver/palladium (Ag/Pd) thick film paste (9695, Electro-Science Laboratories, King of Prussia, Pennsylvania, USA) was screen printed on the substrate. Next, a pH-sensitive layer of RuO<sub>2</sub> based paste (3914, Electro-Science Laboratories, King of Prussia, Pennsylvania, USA) with a resistivity of 10 kΩ/sq was screen printed on the same substrate in such a way that it partially covered the conducting layer. After each printing step, electrodes were dried at 120°C for 15 minutes and



consequently sintered at 900°C for one hour. A copper wire was then soldered onto the free end of the Ag/Pd layer. Lastly, electrodes were covered with a layer of non-corrosive silicone resin (DOWSIL™ 3140 RTV Coating, Dow Chemical Company, Midland, Michigan, USA) to ensure the insulation of the electrical contact. The sensitive area of the RuO<sub>2</sub> layer remained uncovered and open for contact with the electrolyte.

### B. Modification of RuO<sub>2</sub> based electrodes with Nafion

A protective coating of Nafion (Nafion 117 coating solution, 5% in a mixture of water and lower aliphatic alcohols, Sigma Aldrich, Missouri, USA) was deposited on top of the RuO<sub>2</sub> layer using the drop-casting technique. In this process, 30 µL of Nafion (per 1 mm<sup>2</sup> of RuO<sub>2</sub> surface) solution were pipetted on top of the RuO<sub>2</sub> layer. The electrodes were let to air-dry at room temperature for 24 hours.

### C. pH measurement

Both fabricated electrode types (bare RuO<sub>2</sub> electrodes and RuO<sub>2</sub>-Nafion electrodes) were investigated for their pH-sensing performance via standard potentiometric procedure [15]. For that, RuO<sub>2</sub> and RuO<sub>2</sub>-Nafion electrodes were connected to a multichannel voltmeter (9205, National Instruments, Austin, Texas, USA) through an operational amplifier (LMC6044, Texas Instruments, Dallas, Texas, USA). The data was recorded using LABVIEW software (National Instruments, Austin, Texas, USA). All the measurements were conducted in triplicate.

For pH measurements, electrodes were placed in distilled water and subjected to varying pH by the addition of 1 M solution of HCl or 1 M solution of KOH to decrease or increase pH respectively. A standard glass ion-selective silver chloride electrode (Ag|AgCl|KCl, Hydromet, Poland) (ISE) was used as a reference electrode. During the measurement, the investigated solution was continuously stirred using a magnetic stirrer. Furthermore, a commercial glass pH electrode (ELMETRON, Poland) was used to monitor pH adjustment. The fabricated screen-printed electrodes were stored in distilled water for 24 hours prior to any measurement to ensure stable sensitivity [16].

### D. Performance of the RuO<sub>2</sub> and RuO<sub>2</sub>-Nafion electrodes at different temperatures

To observe the influence of temperature on electrodes performance, electrodes were submerged in distilled water at room temperature. The temperature was then gradually increased to 80°C. After the measurement at 80°C, electrodes were allowed to cool down back to the room temperature. The electromotive force (Emf) was recorded throughout the temperature change. The heating was conducted at a constant rate of 0.9°C/min and the rate of cooling was 0.3°C/min. The pH sensitivity, response time and drift rate of the electrodes were investigated at room temperature (22°C) and 80°C. The response time was calculated as the time required to reach a stable Emf value at a given pH while the drift rate was

measured for 5 hours and calculated as the average shift from the stable Emf value at a constant pH in mV/h.

### E. Morphology studies

The surface morphology of the fabricated electrodes was studied with the use of a digital optical microscope (KH 7700, Hirox, New Jersey, USA).

## III. RESULTS AND DISCUSSION

### A. RuO<sub>2</sub> electrode is sensitive to pH due to electrochemical equilibria between Ru<sup>IV</sup> and Ru<sup>III</sup> forms

When electrodes are submerged in water, the hydration of RuO<sub>2</sub> prompts a partial conversion of Ru<sup>IV</sup> to Ru<sup>III</sup> [17]. The reducing Ru<sup>IV</sup> species and their corresponding oxidizing species form a redox couple which is represented by the following equation [1]:



According to the Nernst equation, the electrochemical potential (or electromotive force of the cell when the reference electrode is grounded) depends on the standard electrode potentials and activities of the redox pair. For the RuO<sub>2</sub> electrode, the Nernst equation takes the form of (2):

$$E = E^0 + \frac{R \cdot T}{z \cdot F} \cdot \ln \frac{a_{\text{Ru}^{III}}}{a_{\text{Ru}^{IV}} \cdot a_{\text{H}^+}} \quad (2)$$

where, E is the electrochemical potential, mV; E<sup>0</sup> is the standard potential, mV; R is the universal gas constant, 8.314 J/K·mol; F is the Faraday constant, 96500 °C/mol; n is the number of electrons transferred in the reaction; T is the temperature, K; a<sub>Ru(IV)</sub> and a<sub>Ru(III)</sub> are the activities of redox pair, mol/L;

Taking into account that the values of Ru<sup>III</sup> and Ru<sup>IV</sup> activities are approximate 1, switching from natural logarithm to common logarithm and knowing that pH = -log[H<sup>+</sup>], (3) takes the form of:

$$E = E^0 - 2.303 \frac{R \cdot T}{n \cdot F} \text{pH} \quad (4)$$

From (4), it can be seen that there is a linear dependence between the electromotive force and pH. The slope factor of this plot is called electrode sensitivity. Sensitivity is measured in mV/pH and is one of the main characteristics of an electrode. For single electron process and at room temperature (T=22°C), the sensitivity is equal to 58.3 mV/pH.

### B. Drop-casting of Nafion solution on RuO<sub>2</sub> surface allows to get even coatings of the material

Digital optical microscope images of unmodified RuO<sub>2</sub> electrodes and RuO<sub>2</sub>-Nafion electrodes are presented in Fig. 1. Images were made at the same light exposure. It can be seen that the Nafion layer is evenly spread across the RuO<sub>2</sub> microparticles, creating a uniform protective layer.

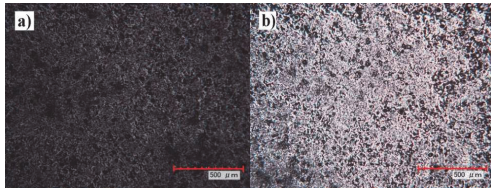


Fig 1. Digital optical microscope images of a) RuO<sub>2</sub> electrodes and b) RuO<sub>2</sub>-Nafion.

### C. RuO<sub>2</sub>-Nafion electrodes showed increased sensitivity

It can be seen that the sensitivity of both electrode types at 22°C was very close to the theoretical value (Table 1). For the RuO<sub>2</sub>-Nafion electrodes, the sensitivity was higher by 3.3 mV/pH in comparison to the unmodified RuO<sub>2</sub> electrodes. This observation is consistent with the results reported previously [7], [10]. The increase in pH sensitivity due to the Nafion layer is not restricted to ruthenium dioxide electrodes [7], [11] but has also been observed for other sensitive materials such as antimony [6], molybdenum sulfide [12] and iridium oxide [18]. The increase in sensitivity after the application of Nafion coating have also been reported for other analytes such as H<sub>2</sub>O<sub>2</sub> [4] and uric acid [5].

At the elevated temperature of 80°C RuO<sub>2</sub>-Nafion electrodes had a sensitivity of  $37.2 \pm 0.8$  mV/pH, whereas the electrodes without Nafion coating had the sensitivity of  $33.4 \pm 1.0$  mV/pH when the expected theoretical sensitivity was 70.1 mV/pH. Both RuO<sub>2</sub> and RuO<sub>2</sub>-Nafion electrodes show good linearity of response to pH change even at elevated temperature ( $R^2 > 0.98$ ). However, a large deviation in sensitivity from the theoretical value was observed (> 33%). This decrease in sensitivity might be associated with the thermal behaviour of Nafion. It is known that the flexibility of polymer chains affects the water uptake capacity of an ionomer and therefore influences the conductivity of the ionomer [19]. It was previously shown that the elasticity of the Nafion membrane decreases with the increase of temperature leading to a 'stiffer' membrane [20] and at a temperature around 80°C Nafion begins to lose its ability to conduct protons [21]. As Nafion begins to lose its ability to conduct protons, the overall contribution of Nafion to enhancing the pH sensitivity of the modified electrode is bound to decrease when moving to higher temperatures.

The response time was found to increase by 20 seconds as a result of electrode modification (Table 1). This is in agreement

Table 1. Characteristics of RuO<sub>2</sub> and RuO<sub>2</sub>-Nafion pH electrodes at 22°C and 80°C.

Temperature		22°C		80°C	
Electrode type		RuO <sub>2</sub>	RuO <sub>2</sub> -Nafion	RuO <sub>2</sub>	RuO <sub>2</sub> -Nafion
E <sup>0</sup> , mV		577.7 ± 10.7	655.8 ± 8.3	424.1 ± 8.8	476.0 ± 8.0
Sensitivity, mV/pH	Theoretical	58.3	58.3	70.1	70.1
	Observed	58.4 ± 0.8	62.6 ± 0.6	33.4 ± 1.0	37.2 ± 0.8
	Deviation, %	+0.1	+3.4	-36.7	-33.0
R <sup>2</sup>		0.995	0.999	0.982	0.987
Response time, s		14 ± 2	42 ± 3	22 ± 3	50 ± 5
Drift rate, mV/h		0.5 ± 0.2	0.4 ± 0.1	34.8 ± 2.4	9.6 ± 3.0

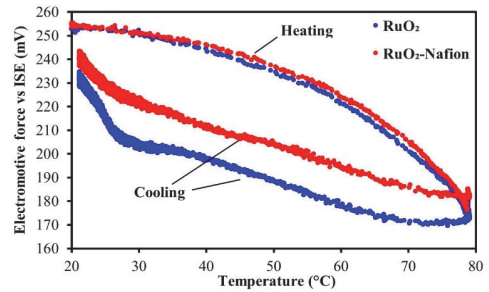


Fig. 2. Change of electromotive force as a function of temperature for RuO<sub>2</sub> (blue) and RuO<sub>2</sub>-Nafion (red)

with previously published results [7], [11]. Since Nafion is selectively permeable to protons, this increase in response time may be due to a slower transfer of protons through the Nafion membrane, especially in basic media where the concentration of protons is low. However, in the study of antimony electrodes, Nafion coating was reported to reduce the response time [6].

The electromotive force during heating up and cooling down is presented in Fig. 2. The difference in electromotive force reading at 22°C before and after heating was  $20.5 \pm 4.3$  mV and  $14.3 \pm 2.3$  mV for unmodified RuO<sub>2</sub> electrodes and RuO<sub>2</sub>-Nafion electrodes respectively.

## IV. CONCLUSION

The pH-sensitive electrodes made from a commercial RuO<sub>2</sub> paste exhibit response close to the theoretical response at room temperature. Modification of these electrodes with a proton selective membrane made of Nafion was found to increase the sensitivity and lower the drift rate even at elevated temperature, nevertheless increasing the response time as well. Upon heating to 80°C both unmodified RuO<sub>2</sub> and modified RuO<sub>2</sub>-Nafion electrodes show linear response with decreased sensitivity, however, electrodes modified with Nafion have slightly higher sensitivity. Our future studies will explore the influence of Nafion on other aspects of pH sensing such as hysteresis, as well as attempt to solve the drawbacks experienced in this study such as longer reaction time and reduced sensitivity at elevated temperature.

#### ACKNOWLEDGMENT

This work was supported by the European Commission through the AQUASENSE (H2020-MSCA-ITN-2018-813680) project. The authors would like to thank Dr Beata Synkiewicz-Musialska for her assistance in the morphological analysis of the fabricated electrodes.

#### REFERENCES

- [1] P. Kurzweil, "Metal oxides and ion-exchanging surfaces as pH sensors in liquids: State-of-the-art and outlook," *Sensors*, vol. 9, no. 6, pp. 4955–4985, 2009.
- [2] L. Manjakkal, D. Szwagierczak, and R. Dahiya, "Metal oxides based electrochemical pH sensors: Current progress and future perspectives," *Prog. Mater. Sci.*, no. December, pp. 1–31, 2019.
- [3] M. Li, Y. T. Li, D. W. Li, and Y. T. Long, "Recent developments and applications of screen-printed electrodes in environmental assays-A review," *Anal. Chim. Acta*, vol. 734, pp. 31–44, 2012.
- [4] J. Ping *et al.*, "A Prussian blue-based amperometric sensor for the determination of hydrogen peroxide residues in milk," *Ionics (Kiel)*, vol. 16, no. 6, pp. 523–527, 2010.
- [5] N. Stozhko, M. Bukharinova, L. Galperin, and K. Brainina, "A nanostructured sensor based on gold nanoparticles and nafion for determination of uric acid," *Biosensors*, vol. 8, no. 1, pp. 5–10, 2018.
- [6] K. Xu, X. Zhang, K. Hou, M. Geng, and L. Zhao, "The effects of antimony thin film thickness on antimony pH electrode coated with nafion membrane," *J. Electrochem. Soc.*, vol. 163, no. 8, pp. B417–B421, 2016.
- [7] M. Lazouskaya, M. Tamm, O. Scheler, K. Uppuluri, and K. Zaraska, "Nafion as a protective membrane for screen-printed pH-sensitive ruthenium oxide electrodes," *Proc. Bienn. Balt. Electron. Conf. BEC*, vol. 2020-Octob, pp. 18–21, 2020.
- [8] W. G. Grot, "Nafion Membrane and its Applications," in *Electrochemistry in Industry*, U. Landau, E. Yeager, and D. Kortan, Eds. Springer, Boston, MA, 1982, pp. 73–87.
- [9] S. J. Peighambaroust, S. Rowshanzamir, and M. Amjadi, *Review of the proton exchange membranes for fuel cell applications*, vol. 35. Elsevier Ltd, 2010.
- [10] W. Lonsdale, M. Wajrak, and K. Alameh, "Effect of conditioning protocol, redox species and material thickness on the pH sensitivity and hysteresis of sputtered RuO<sub>2</sub> electrodes," *Sensors Actuators B Chem.*, vol. 252, pp. 251–256, 2017.
- [11] W. Lonsdale, "Development, manufacture and application of a solid-state pH sensor using ruthenium oxide," Edith Cowan University, 2018.
- [12] P. Awasthi, R. Mukherjee, S. P. O. Kare, and S. Das, "Impedimetric blood pH sensor based on MoS<sub>2</sub>-Nafion coated microelectrode," *RSC Adv.*, vol. 6, no. 104, pp. 102088–102095, 2016.
- [13] A. Cagnini, I. Palchetti, I. Lionti, M. Mascini, and A. P. F. Turner, "Disposable ruthenized screen-printed biosensors for pesticides monitoring," *Sensors Actuators B Chem.*, vol. 24, no. 1–3, pp. 85–89, 1995.
- [14] L. Manjakkal, K. Cvejin, J. Kulawik, K. Zaraska, and D. Szwagierczak, "The effect of sheet resistivity and storage conditions on sensitivity of RuO<sub>2</sub> based pH sensors," *Key Eng. Mater.*, vol. 605, pp. 457–460, 2014.
- [15] R. P. Buck *et al.*, "Measurement of pH. Definition, standards, and procedures (IUPAC Recommendations 2002)," *Pure Appl. Chem.*, vol. 74, no. 11, pp. 2169–2200, 2002.
- [16] K. Pásztor, A. Sekiguchi, N. Shimo, N. Kitamura, and H. Masuhara, "Electrochemically-deposited RuO<sub>2</sub> films as pH sensors," *Sensors Actuators B Chem.*, vol. 13, no. 14, pp. 561–562, 1993.
- [17] L. Manjakkal, K. Cvejin, J. Kulawik, K. Zaraska, D. Szwagierczak, and R. P. Socha, "Fabrication of thick film sensitive RuO<sub>2</sub>-TiO<sub>2</sub> and Ag/AgCl/KCl reference electrodes and their application for pH measurements," *Sensors Actuators, B Chem.*, vol. 204, pp. 57–67, 2014.
- [18] S. A. M. Marzouk, "Improved electrodeposited iridium oxide pH sensor fabricated on etched titanium substrates," *Anal. Chem.*, vol. 75, no. 6, pp. 1258–1266, 2003.
- [19] M. Fumagalli *et al.*, "Fast Water Diffusion and Long-Term Polymer Reorganization during Nafion Membrane Hydration Evidenced by Time-Resolved Small-Angle Neutron Scattering," *J. Phys. Chem. B*, vol. 119, no. 23, pp. 7068–7076, 2015.
- [20] F. Bauer, S. Denneker, and M. Willert-Porada, "Influence of Temperature and Humidity on the Mechanical Properties of Nafion 117 Polymer Electrolyte Membrane," *J. Polym. Sci. B Polym. Phys.*, vol. 43, pp. 786–795, 2004.
- [21] M. Casciola, G. Alberti, M. Sganappa, and R. Narducci, "On the decay of Nafion proton conductivity at high temperature and relative humidity," *J. Power Sources*, vol. 162, no. 1, pp. 141–145, 2006.

## Appendix 6

### Publication VI

M. Lazouskaya, O. Scheler, K. Uppuluri, K. Zaraska, and M. Tamm, "Reusability of RuO<sub>2</sub>-Nafion electrodes, suitable for potentiometric pH measurement," in *IEEE International Conference on Flexible and Printable Sensors and Systems (FLEPS)*, 2022, Vienna, Austria.

© 2022 IEEE. Reprinted, with permission, from M. Lazouskaya, O. Scheler, K. Uppuluri, K. Zaraska, and M. Tamm, "Reusability of RuO<sub>2</sub>-Nafion electrodes, suitable for potentiometric pH measurement," in *IEEE International Conference on Flexible and Printable Sensors and Systems (FLEPS)*, July 2022



# Reusability of RuO<sub>2</sub>-Nafion electrodes, suitable for potentiometric pH measurement

Maryna Lazouskaya<sup>1,2,\*</sup>, Ott Scheler<sup>1</sup>, Kiranmai Uppuluri<sup>3</sup>, Krzysztof Zaraska<sup>3</sup>, and Martti Tamm<sup>2</sup>

<sup>1</sup> Department of Chemistry and Biotechnology, School of Science, Tallinn University of Technology, Tallinn, Estonia

<sup>2</sup> Center of Food and Fermentation Technologies, Tallinn, Estonia

<sup>3</sup> Łukasiewicz Research Network–Institute of Microelectronics and Photonics, Krakow, Poland

\*Corresponding author email: maryna.lazouskaya@tftak.eu

**Abstract**—Nafion™ (Nafion) membrane is known to improve the performance of the electrochemical sensors by acting as a semi-permeable barrier when applied on the electrode's surface. However, the Nafion membrane is soft and can degrade with time. In order to see if the Nafion membrane can be cast repeatedly, we investigated the reusability of Nafion-covered electrodes. In this paper, we present the results of the investigation of the performance of the potentiometric pH-electrodes, based on Ruthenium(IV) oxide (RuO<sub>2</sub>), that were covered with Nafion membrane several times. The electrodes were fabricated by screen printing method and modified with Nafion by drop-casting technique. The investigation of the performance was based on the evaluation of the most important electrode characteristics: sensitivity and linearity, hysteresis, and drift. We have demonstrated that the screen printed RuO<sub>2</sub> electrodes show excellent electrochemical characteristics at room temperature even after coating them with Nafion for the third time.

**Keywords**—pH electrodes, ruthenium(IV) oxide, Nafion, potentiometry

## I. INTRODUCTION

Even though glass electrode is widely used for the measurement of pH, when it comes to measuring in food samples, it is preferred to use something less fragile. An alternative to the conventional glass electrode is a solid-state metal oxide electrode. The idea of utilizing metal oxides for pH sensing was first suggested in 1947 [1] and has been investigated since 1982 [2]. Among the metal oxides, Ruthenium(IV) oxide (RuO<sub>2</sub>) demonstrates the most favourable characteristics: Nernstian sensitivity, fast response and low drift rate [3]. Furthermore, among the various fabrication methods, proposed for electrodes based on metal oxides, the most convenient is screen printing [3]. The screen printing technique allows producing electrodes of different sizes and shapes, fast and at a low cost [4].

Notwithstanding the excellent performance of the screen printed electrodes in aqueous samples [5], when moving on to more complex media, e.g. dairy products, screen printed RuO<sub>2</sub> electrodes do not show good results [6]. We have previously demonstrated that the introduction of a Nafion™ (Nafion) protecting membrane allows the usage of the RuO<sub>2</sub> electrodes for pH measurement in milk [6]. However, the Nafion

membrane is soft, and it can get damaged and degrade with time. Therefore, the aim of this work was to evaluate the possibility of covering the RuO<sub>2</sub> electrodes with a new coating of Nafion membrane when the previous one needs to be replaced.

## II. MATERIALS AND METHODS

### A. Fabrication of the RuO<sub>2</sub> electrodes

The investigated RuO<sub>2</sub> electrodes were fabricated as previously described [5], [6]. Two layers were consequently printed on top of the Alumina substrate: first, a conductive layer of Ag/Pd paste (9695, Electro-Science Laboratories, King of Prussia, Pennsylvania, USA) and second, a pH-sensitive layer of RuO<sub>2</sub>/glass paste (3914, Electro-Science Laboratories, King of Prussia, Pennsylvania, USA). Layers were printed to slightly overlap and not fully cover one another. After printing each layer, electrodes were dried at 120°C for 15 minutes, followed by sintering at 900°C for one hour. After cooling down, a copper wire was connected to the Ag/Pd layer by soldering with Pb/Sn alloy. The Ag/Pd layer connected to the copper wire was then insulated with a non-corrosive silicone resin (DOWSIL™ 3140 RTV Coating, Dow Chemical Company, Midland, Michigan, USA).

### B. Deposition of Nafion membrane

A protective coating of Nafion was introduced on top of the RuO<sub>2</sub> layer by drop-casting technique to create Nafion-covered RuO<sub>2</sub> electrodes (RuO<sub>2</sub>-Nf). For that, 12 μL of 5% Nafion solution, in a mixture of water and lower aliphatic alcohols (Nafion 117, Sigma Aldrich, Missouri, USA) was pipetted on top of the RuO<sub>2</sub> layer. Then electrodes were dried at 80°C for 2 hours in a laboratory incubator (BD 53, Binder, Germany). The procedure was repeated 2 times to achieve 3 layers of Nafion. After deposition of all 3 layers, the RuO<sub>2</sub>-Nf electrodes were let to air-dry overnight at room temperature.

### C. Determination of weight change of Nafion membrane

The solubility of the Nafion membrane was evaluated according to the following formula:

$$\text{Solubility} = \frac{m_n - m_i}{m_n} \cdot 100\% \quad (1)$$

where  $m_n$  is the mass of the initial Nafion membrane, g;  $m_t$  is the mass of the Nafion membrane, weighted some time after placing the RuO<sub>2</sub>-Nf electrode in water, g.

#### D. Removal of the Nafion membrane from the surface of the RuO<sub>2</sub> electrode

To remove the Nafion membrane from the electrode's surface, the RuO<sub>2</sub> electrodes were soaked in 50%(v/v) Ethanol for several minutes and the Nafion membrane was removed using tweezers. The surface of the RuO<sub>2</sub> electrodes was wiped with paper tissue, rinsed with distilled water, and left to air dry at room temperature overnight. A fresh Nafion membrane was deposited on the electrodes the next day. For that, the steps described in section B were repeated.

#### E. Measurement setup

The setup for potentiometric pH measurement generally consists of (i) a galvanic cell and (ii) a potentiometer (a measuring device). In our study, the galvanic cell was built from a fabricated RuO<sub>2</sub>-Nf indicator electrode (IE) and a standard glass ion-selective Ag|AgCl|KCl (HI1053P, Hanna Instruments, USA) reference electrode (RE). The electrodes were connected to the measuring device (Data Acquisition (DAQ) device, USB-6259, National Instruments, USA) through a circuit board via galvanic connections. A high-performance digital power supply (E3631A, Agilent, USA) was used to get an interference-free input voltage of 12 volts to power up the measuring device. The potential difference between the IE and the RE was monitored using the LabVIEW program (National Instruments, USA). All the measurements were conducted in parallel with 3 electrodes for each modification at temperatures of 25, 30, 35 and 40°C.

#### F. Measured electrochemical characteristics

All the essential characteristics of the fabricated electrodes ( $E^0$ , sensitivity, hysteresis, drift rate) were measured by the standard potentiometric measurement.

##### 1) Sensitivity

The sensitivity and  $E^0$  were evaluated by determining the electrochemical potential (potential) in pH buffers in the range of 3.0–11.0. Buffer solutions were prepared before each measurement from corresponding anhydrous salt purchased from Sigma Aldrich (USA). The pH of the buffers was determined with a conventional pH meter (Seven2Go Advanced Single-Channel Portable pH Meter, Mettler Toledo, Switzerland). The potential was recorded 90 seconds after immersing the electrodes in the buffer. The sensitivity of the fabricated electrodes was determined as the slope of the linear function after plotting the measured potential (Y-axis) as a function of pH (X-axis).  $E^0$  was determined by extrapolation of the function until the intersection with the Y-axis.

##### 2) Hysteresis

The hysteresis was determined by exposing the fabricated electrodes to buffer solutions of different pH. For that, the potential of an electrode was recorded for 2 pH cycles: acidic (hysteresis A, pH 3–5–7–5–3) and basic (hysteresis B, pH 11–9–7–9–11). The potential was recorded for 5 minutes in each pH buffer. The electrodes were rinsed with distilled water in

between the measurements. The hysteresis was calculated as a difference in the electrode's potential between 2 measurements in the buffer of the same pH.

##### 3) Drift

To determine the drift rate, the potential of a fabricated electrode was continuously measured for 2 hours, and the drift rate was calculated as the average difference between initial and final potential values per one hour.

### III. RESULTS AND DISCUSSION

#### A. Theoretical aspects of pH measurement with solid-state electrodes

The working principle of the RuO<sub>2</sub> potentiometric pH-electrode is as follows: when the electrode is submerged in water, an electrochemical reaction involving H<sup>+</sup>-ions is taking place:



When we write the Nernst equation for (2):

$$E = E_{Ru^{IV}/Ru^{III}}^0 - \frac{R \cdot T}{n \cdot F} \cdot \ln \frac{a_{Ru^{III}}}{a_{Ru^{IV}} \cdot a_{H^+}} \quad (3)$$

where  $E^0$  is standard potential, V;  $R$  is the universal gas constant, 8.314 J/K·mol;  $T$  is temperature, K;  $n$  is the number of electrons participating in the redox reaction;  $F$  is the Faraday constant, 96485 C/mol;  $a_{Ru^{IV}}$  and  $a_{Ru^{III}}$  are the activities of Ru<sup>IV</sup>O<sub>2</sub> and Ru<sup>III</sup>O(OH) respectively, mol/L,  $a_{H^+}$  is the activity of H<sup>+</sup> ions, mol/L.

Since a RuO<sub>2</sub> electrode is a solid-state electrode,  $a_{Ru^{IV}}$  and  $a_{Ru^{III}}$  are equal to 1. At room temperature ( $T = 25$  °C), (3) takes the following form:

$$E = E_{Ru^{IV}/Ru^{III}}^0 - 0.0592 \cdot pH \quad (4)$$

The value of 0.0592 volts (or 59.2 Millivolts) is called the sensitivity of an electrode. Since it is calculated from known values of constants, it is supposed to be the same for all the electrodes when the same number of electrons participate in the reaction. It is used as a measure of the electrode's performance.

Other important characteristics of an electrode are hysteresis and drift rate. Hysteresis is a measure of the impact of measurement in samples on one another. It was shown that for solid-state electrodes when consequently measuring in the samples of different pH, the previous sample can impact the accuracy of measurement in the next sample [7]–[10]. This phenomenon is associated with the structural changes in the double layer on the surface of an electrode when the electrode is exposed to a solution of a different pH [3]. Hysteresis is measured in millivolts.

Drift rate is associated with unspecific fluctuations of the electrode's potential over time. This characteristic should be taken into account when a continuous measurement is performed. Drift rate is usually measured in millivolts per hour.

*B. Almost half the weight of the Nafion membrane dissolves after one month of usage*

First, we investigated the stability of the Nafion membrane. For that, we were monitoring the change in weight of the Nafion membrane over time. The results are presented in Table I. It can be seen, that after one day of storing the RuO<sub>2</sub>-Nf electrodes in water, the weight of the Nafion membrane increased by 1.3%. This can be associated with water uptake. However, after one week, a decrease in the weight of the Nafion membrane is observed. The decrease in weight reaches 48.5% after one month of observation and indicates a limited lifetime of the Nafion membrane.

TABLE I. SOLUBILITY OF THE NAFION MEMBRANE

	Time		
	1 day	1 week	1 month
Solubility, %	+1.29 ± 0.07	-1.01 ± 1.01	-48.52 ± 3.92

*C. RuO<sub>2</sub> electrodes can be successfully covered with Nafion 3 times for measurement at room temperature*

To see if the electrodes can be used even after the Nafion membrane wears off, we attempted to remove the Nafion membrane and cover them with a fresh membrane. The performance of the electrodes was evaluated based on the following parameters: sensitivity, E<sup>0</sup>, R<sup>2</sup>, hysteresis A, hysteresis B, and drift. The measured parameters were used to build a comparison matrix (Table II) as described in our previous work [6]. The results of all the measurements are presented in Table III. From Table II it can be seen that the electrodes showed good performance at room temperature even after coating them with Nafion for the third time. However, the performance gradually impaired with the increase of temperature for the electrodes covered with Nafion

for the second and third time. Furthermore, the main characteristic of the electrode, its sensitivity, was very low for the electrodes covered with Nafion for the third time. Thus, electrodes can be covered with Nafion repeatedly, however, only to be used at room temperature.

TABLE II. COMPARISON MATRIX FOR THE PERFORMANCE OF RuO<sub>2</sub>-Nf ELECTRODES

Drying Temperature \ Temperature of the sample	25°C	30°C	35°C	40°C
	First coating	5	5	6
Second coating	5	5	4	2
Third coating	5	4	2	2

IV. CONCLUSIONS

The screen printed RuO<sub>2</sub> pH-electrode covered with a protective Nafion membrane showed excellent performance at room temperature even after 2 renewals of the Nafion membrane. The temperature of the sample had a negative effect on the performance of the fabricated electrodes. In our future studies, we will further explore the possibility to recover the RuO<sub>2</sub> electrodes with Nafion membrane to improve the performance of the RuO<sub>2</sub>-Nf electrodes. We will investigate wider temperature diapason and determine the number of possible renewals of the Nafion membrane.

ACKNOWLEDGEMENT

This work was supported by the European Commission through the AQUASENSE project [H2020-MSCA-ITN-2018-813680]. Ott Scheler acknowledges support from the Tallinn University of Technology development program 2016–2022 [project code 2014-2020.4.01.16-0032].

TABLE III. CHARACTERISTICS OF RuO<sub>2</sub>-Nf ELECTRODES DRIED AT DIFFERENT TEMPERATURES, MEASURED AT VARYING SAMPLE TEMPERATURES.

Temperature, °C	Sensitivity, mV/pH	Theoretical sensitivity, mV/pH	E <sup>0</sup> , mV	R <sup>2</sup>	Hysteresis A, mV	Hysteresis B, mV	Drift, mV/h
<b>First coating</b>							
25	53.5 ± 2.3	59.2	640.7 ± 75.7	0.985	8 ± 1	20 ± 6	5-20
30	54.0 ± 0.8	60.2	548.1 ± 16.3	0.979	15 ± 6	17 ± 1	5-15
35	54.5 ± 2.2	61.2	506.2 ± 41.9	0.985	12 ± 2	15 ± 9	10-20
40	54.7 ± 2.2	62.2	583.6 ± 58.2	0.995	15 ± 7	20 ± 10	10-15
<b>Second coating</b>							
25	49.5 ± 5.8	59.2	537.9 ± 23.4	0.994	24 ± 7	9 ± 2	0-15
30	40.4 ± 6.8	60.2	350.7 ± 18.1	0.952	9 ± 4	11 ± 3	0-20
35	47.8 ± 5.0	61.2	425.9 ± 6.5	0.977	20 ± 7	20 ± 4	0-20
40	33.3 ± 4.8	62.2	259.6 ± 80.4	0.876	28 ± 1	8 ± 7	0-15
<b>Third coating</b>							
25	53.7 ± 1.5	59.2	522.8 ± 22.3	0.975	20 ± 4	4 ± 1	10-20
30	27.7 ± 7.4	60.2	342.6 ± 117.6	0.966	19 ± 1	7 ± 4	5-15
35	28.1 ± 5.8	61.2	260.5 ± 51.0	0.941	24 ± 4	20 ± 4	10-20
40	13.7 ± 4.2	62.2	67.7 ± 64.8	0.831	22 ± 5	10 ± 2	10-20



## REFERENCES

- [1] G. A. Perley and J. B. Godshalk, "Cell for pH measurements," 2416949, 1947.
- [2] T. Katsube, I. Lauks, and J. N. Zemel, "pH-sensitive sputtered iridium oxide films," *Sensors and Actuators*, vol. 2, pp. 399–410, 1982.
- [3] L. Manjakkal, D. Szwagierczak, and R. Dahiya, "Metal oxides based electrochemical pH sensors: Current progress and future perspectives," *Prog. Mater. Sci.*, vol. 109, pp. 1–31, 2020.
- [4] Y. Zhang *et al.*, "Ink formulation, scalable applications and challenging perspectives of screen printing for emerging printed microelectronics," *J. Energy Chem.*, 2021.
- [5] K. Uppuluri, M. Lazouskaya, D. Szwagierczak, K. Zaraska, and M. Tamm, "Fabrication, potentiometric characterization, and application of screen-printed RuO<sub>2</sub> pH electrodes for water quality testing," *Sensors*, vol. 21, no. 5399, 2021.
- [6] M. Lazouskaya, O. Scheler, V. Mikli, K. Uppuluri, K. Zaraska, and M. Tamm, "Nafion Protective Membrane Enables Using Ruthenium Oxide Electrodes for pH Measurement in Milk," *J. Electrochem. Soc.*, vol. 168, no. 107511, 2021.
- [7] L. Manjakkal, K. Cvejin, J. Kulawik, K. Zaraska, D. Szwagierczak, and R. P. Socha, "Fabrication of thick film sensitive RuO<sub>2</sub>-TiO<sub>2</sub> and Ag/AgCl/KCl reference electrodes and their application for pH measurements," *Sensors Actuators, B Chem.*, vol. 204, pp. 57–67, 2014.
- [8] B. Xu and W. Zhang, "Modification of vertically aligned carbon nanotubes with RuO<sub>2</sub> for a solid-state pH sensor," *Electrochim. Acta*, vol. 55, pp. 2859–2864, 2010.
- [9] W. Lonsdale, M. Wajrak, and K. Alameh, "Effect of conditioning protocol, redox species and material thickness on the pH sensitivity and hysteresis of sputtered RuO<sub>2</sub> electrodes," *Sensors Actuators B Chem.*, vol. 252, pp. 251–256, 2017.
- [10] H. N. McMurray, P. Douglas, and D. Abbot, "Novel thick-film pH sensors based on ruthenium dioxide-glass composites," *Sensors Actuators B Chem.*, vol. 28, no. 1, pp. 9–15, 1995.

## Appendix 7

### Publication VII

M. Lazouskaya, I. Vetik, O. Scheler, K. Uppuluri, N. Razmi, K. Zaraska, and M. Tamm, "Cleaning procedure for the screen printed RuO<sub>2</sub>-based pH electrodes," in *IEEE Sensors Conference*, 2022, Dallas, Texas, USA.

© 2022 IEEE. Reprinted, with permission, from M. Lazouskaya, I. Vetik, O. Scheler, K. Uppuluri, N. Razmi, K. Zaraska, and M. Tamm, "Cleaning procedure for the screen printed RuO<sub>2</sub>-based pH electrodes," in *IEEE Sensors Conference*, October 2022



# Cleaning Procedure for the Screen-Printed RuO<sub>2</sub> pH Electrodes

Maryna Lazouskaya<sup>1,2,\*</sup>, Iuliia Vetik<sup>1</sup>, Kiranmai Uppuluri<sup>3</sup>, Nasrin Razmi<sup>4</sup> and Ott Scheler<sup>1</sup>

<sup>1</sup> Department of Chemistry and Biotechnology, School of Science, Tallinn University of Technology, Tallinn, Estonia

<sup>2</sup> Center of Food and Fermentation Technologies, Tallinn, Estonia

<sup>3</sup> Lukasiewicz Research Network—Institute of Microelectronics and Photonics, Krakow, Poland

<sup>4</sup> Department of Science and Technology, Physics and Electronics, Linköping University, Norrköping, Sweden

\*Email address of the corresponding author: [malazo@taltech.ee](mailto:malazo@taltech.ee)

ORCID number of the corresponding author: 0000-0003-2411-4267

**Abstract**—Screen-printed RuO<sub>2</sub> pH electrodes are suitable for pH determination not only in water samples but also in different food matrixes, e.g., beverages, juices and milk. Nevertheless, the application of the screen-printed RuO<sub>2</sub> electrodes in milk is impossible without covering the electrodes with a protective Nafion membrane that prevents the contamination of the pH-sensitive area of the electrode with sample residues. However, not much attention has been paid to the cleaning procedure of Nafion-covered screen-printed RuO<sub>2</sub> electrodes (RuO<sub>2</sub>-Nf). In this paper, we show that cleaning the electrodes by soaking them in the solution of 5% pepsin in 0.1 M HCl allows restoring the electrode to its initial state for measuring pH in food samples.

**Keywords**—ruthenium oxide, screen printing, pH electrodes, cleaning procedure

## I. INTRODUCTION

Ruthenium(IV) oxide (RuO<sub>2</sub>) electrode is a well-known alternative to a fragile glass electrode used in potentiometric pH measurement. Among the investigated pH-sensitive materials, thick and thin films of RuO<sub>2</sub> were shown to have the best sensitivity and selectivity [1], Nernstian response even in the presence of strong oxidizing and reducing agents [2], and unaltered performance even in the presence of colonies of organic sediments [3]. The RuO<sub>2</sub> electrodes were previously shown to have excellent pH sensitivity in various food samples, such as juices, beers and even dairy products [4]–[8].

Various fabrication methods were reported for the RuO<sub>2</sub> electrodes over the years, including magnetron sputtering [4], electrodeposition [9], thermal deposition [10] and screen printing [3]. Among them, screen printing allows to fabricate the RuO<sub>2</sub> electrodes with the best characteristics and is rapid and easily scalable [11].

The screen-printed RuO<sub>2</sub> electrode measures pH similarly to a conventional glass electrode: the electrochemical potential of a RuO<sub>2</sub> electrode is directly proportional to pH. Thus, if we calibrate the electrode's potential against standard buffer solutions, we can determine the pH of any sample from the measured potential. However, in practice, it is not that simple. Sample composition and texture can affect the precision of the pH measurement due to the

This work was supported by the European Commission through the AQUASENSE (H2020-MSCA-ITN-2018-813680) project. Ott Scheler acknowledges support from the Tallinn University of Technology development program 2016–2022 (project code 2014-2020.4.01.16-0032).

contamination of the electrode. Previously, we have demonstrated that modification of the screen-printed RuO<sub>2</sub> electrodes with a Nafion membrane allows avoiding this contamination risk, and therefore allows using RuO<sub>2</sub> electrodes in milk [8].

Nevertheless, little attention has been paid so far to establish a proper cleaning procedure for the solid-state electrodes (Fig. 1). Therefore, the aim of this work was to evaluate the most common cleaning approaches, known for the conventional glass electrode and determine what works the best for the screen printed RuO<sub>2</sub> electrodes.

## II. MATERIALS AND METHODS

### A. Fabrication of the RuO<sub>2</sub> electrodes

The RuO<sub>2</sub> electrodes were fabricated as previously described [12]. First, a layer of Ag/Pd conductive paste (9695, Electro-Science Laboratories, USA) was printed on top of Al<sub>2</sub>O<sub>3</sub> substrate, dried at 120°C for 15 minutes, followed by sintering at 900°C for one hour. Next, a layer of pH-sensitive RuO<sub>2</sub>/glass paste (3914, Electro-Science Laboratories, USA) was printed, dried at 120°C for 15 minutes and sintered at 900°C for one hour. The RuO<sub>2</sub> layer was printed to slightly overlap the Ag/Pd layer. After cooling down, a copper wire was soldered to the Ag/Pd layer with Pb/Sn alloy. The electrical connection was then covered with a non-corrosive silicone resin (DOWSIL™ 3140 RTV Coating, Dow Chemical Company, USA) for insulation purposes.

### B. Modification of the RuO<sub>2</sub> electrodes with Nafion membrane

The Nafion membrane was deposited on the RuO<sub>2</sub> electrodes by drop-casting technique as previously described [8]. For that, 10 μL of 5% solution of Nafion in a mixture of lower aliphatic alcohols and water (Nafion 117, Sigma

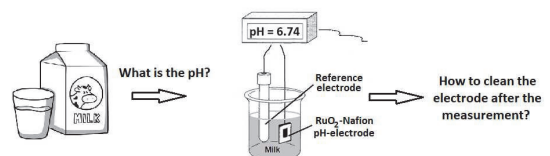


Fig. 1 At present, there are no recommendations regarding how the screen-printed electrodes should be cleaned after the measurement in the samples that can contaminate the electrode (e.g., milk).

Aldrich, USA was pipetted on the electrodes to cover the RuO<sub>2</sub> layer. The electrodes were placed into a laboratory incubator (BD 53, Binder, Germany) for 2 hours to dry at 80°C. The procedure was repeated two more times to create a thicker Nafion membrane. The electrodes were left to air-dry at room temperature overnight.

### C. Setup

A standard potentiometric method was used to determine the sensitivity of the fabricated electrodes. A fabricated RuO<sub>2</sub>-Nf electrode was used as an indicator electrode (IE) and a standard glass ion-selective electrode (Ag | AgCl | KCl, HI1053P, Hanna Instruments, USA) was used as a reference electrode (RE). The electrodes were connected to the measuring device (USB-6259, National Instruments, USA) via a circuit board by galvanic connections. The measuring device was powered up by a high-performance digital power supply (E3631A, Agilent, USA) with an input voltage of 12 Volts. The potential difference between IE and RE was measured and recorded using the LabVIEW program (National Instruments, USA).

### D. Sensitivity measurement

The sensitivity of a fabricated RuO<sub>2</sub>-Nf electrode was determined by exposing the electrodes to the buffers with pH in the range of 3.0 ... 11.0 and recording the potential of the electrode 90 seconds after immersing the electrodes in the buffer. The buffer solutions were freshly prepared before each measurement from anhydrous salts (Sigma Aldrich, USA). The pH of the buffers was double-checked with a conventional pH meter (Seven2Go Advanced Single-Channel Portable pH Meter, Mettler Toledo, Switzerland).

The sensitivity of the fabricated electrodes was determined as the slope of the linear dependency of the potential of an electrode on the pH of the buffer solution. For that, the dependency of the potential of an electrode (Y-axis) as a function of pH (X-axis) was plotted and the equation was extracted by the method of least squares. The sensitivity was determined for each electrode 5 times:

- initial sensitivity after reaching stable sensitivity values;
- after usage in milk;
- straight after cleaning;
- 12 hours after cleaning;
- 24 hours after cleaning.

### E. Measurement of the potential of the electrodes in milk samples

To study the behaviour of the RuO<sub>2</sub>-Nf electrodes in milk samples, the electrodes were placed into a milk sample at room temperature and the potential of an electrode was recorded for 1 hour. Three milk samples were tested: whole milk containing 2.5% fat (ultra pasteurised Latte Piim, Tere, Estonia), whole milk filtered through a filtering bag with a porosity of 63 µm (BagPage F, Interscience, France) and reconstructed skim milk (RSM). Reconstructed skim milk was prepared as previously described [13]. Briefly, 10 g of skimmed milk powder (Valio Ltd., Turku, Finland) was dissolved in 100 mL of Milli-Q water to yield a final concentration of 10% (w/v). Then, an aqueous solution of CaCl<sub>2</sub> was added to the solution of skimmed milk to produce a final concentration of 5 mM. The resulting mixture was thoroughly stirred for 1 h at room temperature.

TABLE I. CLEANING METHODS

Approach	How it was performed
Mechanical cleaning	Electrodes were cleaned with a soft sponge and surfactants, then rinsed with Milli-Q water
Mechanical cleaning and soaking in 0.1 M HCl	Electrodes were soaked in 0.1 M HCl for 10 minutes, and then were cleaned mechanically as described above
5% pepsin in 0.1 M HCl	Electrodes were soaked in 0.1 M HCl with added 5% of pepsin for 10 minutes and then rinsed with Milli-Q water
0.4 M HCl	Electrodes were soaked in 0.4 M HCl for 10 minutes and then rinsed with Milli-Q water

### F. Cleaning approaches

Four main approaches, indicated in Table 1, were selected to identify the most appropriate way to clean the screen-printed RuO<sub>2</sub> electrodes. The approaches were selected as the most commonly advised for maintaining the conventional glass electrode: mechanical cleaning with surfactants is used for food samples containing fats and oils, cleaning with acidic pepsin solution is advised to remove proteins' residues and acidic cleaning is advised to remove mineral deposits [14].

## III. RESULTS AND DISCUSSION

### A. RuO<sub>2</sub> electrodes measure pH similarly to the glass electrode

The response of the RuO<sub>2</sub> to the pH change can be described by (1) [1]:

$$Ru^{IV}O_2 + \bar{e} + H^+ = Ru^{III}O(OH) \quad (1)$$

The Nernst equation for this process takes the form of (2)

$$E = E^0 + R \cdot T / F \cdot \ln(a_{Ru^{III}} / (a_{Ru^{IV}} \cdot a_{H^+})) \quad (2)$$

where E is the electrochemical potential, V; E<sup>0</sup> is the standard electrochemical potential, V; R is the universal gas constant, 8.314 J/mol·K; T is temperature, K; F is the Faraday constant, 96485 J;  $a_{Ru^{III}}$ ,  $a_{Ru^{IV}}$  and  $a_{H^+}$  are the activities of Ru<sup>III</sup>O(OH), Ru<sup>IV</sup>O<sub>2</sub> and H<sup>+</sup> respectively.

Considering that pH = -lg<sub>10</sub>a<sub>H<sup>+</sup></sub> and the values of metals activities approximate 1 in a solid state, after substituting the constants, at room temperature (22°C) (2) takes the form of (3):

$$E = E^0 + 0.0583 \cdot \text{pH} \quad (3)$$

Equation (3) allows determining the pH of a sample with a RuO<sub>2</sub> electrode, similarly to the conventional glass electrode. Furthermore, the value of 0.0583 Volts (or 58.3 milliVolts) is called theoretical Nernstian sensitivity and can be used to evaluate the performance of an electrode.

### B. RuO<sub>2</sub> electrodes showed behaviour similar to that of the conventional glass electrode

Since the screen-printed RuO<sub>2</sub> electrodes cease to work in complex food samples, containing fats and proteins, such as milk (Fig. 2a), and to see if the fabricated RuO<sub>2</sub>-Nf electrodes are sensitive to the milk sample, we tested the fabricated RuO<sub>2</sub>-Nf electrodes in (i) whole milk, (ii) fatless

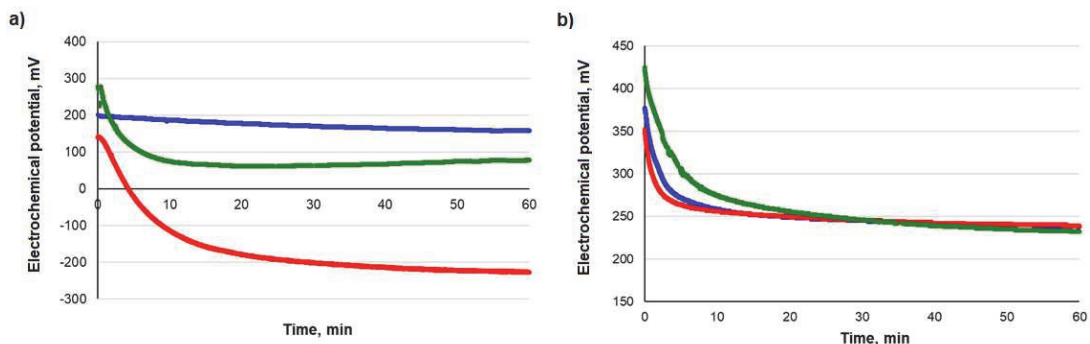


Fig. 2 Change of the potential (Y-axis) of the fabricated RuO<sub>2</sub> (a) and RuO<sub>2</sub>-Nf (b) electrodes with time (X-axis) measured in whole milk (red), filtered whole milk (blue) and RSM (green). While the RuO<sub>2</sub> electrodes showed significant potential drop when measuring in whole milk and RSM, the RuO<sub>2</sub>-Nf electrodes showed excellent performance in all three milk samples.

milk reconstructed from milk powder and (iii) milk filtered from big colloidal clusters. From Fig. 2, it can be seen that the RuO<sub>2</sub>-Nf electrodes showed improved behaviour, compared to that of the RuO<sub>2</sub> electrodes and can be successfully used in all three milk samples.

### C. Acidic pepsin solutions allow restoring the RuO<sub>2</sub> electrodes to the initial state and a combination of surfactants and acidic cleaning allows to improve electrode performance

The fabricated RuO<sub>2</sub>-Nf electrodes showed improved sensitivity after each cleaning procedure (Fig. 3). However, it can be seen that some conditioning in distilled water is required after the cleaning. This conditioning might be associated with the re-formation of the double layer on the surface of the electrode that participates in the pH-response of the electrode [11]. For the electrodes, cleaned with surfactants, the sensitivities after cleaning and conditioning for 24 hours exceeded the initial sensitivities that might be

associated with damaging the electrodes during cleaning. For the electrodes cleaned with 0.4 M HCl, the sensitivity decreased to  $5.0 \pm 3.0$  mV/pH after cleaning. It is unclear why this drop in sensitivity takes place and how it might affect the RuO<sub>2</sub>-Nf electrodes. Further investigation is necessary. The electrodes cleaned with the acidic pepsin solution showed the smallest change in sensitivity after cleaning and conditioning in distilled water for 24 hours and therefore should be preferred for the cleaning of the screen-printed RuO<sub>2</sub>-Nf electrodes after usage in real-life food samples.

## IV. CONCLUSION

In this study, we have demonstrated that the utilization of acidic pepsin solution for the cleaning of the screen-printed RuO<sub>2</sub>-Nf electrodes is the best way to clean the electrodes after measurement in milk, which is known to be one of the complex food samples from the point of the composition. The impact of the cleaning procedure on the sensitivity of the screen-printed RuO<sub>2</sub> electrodes was investigated for the first time. These results can be of interest to food researchers since most of the reported solid-state electrodes are suitable only for one measurement and should be discarded afterwards. Our findings allow for repeatable usage of the screen-printed RuO<sub>2</sub>-Nf electrodes.

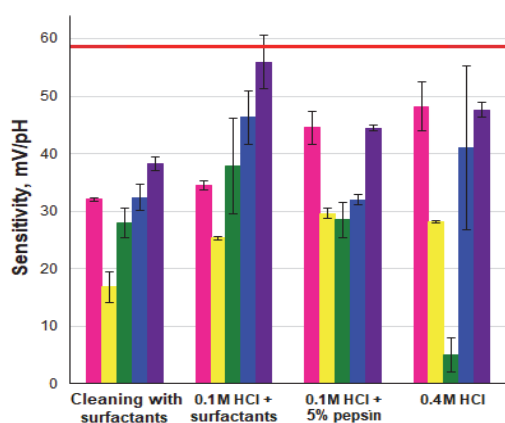


Fig. 3 Sensitivity of the RuO<sub>2</sub>-Nf electrodes after different cleaning procedures (Ox): initial sensitivity (pink), sensitivity after using in milk (yellow), sensitivity straight after cleaning (green), sensitivity 12 hours after cleaning (blue) and sensitivity 24 hours after cleaning (purple). Red line indicates theoretical Nernstian sensitivity. The RuO<sub>2</sub> electrodes were restored to the initial state after cleaning with an acidic pepsin solutions (5% pepsin in 0.1 M HCl) and a combination of surfactants and acidic cleaning (combination of mechanical cleaning with surfactants and acidic cleaning with 0.1 M HCl) improved electrode's performance.

## REFERENCES

- [1] P. Kurzweil, "Metal oxides and ion-exchanging surfaces as pH sensors in liquids: State-of-the-art and outlook," *Sensors*, vol. 9, no. 6, pp. 4955–4985, 2009.
- [2] R. Fog, A.; Buck, "Electronic semiconducting oxides as pH sensors," *Sensors and Actuators*, vol. 5, pp. 137–146, 1984.
- [3] S. Zhuiykov, "Morphology of Pt-doped nanofabricated RuO<sub>2</sub> sensing electrodes and their properties in water quality monitoring sensors," *Sensors Actuators, B Chem.*, vol. 136, no. 1, pp. 248–256, 2009.
- [4] W. Lonsdale, M. Wajrak, and K. Alameh, "Manufacture and application of RuO<sub>2</sub> solid-state metal-oxide pH sensor to common beverages," *Talanta*, vol. 180, no. December 2017, pp. 277–281, 2018.
- [5] L. Manjakkal, K. Cvejic, J. Kulawik, K. Zaraska, D. Szwagierczak, and G. Stojanovic, "Sensing mechanism of RuO<sub>2</sub>-SnO<sub>2</sub> thick film pH sensors studied by potentiometric method and electrochemical impedance spectroscopy," *J. Electroanal. Chem.*, vol. 759, pp. 82–90, 2015.
- [6] K. Xu, X. Zhang, C. Chen, and M. Geng, "Development and performance of an all-solid-stated pH sensor based on modified membranes," *Int. J. Electrochem. Sci.*, vol. 13, no. 3, pp. 3080–3090, 2018.
- [7] Q. Li *et al.*, "Stable thin-film reference electrode on plastic substrate for all-solid-state ion-sensitive field-effect transistor sensing system," *IEEE Electron Device Lett.*, vol. 38, no. 10, pp. 1469–1472, 2017.
- [8] M. Lazouskaya, O. Scheler, V. Mikli, K. Uppuluri, K. Zaraska, and M. Tamm, "Nafion protective membrane enables using ruthenium oxide electrodes for pH measurement in milk," *J. Electrochem. Soc.*, vol. 168, no. 107511, 2021.
- [9] K. Pásztor, A. Sekiguchi, N. Shimo, N. Kitamura, and H. Masuhara, "Electrochemically-deposited RuO<sub>2</sub> films as pH sensors," *Sensors Actuators B. Chem.*, vol. 13, no. 14, pp. 561–562, 1993.
- [10] L. A. Pocrifka, C. Gonçalves, P. Grossi, P. C. Colpa, and E. C. Pereira, "Development of RuO<sub>2</sub>-TiO<sub>2</sub> (70-30) mol% for pH measurements," *Sensors Actuators, B Chem.*, vol. 113, no. 2, pp. 1012–1016, 2006.
- [11] L. Manjakkal, D. Szwagierczak, and R. Dahiya, "Metal oxides based electrochemical pH sensors: Current progress and future perspectives," *Prog. Mater. Sci.*, vol. 109, pp. 1–31, 2020.
- [12] K. Uppuluri, M. Lazouskaya, D. Szwagierczak, K. Zaraska, and M. Tamm, "Fabrication, potentiometric characterization, and application of screen-printed RuO<sub>2</sub> pH electrodes for water quality testing," *Sensors*, vol. 21, no. 5399, 2021.
- [13] M. Lazouskaya *et al.*, "Front-face fluorimeter for the determination of cutting time of cheese curd," *Foods*, vol. 10, no. 576, pp. 1–13, 2021.
- [14] Hach Company, "pH electrode cleaning & maintenance guide," 2014.

# Curriculum vitae

## Personal data

Name: Maryna Lazouskaya  
Date of birth: 03 May 1992  
Place of birth: Belarus  
Citizenship: Belarus

## Contact data

E-mail: [maryna.lazouskaya92@gmail.com](mailto:maryna.lazouskaya92@gmail.com)

## Education

2019–2023 Tallinn University of Technology – PhD Chemistry  
2015–2016 Graduate School of the National Academy of Sciences of  
Belarus – MSc Chemistry  
2010–2015 Belarussian State University – BSc Physical Chemistry

## Language competence

Russian Native  
Belarusian Native  
English Fluent  
Korean Intermediate  
Polish Intermediate  
German Beginner  
Estonian Beginner

## Professional employment

2022–2023 Visiting Scholar, Boise State University, Boise, Idaho, USA  
2019–2022 Researcher at the Center of Food and Fermentation  
Technologies (TFTAK), Tallinn, Estonia  
2019–2019 Chemist-engineer at FACOM TECHNOLOGIES LTD, Minsk  
Belarus  
2015–2018 Junior Researcher (chemist) at Institute of Chemistry of  
New Materials of National Academy of Sciences of Belarus,  
Minsk Belarus  
2014–2015 Laboratory technician (chemist) at Institute of Chemistry  
of New Materials of National Academy of Sciences of  
Belarus, Minsk Belarus



## Elulookirjeldus

### Isikuandmed

Nimi: Maryna Lazouskaya  
Sünniaeg: 3. mai 1992  
Sünnikoht: Valgevene  
Kodakondsus: Valgevene

### Kontaktandmed

E-post: [maryna.lazouskaya92@gmail.com](mailto:maryna.lazouskaya92@gmail.com)

### Hariduskäik

2019–2023 Tallinna Tehnikaülikool – PhD Keemia  
2015–2016 Valgevene Riikliku Teaduste Akadeemia Kõrgkool – MSc Keemia  
2010–2015 Valgevene Riiklik Ülikool – BSc Füüsikaline keemia

### Keelteoskus

Vene keel Emakeel  
Valgevene keel Emakeel  
Inglise keel Kõrgtase  
Korea keel Kesktase  
Poola keel Kesktase  
Saksa keel Algaja  
Eesti keel Algaja

### Teenistuskäik

2022–2023 Boise Osariigi Ülikool, Külalisteadlane  
2019–2022 AS Toidu- ja Fermentatsioonitehnoloogia Arenduskeskus, Teadur  
2019–2019 FACOM TECHNOLOGIES LTD, Keemiainsener  
2015–2018 Valgevene Riikliku Teaduste Akadeemia uute materjalide keemia instituut, Nooremteadur  
2014–2015 Valgevene Riikliku Teaduste Akadeemia uute materjalide keemia instituut, Tehniline töötaja

ISSN 2585-6901 (PDF)  
ISBN 978-9949-83-969-8 (PDF)